AD-A133 771   LECTURES ON COMPOSITE MATERIALS FOR AIRCRAFT STRUCTURES   1/3
(U) AERONAUTICAL RESEARCH LABS MELBOURNE (AUSTRALIA)
B C HOSKIN ET AL. OCT 82 ARL/STRUC-394

UNCLASSIFIED   F/G 11/4   NL
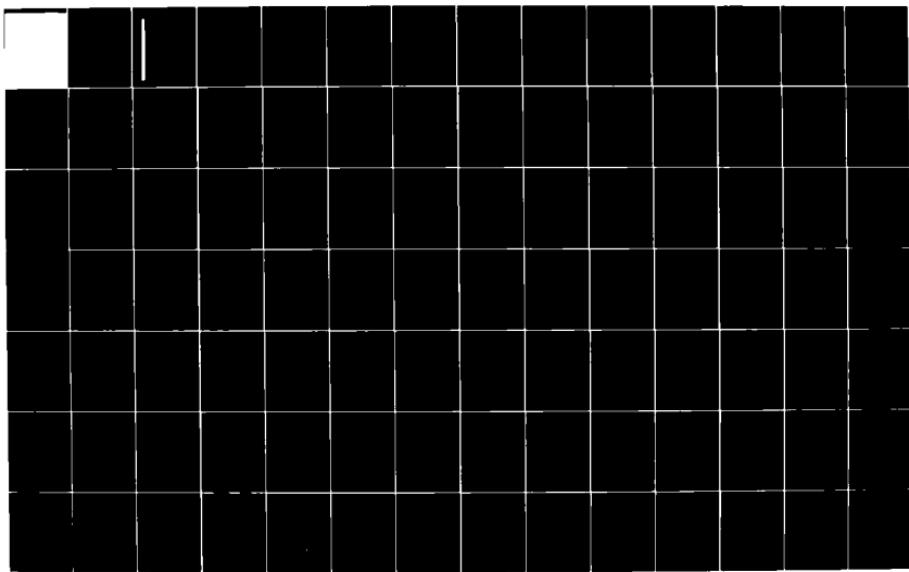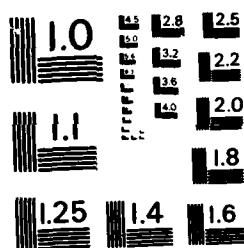
MICROCOPY RESOLUTION TEST CHART

NATIONAL BUREAU OF STANDARDS-1963-A

ARL-STRUC-REPORT-394/
ARL-MAT-REPORT-114

AR-002-919

AD-A133771

DEPARTMENT OF DEFENCE SUPPORT

DEFENCE SCIENCE AND TECHNOLOGY ORGANISATION

AERONAUTICAL RESEARCH LABORATORIES

MELBOURNE, VICTORIA

STRUCTURES REPORT 394/
MATERIALS REPORT 114

LECTURES ON COMPOSITE MATERIALS FOR
AIRCRAFT STRUCTURES

Edited by

B.C. HOSKIN and A.A. BAKER

DTIC
ELECTE
OCT 1 9 1983
E

DTIC FILE COPY

COPY No

OCTOBER 1982

83 09 26 012

AR-002-919

DEPARTMENT OF DEFENCE SUPPORT

DEFENCE SCIENCE AND TECHNOLOGY ORGANISATION

AERONAUTICAL RESEARCH LABORATORIES

STRUCTURES REPORT 394

MATERIALS REPORT 114

LECTURES

ON

COMPOSITE MATERIALS FOR AIRCRAFT STRUCTURES

Edited by

B.C. HOSKIN and A.A. BAKER

SUMMARY

This report is an edited version of notes prepared in connection with
a series of lectures on Composite Materials for Aircraft Structures that
was given at the Aeronautical Research Laboratories during November 1981.
The aim of the lectures was to provide a broad introduction to virtually
all aspects of the technology of composite materials for aircraft structural
applications. Topics covered included: the basic theory of fibre
reinforcement; material characteristics of the commonly used fibre, resin,
and composite systems; component form and manufacture; structural mechanics
of composite laminates; joining composites; environmental effects,
durability and damage tolerance; NDI procedures; repair procedures; aircraft
applications; airworthiness considerations.

POSTAL ADDRESS: Director, Aeronautical Research Laboratories,
                  P.O. Box 4331, Melbourne, Victoria, 3001, Australia.

FOREWORD

    This report is an edited version of notes that were prepared
in connection with a series of lectures that was given at the
Aeronautical Research Laboratories, Melbourne, during November 1981.
All lecturers were officers in either Structures or Materials Division,
ARL. The names of the lecturers, along with their topics, are given in
the list of contents. The lectures originated with a request to ARL
from the Department of Transport (Airworthiness Branch).

CONTENTS

DISTRIBUTION

DOCUMENT CONTROL DATA

<u>Lecture 1</u>

<u>INTRODUCTION</u>

B.C. HOSKIN

1. <u>GENERAL</u>

A major development in aeronautics, which has come to the fore
especially over the past decade or so, has been the use of composite
materials in place of metals in aircraft structures. In general, a com-
posite material can be defined simply as a material which consists of two
(or more) identifiably distinct constituent materials. The composite
materials used for aircraft structures belong to the class known as "fibre
composites" (or, sometimes, "fibre reinforced plastics") comprising
continuous fibres embedded in a resin (or "plastic") matrix. It is the
fibres which provide such a composite with its key structural properties,
the matrix serving mainly to bond the fibres into a structural entity.
The prime reason for using composite materials is that substantial weight
savings can be achieved because of their superior strength-to-weight and
stiffness-to-weight ratios, as compared with the conventional materials
of aircraft construction such as the aluminium alloys. Weight savings of
the order of 25% are generally considered to be achievable using current
composites in place of metals.

There is a distinct lack of uniformity in the names given to
composite materials. In the USA the usual practice is to write the name
in the format "fibre/matrix". Since, for aircraft structural applications,
the main fibres presently used are graphite, boron, aramid and glass, and
the main matrix material is epoxy resin, the main composites in the US
terminology are graphite/epoxy, boron/epoxy, aramid/epoxy and glass/epoxy.
(Naturally, if another type of matrix material is used that is reflected
in the name; for example, there has been some interest in graphite/
polyimide composites.) This notation is reasonably explicit, and a further
advantage is that it can be readily adapted to describe specific composite
systems. For example, a common US graphite/epoxy system uses Thornel T300
fibres and Narmco 5208 resin; this is generally abbreviated to "T300/5208".
Another common US graphite/epoxy system uses Hercules AS fibres and
Hercules 3501-6 resin; this is likewise abbreviated to "AS/3501-6". The
US terminology will be adopted here but, before passing on, mention will be
made of the main alternatives. In the UK, where graphite fibres were
first developed, they have always been called "carbon fibres" and the
associated composite is simply called "carbon fibre composite". Aramid
fibres are organic fibres first developed by Du Pont and the Du Pont
proprietary name of "Kevlar" is commonly used; originally the same material
was known as "PRD-49". Finally, at one time the terms "carbon fibre
reinforced plastic", "boron fibre reinforced plastic" and "glass fibre
reinforced plastic" were in wide use; this terminology seems to be lapsing
partly because it suggests that the fibres act in a supporting role to the
plastic matrix whereas the real situation is quite the reverse. The
terminology has been summarised in Table 1 below.

1

**TABLE 1: Main Composite Materials for Aircraft
Structural Applications**

These Lectures	Equivalent Nomenclature
Graphite/epoxy (Gr/Ep)	Carbon fibre composite (CFC) Carbon fibre reinforced plastic (CFRP)
Boron/epoxy (B/Ep)	Boron fibre reinforced plastic (BFRP)
Aramid/epoxy (Ar/Ep)	Kevlar/epoxy PRD-49/epoxy
Glass/epoxy	Glass fibre reinforced plastic (GFRP or GRP)

2. OVERVIEW OF USE OF COMPOSITE MATERIALS IN AIRCRAFT STRUCTURES

Of the materials being considered here, glass fibre composites
were the first to be used for aircraft structures. As far back as 1944 a
Vultee BT-15 trainer aircraft was made and flown with the aft fuselage
skin made of glass fibre composite sandwich panels (composite facings on a
balsa wood core). However, whilst over the succeeding years glass fibre
composites, especially in the form of glass/epoxy, have become quite widely
used in aircraft structures, this use has been mainly confined to items
such as control surfaces, fairings, interior fittings and canopies; this
is the way glass fibre composites are utilised in, for example, the
Boeing 747. The reason why these composites have not been generally employed
for major structural components is that, although their strength-to-weight
ratio compares very favourably with that for metals, their stiffness-to-
weight ratio does not and stiffness is often as important a design
requirement as strength, especially for high speed aircraft. One application
of glass/epoxy that is being widely pursued, however, is in helicopter rotor
blades.

The potential for the widespread use of composites in aircraft
structures came about with the more or less simultaneous invention, around
1960, of graphite fibres in the UK and boron fibres in the USA. The so-
called "advanced composite materials" based on either of these fibre types,
generally with an epoxy matrix, are markedly superior to conventional
aircraft materials in both strength and stiffness properties. Initially
the development of boron/epoxy proceeded the more rapidly and virtually
entirely in USA. By 1970, the US had made and flown major boron/epoxy
demonstrator items, including an F-111 horizontal tail and 50 F-4 rudders.
On the basis of the experience so gained, boron/epoxy was incorporated in
the US high-performance military aircraft then being designed. Thus, the
skin of the horizontal tail of the F-14, and the skin of both the horizontal
and vertical tails of the F-15, are made of boron/epoxy. The development
of graphite/epoxy went on much more slowly in the UK, generally only small
demonstrator items such as rudder trim tabs for a Strikemaster and a
spoiler for Jaguar being made around this time.

2

However, by the mid-1970s, the US had decided to switch from boron/epoxy to graphite/epoxy. The reason was primarily the cost of the material; by 1979 the cost of graphite/epoxy in the USA in the form that it is procured by the aircraft manufacturer (namely, "pre-preg") was $40 per lb. and falling whilst that of boron/epoxy was $180 per lb. and rising. Having made the switch, the US has been quick to incorporate graphite/ epoxy in its high performance military aircraft. In the F-16, graphite/ epoxy is used for the skin of the horizontal and vertical tails and for various control surfaces; it comprises about 3% of the structural weight. A more extensive use of graphite/epoxy is made in the F/A-18 (Fig. 1); there the wing skins, horizontal and vertical tail skins, the fuselage dorsal cover and avionics door, and many of the control surfaces are graphite/ epoxy which comprises 9% of the structural weight (and 35% of the surface area). In the AV-8B (Fig. 2), almost the complete wing, i.e., skin plus sub-structure, is made of graphite/epoxy; it is also used in the horizontal tail, forward fuselage and various control surfaces and comprises about 26% of the structural weight. The horizontal tail (skin and sub-structure) of a prototype B-1 bomber was graphite/epoxy.

As regards European military aircraft, a graphite/epoxy taileron (i.e., all-moving horizontal tail) is being developed for the Tornado by the UK and West Germany, and the French Mirage 2000 uses both boron and graphite composites for its tail unit and control surfaces.

Applications of advanced composites in civil aircraft have lagged behind those in military aircraft; however, interest is now quickening. Various graphite/epoxy demonstrator items have been made in USA. Early such items included Boeing 737 spoilers, of which 111 were made and fitted to the aircraft of seven airlines operating throughout the world; by mid-1981 the high time spoiler had achieved approximately 22,000 flight hours and no significant problems had been encountered. The substantial weight savings that can be achieved using composites can lead to substantial fuel savings and, because of this, a major development of composite aircraft structures is being undertaken within the framework of the NASA Aircraft Energy Efficiency (ACEE) program. The aim of this development is to provide the technology and confidence so that commercial transport manufacturers can commit themselves to the use of composites in their future aircraft; the time-scale is for composites to be used for secondary structure from 1980 onwards and for primary structure from 1985 onwards. Demonstrator items included in the ACEE composites program are shown in Table 2 below along with the saving in weight as compared with existing metal components.

TABLE 2: Graphite/Epoxy Demonstrators in ACEE Program
        (see p.8 of ref. 9)

Type of Structure	Item	Weight Saving %
Secondary	McDonnell-Douglas DC-10 rudder	26.8
	Boeing 727 elevator	25.6
	Lockheed L-1011 aileron	26.3
Primary	McDonnell-Douglas DC-10 vertical tail	20.2
	Boeing 737 horizontal tail	27.1
	Lockheed L-1011 vertical tail	27.9

Consistently with the above time-scales the Boeing 757 and 767 aircraft, scheduled to go into service soon, use graphite/epoxy for many of the control surfaces (Fig. 3). Special mention should be made of the Lear Fan 2100 (Fig. 4) which is a small passenger aircraft; this is sometimes referred to as the "all-composite" aircraft because almost all the airframe is made of composites, mainly graphite/epoxy. The Lear Fan 2100 first flew in January 1981 and, naturally, its service performance will be of special interest.

Composites have also been used in space vehicle structures e.g. the 15 m long cargo bay doors in the Space Shuttle are graphite/epoxy. There have been many applications of graphite/epoxy in satellite structures where another advantage of the material (besides the weight savings aspect) is its low coefficient of thermal expansion; this permits the maintenance of dimensional stability under large temperature variations.

So far no mention has been made of aramid/epoxy which is also classed as an advanced composite. This is quite widely used in aircraft structures but largely in roles previously filled by glass/epoxy. However, there is interest in a hybrid aramid-graphite composite for more general use. In the Boeing 767, for example, this hybrid is used for the wing-to-fuselage fairing, undercarriage doors, engine cowlings and fixed trailing edge panels. One shortcoming of aramid composites which has militated against their wider use in primary structure has been their rather low compressive strength.

In summary, fibre composite materials are already being used to a significant extent in aircraft structures and that use seems certain to extend; a consolidated list of some major applications is given in Table 3. Currently graphite/epoxy and, to a lesser extent, aramid/epoxy are seen as the most important composites for aircraft structural applications.

TABLE 3: Some Aircraft Applications of Advanced Composites

Aircraft	Composite	Application
F-14	B/Ep	Horizontal tail skin
F-15	B/Ep	Horizontal tail skin
	"	Vertical tail skin
	Gr/Ep	Speed brake
F-16	Gr/Ep	Horizontal tail skin
	"	Vertical tail skin
	"	Control surfaces
F/A-18	Gr/Ep	Wing skin
	"	Horizontal tail skin
	"	Vertical tail skin
	"	Control surfaces
	"	Dorsal cover, avionics door
AV-8B	Gr/Ep	Wing skin and substructure
	"	Horizontal tail skin
	"	Forward fuselage
	"	Control surfaces
B-1 (prototype)	Gr/Ep	Horizontal tail skin and substructure
Boeing 757&767	Gr/Ep	Control surfaces
	Ar-Gr/Ep	Fairings, U/C doors, cowlings
Lear Fan 2100	Gr/Ep	"Almost all" structure

3. SCOPE OF LECTURES

The importance of composite materials for aircraft structural applications is evident from the above discussion. However, in virtually all aspects, the use of these materials involves a very different technology to that for metals. The materials themselves are intrinsically different, manufacturing procedures are different, structural design procedures are different, and the in-service performance of the materials is different particularly as regards the causes and nature of damage that may be sustained. All these matters are addressed in these lectures which are aimed at providing a broad introduction to the technology of composite materials for aircraft structural applications.

In Lecture 2 the basic principles of fibre composites are described, a general account being given of how the properties of the heterogeneous composite derive from the properties of its constituents viz., fibres plus matrix. This topic is often referred to as the "micro-mechanics" of composites.

The next three lectures are concerned with the physical and mechanical properties of composite materials. The properties of the commonly used fibres, in particular, graphite, boron, aramid and glass are described in Lecture 3. This is followed in Lecture 4 by a description of the resins used as matrix materials, especially the widely used epoxy resins. Then, in Lecture 5, the properties of the main composites - graphite/epoxy, boron/epoxy, aramid/epoxy and glass/epoxy - are described.

The procedures involved in manufacturing a composite component are outlined in Lecture 6. Most attention is paid to the case where the material comes in the form of a tape or broadgoods but some reference is also made to filament-winding processes.

The next four lectures are related to structural applications of composites. In Lecture 7, the basic theory that is needed for composite structural analysis is presented. This involves concepts from anisotropic elasticity (because the mechanical properties of composites are highly directionally-dependent and, indeed, the key to the successful application of composites lies in the proper utilisation of this directional dependence) and from laminate theory (because composite structures are usually made as multi-ply laminates). The subject of joints is an especially important one for composite structures, and both mechanically fastened and adhesively bonded joints are commonly encountered; these are discussed in Lecture 8. Factors affecting the in-service performance, or durability, of composite aircraft structures are taken up in Lecture 9. These factors include environmental effects (especially the effects of moisture absorption and high temperatures); the fatigue of composites is also discussed in this lecture. The damage tolerance characteristics of composites, especially as regards damage caused by low energy impacts, are described in Lecture 10.

Non-destructive inspection (NDI) methods for use in the factory and in the field are described in Lecture 11. Procedures used for repairing composite structures, again either in the factory or in the field, are discussed in Lecture 12.

The types of composite construction being used in current aircraft are described in Lecture 13 and, finally, in Lecture 14 some account is given of matters which need special consideration in the airworthiness certification of aircraft containing major composite components.

4. COMPOSITE MATERIALS FOR OTHER AERONAUTICAL APPLICATIONS

Whilst these lectures are concerned with composite materials for aircraft structures, other types of composites are being investigated for a variety of possible aeronautical applications. One particularly active area is in the development of metal matrix composites for jet engine components. For instance, boron/aluminium composites (i.e., boron fibres in an aluminium alloy matrix) are being studied for use in fan blades; also, for hot end components such as turbine blades there is interest in tungsten/superalloy composites.

Composites not based on continuous fibre reinforcement, but rather comprising particles of one material embedded in a matrix of another material - the so-called "particulate composites" - are also receiving attention. (The most homely of all composites, namely concrete, is of this form consisting of particles of stone in a cement matrix. Reinforced concrete is, of course, also a composite, but it is akin to a fibre composite with the steel reinforcing rods playing the part of the fibres). The whisker composites, where the reinforcement is supplied by very small crystals (or "whiskers"), are examples of particulate composites; however, these are still largely in a developmental stage.

5. BIBLIOGRAPHIC COMMENTS

There is an extensive, and rapidly growing, literature on composite materials. Only some of the more general references will be mentioned below.

Reasonably broad, yet still reasonably succinct, accounts of the field have been given by Jones (1) and Aggarwal and Broutman (2). The most ambitious work to date is the eight volume treatise, edited by Broutman and Krock (3).

The US Military Handbook (4) contains quite an extensive discussion on composites for aerospace applications, although the materials data included in the 1971 edition are limited to glass and boron composites. The several publications, (5), (6), (7) and (8), by the NATO Advisory Group for Aerospace Research and Development (AGARD) provide a useful background on the way in which composites have been taken up for aeronautical applications. Several specific applications of composites in aircraft structures are described in detail in refs. (9) and (10).

Some idea of the many aspects of composites on which research is being undertaken can be obtained by consulting the conference proceedings regularly published by the American Society for Testing and Materials; see refs. (11) to (15). The state-of-the-art review by Gerharz and Schutz (16) contains an extensive bibliography. Various other items are listed as refs. (17) to (26).

REFERENCES

1. Jones, R.M., Mechanics of Composite Materials, McGraw-Hill Kogakusha Ltd., Tokyo, 1975.

2. Aggarwal, B.D. and Broutman, L.J., Analysis and Performance of Fiber Composites, Wiley, New York, 1980.

3. Broutman, L.J., and Krock, R.H. (eds.), Composite Materials, vols. 1 to 8, Interscience, New York, 1975.

4. Anon., Plastics for Aerospace Vehicles, Part 1, Reinforced Plastics, MIL-HDBK-17A, US Department of Defense, Washington, 1971.

5. Anon., The Potentials of Composite Structures in the Design of Aircraft, AGARD Advisory Report No. 10, 1967.

6. Anon., Composite Materials, AGARD Conference Proceedings No. 63, 1970.

7. Rosen, B.W. (ed.), Composite Materials, AGARD Lecture Series No. 55, 1972.

8. Anon., Certification Procedures for Composite Structures, AGARD Report No. 660, 1977.

9. Lenoe, E.M., Oplinger, D.W., and Burke, J.J. (eds.), Fibrous Composites in Structural Design, Plenum Press, New York, 1980.

10. Anon., The 1980s – Pay-Off Decade for Advanced Materials, Science of Advanced Materials and Process Engineering Series, vol. 25, Society for the Advancement of Material and Process Engineering (SAMPE), 1980.

11. Anon., Composite Materials: Testing and Design, ASTM STP 460, 1969.

12. Anon., Composite Materials: Testing and Design (Second Conference), ASTM STP 497, 1972.

13. Anon., Composite Materials: Testing and Design (Third Conference), ASTM STP 546, 1974.

14. Anon., Composite Materials: Testing and Design (Fourth Conference), ASTM STP 617, 1977.

15. Tsai, S.W. (ed.), Composite Materials: Testing and Design (Fifth Conference), ASTM STP 674, 1979.

16. Gerharz, J.J. and Schutz, D., Literature Research on the Mechanical Properties of Fibre Composite Materials – Analysis of the State of the Art, vol. 1, Royal Aircraft Establishment, Farnborough, Library Translation 2045, August 1980.

17. Tsai, S.W. and Hahn, H.T., Introduction to Composite Materials, Technomic Publishing Co., Westport, 1980.

18. Schwartz, R.T. and Schwartz, H.S. (eds.), Fundamental Aspects of Fibre Reinforced Plastic Components, Interscience, New York, 1968.

19. Tsai, S.W., Halpin, J.C., and Pagano, N.J. (eds.), Composite Materials Workshop, Technomic Publishing Co., Stamford, 1968.

20. Wendt, F.W., Liebowitz, H. and Perrone, N. (eds.), Mechanics of Composite Materials, Proc. of Fifth Symposium on Naval Structural Mechanics, Pergamon, Oxford, 1970.

21. Dietz, A.G.H. (ed.), Composites Engineering Laminates, MIT Press, Cambridge, Mass., 1969.

22. Gill, R.M., Carbon Fibres in Composite Materials, Iliffe, London, 1972.

23. Salkind, M.J. and Holister, G.S. (eds.), Applications of Composite Materials, ASTM STP 524, 1973.

24. Lubin, G. (ed.), Handbook of Fibreglass and Advanced Plastics Composites, Van Nostrand Reinhold, New York, 1969.

25. Vinson, J.R. and Chou T-W, Composite Materials and their use in Structures, Applied Science Publishers, London 1975.

26. Langley, M. (ed.), Carbon Fibres in Engineering, McGraw-Hill, London, 1973.
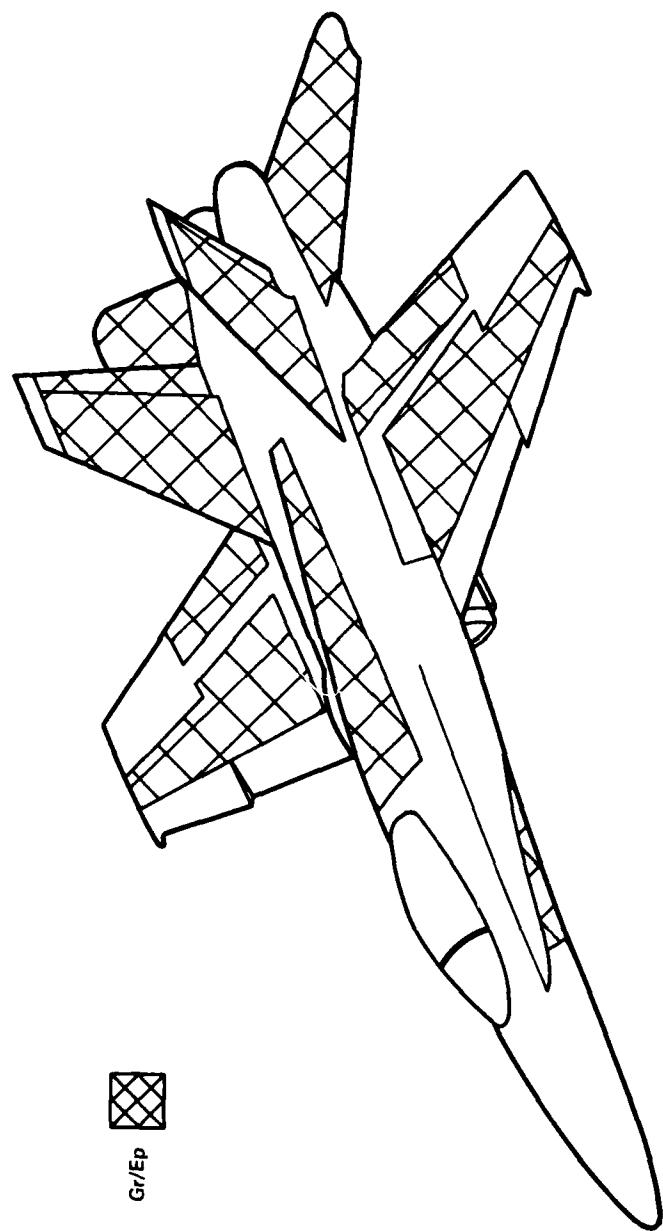
FIG. 1 GRAPHITE/EPOXY APPLICATIONS ON F/A-18

Gr/Ep

9
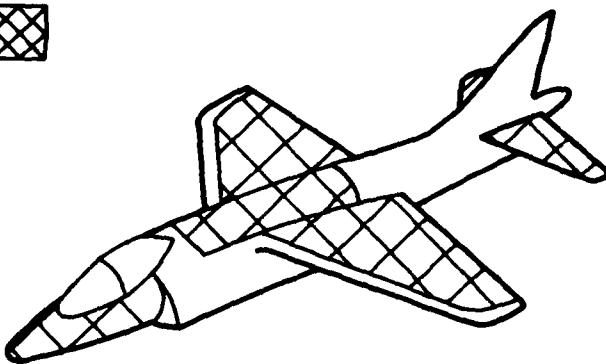
Gr/Ep

FIG. 2 USE OF GRAPHITE/EPOXY IN AV-8B (HARRIER)

Gr/Ep

Hybrid Gr-Aramid/Ep

NLG doors

MLG doors
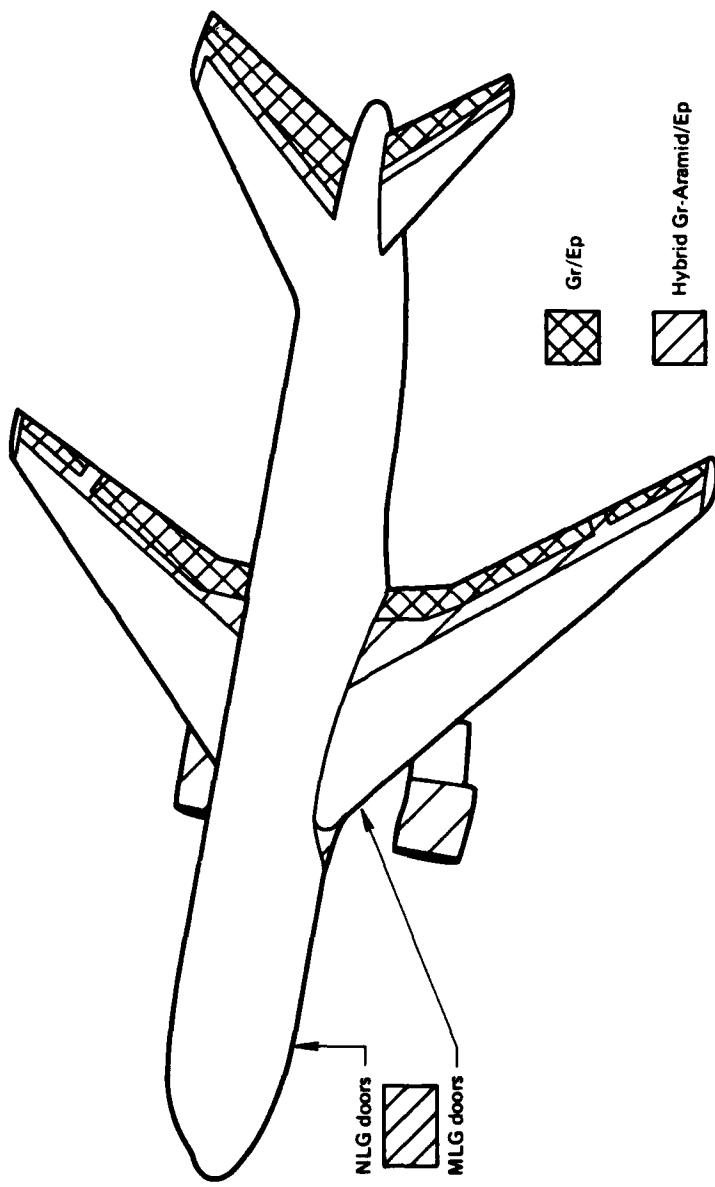
FIG. 3 ADVANCED COMPOSITES IN BOEING 767

11
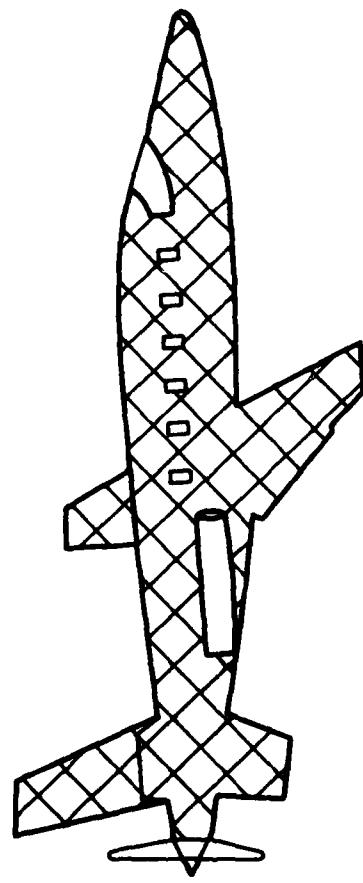
Gr/Ep

FIG. 4 LEAR FAN 2100 "ALL-COMPOSITE" AIRCRAFT

Lecture 2

BASIC PRINCIPLES OF FIBRE COMPOSITE MATERIALS

A.A. BAKER and A.W. RACHINGER

1. GENERAL

   ### 1.1 Introduction to Fibre Composite Systems

   A fibre composite material usually consists of one or more
filamentary phases embedded in a continuous matrix phase. The aspect
ratio (i.e., ratio of length to diameter) of the filaments may vary from
about 10 to infinity (for continuous fibres). Their scale, in relation
to the bulk material, may range from microscopic (e.g., 8 μm) diameter
graphite fibres in an epoxy matrix) to gross macroscopic (e.g., 25mm
diameter steel tendons in concrete). These lectures are concerned mainly
with continuous fibres which have diameters in the microcopic range.

   Composite constituents (fibres and matrices) can be conveniently
classified according to their moduli and ductilities. Within the composite,
the fibres may, in general, be in the form of continuous fibres,
discontinuous fibres or whiskers and may be aligned to varying degrees,
or randomly oriented. In Fig. 1 this classification is illustrated for a
number of common fibres and matrices and several examples of composites
formed from these materials are shown. The systems of particular interest
here are in the brittle fibre/brittle matrix category with the fibres
being very much stiffer and stronger than the matrix. These include aramid/
epoxy, boron/epoxy, glass/epoxy and graphite/epoxy.

   ### 1.2 Micromechanical Versus Macromechanical View of Composites

   Fibre composites can be studied from two points of view: micro-
mechanics and macromechanics. Micromechanical analyses are aimed at
providing an understanding of the behaviour of composites (generally uni-
directional composites) in terms of the properties and interactions of the
fibres and matrix. Approximate models are used to simulate the micro-
structure of the composite and hence predict its "average" properties
(such as strength and stiffness) in terms of the properties and behaviour of
the constituents.

   Advanced composite structures are usually in the form of uni-
directional plies laminated together at various orientations, or filament-
wound configurations. In aircraft applications, the laminated
multi-directional lay-up is certainly the most common, and macromechanics
is used to design, or predict, the behaviour of such structures on the basis
of the "average" properties of the unidirectional material: namely, the
longitudinal modulus (E_1), the transverse modulus (E_2), the major Poisson's
ratio (v_{12}) and the in-plane shear modulus (G_{12}), as well as the
appropriate strength values.

13

Micromechanics is aimed at predicting and understanding these "average" properties in terms of the detailed microscopic behaviour of the material, rather than generating accurate design data; macromechanics draws mainly on the results obtained from physical and mechanical testing of uni-directional composites.

1.3 Micromechanics

As already mentioned, micromechanics utilises microscopic models of composites, in which the fibres and the matrix are separately modelled. In most simple models, the fibres are assumed to be

- homogeneous
- linearly elastic
- isotropic
- regularly spaced
- perfectly aligned
- of uniform length

and the matrix is assumed to be

- homogeneous
- linearly elastic
- isotropic

The fibre/matrix interface is assumed to be perfect, with no voids or disbonds.

More complex models, representing more realistic situations, may include

- voids
- disbonds
- flawed fibres (including statistical variations in flaw severity)
- wavy fibres
- non-uniform fibre dispersions
- fibre length variations

Micromechanics can, itself, be approached from two points of view:

(1) "The mechanics of materials" approach which attempts to predict the behaviour of approximate models of the composite material, and

(2) "The theory of elasticity" approach which is often aimed at producing upper and lower bound solutions, exact solutions for very specific systems, or numerical solutions.

14

A common aim of both of these approaches is to determine the elastic constants and strengths of composites in terms of their constituent properties. As previously stated, the main elastic constants for unidirectional fibre composites are:

E_1 longitudinal modulus (i.e., modulus in fibre direction),

E_2 transverse modulus,

ν_{12} major Poisson's ratio (i.e., ratio of contraction in the transverse direction consequent on an extension in the fibre direction),

G_{12} in-plane shear modulus.

The main strength values required are:

σ_1^u longitudinal strength (both tensile and compressive),

σ_2^u transverse strength (both tensile and compressive),

τ_{12}^u shear strength.

2. THE ELASTIC CONSTANTS

2.1 Mechanics of Materials Approach

The simple model used in the following analyses is a single, uni-directional ply, or "lamina", as depicted in Fig. 2. Note that the representative volume element shown is the full thickness of the single ply, and the simplified "two dimensional" element is used in the following analyses. The key assumptions used in connection with this model are indicated on Fig. 3.

E_1, Longitudinal Modulus:

In Fig. 3(a) is shown the representative volume element under an applied stress, σ_1. The resultant strain, ϵ_1 is assumed to be common to both the fibre and matrix. The stresses felt by the fibre, matrix and the composite are, respectively, σ_f, σ_m and σ_1, and taking E_f and E_m as the fibre and matrix moduli respectively, then

$$\sigma_f = E_f\, \epsilon_1$$
$$\sigma_m = E_m\, \epsilon_1 \qquad\qquad (2.1)$$
$$\sigma_1 = E_1\, \epsilon_1$$

The applied stress acts over a cross-sectional area A, consisting of A_f, the fibre cross-section, and A_m, the matrix cross-section. Since the fibres and matrix are acting in parallel to carry the load:

$$\sigma_1 A = \sigma_f A_f + \sigma_m A_m$$
$$\text{or} \qquad \sigma_1 = \sigma_f V_f + \sigma_m V_m \qquad\qquad (2.2)$$

15

where $V_f = A_f/A$ = fibre volume fraction,

and $V_m = A_m/A = 1 - V_f$ = matrix volume fraction.

Substituting eqns (2.1) into (2.2) gives:

$$E_1 = E_f V_f + E_m V_m. \tag{2.3}$$

Equation (2.3) is a "Rule of Mixtures"-type relationship which relates the composite property to the weighted sum of the constituent properties. Experimental verification of eqn (2.3) has been obtained for many fibre/resin systems; examples of the variation of E_1 with V_f for two glass/polyester resin systems are shown in Fig. 4.

E_2, Transverse Modulus:

As shown in Fig. 3(b), the fibre and matrix are assumed to act in series, both carrying the same applied stress, σ_2. The transverse strains for the fibre, matrix and composite are thus respectively:

$$\begin{aligned} \varepsilon_f &= \sigma_2/E_f \\ \varepsilon_m &= \sigma_2/E_m \\ \varepsilon_2 &= \sigma_2/E_2 \end{aligned} \tag{2.4}$$

Deformations are additive over the width, W, so that,

$$\Delta W = \Delta W_f + \Delta W_m$$

or

$$\varepsilon_2 W = \varepsilon_f (V_f W) + \varepsilon_m (V_m W). \tag{2.5}$$

Substitution of eqns (2.4) into (2.5) yields:

$$1/E_2 = V_f/E_f + V_m/E_m. \tag{2.6}$$

Experimental results are in reasonable agreement with eqn (2.6) as shown, for example, in Fig. 5.

Several interesting features emerge from eqns (2.3) and (2.6). In high performance composites, the fibre moduli are much greater than the resin moduli, so, in the typical fibre volume fraction range of 50 to 60%, the matrix has only a small effect upon E_1 whilst the fibres have only a

small effect on E_2. In other words:

$$E_1 \approx E_f V_f,$$
$$E_2 \approx E_m / V_m.$$

ν_{12}, Major Poisson's Ratio:

The major Poisson's ratio is defined by:

$$\nu_{12} = -\epsilon_2 / \epsilon_1 \qquad\qquad (2.7)$$

where the only applied stress is σ_1 (Fig. 3(c)).

The transverse deformation is given by:

$$\Delta W = \Delta W_f + \Delta W_m$$

or,

$$\epsilon_2 W = -\nu_f \epsilon_1 (V_f W) - \nu_m \epsilon_1 (V_m W), \qquad\qquad (2.8)$$

since the fibres and matrix have equal strains in the longitudinal direction and, in general,

$$\nu = -\epsilon_2 / \epsilon_1$$

Substitution of eqn (2.7) into eqn (2.8) for ϵ_2 gives the result:

$$\nu_{12} = \nu_f V_f + \nu_m V_m$$

which is another "Rule of Mixtures" expression.

G_{12}, In-Plane Shear Modulus:

The applied shear stresses and resultant deformations of the representative volume element are shown in Fig. 3(d). The shear stresses felt by the fibre and matrix are assumed equal and the composite is assumed to behave linearly in shear (which is, in fact, not true for many systems).

The total shear deformation is given by:

$$\Delta = \gamma W$$

where γ is the shear strain of the composite. The deformation, Δ, consists of two additive components so that

$$\Delta = \Delta_f + \Delta_m$$
$$= \gamma_f(V_f W) + \gamma_m(V_m W) \qquad (2.9)$$

Since equal shear stresses are assumed:

$$\gamma_f = \tau/G_f$$
$$\gamma_m = \tau/G_m \qquad (2.10)$$
$$\gamma = \tau/G_{12}$$

Substitution of eqns (2.10) into eqn (2.9) yields

$$1/G_{12} = V_f/G_f + V_m/G_m$$

Since G_m is very much smaller than G_f, the value of G_m has the major effect on G_{12} for typical 50-60% V_f values; the situation is analogous to that for the transverse modulus E_2.

2.2 Refinements to Mechanics of Materials Approach for E_1 and E_2

Prediction of E_1:

Equation (2.3) is considered to provide a good estimate of the longitudinal modulus, E_1. However, it does not allow for the triaxial stress condition in the matrix resulting from the constraint caused by the fibres. Ekvall (3) has produced a modified version of the equation to allow for this effect:

$$E_1 = E_f V_f + E_m' V_m$$

where

$$E_m' = E_m/(1 - 2v_m^2)$$

and v_m is Poisson's ratio for the matrix material. However, the modification is not large for values of v_m of approximately 0.3.

Prediction of E_2:

Equation (2.6) is considered to provide only an approximate estimate of the transverse modulus, E_2. This is because, for loading in the transverse direction, biaxial effects resulting from differences in contraction in the

18

longitudinal (fibre) direction between the fibre and the matrix become significant. The contraction difference arises because the two phases experience different strains and is even more marked if there is a difference in their Poisson's ratios.

The modified version of equation (2.6) produced by Ekvall (3) is

$$\frac{1}{E_2} = \frac{V_f}{E_f} + \frac{V_m}{E_m} - \frac{V_f}{E_f} \frac{[(E_f \nu_m / E_m) - \nu_f]^2}{[(V_f E_f / V_m E_m) + 1]}$$

2.3 Theory of Elasticity Approach to the Elastic Constants

The theory of elasticity approach to the determination of the elastic constants for composites is based on a wide variety of models and energy-balance treatments. A detailed discussion of these approaches is beyond the scope of this lecture; however some aspects are outlined below.

Energy Approach:

Bounding (or variational) derivations use energy balance considerations to produce upper and lower bounds on the elastic constants. The usefulness of the results, of course, depends upon the closeness of the bounds, as demonstrated in the following example.

Considering the stressed element shown in Fig. 3(a), it can be shown (4) that the lower bound on the longitudinal modulus, E_1, is given by:

$$1/E_1 \leq V_m/E_m + V_f/E_f \qquad \text{(compare with eqn (2.6))}$$

while the upper bound is given by:

$$E_1 \leq \frac{1 - \nu_f - 4\nu_f \nu_{12} + 2\nu_{12}^2}{1 - \nu_f - \nu_f^2} E_f V_f + \frac{1 - \nu_m - 4\nu_m \nu_{12} + 2\nu_{12}^2}{1 - \nu_m - 2\nu_m^2} E_m V_m$$

where

$$\nu_{12} = \frac{(1 - \nu_m - 2\nu_m^2) \nu_f E_f V_f + (1 - \nu_f - 2\nu_f^2) \nu_m E_m V_m}{(1 - \nu_m - 2\nu_m^2) E_f V_f + (1 - \nu_f - 2\nu_f^2) E_m V_m}$$

It is of interest to note that if $\nu_{12} = \nu_f = \nu_m$, the upper bound solution becomes:

$$E_1 \leq E_f V_f + E_m V_m \qquad ,$$

19

the same result as eqn (2.3), which implies an equality of ν_f and ν_m in the mechanics of materials approach.

In this example, the bounding solutions are not very useful because the bounds are too far apart, the lower bound being the transverse modulus as predicted by the mechanics of materials approach.

Direct Approaches:

Here, various representative models of elastic inclusions in an elastic matrix are employed to obtain exact solutions for the stiffness properties. Typical volume elements assumed for a hexagonal and a square fibre distribution are shown in Fig. 6. In many cases the solutions are highly complex and of limited practical use. Regular fibre distributions do not occur in practical composites. Rather, the array is random and the analysis for regular arrays must be modified to allow for the extent of contact between fibres; this is called the "degree of contiguity" (ref. 5) and is measured by a coefficient, c, which can vary from c = 0 for isolated fibres to c = 1 for contacting fibres. This situation is illustrated in Fig. 7. The effective value of c may be determined experimentally. The degree of contiguity has more effect on E_2 and G_{12} than on E_1. These matters, and other simplifying approaches, such as the Halpin-Tsai equations, are discussed more fully in ref. 1.

3. MECHANICS OF MATERIALS APPROACH TO STRENGTH

3.1 Simple Estimate of Tensile Strength

The simplest analysis of longitudinal tensile strength assumes that all fibres break at the same stress level, at the same time, and in the same plane. Although this assumption is grossly unrealistic, it provides a starting point for further analysis.

As with the model used to determine E_1, the fibres and matrix are assumed to carry equal strains. In advanced epoxy-matrix composites, the strain to failure capability of the stiff fibres, ε_f^u, is markedly less than that of the matrix, ε_m^u, as shown in Fig. 8(a). The fibres will thus fail first, and the total load will be transferred to the matrix. Two composite failure modes can be envisaged depending on the fibre volume fraction, V_f. At high V_f, the matrix alone is not capable of bearing the full load, and fractures immediately after fibre fracture. The composite strength is thus given by:

$$\sigma_1^u = \sigma_f^u V_f + \sigma_m' V_m$$

where σ_m' is defined in Fig. 8(a) as the stress carried by the matrix material at the fibre breaking strain. At low V_f, there is enough matrix material to carry the full load after the fibres fracture and the composite strength is then given by:

$$\sigma_1^u = \sigma_m^u V_m$$

σ_1^u is plotted as a function of V_f in Fig. 8(b) and it can be readily seen that the value of V_f corresponding to a change in failure mode is given by:

$$V_f' = (\sigma_m^u - \sigma_m') / (\sigma_f^u + \sigma_m^u - \sigma_m')$$

Note also that there is a minimum volume fraction, V_{min}, below which composite strength is actually less than the inherent matrix strength:

$$V_{min} = (\sigma_m^u - \sigma_m') / (\sigma_f^u - \sigma_m')$$

For high strength, high modulus, fibres in relatively weak, low modulus, epoxy matrices, σ_m', V_f' and V_{min} will be quite small.

Analogous treatments can be applied to systems in which the matrix fails first, but obviously the physical characteristics of the fracture modes will be quite different.

3.2 Statistical Analysis of Tensile Strength

General:

The foregoing analysis of tensile strength assumed simultaneous fracture of equal strength fibres in one plane. In reality, the situation is much more complex, because of the brittle (flaw-sensitive) nature of the fibres and the fibre/matrix interaction. These two features are discussed below.

Brittle fibres contain surface flaws or imperfections which produce "weak spots" along the fibre length. Fibre fractures will occur at these flaws at more or less random positions throughout the composite. Therefore, fracture will not occur in a single plane. In the most simple case in which the imperfect fibres all have the same strength, and the matrix is unable to grip the broken fibres, the strength of the composite would be as calculated in Section 3.1.

For brittle fibres, however, flaws vary not only in position, but also in severity. In Fig. 9 is shown the way in which fibre strength varies as a result of this variation in flaw severity and the markedly different characteristics of non-flaw-sensitive fibres (such as ductile metals). It would therefore be expected that fibre fractures would occur throughout a range of stress levels, up to ultimate composite failure. This is indeed the case, as shown in Fig. 10.

Another important characteristic of composite fracture is the fibre/matrix interaction in the vicinity of a fibre fracture. Rather than becoming ineffective, a broken fibre can still contribute to composite strength because the matrix is able to transfer stress back into the fibre

21

from the broken end, as shown in Fig. 11. High shear stresses are developed in the matrix and these decay away a short distance from the break, while at the same time the tensile stress carried by the fibre increases from zero at the broken end, to the full stress carried by unbroken fibres. The characteristic length over which this stress build-up occurs is known as the ineffective length, δ (Fig. 11).* The ineffective length can be determined experimentally by measuring the stress required to pull fibres of various lengths from a matrix (2).

If the fibre/matrix bond strength is low, the high shear stresses will cause fibre/matrix debonding, as shown in Fig. 12(a). It is also possible that the stress elevation felt by fibres adjacent to the fractured fibre (Fig. 11) is sufficient to cause further fibre fractures, and crack propagation through the matrix in the brittle fashion shown in Fig. 12(b). In addition to the stress concentration felt by fibres resulting from the ineffectiveness of adjacent fractured fibres near the broken ends, there is also a stress concentration associated with the crack in the matrix surrounding the fibre fracture. This latter aspect will be discussed in Section 4.

If fibre/matrix debonding, crack propagation and fibre fracture propagation are not dominant failure mechanisms, the composite will accumulate damage under increasing stress, and failure will occur by the cumulative damage mechanism outlined below, and shown in Fig. 12(c).

Rosen's Model of Cumulative Damage:

The strength of individual fibres is dependent on the probability of finding a flaw, and therefore on the fibre length. It has been shown that the strength/length relationship takes the form of a Weibull distribution of the form:

$$f(\sigma) = L\ \alpha\ \beta\ \sigma^{\beta-1}\ \exp(-L\ \alpha\ \sigma^{\beta})$$

where $f(\sigma)$ is the probability density function for fibre strength,
$\quad$ L $\quad$ is fibre length,
$\quad$ α, β are material constants.

The constant α determines the position of the Weibull distribution, while the constant β determines its shape. Both α and β are experimentally accessible quantities and can be determined, for example, from a log-log plot of mean fibre strength for fibres of given lengths versus fibre length.

Daniels (6) showed that the strength of a bundle of N fibres having such a Weibull distribution can be described by a normal distribution where mean value, $\bar{\sigma}_{BL}$, is a function of fibre length:

$$\bar{\sigma}_{BL} = (L\ \alpha\ \beta)^{-1/\beta}\ \exp(-1/\beta)$$

----
* Often, the term "critical transfer length" is used in this context; the critical transfer length being twice the ineffective length.

and whose standard deviation is proportional to $N^{-\frac{1}{2}}$. Thus for very large N, all bundles tend toward the same strength value, $\bar{\sigma}_{BL}$. (In the other words, the strength distribution function tends towards the "unique strength distribution" shown in Fig. 9(b).)

Rosen models the composite as a chain of bundles (Fig. 13), the length of each bundle (or chain link) being the ineffective length δ. For very large N, the strength of each bundle or chain link will be the same and the strength of the whole chain (or composite) will be equal to the link strength which is given by:

$$\bar{\sigma}_{B\delta} = (\delta \ \alpha \ \beta)^{-1/\beta} \ \exp(-1/\beta)$$

Thus it is possible to compare the strengths of a bundle of "dry" fibres of length L and a composite with ineffective length δ as follows:

$$\bar{\sigma}_{B\delta}/\bar{\sigma}_{BL} = (L/\delta)^{1/\beta}$$

For glass fibres in an epoxy matrix $\beta \cong 10$, $\delta \cong 10^{-3}$ mm (about a fibre diameter), so if L = 100 mm then

$$\bar{\sigma}_{B\delta}/\bar{\sigma}_{BL} = (100/10^{-3})^{1/10} = 10^{\frac{1}{2}} \sim 3$$

This is thus the strengthening obtained by composite action.

3.3 Mechanics of Materials Approach to Compressive Strength

The previously introduced equations relating to tensile failure do not apply to compressive strength because fibres do not fail in simple compression. Rather, they fail by local buckling. This behaviour is very complicated since it is dependent on the presence of residual stresses in the matrix caused by different fibre and matrix expansion coefficients. It has been shown, for example, that glass fibres in an epoxy matrix will buckle after cool down from the resin cure temperature. As may be expected, by assuming that the fibres act as circular columns on an elastic foundation, the wavelength of the buckling increases with fibre diameter.

Two pure buckling modes can be envisaged (Fig. 14): (i) the extensional mode, in which the matrix is stretched and compressed in an out-of-phase manner, or (ii) the shear mode in which the fibres buckle in phase and the matrix is sheared. The most likely mode is that producing the lowest energy in the system. While mixed modes are possible they would require more energy than either of the pure modes.

The analysis of buckling is based on the energy method in which the change in strain energy of the fibres ΔU_f and of the matrix ΔU_m, as the composite changes from the compressed but unbuckled state to the buckled state, is equated to the work done ΔW, by the external loads:

$$\Delta U_f + \Delta U_m = \Delta W$$

In the model, the composite is considered two-dimensional, the fibres are treated as plates normal to the plane of Fig. 15 (rather than rods) and the buckling pattern is assumed to be sinusoidal. The resulting buckling stress for the extensional mode is:

$$\sigma_{cmax} = 2V_f \{ (V_f E_m E_f)/3(1-V_f) \}^{\frac{1}{2}}$$

and for the shear mode:

$$\sigma_{cmax} = G_m/(1-V_f)$$

As V_f tends to zero, σ_{cmax} for the extensional mode tends to zero but as V_f tends to unity, σ_{cmax} for the extensional mode becomes very large compared with σ_{cmax} for the shear mode so the extensional mode would be expected to apply for only small V_f. From Ref. 2, assuming $E_f \gg E_m$ and $\nu_m = 1/3$, with $G_m = E_m/2(1+\nu_m)$, then the transition occurs at $(E_m/10E_f)^{1/3}$, or at $V_f = 10\%$ for $E_f/E_m = 100$, and at $V_f = 22\%$ for $E_f/E_m = 10$. It has been found that these equations tend to over-predict considerably the compressive strength.

One exception is boron/epoxy, whose actual compressive strength is only about 63% lower than that predicted. The problem, generally, is that the predicted failure strains are much higher than the matrix yield strain (e.g. 5% in the case of glass/epoxy). As an approximation to the inelastic behaviour, the theory was expanded in Ref. (7) using a gradually reducing matrix shear modulus. This gives more reasonable agreement with experimental results.

A very simple approach which appears to predict the experimental behaviour in some cases is obtained by assuming failure occurs when the matrix reaches its yield stress, σ_m^y. Thus, at failure

$$\sigma_{cmax} = \sigma_f V_f + \sigma_m^y V_m$$

where the fibre stress, σ_f, is given by strain compatibility as

$$\sigma_f = \sigma_m^y E_f/E_m = \epsilon_m^y E_f$$

Taking ϵ_m^y for an epoxy resin as 0.02 and E_f = 70 GPa for glass fibres,

then σ_f = 0.02 X 70 GPa = 1.4 GPa,

and so $\sigma_c^u = \sigma_f V_f$ = 1.4 X 0.6 = 0.84 GPa (ignoring the small contribution from the matrix).

This result is in reasonable agreement with typically observed values.

3.4 Off-Axis Strength in Tension

The failure of an oriented, but still unidirectional composite can be envisaged as occurring in any of three modes:

(i) Failure normal to the fibres (as occurs with straight tension in the fibre direction),

(ii) Failure parallel to the fibres by matrix rupture or fibre/matrix interface tensile failure,

(iii) Failure by shear of the matrix or fibre/matrix interface.

If the fibres make an angle ϕ with the direction of applied tensile stress σ, then, as shown in Fig. 16, the stresses can be resolved as follows:

Tensile stress parallel to fibres $\sigma_1 = \sigma \cos^2 \phi$

Tensile stress normal to fibres $\sigma_2 = \sigma \sin^2 \phi$

Shear stress parallel to fibres $\tau_{12} = \frac{1}{2} \sigma \sin 2\phi$

If σ_1^u, σ_2^u and τ^u represent the composite strengths in direct tension ($\phi = 0°$), transverse tension ($\phi = 90°$) and shear ($\phi = 45°$) respectively, then the failure stress, σ, for each mode can be expressed as follows:

Mode (i) $\sigma = \sigma_1^u/\cos^2 \phi$

Mode (ii) $\sigma = \sigma_2^u/\sin^2 \phi$

Mode (iii) $\sigma = 2\tau^u/\sin 2 \phi$

Thus the failure mode changes with ϕ as shown in Fig. 17. Although these results are obeyed quite well for many systems (Fig. 17) and observed fracture modes are as predicted, the interaction of stresses and the occurrence of mixed-mode fractures are not accounted for. Reference (2) presents a more detailed analysis which does account for complex stress states.

Fig. 17 shows that strength falls rapidly with increasing ϕ. However, if plies are placed at $+\phi$ and $-\phi$ the rate of fall off is very much less, even to values of ϕ as high as 30°.

4. FRACTURE TOUGHNESS

4.1 Fracture Surface Energy

A measure of the toughness, or resistance of a material to crack propagation, is its fracture surface energy (γ). This is defined as the minimum amount of energy required to create unit area of free surface, and is usually given in units of KJ/m². Since two free surfaces are produced, R (for crack resistance), equal to 2γ, is the term often employed in fracture calculations.

It is a matter of considerable importance that for crack propagation normal to the fibres, (Fig.18(a))the fracture energy of a composite consisting of brittle fibres in a brittle matrix is usually very much greater than is predicted by a simple rule of mixtures relationship. In general $R_1 >> V_f R_f + V_m R_m$. For example, in the case of a typical graphite/epoxy composite $R_m \approx 1$ KJ/m² for the bulk epoxy resin and $R_f \approx 0.1$ KJ/m² for the graphite material. However, the fracture surface energy of a unidirectional composite, R_C (if the crack is made to propagate normal to the fibres) is typically 25 to 50 KJ/m².

In contrast, for crack propagation parallel to the fibres (Fig. 18(b)) the fracture surface energy R_2 is of the order of R_m if the crack propagates solely through the matrix; however, R_m may be lower if the crack propagates, partially, through the weaker fibre/matrix interface. Because $R_2 << R_1$ crack propagation parallel to the fibres, or splitting (Fig. 18(c)), may occur even when the starting crack is normal to the fibres. This important matter will be discussed more fully later.

Contributions to the Fracture Energy:

Considering crack propagation normal to the fibres (Fig. 18(a)), the total work of fracture can be attributed to a number of sources as shown in Fig. 19 and Table 1, below, taken from Ref. 8. In the case of the brittle fibre/brittle matrix composite (Fig. 19(a)),crack growth proceeds by pulling fibres out of the matrix behind the crack front, and fracturing fibres ahead of the crack tip. Energy is absorbed during pull out if the shear stress at the fibre-matrix interface is maintained whilst the fracture surface is separating. If the fibre-matrix interface is relatively weak, local stresses will cause the fibres to be debonded from the matrix, with a resultant loss of stored strain energy. Stored strain energy is also lost by stress relaxation over the transfer length when the fibre fractures. Finally, strain energy is also lost from the fibre by crack-bridging if the fibre spans the opening crack prior to fracture.

If the matrix is ductile, as in a metal matrix composite, energy is also absorbed by matrix plastic deformation. This situation is illustrated in Fig.19(b) for the case where the fibre is very strongly bonded to the matrix so that little fibre pull out occurs.

TABLE 1: Fracture Mechanisms

MODEL	γ
Pull-out (short fibres of length L)	$\dfrac{V_f \, \sigma_f^u \, \delta^2}{3L}$ (L > 2δ)
	$\dfrac{V_f \, \sigma_f^u \, L^2}{24\delta}$ (L < 2δ)
Debonding	$\dfrac{V_f \, \sigma_f^{u2} \, y}{4E_f}$
Stress-relaxation	$< \dfrac{V_f \, \sigma_f^{u2} \, \delta}{3E_f}$
Crack-bridging	$\dfrac{2V_f \, r \, \sigma_f^{u*}}{\tau_i \, E_f} \times \dfrac{(1-\nu_f)(1-2\nu_f)}{12(1-\nu_f)}$
Matrix plastic deformation	$\dfrac{(1-V_f)^2}{V_f} \times \dfrac{\sigma_m^u \, r}{\tau_m} \times U$

The notation in Table 1 is:

y debonded length of fibre

r fibre radius

τ_i shear strength of interface

τ_m shear strength of matrix

U work to fracture unit volume of matrix

*δ ineffective length (= $\frac{1}{2} \sigma_f^u \, r/\tau_i$)

The work of fracture contribution for pull-out refers to short constant-strength fibres. The expression would have to be modified for a statistical flaw distribution in continuous fibres. The contribution due to creation of new surface of fibres and matrix can be ignored in brittle systems, as too can contributions from matrix yield.

4.2 Fracture Mechanics

The energetic requirement for crack propagation is that the energy release rate (equal to the "fixed grips" strain energy release rate) G must equal the fracture surface energy R. At the critical condition,

$$G = G_c = R$$

In many cases it is more convenient to work in terms of the stress intensity factor K. For an isotropic material in the crack opening mode K_I is related to G through Irwin's equation: $K_I^2 = EG$ and $K_{Ic}^2 = EG$ at failure.

In the simple case of a small centre crack in a sheet under tension

$$K_I = \sigma(\pi a)^{\frac{1}{2}}$$

where σ is the applied stress and 2a the crack length. Thus, the stress σ_f at failure is given by

$$\sigma_f = \left(\frac{ER}{\pi a}\right)^{\frac{1}{2}} ,$$

which is the familiar Griffith equation.

A relationship between G and K can also be obtained for a fibre composite material by modelling it as a continuous linear orthotropic material with the crack propagating on one of the planes of symmetry. Using the analysis for such materials given in ref. (9),

$$G = K_I^2 \left(\frac{a_{11}\, a_{22}}{2}\right)^{\frac{1}{2}} \left[\left(\frac{a_{22}}{a_{11}}\right)^{\frac{1}{2}} + \left(\frac{a_{66} + 2a_{12}}{2a_{11}}\right)\right]^{\frac{1}{2}}$$

The factor involving the "a" terms can be considered as the reciprocal of the effective modulus (E') of the composite. For the simple case illustrated in Fig. 18(a)*, assuming the load is in the 2-direction,

$$a_{22} = \frac{1}{E_{11}} \qquad a_{11} = \frac{1}{E_{22}}$$

$$a_{66} = \frac{1}{G_{12}} \qquad a_{12} = -\nu_{12}/E_{11} = -\nu_{21}/E_{22}$$

----

* Note that in this treatment the "1" and "2" axes are interchanged, which
   is not consistent with standard notation for composites; it appears,
   however, to be conventional in fracture mechanics treatment of this type.

Taking, as values typical of a graphite/epoxy composite, $E_{11} = 140$ GPa, $E_{22} = 12$ GPa, $G_{12} = 6$ GPa, $\nu_{12} = 0.25$ and $\nu_{21} = 0.0213$, then $E' \approx 0.4E_{11}$. If, alternatively, the crack is considered to lie parallel to the fibres (Fig. 18(b)) then $E' \approx 2E_{22}$.

As long as crack propagation occurs on a plane of symmetry, the relationship between K_I, σ and a for the linear orthotropic material remains the same as that for the isotropic material. Thus, referring back to the unidirectional composite, it can be seen that for a given crack length, a, and normal stress, σ, a crack parallel to the fibres produces a larger G than one normal to the fibres. This results from the lower compliance of the composite when stressed in the fibre direction.

In the fibre composite material the orientation dependence of R must also be taken into consideration. In general, a composite is notch sensitive to cracks running parallel to the fibres (Fig. 18(b)) and the fracture mechanics principles described above may be directly employed. However, the composite may not be notch sensitive in the situation shown in Fig. 18(a). In some cases (2), the composite may become notch sensitive when $a \gg \delta$, the ineffective length, since the strain concentration in the matrix may then lead to fibre fractures at the crack tip. The crack would then become more effective with increasing a, as required in fracture mechanics considerations. However, in other cases gross failure of the fibre/matrix interface may occur resulting in the splitting mode of failure illustrated in Fig. 18(c). This situation, which occurs in more weakly bonded composites, results in complete notch-insensitivity (failure at the net section strength.) Both of these situations are illustrated in some experimental work on graphite/epoxy composites in Fig. 20, taken from ref. (8).

The conditions for crack turning or splitting can be approached from energy considerations (10). For the cracking illustrated in Fig. 18(c) to occur in a unidirectional composite, it is necessary that

$$\frac{G_1}{G_2} < \frac{R_1}{R_2}$$

where G_1 is the energy release rate for self-similar propagation and G_2 is the release rate for splitting. Typically, for graphite/epoxy R_1/R_2 is in the range 25 to 50 and G_1/G_2 is about 20 so splitting is generally predicted.

As mentioned earlier, most advanced composite structures are made up of laminates in the form of unidirectional plies laminated together at various orientations. The fracture behaviour of these materials is considered in Lecture 10. However, it is worth mentioning here that a similar approach to that just described can be taken for this highly complex situation (11). The direction of crack growth is based on the R_1/R_2 ratio for each ply, and the G_1/G_2 ratio for the laminate. The energy release rates are calculated by finite element procedures and recalculated after each increment of crack growth until the point of catastrophic failure.

REFERENCES

1. Jones, R.M., *Mechanics of Composite Materials*, McGraw-Hill, New York, 1975.

2. Kelly, A., *Strong Solids*, Oxford University Press, 1973.

3. Ekvall, J.C., Structural Behaviour of Monofilament Composites, Proc. AIAA, 6th Structures and Materials Conf., AIAA, New York, April 1965.

4. Fung, Y.C., Foundations of Solid Mechanics, Englewood Cliffs, N.J., Prentice-Hall, Inc., 1965.

5. Tsai, S.W., *Structural Behaviour of Composite Materials*, NASA CR-71, July 1964.

6. Daniels, H.E., The Statistical Theory of the Strength of Bundles of *Threads I*, Proc. R. Soc. A183, 405, 1945.

7. Dow, Norris F. and Rosen, W.B., Evaluations of Filament-Reinforced Composites for Aerospace Structural Applications, NASA CR-207, April 1965.

8. Philips, D.C. and Tetelman, A.S., The Fracture Toughness of Fibre Composites, *Composites*, pp. 216-223, September 1972.

9. Sih, G., Paris,P.C. and Irwin, G.R., On Cracks in Rectilinearly Anisotropic Bodies, *International Journal of Fracture Mechanics*, vol. 1, p. 189, 1965.

10. Harrison, N.L., Splitting of Fibre-Reinforced Materials, *Fibre Science and Technology*, vol. 6, p. 25, 1973.

11. Griffith, W.I., Kanninen, M.F. and Rybicki, E.F., A Fracture Mechanics Approach to the Analysis of Graphite/Epoxy Laminated Precracked Tension Panels, ASTM Special Technical Publication 696, 1979.

COMPOSITE

Aligned / Random → Chopped → CONTINUOUS / UNIDIRECTIONAL — Woven / Wound / Laminated

Whiskers

GRAPHITE/EPOXY
BORON/EPOXY
ARAMID/EPOXY
GLASS/EPOXY

Boron/Aluminium
Tungsten/superalloy
Graphite/Carbon
Glass/Polyester
Graphite/Glass
Glass/Nylon
Steel/Concrete
Polyester/Rubber (tyres)
Hair/plaster
Nylon/Polyethylene (hose)
SiC whiskers/aluminium

MATRICES

High E
 Brittle
 carbon
 glass
 ceramic
 cement
 Ductile
 tungsten
 iron
 copper
 aluminium

LOW E
 BRITTLE
 epoxy
 polyester
 phenolic
 rubber
 Ductile
 polysulphone
 polypropylene

FIBRES

HIGH E
 BRITTLE
 graphite
 boron
 glass
 aramid
 FP (alumina)
 Ductile
 tungsten
 steel

Low E
 Brittle
 cotton
 hair
 Ductile
 nylon

FIG 1   CLASSIFICATION OF COMPOSITES ACCORDING TO FIBRE & MATRIX PROPERTIES

31
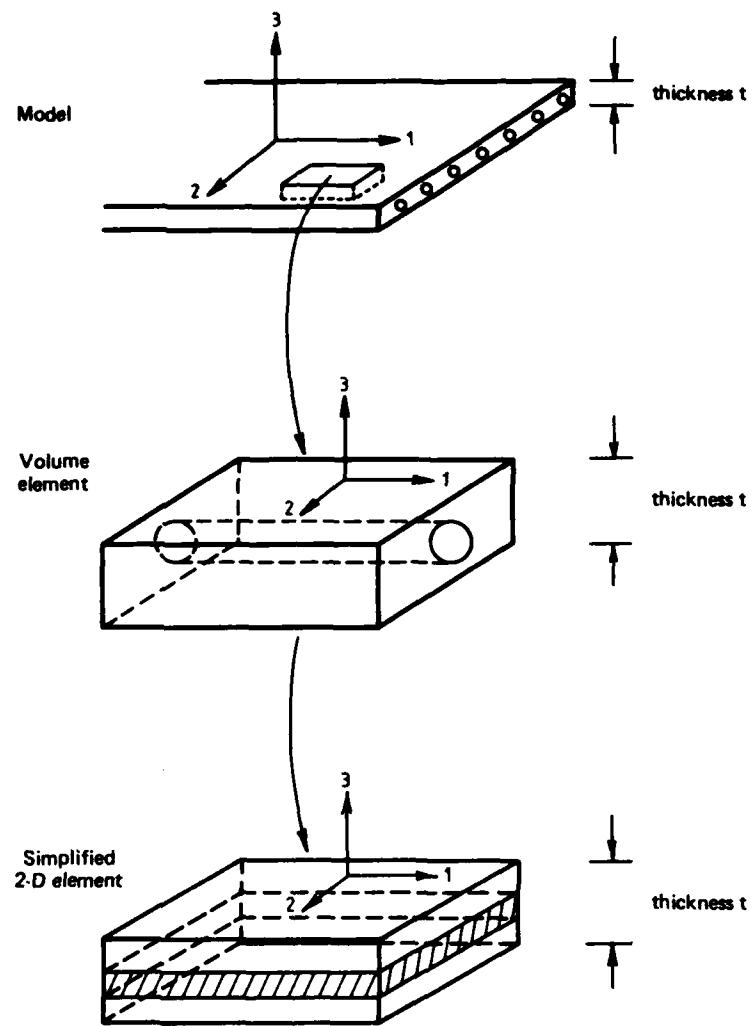
FIG 2   MODEL AND REPRESENTATIVE VOLUME ELEMENT OF A SINGLE,
UNIDIRECTIONAL PLY

32
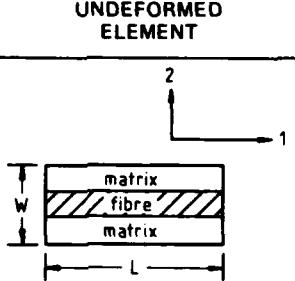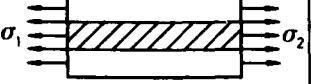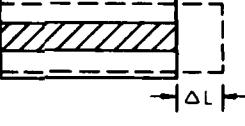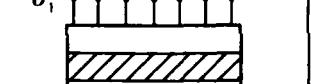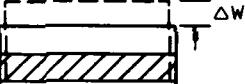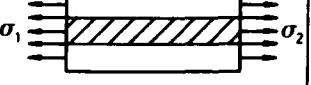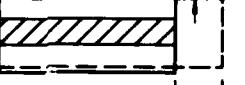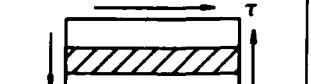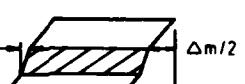
	UNDEFORMED ELEMENT	
	2 ← 1 matrix / fibre / matrix W, L	
APPLIED STRESSES	**DEFORMATIONS**	**ASSUMPTIONS**
σ_1 ← → σ_2 a. Determination of E_1	ΔL	$\epsilon_1 = \epsilon_{1f} = \epsilon_{1m}$ $v_f = v_m$
σ_1 ↑ σ_2 ↓ b. Determination of E_2	ΔW	$\sigma_2 = \sigma_{2f} = \sigma_{2m}$
σ_1 ← → σ_2 c. Determination of v_{12}	$\Delta W/2$ ΔL	$\epsilon_1 = \epsilon_{1f} = \epsilon_{1m}$
τ d. Determination of G_{12}	Δf $\Delta m/2$ Δ	$\tau = \tau_f = \tau_m$ Linear shear behavior

FIG 3   MODELS FOR THE DETERMINATION OF ELASTIC CONSTANTS BY THE "MECHANICS OF MATERIALS APPROACH"
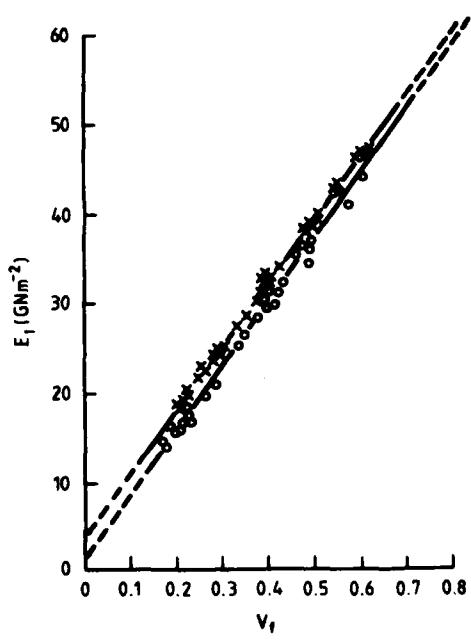
FIG 4   E$_1$ VERSUS V$_f$ FOR TWO GLASS/POLYESTER SYSTEMS

34
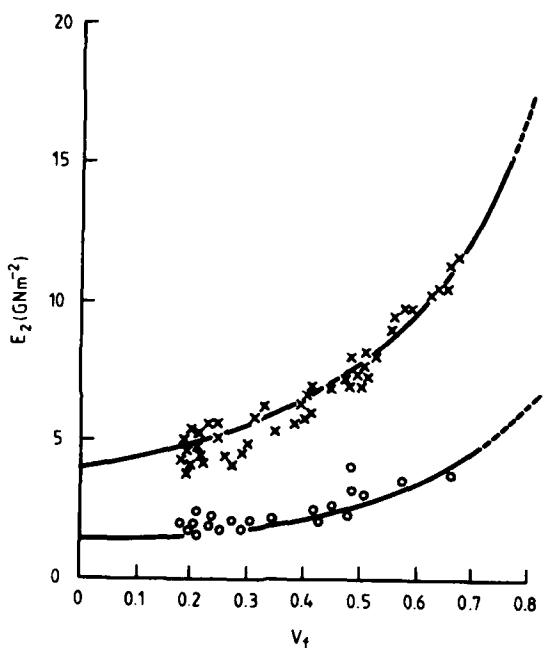
FIG 5   E$_2$ VERSUS V$_f$ FOR TWO GLASS/POLYESTER SYSTEMS

35
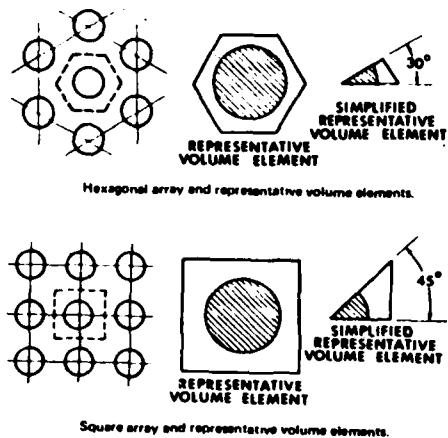
FIG. 6   TYPICAL MODELS OF COMPOSITES FOR EXACT ELASTICITY SOLUTIONS
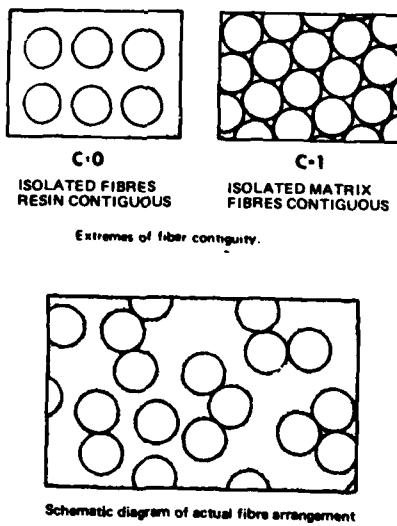
**FIG. 7   THE CONCEPT OF CONTIGUITY USED FOR SEMI-EMPIRICAL
ELASTICITY SOLUTIONS**

36

(a)

Stress

σ_f^u — Fibre

σ_m^u
σ_m' — Matrix

ϵ_f^u ϵ_m^u

Strain

(b)

Stress

$\sigma_1^u = \sigma_f^u V_f + \sigma_m' V_m$

σ_m^u

$\sigma_1^u = \sigma_m^u V_m$

σ_f^u

0   V_f' V_{min} $V_f \longrightarrow$ 1.0

Fibre volume fraction
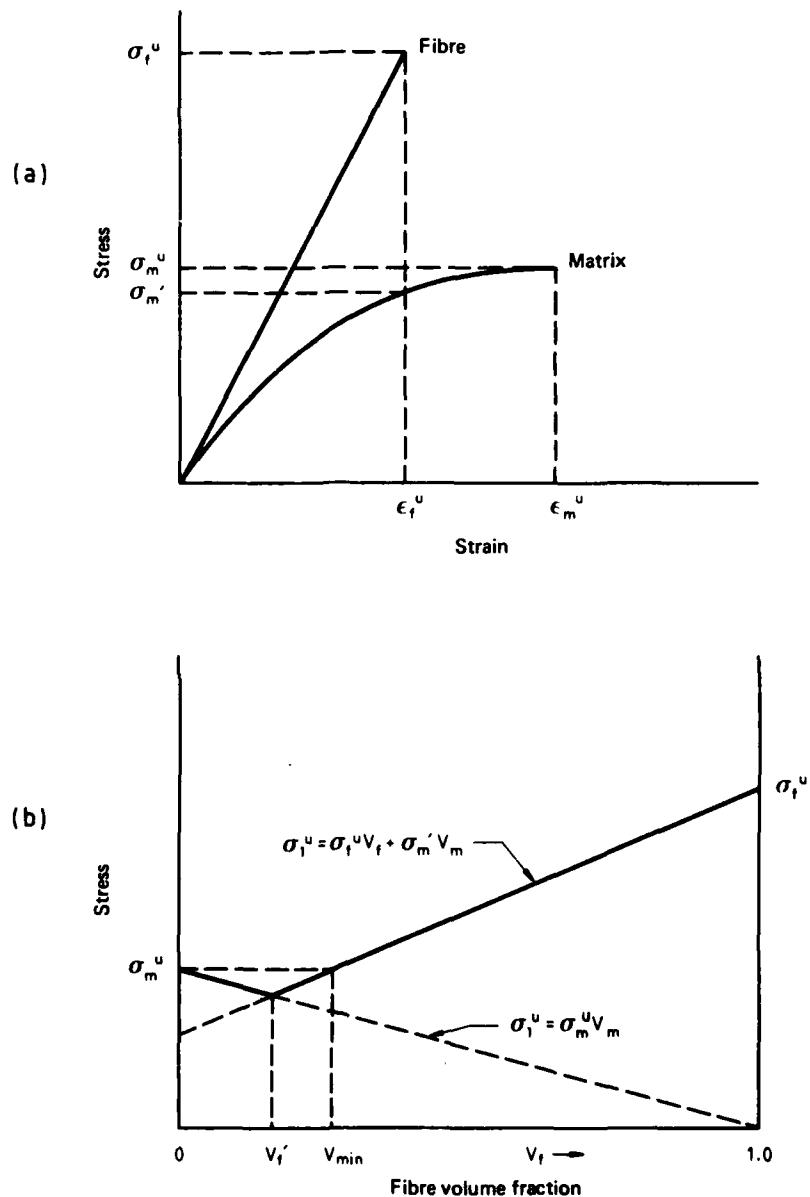
FIG 8   RULE OF MIXTURES PREDICTION OF σ_1^u for $\epsilon_f^u < \epsilon_m^u$

37

f(σ)

$\delta(\sigma_o)$

f(σ)

σ

σ_o σ

a VARIABLE STRENGTH
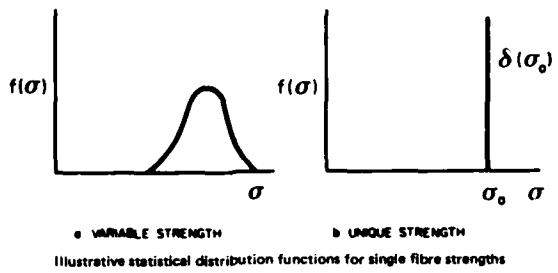
b UNIQUE STRENGTH

Illustrative statistical distribution functions for single fibre strengths

Graphite fibres
Type 2.11R
50 mm length
125 results

10 12 14 16 18 20 22 24 26 28 30 32 34 36 38 40 42

Fibre strength MN/m^2 x 10^{-2}
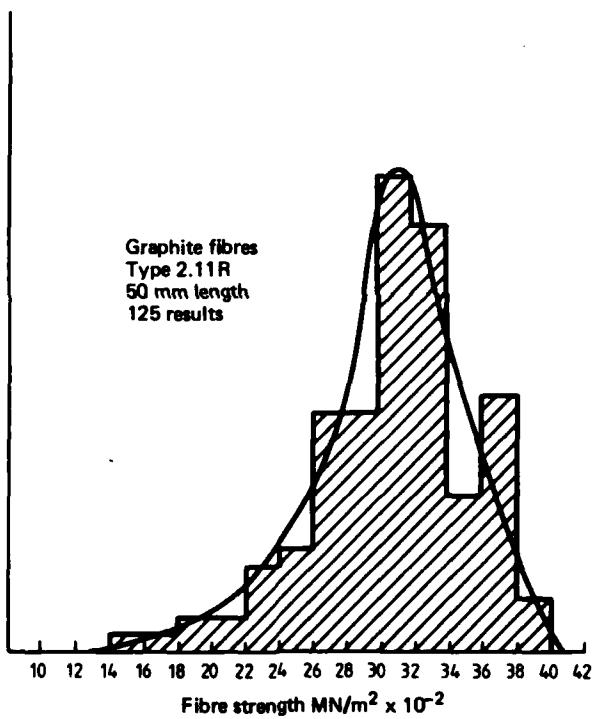
FIG. 9 COMPARISON OF VARIABLE AND UNIQUE STRENGTH FIBRES

140

Number
of breaks   70

0

0   0.2   0.4   0.6   0.8   1.0

Fraction of Ultimate Load
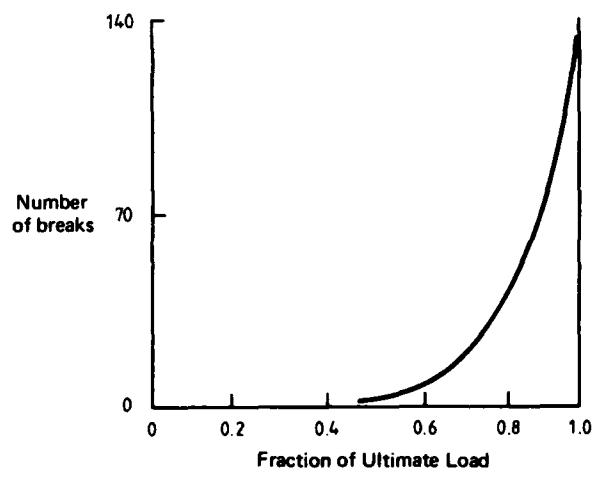
FIG. 10   NUMBER OF FIBRE FRACTURES VS. FRACTION OF ULTIMATE
COMPOSITE STRENGTH

39
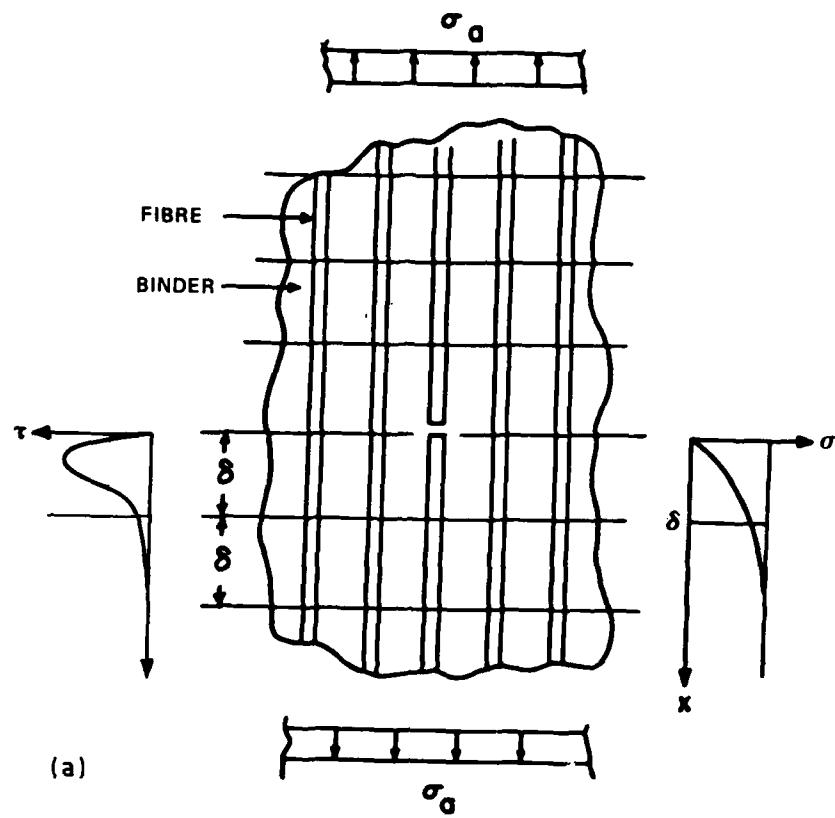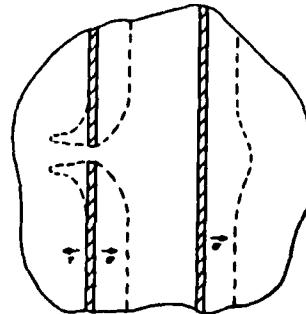
FIG 11   ROSEN'S MODEL SHOWING
         (a) Ineffective length at break
         (b) Perturbation of stress in adjacent fibre

(a) Fibre bundle   (b) Crack   (c) Statistical
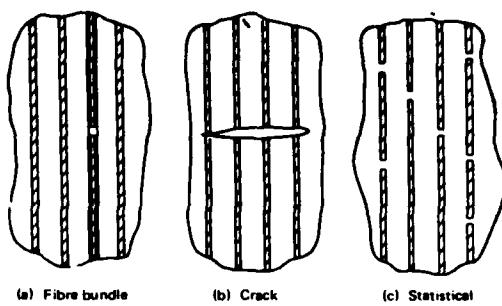
FIG 12   POSSIBLE COMPOSITE TENSILE FAILURE MODES

Cross sectional layer
of N fibres

Cylindrical specimen of
n layers (n = L/δ)
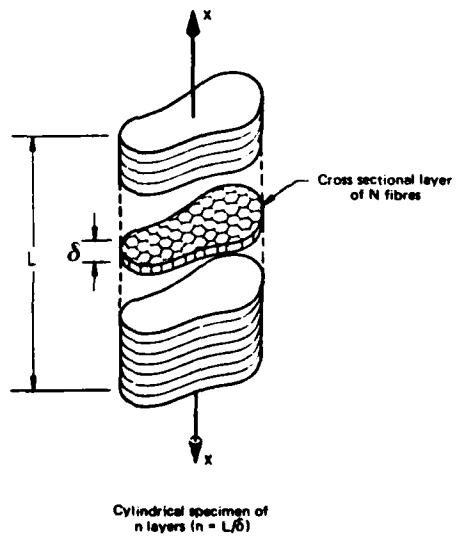
FIG 13   ROSEN'S MODEL — CHAIN OF FIBRE BUNDLES

41
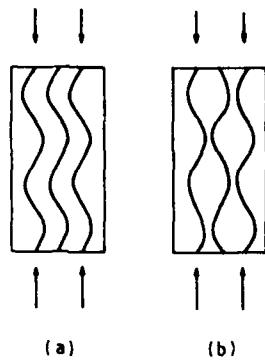
FIG. 14 TWO PURE BUCKLING MODES FOR UNIDIRECTIONAL COMPOSITES
IN COMPRESSION
(a) Shear or in-phase mode
(b) Extensional or out-of-phase mode
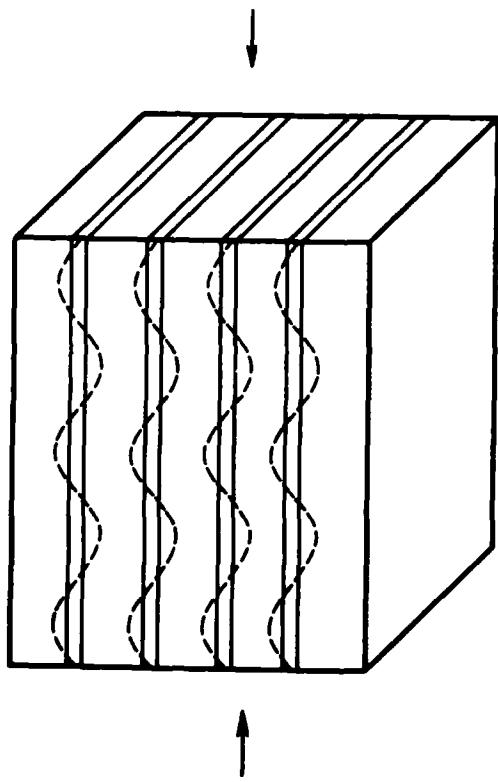
FIG 15 MODEL FOR BUCKLING FIBRES IN UNIDIRECTIONAL COMPOSITE UNDER
COMPRESSION – FIBRES ARE CONSIDERED PLATES RATHER THAN RODS.
BUCKLING IS ASSUMED SINUSOIDAL

42

$$F_p = F \cos \phi$$
$$F_T = F \sin \phi$$

$$A_p = A / \sin \phi$$
$$A_T = A / \cos \phi$$
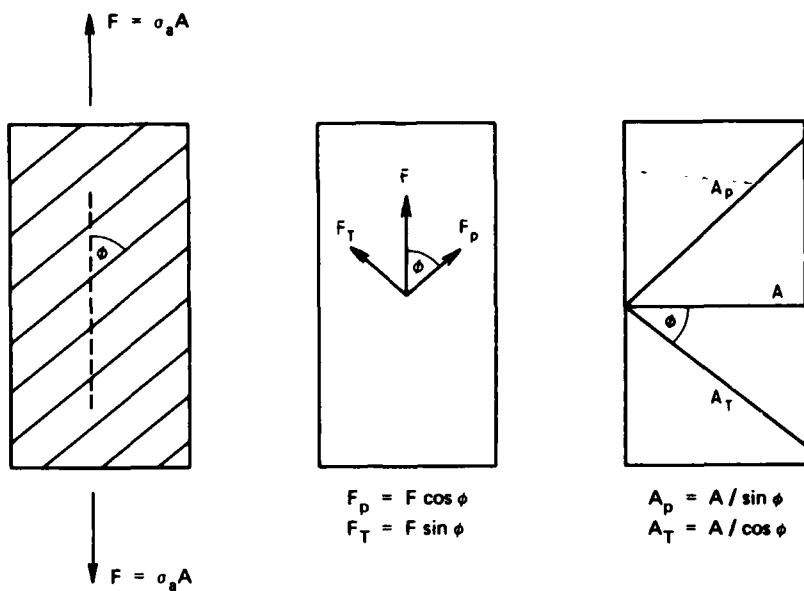
FIG. 16   RESOLUTION OF FORCES AND AREA IN OFF-AXIS TENSION

$$\sigma = \sigma_1^u / \cos^2 \phi$$

$$\sigma = 2\tau^u / \sin 2\phi$$

$$\sigma = \sigma_2^u / \sin^2 \phi$$
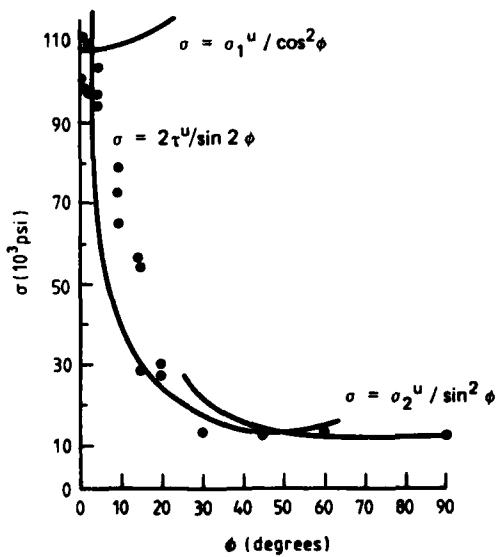
FIG. 17   EXAMPLE OF THE VARIATION OF TENSILE STRENGTH VERSUS ORIENTATION
FOR UNIDIRECTIONAL COMPOSITES

43
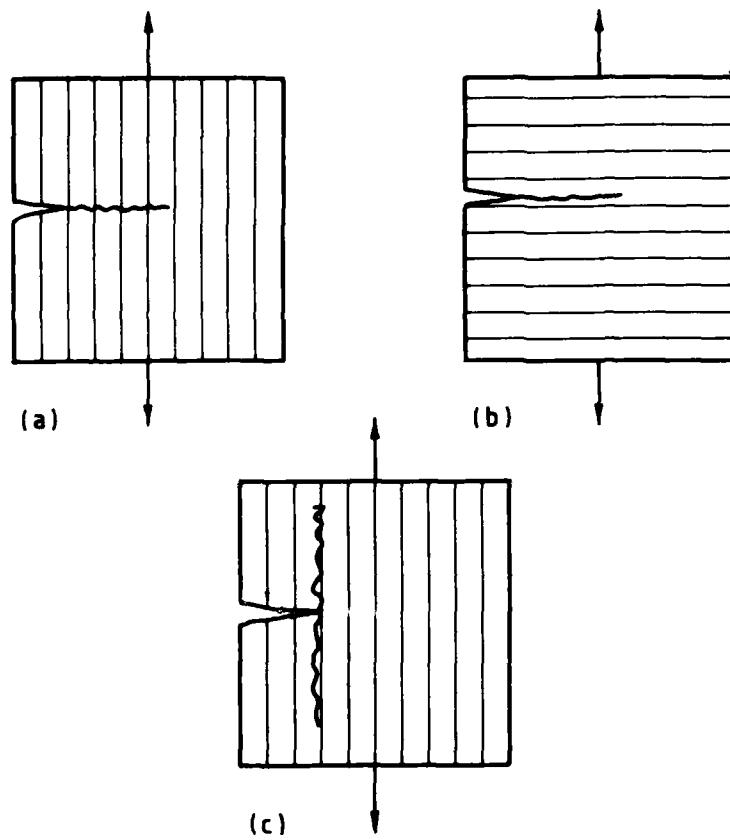
FIG. 18 THE THREE BASIC MODES OF CRACK PROPAGATION IN UNIDIRECTIONAL
FIBRE COMPOSITES SUBJECTED TO SIMPLE TENSILE LOADING
(a) normal to the fibres
(b) parallel to the fibres and (c) splitting
Modes (a) and (b) are self similar modes of propagation

44

Lecture 3

FIBRE SYSTEMS

J.G. WILLIAMS

1. INTRODUCTION

1.1 General

The strength of a brittle material is controlled by the presence
of flaws. As the probability of finding a flaw of a particular severity
depends on the volume of material, a fibre with a low volume per unit length
generally appears stronger on the average than the bulk material. This
effect is illustrated in Fig. 1 where probability distributions of strengths
are shown for a hypothetical brittle material tested in tension in bulk, and
in fibrous form. As indicated schematically, the bulk material has a lower
coefficient of variation and a lower average strength.

For crystalline materials, more favourable orientation of the
crystallites within the fibre may also give rise to increased strength and
modulus compared to the bulk material. For example, polymer chains may be
aligned along the fibre axis by a stretching process. Carbon fibres have
graphitic crystals aligned along the fibre resulting from the structure of the
polymer and retained during manufacture. The strength of the graphite crystal
is anisotropic and this orientation of the crystallites gives high strength
in the fibre direction.

The density of a material is of importance when considering its
possible value as a reinforcing fibre. In many applications, the final
weight is a dominant factor. This is especially true of aerospace applica-
tions and is gaining significance in some land-based uses. The density of a
material is a function of the atomic number of the constituent atoms. Light
fibres are therefore generally based on elements or groups of elements with
low atomic number including C,N,O,Be,B and Si. Of these,even glass, basically
Si and O, is considered heavy with a specific gravity of around 2.4-2.5.

The principal materials from which fibres can at present be
produced economically for use in composites requiring high strength and
stiffness are:

    (i) silica-based glass - "electrical" grade (E-glass)
                            - high strength grade (S-glass)

    (ii) carbon - graphitised grades

    (iii) boron

    (iv) aromatic polyamides - "aramids".

45

The potential of these materials is seen in Table 1 where the strength and modulus of fibres is compared with structural materials. In many applications, including aerospace uses, the weight of a component with adequate strength or rigidity is an important design factor. Materials for such applications can be compared on the basis of specific properties obtained by dividing the appropriate property value by the specific gravity.

TABLE 1: Comparison of the Properties of Structural Materials and Fibres

Material	Specific Gravity	Tensile Strength GPa	Elastic Modulus GPa	Specific Strength GPa	Specific Modulus GPa
Aluminium L65 Alloy	2.8	0.46	72	0.17	26
Titanium DTD 5173	4.5	0.93	110	0.21	24
Steel S97 Alloy	7.8	0.99	207	0.13	27
E-glass	2.54	2.6	84	0.98	33
S-glass	2.49	4.6	72	.1.85	29
Carbon (Graphite) Type I	2.0	1.9	400	0.95	200
Carbon (Graphite) Type II	1.7	2.6	200	1.52	118
Boron	2.5	3.5	420	1.40	168
Aramid ('Kevlar')	1.44	2.8	130	1.94	90

When the fibres are embedded in a matrix which has little load-bearing capability, many composite specific properties are reduced in proportion to the volume fraction of fibre; in Fig. 2 a comparison is shown of the specific properties of some structural materials and unidirectional composites loaded in the fibre direction.

For further accounts of the matters discussed here see, for example, refs. (1) and (2).

1.2   Filamentary Single Crystals (Whiskers)

Some materials can be formed into filamentary single crystals with diameters in the range 1 to 10 μm, and length to diameter ratios up to 10000. Under certain growth conditions these materials have been found to have very high strengths. This has been associated with their crystalline perfection which minimises the occurrence of defects responsible for the low strength of the materials in bulk form. Whiskers with low density have been formed from B, B_4C, Al_2O_3, SiC and Si_3N_4. Composites formed using such whiskers embedded in a suitable matrix have high strength and modulus. These materials, however, are outside the scope of this lecture and will not be further considered; Reference (3) gives a more detailed account.

46

2. MANUFACTURE OF COMMERCIAL FIBRES

2.1 Glass Fibres

Several types of glass may be used in the manufacture of glass fibre (4). The main type is E-glass - a type originally intended for the electrical industry. E-glass is based on a mix of silica (SiO_2), alumina (Al_2O_3), boric acid (H_3BO_3) and calcium carbonate ($CaCO_3$). Another type of glass is S-glass (S for strength). This is based on silica, alumina and magnesia (MgO). The glass is usually premixed and supplied to the fibre manufacturer as glass marbles.

Fibres are formed by melting the marbles in a crucible at a carefully controlled temperature. The process is illustrated in Fig. 3. The melt has low viscosity and gravity feeds through a number of fine holes (200-400 holes of 1-2 mm diameter) in a platinum bushing. A winding device draws the filament bundle away at very high speed (50-100 m/s). The molten glass vitrifies within a few millimetres of the bushing and is cooled rapidly by an aqueous spray containing processing aids. These are discussed below. The fibres produced may be of any diameter but most common filaments have a diameter about 12 μm.

2.2 Carbon and Graphite Fibres

Many forms of carbon fibre are available. Low cost fibres are produced by pyrolysis of many organic, fibrous materials under controlled conditions. These fibres consist of largely amorphous carbon and have low strength and stiffness. They are used as a high temperature insulation and for the manufacture of electrically - conducting, general-purpose composites.

Advanced carbon (graphite) fibres can be produced from particular precursor fibres. Some manufacturers use polyacrylonitrile (PAN) or cellulose-based (rayon) fibres. Recent developments use fibres spun from pitch. The PAN process is illustrated in Fig. 4. The first stage involves a controlled oxidation of a "tow" of about 10000 filaments. Complex reactions between the aligned polymer chains of the precursor form crosslinks and an extended carbon network retaining the original alignment along the fibre axis is formed. For fibres based on pitch filament as a precursor, this stage is carried out with the fibres under tension. As this and the subsequent step require diffusion of waste gases to the fibre surface, the diameter of the fibre produced is limited. Fibres usually have a diameter of about 8 μm. The second stage is pyrolysis under an inert atmosphere. Most non-carbonaceous atoms are lost during this process. The final stage exposes the carbon filament to high temperature to facilitate formation of extended graphite ribbons, aligned along the fibre axis. The end result is a fibre with high modulus and strength. As the temperature of the final treatment is increased, the degree of "graphitisation" increases and the fibre achieves a higher modulus. The strength of the fibre is affected by the number of flaws and defects present and their magnitude (5). At higher heat-treatment temperatures the flaws degrade the strength significantly. The fibre may be produced by controlling the process to optimise either modulus or strength resulting in either high strength (Type HS or I) or high modulus (Type HM or II) fibres. Some economy can be obtained, for example by reducing the final heat-treatment temperature which results in production of a general purpose fibre with reasonable, but lower, strength and modulus (Type A).

47

A fourth variety of fibre is produced from a PAN precursor fibre having a "dog-bone" cross-section. This overcomes, in part, the conflict during the optimisation of the process and results in high-strength, high-modulus fibres. This may be related to a reduction in the distance necessary for evolved gases to diffuse out of the fibre without leading to high internal stresses (6), (7). The cross-section, however, prevents the formation of high fibre content composites.

2.3 Boron Fibres

Boron fibres are produced by a vapour deposition process which is illustrated in Fig. 5. A fine tungsten wire is heated by a passage of an electric current, in an atmosphere containing a boron trihalide (usually boron trichloride) and hydrogen. The reaction is:

$$2BCl_3 + 3H_2 \rightarrow 2B + 6HCl$$

With carefully controlled temperature, boron deposits evenly on the wire. The tungsten is largely converted to tungsten boride and remains in the fibre as a semi-conducting core. The process is limited to single fibre production. Pure tungsten is used as the core because of its high strength at elevated temperatures but the initial diameter is limited by its strength. The boron filament produced must have a high diameter to ensure that the residual tungsten core has insignificant effects on the final fibre properties (8). Tungsten cored fibres normally are produced with a diameter of about 125 μm. The bending stiffness of an individual fibre is dependent on the fourth power of the radius and thus thick fibres are difficult to manipulate into complex shapes. The tightest radius bend an individual fibre can be formed into depends on the ultimate elongation of the fibre and its radius; boron composites will fracture if the radius of curvature is less than about 8 mm. It is thus not possible to weave boron filaments into a conventional cloth.

Recent developments use a carbon fibre as the core material. This gives a lighter fibre due to the low density of the carbon core; also a smaller fibre diameter can be employed.

Compressive properties of a unidirectional composite, in the fibre direction, may be limited by the columnar stability of individual fibres, by the fibre-matrix bond strength, and by the shear modulus of the matrix. Failure of carbon and glass composites in compression is initiated when the fibres buckle after the bond strength or matrix shear yield strength is exceeded (9); boron fibres, because of their larger diameter, resist this buckling and consequently boron reinforced composites have excellent compressive strength (10). As boron is exceedingly hard (9 Moh), derived composites can be machined only with great difficulty, with diamond-tipped tools.

2.4 Aramid Fibres

These fibres are the latest type to be released commercially. They are polyamide fibres closely related to conventional nylons but the flexible aliphatic chains are replaced by aromatic rings. The polymer is formed by condensation of aromatic diacid derivatives with aromatic

48

diamines. The only commercially available fibre is Kevlar marketed by
duPont. This is based on the condensation product of terephthalic acid
and para phenylene diamine (11).

These materials have long been known to have appropriate
properties for use as reinforcements but they are generally intractable
polymers. The commercial availability of advanced solvents and spinning
techniques made production of aramid fibres commercially feasible. The
acid and amine are condensed in suitable solvents and formed into fibres
by extruding a solution in sulphuric acid into a neutralising bath when the
fibre is precipitated. The polymer in the raw fibre is oriented along the
fibre axis, as for most polymer fibres, by extended elongation of the
fibre during, and immediately following, the spinning process. The fibre
diameter is limited by the need to lose trace solvent from the finished
fibre.

Three types of Kevlar are available differing in the draw ratio
of the final step. The first grade, called simply Kevlar, is intended for
reinforcement of tyres. The second, Kevlar 29, is used to reinforce rubber
goods such as cordage and belting. The third, Kevlar 49, is used in
engineering composites.

The structure of the fibre is itself a composite, with long stiff
fibrils running along the fibre axis, and embedded in a softer matrix. This
microstructure imparts two important properties to Kevlar. The composite
compressive strength is significantly lower than with other advanced fibres
as fibre buckling is enhanced by fibril buckling (12). On the other hand,
the fracture toughness of the composite is greatly increased, as considerable
energy is absorbed by the failing composite by cracks running between fibrils.
Failed specimens often give the appearance of broomsticks due to this
failure mode. Machining of Kevlar composites requires careful design or
modification of cutting tools (13).

3.   FORMS IN WHICH FIBRE IS SUPPLIED

3.1   Textile Terminology and Filament Forms

A number of special terms are used, derived from the textile trade.
A single fibre is usually called a filament. A collection of filaments
usually produced simultaneously is termed an end or sometimes a strand.
Several ends may again be combined into a roving or a tow. Typical rovings
may contain 50-60 ends and 3000-4000 filaments. If a strand is twisted to
hold the filaments together it becomes a yarn which may be further combined
into assembled, plied, and cabled yarns. Complex yarns are not common in
reinforcement applications, as excessive twist in the yarn reduces the ease
with which resin can displace entrapped air (wet-out) from the filament
bundle. Some twist, however, helps compact the yarn resulting, ultimately,
in a composite with higher fibre content.

3.2   Woven Broadgoods

Both roving and yarn may be woven to give, respectively, woven
roving and cloth (4). Woven roving uses the fibre strength efficiently, but
as the roving is not compact, generally derived composites have high resin

contents. It is normally used to build thick sections rapidly as it will wet-out easily with resin. Cloth is slightly weaker on the basis of fibre volume fraction than roving due, in part, to the increased damage caused during processing and, in part, to effect of the fibre twist. Cloth allows a good wet-out by resin and, as it is compact, gives a high fibre content laminate. During the weaving process, woven rovings and cloth may be produced in a wide variety of forms. The ratio of the number of filaments across the cloth roll (weft direction) to the number along the roll (warp direction) can easily be varied from effectively unidirectional, with only sufficient warp filaments to hold the cloth together, to even warp and weft. Hybrid cloths are produced with different fibres in warp and weft directions e.g., graphite warp and glass weft.

The weaving pattern affects the way the cloth handles and the final composite properties. In plain weave, the weft alternately goes over and under successive warps. Special weave patterns, where the warp fibres cross different numbers of weft fibres result in satin and crowsfoot cloths (4). In these, the cloth drapes over complex shapes more readily but is easily disturbed to give alignment errors. The strength and stiffness tend to be higher as the fibres, on average, are straighter.

3.3 Non-woven Broadgoods

Another form in which fibres may be supplied is chopped strand mat (CSM). This form is produced by chopping the fibres, (usually glass), into lengths about 25-50 mm long and distributing them randomly on a flat surface. A water-soluble binder is sprayed onto the mat to hold the fibres together and the sheet is compacted. In use, the binder is designed to dissolve in the resin system to give a random orientation of the reinforcement in the plane of the mat. Much chopped strand mat is designed for use with polyester and vinyl ester resins. The binder does not dissolve in epoxy resins and hence cannot be used with them. Some epoxy-compatible CSM is produced in Europe and USA.

Some fibres may be produced in felt form, where short fibres are held in a light cloth with the fibres normal to the plane of the support cloth. This is occasionally used in an attempt to produce "through-the-thickness" reinforcement.

Some composites, particularly if based on thick woven roving, tend to have a resin rich layer between laminates. Felt or CSM may be used to reinforce this layer to prevent interlaminar shear failure.

3.4 Tapes

Automated machinery is often employed in composite production facilities especially for aerospace applications. Many of these machines are designed to use tapes. The tapes may be unidirectional when fibres or tows are aligned primarily along the tape direction or may be conventionally woven, usually using a plain weave. Unidirectional tapes may be (i) held together with a light cross-weave of the same fibre or a lower-cost fibre, or (ii) may be supported on a light glass cloth (scrim), or (iii) may be on an inert backing sheet. Tapes are often supplied pre-impregnated with the required resin system which serves to hold the fibres together on the backing material.

Boron fibres, which are too stiff to weave, are normally supplied as pre-preg tape on a glass scrim.

4.   SIZES, FINISHES AND FIBRE SURFACE TREATMENTS

During processing of the original fibre into the form in which it will be finally protected by the matrix, considerable damage can be expected. This is particularly true of glass fibres which are brittle and have a high coefficient of friction (for glass on glass, this is around unity). Mishandling results in the formation of micro-cracks in the surface which substantially weaken the brittle fibre. To reduce this damage, a coating is applied to the fibre as early as possible (on exit from the spinerette for glass). This coating material, termed a *finish* or *size*, serves several functions. It acts:

(i)   as a binder to keep the filaments together
       (especially in CSM, see above)

(ii)   as a lubricant to reduce the inter-filament
       coefficient of friction,

(iii) as a coupling agent to promote durable bonding
       between fibre and matrix,

(iv)   as a wetting agent to assist in resin wet-out.

Typical sizes for glass include amino silanes and proprietary chrome finishes (Volan). The size is often designed for use with particular classes of resin (e.g. amino silanes for epoxy resin). For many fibres systems, the size is applied early in manufacture and is designed to dissolve in the resin system during use. It may be suitable only for specific resins. For woven fabrics, the mechanical degradation of the fibre can be severe and very heavy duty textile finishes are used which are usually removed after weaving to be replaced by a conventional finish as above.

For some fibres, particularly graphite, the surface may be etched in either the gas phase or liquid phase by oxidising agents including chlorine and bromine, nitric acid and chlorates. This improves wettability by the resin and encourages formation of a strong durable fibre-matrix bond. Some strength improvement by removal of surface flaws has been demonstrated (9), (14).

51

REFERENCES

1. Langley, M. (editor), Carbon Fibres in Engineering, McGraw-Hill, London, 1973.

2. Galasso, F.S., High Modulus Fibres and Composites, Gordon and Breach, New York, 1969.

3. Levitt, A.P., Whisker Technology, Wiley-Interscience New York, 1970.

4. (a) Anon., Woven Glass Fibre Fabrics for Plastic Reinforcement, BS 3396 Pt. 1, 1966.
    (b) Anon., Glass Fibre Rovings, BS 3639, 1969.
    (c) Anon., Woven Roving Fabrics of E Glass Fibre, BS 3749, 1974.

5. Johnson, D.J. and Tyson, C.N., The Fine Structure of Graphitised Fibres, J. Physics D, vol. 2, pp. 787-795, 1969.

6. LeMaistre, C.W. and Diefenderf, R.J., Origin of Structure in Carbon Fibres, Carbon Symposium 1971 (Pub 1972) 77-8 Editor J.D. Buckley, American Ceramic Society.

7. LeMaistre, C.W., The Related Effects of Microstructure and Thermal Expansion Anisotropy to the Strengths of Carbon Fibres, WRE Tech. Memo. 587 (WR&D), 1972.

8. Galasso, F. and Paton, A., The Tungsten Borides in Boron Fibres, Trans. AIME, vol. 236, pp. 1751-1752, 1966.

9. Weaver, C.W. and Williams, J.G., Deformation of a Carbon Epoxy Composite under Hydrostatic Pressure, J. Mat. Sci., vol. 10, pp. 1323-1333, 1975.

10. Greszczuk, L.B., Micro-buckling of Unidirectional Composites, AFML TR-71-231, 1971.

11. Dobb, M.G., Johnson, D.J. and Saville, B.P., Compressional Behaviour of Kevlar Fibres, Polymer, vol. 22, pp. 960-965, 1981.

12. Kulkarni, S.V., Rice, J.S. and Rosen, B.W. An Investigation of the Compressive Strength of Kevlar 49/Epoxy Composites, Composites, vol. 6, pp. 217-225, 1975.

13. Anon., A Guide to Cutting and Machining Kevlar Aramid, Du Pont Publication.

14. Johnson, J.W. Factors Affecting the Tensile Strength of Carbon-Graphite Fibers, Applied Polymer Symposia, No. 9, pp. 229-243, 1969.
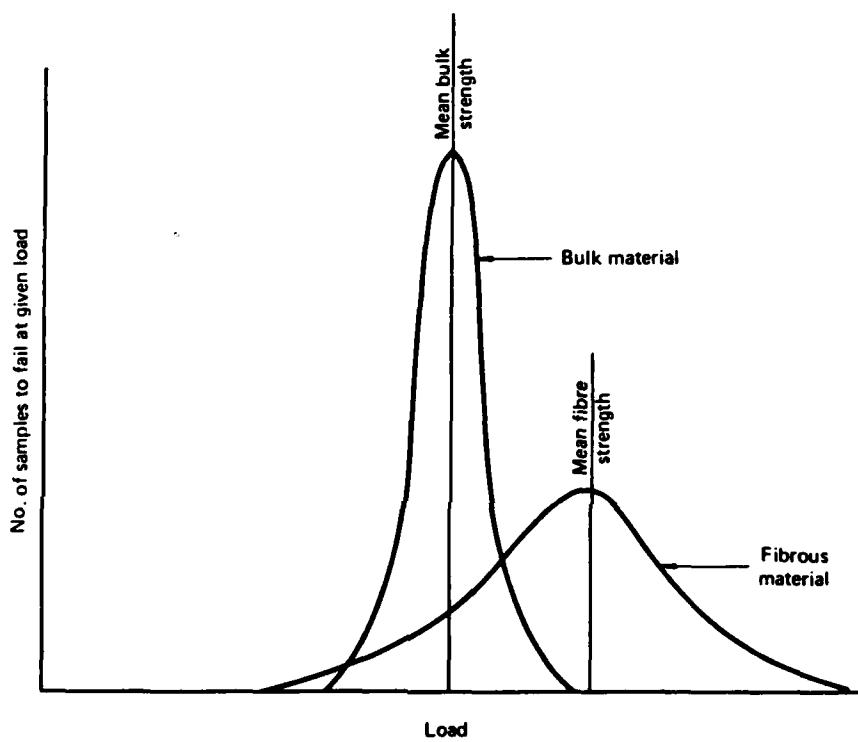
FIG 1   EFFECT OF SAMPLE CROSS-SECTION ON DISTRIBUTION OF STRENGTH
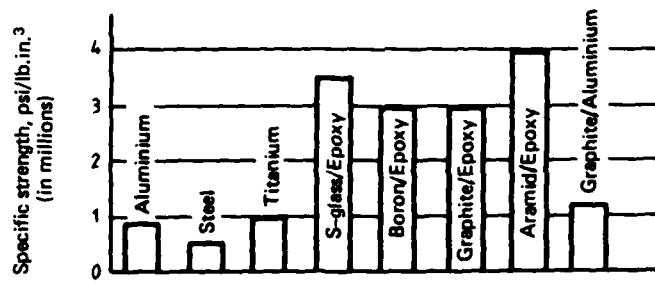
A comparison of composites and metals by specific strength (ultimate tensile strength/density)
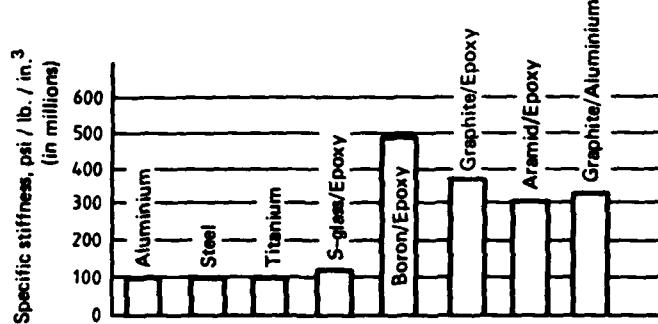
A comparison of composites and metals by specific stiffness (modulus/density)

Composite data shown are for 0° unidirectional laminates.

FIG 2   COMPARISON OF SPECIFIC STRENGTH AND STIFFNESS OF COMPOSITES AND
         OTHER MATERIALS
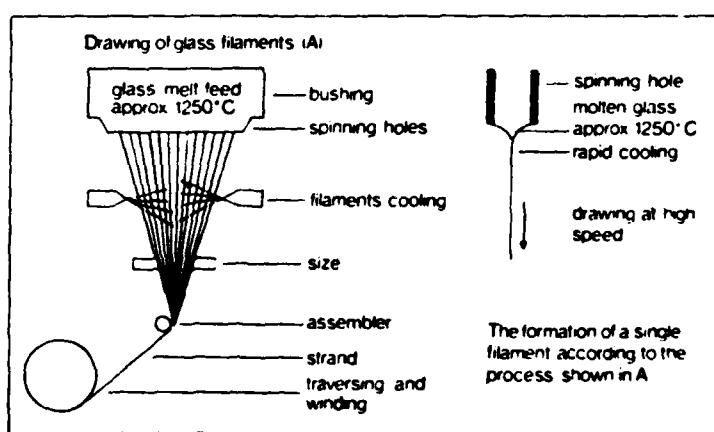
FIG 3   SCHEMATIC ILLUSTRATION OF THE PROCESS OF MELT – SPINNING GLASS
         FIBRES
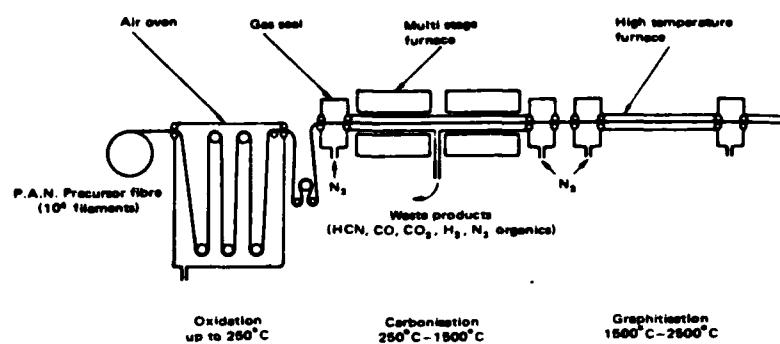
FIG 4   SCHEMATIC ILLUSTRATION OF THE PROCESS USED FOR MANUFACTURING
CARBON FIBRES
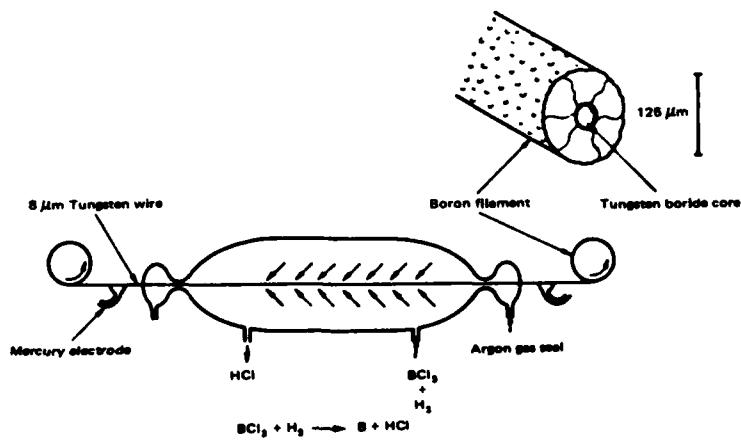
FIG 5   SCHEMATIC ILLUSTRATION OF THE PROCESS USED FOR MANUFACTURING
BORON FIBRES

55

Lecture 4

RESIN SYSTEMS

J.G. WILLIAMS

1.   INTRODUCTION

   1.1   The Functions of the Matrix

          The matrix in a composite serves three main functions. It holds
   the fibres together; it distributes load between fibres; and it protects
   the fibres from the environment.

          The ideal material from which a matrix is derived should be,
   initially, a low viscosity liquid which can be converted readily to a tough
   durable solid, adequately bonded to the reinforcing fibre. While the function
   of the fibrous reinforcement is to carry the load in the composite, the
   mechanical properties of the matrix can significantly affect the way, and the
   efficiency with which, the fibres operate. For example, in a fibre bundle in
   the absence of matrix, the straightest fibres bear a high proportion of the
   load. The matrix causes the stress to be distributed more evenly between
   all fibres by causing all fibres to suffer the same strain. The stress is
   transmitted by a shear process which requires good bonding between fibre and
   matrix and also high shear strength and modulus for the matrix itself.

          As the load is carried primarily by the fibres, the overall
   composite elongation is limited by the elongation to failure of the fibres.
   This is usually 1-1.5%. The significant property of the matrix is that it
   should not crack. Resin systems for advanced composites tend to behave in a
   brittle manner with low strain to failure and with a high modulus compared to
   systems designed for non-reinforced applications.

          Across the fibre direction the mechanical properties of the
   matrix and the bond between fibre and matrix dominate the physical properties
   of the composite. The matrix is much weaker and more compliant than the
   fibre and hence direct transverse loading of the matrix is avoided as far as
   possible during design of a composite component.

          The matrix and matrix-fibre interaction can have a significant
   effect on crack propagation through the composite. If the matrix shear
   strength and modulus, and the fibre-matrix bond strength are too high, a
   crack may propagate through fibre and matrix, without turning. The composite
   will then behave as a brittle material and failed specimens will show clean
   fracture surfaces. If the bond strength is too low, the fibres will act
   as a fibre bundle and the composite will be weak. At an intermediate bond
   strength, cracks propagating transversely through resin or fibre may turn at
   the interface and travel along the fibre direction. This results in
   absorption of considerable energy, and composites which fail by this mode
   are tough materials.   Failed specimens will show considerable fibre pull-
   out and the fracture surface will be very rough with lengths of bare fibre
   visible.

A compromise is needed between a system with high bond strength (for efficient load transfer between fibres but poor fracture toughness) and systems with lower bond strength (which will not be as efficient but will have higher toughness). Composites used in situations where stress levels and directions are not defined, or which are manufactured under conditions which reduce fibre alignment accuracy, usually require softer, more forgiving matrices. Advanced composites, used in situations where stress levels are well defined, and which are manufactured with careful control of fibre alignment, can make better use of ultimate fibre properties by using matrices with high modulus and high bond strength.

Some general references on resin matrices are given in (1-4).

1.2 Resin Types

The major types of resin used in production of composite components are epoxy, polyester and vinylester, and phenolic resins. The most common matrix is polyester resin as this is used in composite applications for fairly low stress situations. The majority of advanced composite applications call for the use of epoxy resins. The search for improved matrices continues, especially to allow production of composites suitable for use at higher temperatures and with lower moisture sensitivity. Comparative physical properties of typical matrix resins are shown in Table 1.

TABLE 1: Comparative Properties of Resin Matrices

Property (1)	Unit	Epoxy Resins			Polyester	Phenolic
		R.T. Cured	Heat Cured	Advanced (2)		
Spec. Gravity	-	1.1-1.3	1.2-1.4	1.3	1.2	1.2-1.3
Tensile Strength	MPa	50-70	70-90	60	50-60	50-60
Tensile Modulus	GPa	2-3	2.5-3	3.5	2-3	5-11
Elongation to Failure	%	2-6	2-5	2	2-3	1.2
Compr. Strength	MPa	80-100	120-130	300	120-140	70-200
Max. Operating Temp. (3)	°C	70-100	100-180	180	60-80	100-125

NOTES: (1) Values quoted obtained using relevant ASTM standard methods.

(2) A typical grade recommended for use with advanced fibres.

(3) Quoted is the heat distortion temperature which measures the onset of the glass transition region, approximately.

2.   EPOXY RESINS

2.1   General

Epoxy resins are a class of compounds which contain two or more epoxide groups. The major types are formed by reacting polyphenols with epichlorhydrin under basic conditions. If the polyphenol is diphenylol propane the most usual epoxy resin is obtained. Trade names include such materials as Epikote or Epon 828 DOW DER 331, Araldite F or 6010 etc. The resin is supplied as a viscous, clear to light-yellow liquid.

Many other epoxy resins are manufactured for special purposes. The polyhydric phenol may be replaced by aminophenols or polyamine compounds. The triglycidyl ether of aminophenol and the tetraglycidyl ether of diaminodiphenyl methane (DDM) are finding widespread use in advanced composites and adhesives. Structures of resins and typical curing agents are shown in Figure 1.

All epoxy resins can be self-polymerised using suitable catalysts, but the majority of applications make use of curing agents. The major classes of curing agents are aliphatic amines which give cold curing systems, and aromatic amines and polyanhydrides which give heat curing systems. The condensation is a strict chemical reaction and the rate cannot be adjusted by changing mixing ratios (compare polyesters, below). The chemical reaction between resin and curing agent is strongly exothermic in the liquid state. As the condensation proceeds, gel particles precipitate from the reactant mixture. The reaction rate in the gel is controlled by diffusion of the reactants to active sites and the rate is reduced compared to what it is in the liquid state. Eventually all the liquid gels, probably forming a dispersion of well-advanced particles in a less well advanced matrix. Reaction continues in the solid state until the resin is sufficiently crosslinked to become a glass. Diffusion of the reacting species in the glassy state is very slow and the reaction effectively stops at that point.

The occurrence of rubbery and glassy states is characteristic of amorphous polymers. At low temperatures all polymers become glassy and at high temperatures they may become rubbery. The temperature region over which the transition occurs is called the glass transition temperature (T_g). The exact temperature is a function of how the measurement is made.

Most practical determinations place some physical stress on the sample and determine the effect of temperature. The speed of application of the stress and the rate of change of temperature have a pronounced effect on the observed temperature of the glass transition. Many rubbery plastics will fail in a glassy manner if tested at a high enough speed.

The glass transition temperature is a rough indication of the maximum operating temperature for that system. As the polymerisation of epoxy resins stops in the glassy state, it is very difficult to design a system which will be capable of operation much over the maximum temperature in the cure cycle. Systems cured at room temperature, using aliphatic polyamine curing agents are not suitable for use at temperatures much over 50°C. With postcure at temperatures over 100°C, maximum operating temperatures may be increased to 90-100°C. Systems cured with aromatic

polyamines or anhydrides are usually cured at temperatures around 100-150°C, may often be postcured at 150-250°C, and have maximum operating temperatures in the range 100-250°C.

Cure can be accelerated by the use of suitable catalysts but the maximum rate is slower than for polyesters (see below). As the epoxide-curing agent is strongly exothermic (generates heat), the use of excessive quantities of catalyst or inappropriately high cure temperatures will result in thermal degradation of the matrix in thick sections.

2.2 Formulating with Epoxy Resins

The properties of the final cured matrix are partially defined by the choice of resin and curing agent. They may be further modified by a range of additives including:

> (i) Diluents added to reduce viscosity before cure to aid handling, wet-out etc. (Usually these cause decreases in maximum operating temperatures).

> (ii) Flexibilisers added to reduce elastic modulus and increase elongation to failure.

> (iii) Rubber-toughening agents which precipitate from the reacting matrix as rubbery particles, which modify crack propagation in the matrix.

> (iv) Inert fillers, including hollow fillers, added to alter density, cost, and mean matrix modulus.

Modification of properties is a specialised task and is not usually left to the user. Many commercial formulations are available from suppliers.

2.3 Environmental Durability

One of the functions of the matrix is to protect the fibres from the environment. Two components of the atmosphere which will degrade resins are ultraviolet light and moisture. All resins containing aromatic groups can absorb sufficient UV radiation to cause bond scission. Of the resins discussed, phenolics are most sensitive, then epoxy resins; polyesters are least sensitive. All resins may be protected from radiation by the use of surface coatings.

Attack by moisture is a more difficult problem. All fibres to which resins will form a bond are preferentially wet by water. Water, therefore, if allowed access to the fibre-resin interface, may result in debonding, and a loss of composite stiffness and strength.

The controlling factor, in the degradation by moisture ingress, is the diffusion constant of water vapour. As water is a very polar molecule, the diffusion mechanism involves hydrogen bonding with polar sites in the polymer molecule. Epoxy resins are the most polar of the normal

resins as they contain hydroxyl groups, ether groups and C-N bonds. Polyesters are less polar due to the high concentration of polystyrene links and low concentration of ester links. Phenolics have the lowest polarity. Water permeability is therefore highest for epoxy resins and lowest for phenolics.

The equilibrium moisture uptake of the resin is also related to the diffusion constant and polarity of the resin. Water acts as a plasticiser of the resin system and degrades the mechanical properties at room temperature slightly. More significantly, it can reduce the glass transition temperature and limit the high temperature performance of the matrix. As moisture is strongly bonded to the epoxy system even at high temperatures it is only lost slowly. High performance aircraft may experience "thermal spikes" by cruising at high altitude where skin temperatures may fall to around -50°C and then sprinting to supersonic speeds where aerodynamic heating may raise skin temperatures to well over 100°C in a few seconds. Special care needs to be taken that moisture absorption has not degraded the high temperature performance of composite used in these situations.

It should also be mentioned that moisture trapped in voids and cracks can be vaporised under these conditions and this can result in matrix cracking. Similarly, low temperatures can freeze entrapped moisture and the resulting expansion can also initiate matrix cracking.

2.4 Advantages and Disadvantages of Epoxy Resins

The main advantages of epoxy resins are:

(i) May be formulated for optimum properties for particular applications.

(ii) Fracture toughness may be controlled.

(iii) Are moderately convenient to use.

The main disadvantages are:

(i) Expensive compared to polyesters (specialty resins can be very expensive).

(ii) Less convenient than polyesters due to relatively slow cure and high viscosity.

(iii) Limited resistance to some organic materials (particularly organic acids and phenols), and limited high temperature performance.

3. POLYESTER RESINS

3.1 General

Polyester resins are formed by condensation of a mixture of dibasic acids with dihydric alcohols (glycols) or dihydric phenols. The dibasic acid mix contains unsaturated acids. The components are illustrated in Figure 2. The condensation is carried out to give a prepolymer

60

of low melting point and good solubility in liquid styrene. The molecular
weight of the prepolymer is a few thousand and it usually contains an
average of five unsaturated links. The polyester is supplied as a solution
in styrene monomer (35% styrene W/W). When a source of free radicals is
added (the initiator), and often a catalyst (the accelerator) as well, the
styrene polymerises. The polymerising styrene reacts with the unsaturated
sites in the polyester to form a three dimensional crosslinked network based
in part on polystyrene and in part on the polyester prepolymer.

3.2 Types of Polyester

The major commercial variations of polyesters are based on
modification of the polyester component by partial replacement of saturated
acid or glycol by alternative materials. For example, resins of improved
strength and durability are obtained by replacing the normal ortho phthalic
acid by isophthalic acid ("isophthalic polyesters") or by the use of
diphenylol propane in place of some glycol ("DPP resins"). Another common
variation is the use of adipic acid which improves flexibility and increases
failure strain of the cured matrix.

3.3 Cure of Polyesters

The most commonly used initiator for cure of polyester resins
is methyl-ethyl ketone peroxide (MEKP), usually supplied as a solution in
dimethyl phthalate. Cobalt naphthenate, supplied as a solution in naphtha,
is used as an accelerator with MEKP. MEKP is an extremely hazardous
material and can cause permanent eye damage, skin burns, etc. and can lead
to serious fires and explosions if used incorrectly. Of particular importance
is the admixture of initiator and accelerator which will spontaneously
inflame and may explode. This occurs if the two materials are accidently
added successively to the resin without intermediate stirring.

The speed of the polyester polymerisation may be controlled
over a wide range by adjustment of the quantities of initiator (0.5 - 3% wt.
resin) and accelerator (0.05 - 0.5% wt. resin) added.

The polyester polymerisation is strongly exothermic and the use
of high levels of initiator and accelerator will cause severe thermal damage
in thick sections. The use of massive moulds and the incorporation of
fillers reduce exotherm by increasing the system thermal mass.

Another common initiator is benzoyl peroxide (BzP) which is sold
as a paste in dimethyl phthalate. The appropriate accelerator for BzP is a
tertiary amine. It should be noted that the accelerators for MEKP and BzP
are not interchangeable. Systems cured with BzP without accelerator, or at
very low accelerator contents, are stable at room temperature and are cured
at elevated temperature. A range of initiators similar to BzP is available
which will allow crosslinking to initiate rapidly at particular limiting
temperatures e.g. BzP is stable to 70°C while ditertiary butyl peroxide is
stable to 140°C. Heat cured polyesters are generally used in matched die
moulding where fast cycle times are required.

3.4 Advantages and Disadvantages of Polyesters

The major advantages of polyesters are:

(i)   Initial low viscosity which allows easy wet-out
      of reinforcement.

(ii) Low cost (all raw materials are readily available
      and relatively cheap).

(iii) Cure conditions can be easily modified with little
      operator experience.

(iv) They can readily be manufactured in a range of modi-
      fications for particular applications.

(v)   They have good environmental durability.

The major disadvantages are:

(i)   High exotherm and high shrinkage on cure. Both
      factors head to a poor fibre-matrix bond strength
      due to in-built stress.

(ii) Systems with adequate shear strength tend to be
      brittle and toughening additives appear ineffective.

(iii) They have poor resistance to alkali even when the
      alkali is very dilute.

4.   VINYL-ESTER RESINS

A resin system very closely related to polyesters is obtained
by using unsaturated hydroxylic compounds (e.g. vinyl alcohol) in place
of some of the glycol in a polyester, and by eliminating the unsaturated
acid. These materials are known as vinyl-ester resins and are sold in
styrene monomer solution and used as for polyesters. The major
advantage of these materials is an improved bond strength between fibre and
matrix. Generally, however, they are similar to polyesters.

5.   PHENOLIC RESINS

5.1   General

When phenol is condensed with formaldehyde under alkaline
conditions polymerisation occurs. If the system is carefully controlled,
polymerisation can be stopped while the polymer is still fusible and
soluble. This prepolymer is termed a resol. It will polymerise under the
influence of heat or of acidic or basic catalysts to give a densely cross-
linked material of complex chemical structure. (See Figure 3). Water and
other volatile by-products are formed, and this requires that the poly-
merisation should be carried out under high pressure to avoid the formation
of a friable foam. Cured resol-type phenolics usually have a high void content.

62

If the prepolymerisation is carried out under acid conditions, a different polymerisation path is followed and a novolak resin is produced. This will not self-polymerise but can be crosslinked under the influence of a complex amine, usually hexamethylene tetramine. (See Figure 4). Other materials, including paraldehyde, are occasionally used. Polymerisation of the prepolymer is carried out under pressure as volatile by-products are also formed in this reaction.

5.2 Properties of Phenolic Resins

Phenolic prepolymers for use in composites are solids and are usually supplied in solution. Due to the dilution effect, the solutions are stable at room temperature. Fibres, usually in the form of cloth or matt, are impregnated with the solution and the solvent evaporated off. The resultant treated fabric may be heat-treated to partially-polymerise the resin system. This material is termed a pre-preg (from "pre impregnated") and if the resin has been heat-treated it is called a B stage pre-preg (A stage is liquid or sticky solid pre-polymer; B stage is a fusible solid with low tack; C stage is fully cured). Sheets of pre-preg can then be assembled with the required orientation and consolidated under pressure during heat-curing. While all heat-curing resins including epoxy and poly-ester resins are commonly used in this fashion, phenolic resins can only be used as pre-pregs.

5.3 Advantages and Disadvantages of Phenolic Resins

The principle advantage of phenolic resins is their excellent resistance to high temperature, especially under oxidising conditions. This particularly affects their ablation properties i.e., the speed at which they burn-off when directly exposed to flame. Under these conditions phenolics char readily giving a good yield of a superficial layer of porous carbon. This protects the underlying composite, while the carbon slowly burns away. Other resins usually give a poor char yield and burn away to gaseous products relatively quickly.

The disadvantages of phenolics include:

(i) Their difficulty of use due to the high pressures needed during polymerisation.

(ii) They usually are dark-brown to black.

(iii) The mechanical properties of derived composites are lower than for composites based on other resins due to the high content of voids.

6. OTHER RESINS

A wide variety of resins have been developed in attempts to allow the use of composites at higher temperatures (e.g. 250-350°C). Commercially available in limited quantities are, for example, polyimides (PI) and polybenzimidazoles (BPI). These are complex highly aromatic materials frequently containing heterocyclic fused rings. They are produced

from tetrafunctional aromatic acids and aromatic diamines (PI) or tetramines (PBI). Thermal treatment of this prepolymer, frequently in the presence of acid anhydrides and basic catalysts, results in the formation of crosslinked networks. Their thermal resistance achieved to date allows continuous exposure to about 300°C and they can withstand short exposures to up to 420°C.

They are both difficult to use and require the pre-preg process and high temperatures and high pressures for cure. PI has better temperature resistance than PBI but is harder to use.

7. CARBON-CARBON COMPOSITES

A special type of advanced composite finding application in the aerospace field is the so-called carbon-carbon composite. This material is usually obtained by pyrolysis of a carbon reinforced phenolic matrix under pressure. As described above, phenolic resins yield a high proportion of amorphous carbon char under such conditions especially when air is excluded. The product is carbon fibre reinforced amorphous carbon. This material tends to be very porous and may be reimpregnated and refined to reduce the void content. The finished material is capable of withstanding very high temperatures for prolonged periods if oxygen is excluded. It finds applications as a brake-lining compound, in rocket exhaust nozzles, and other high temperature applications.

REFERENCES

1. Saunders, K.J., Organic Polymer Chemistry, Chapman and Hall Ltd., London, 1973.

2. Lee, H. and Neville, K., Handbook of Epoxy Resins, McGraw-Hill, New York, 1967.

3. Boenig, H.V., Unsaturated Polyesters, Elsevier, Amsterdam, 1964.

4. Lubin, G. (ed.), Handbook of Fibreglass and Advanced Plastics Composites, Van Nostrand Reinhold, New York, 1969.
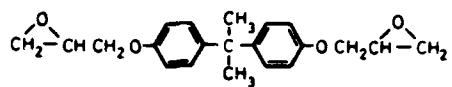
DPP-based Epoxy Resin (standard type)
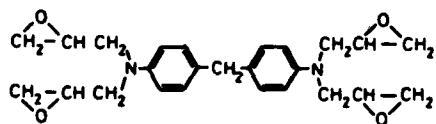
Tetraglycidyl ether of DDM (advanced resin)

$$H_2NCH_2CH_2NHCH_2CH_2NH_2$$
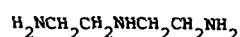
DET: room temperature curing agent
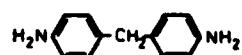
DDM: heat curing agent

FIG. 1 STRUCTURE OF EPOXY RESINS AND CURING AGENTS

66

Propylene glycol

$$\begin{array}{l} CH_2OH \\ | \\ CHMeOH \end{array}$$

Phthalic anhydride

$$\underset{}{\bigcirc}\begin{array}{l} CO \\ CO \end{array}\!\!>\!\!O$$

Maleic anhydride

$$\begin{array}{l} CH\,CO \\ \| \\ CH\,CO \end{array}\!\!>\!\!O$$

Hydroquinone

$$HO\!-\!\bigcirc\!-\!OH$$

Monomeric styrene

$$\bigcirc\!-\!CH\!:\!CH_2$$
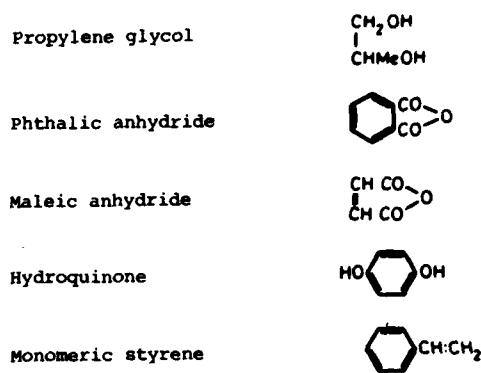
FIG. 2 COMPONENTS OF A POLYESTER RESIN
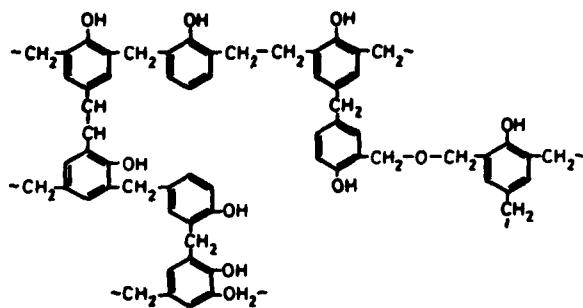
FIG. 3 STRUCTURE OF A CROSSLINKED PHENOLIC RESIN - RESOL TYPE
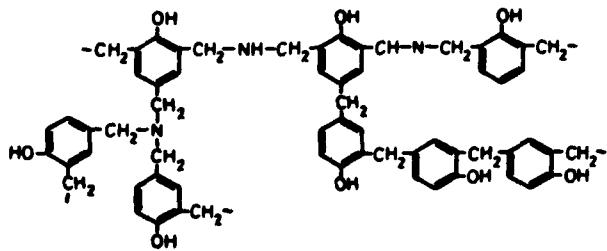
FIG. 4 STRUCTURE OF A CROSSLINKED PHENOLIC RESIN - NOVALAC TYPE

Lecure 5

COMPOSITE SYSTEMS

M.J. DAVIS and A.W. RACHINGER

1.   INTRODUCTION

In the preceding lectures, the properties and nature of fibres and resins were discussed. This lecture will cover the characteristics of composite systems constituted from these materials. In Lecture 2, micro-mechanical analyses were used to predict composite properties from a knowledge of constituent properties and from an understanding of the fibre/matrix interactions in the "composite state." It is important to realise however, that such analyses are approximate because they rely on much simplified models of very complex systems. Micromechanical analyses alone are not sufficient for design purposes, and mechanical testing data from real composite materials are required. Therefore, considerable emphasis is placed on testing procedures in this lecture. The elastic constants and strength values required for designing laminates are presented, the testing procedures for their determination are discussed, and the importance of the generally anisotropic nature of composites in the context of mechanical testing is demonstrated. Selected mechanical properties of several composite systems are discussed and compared with those of more conventional aircraft materials, and finally the novel technique of hybridisation of composites is introduced. References 12 and 13 provide a detailed coverage of the material presented in this lecture.

2.   AVAILABLE FORMS OF MATERIAL

Advanced composites are usually supplied in the form of continuous tape or sheet. As shown in Fig. 1, the smaller diameter fibres are grouped as tows or yarns, while larger diameter fibres such as boron are in the form of monofilaments. With modern textile technology, a variety of woven forms are also available. Such forms allow easy combination of fibre types to produce hybrid composites such as aramid-glass, aramid-graphite and graphite-glass.

In non-woven unidirectional material, cross-stitches of the constituent fibre or glass fibre are sometimes used to aid collimation of the fibres. Boron filaments are only available in unidirectional form (they cannot be woven because of their large diameter), but are easily collimated and are held in place with a light glass scrim. Although boron is most commonly supplied as a tape, "continuous" sheets are also available.

Fibres may be supplied in the dry condition or pre-impregnated with resin, which aids in collimation and handling. The handling of these "pre-pregs" is also aided by partial curing (B-staging) of the resin to provide tackiness. The major disadvantage of pre-pregs is their limited shelf-life (even at -20°C) and the effect of resin cure advancement on processing variables.

68

Unidirectional and laminated composites are fabricated from stacked layers of pre-preg by heat-curing of the epoxy. Vacuum is generally applied during the initial stages of cure to aid in the removal of voids; then pressure is applied as the resin gels to remove excess resin. Usually a fibre volume fraction of 50-60% is most desirable. Further details of the fabrication process are discussed in Lecture 6.

3. PROPERTIES OF ADVANCED COMPOSITE SYSTEMS

3.1 General Comments

Experimental studies and theoretical analyses have shown that the properties of a fibre/matrix system depend not only on the properties of the constituents alone, but also upon their manner of interaction in "combined form". It has been shown, for example, that broken fibres within a composite can still contribute to load-bearing (Lecture 2) and that the microstructure of resins within composites (especially in close proximity to fibres) may be very different to that of the bulk material. Because of such complex features of a "composite system", the results of micro-mechanical analyses which rely on simplified models are only approximate, and physical testing of material is the only true guide for designing.

None the less, it is useful to use such analyses here, in a semi-quantitative way, to explain some of the properties of the composite systems to be discussed. In particular, it should be noted that the exceptionally high moduli and strengths of high performance fibres are not fully realized in the composite system. This follows from predicted law-of-mixtures expressions of the forms:

$$E_1 \cong E_f V_f \qquad \text{(ignoring the contribution}$$

and

$$\sigma_1 \cong \sigma_f V_f \qquad \text{from the matrix)}$$

where

E_1 = modulus of composite in fibre direction,

E_f = fibre modulus,

σ_1 = tensile strength of composite in fibre direction,

σ_f = fibre tensile strength,

V_f = fibre volume fraction.

Thus, in typical systems with about 60% fibre volume fractions, one could expect to achieve about 60% of the inherent fibre strengths and moduli in the longitudinal direction for a unidirectional composite. Values will be considerably less for multi-directional laminates and woven forms such as cloth.

The resin-sensitive, or "matrix dominated", (transverse and shear) properties are obviously much lower than the "fibre-dominated" properties in advanced composites as indicated by relations of the form

$$1/E_2 = V_f/E_f + V_m/E_m \approx V_m/E_m$$

and

$$1/G_{12} = V_f/G_f + V_m/G_m \approx V_m/G_m$$

where

E_m, G_m = matrix extensional and shear modulus, respectively,

G_f = fibre shear modulus,

E_2 = transverse modulus of composite,

G_{12} = in-plane shear modulus of composite,

V_m = matrix volume fraction.

However, these properties are certainly of importance in design considerations.

In Table 1 are shown typical values for the systems of interest. It is evident that the fibre-dominated properties are far superior to the matrix-dominated properties. Longitudinal strength values are typically 10 to 100 times greater than corresponding transverse and shear values, and longitudinal moduli are similarly much greater than transverse and shear moduli. It is interesting to note that Poisson's Ratio (v_{12}) may vary, depending on whether tensile or compressive stress is applied, and may also be a function of magnitude of the applied stress; however, the latter effect is not significant in most structural applications in which design limits of around 4000 micro strain are used to account for effects of environment, damage etc . (Furthermore, Poisson's Ratio may exceed 0.5 in anisotropic materials. For isotropic materials such as metals, Poisson's Ratio is always less than 0.5). Finally, it should be noted that while it is reasonable to assume that moduli are equal under tension and compression (at least at low strains), it is clearly evident from Table 1 that strengths in tension and compression are markedly different.

Good design with composites utilizes as fully as possible, the superior fibre-dominated properties. These properties are the subject of the following section, in which a comparison is made between advanced composites and more conventional aircraft materials.

3.2   Properties of Advanced Composites

High performance composites in general exhibit high strength and stiffness, low density and good resistance to fatigue and corrosion, properties which make them very well suited to many aircraft and aerospace

70

applications. Table 2 shows the markedly superior strength-to-weight and stiffness-to-weight properties of several composite systems compared to more conventional engineering materials. Boron/epoxy, for example, has four times the stiffness of an equivalent weight of steel and graphite/epoxy is five times stronger than the same weight of L65 aluminium alloy. It should be noted, however, that the properties shown here are for 0° uni-directional materials and are thus the maximum attainable values. In the multi-directional laminates encountered in practice, there will generally be substantial reductions from these values; for example, a typical laminate for a wing skin is likely to have an extensional modulus approximately half the uni-directional value.

It is also important to note that while many design applications are based on strength-to-weight and stiffness-to-weight properties, these are by no means the only criteria. Material efficiencies or "indices of merit" can be calculated for various structural forms (see refs. (1) and (2)); for example, the material efficiency of a thin panel which fails by buckling under compression is proportional to $E^{1/3}/\rho$ whilst that of a thin-walled tube which buckles under compression is proportional to $E^{\frac{1}{2}}/\rho$, where ρ denotes the density. The desirability of one material over another will thus depend on the details of the structure being considered. Even so, the strength and stiffness advantages of fibre composites on a weight basis are quite evident.

Typical tensile stress-strain curves are shown in Fig. 2. It can be clearly seen that glass/epoxy and aramid/epoxy, while having high tensile strengths, are not nearly as stiff as boron/epoxy and graphite/epoxy. A further disadvantage of aramid/epoxy is its very poor compression strength, but this is often overcome by hybridization with other fibre types as discussed later. Certainly, the major advantage of aramid/epoxy and glass/epoxy is their low cost, aramid and glass fibres costing less than $20/kg compared with graphite and boron fibres at $100/kg and $630/kg respectively.*

Finally, it should be noted that advanced composites in general have much lower coefficients of thermal expansion than most metals. For example, for graphite/epoxy $\alpha = 0.5 \times 10^{-6}$ °C^{-1} compared with 23×10^{-6} °C^{-1} for aluminium alloys. This mismatch can cause problems with adhesively bonded composite/metal joints, as will be discussed in Lecture 8. The thermal expansion co-efficient is also often markedly anisotropic in composites.

----

*The costs of graphite and boron fibres are presently undergoing changes. As graphite usage increases, its cost decreases, with some types of fibre now costing less than $100/kg. As boron usage has not increased, its cost continues to rise.

TABLE 1: Typical Properties of Unidirectional Composites

| | STRENGTH (GPa) | | | | MODULUS (GPa) | | | SHEAR STRENGTH (GPa) | POISSON'S RATIO (ν_{12}) |
| | LONGITUDINAL | | TRANSVERSE | | | | | | |
	TENSILE	COMPRESSIVE	TENSILE	COMPRESSIVE	LONGITUDINAL	TRANSVERSE	SHEAR		
Graphite/Epoxy (V_f = 60%)	1.1	0.7	0.02	0.13	130	7	6	0.06	0.28
Boron/Epoxy (V_f = 50%)	1.3	2.5	0.06	0.20	200	19	6	0.07	0.23
Glass/Epoxy (V_f = 45%)	1.1	0.6	0.03	0.12	40	8	4	0.07	0.26
Aramid/Epoxy (V_f = 60%)	1.4	0.2	0.01	0.05	80	6	2	0.03	0.34

TABLE 2: Comparative Properties of Composites and Metallic Aircraft Materials

* Units: GPa
Unidirectional Composites, 60% V_f

	BORON/ EPOXY	GRAPHITE/ EPOXY TYPE I	GRAPHITE/ EPOXY TYPE II	ARAMID/ EPOXY KEVLAR-49	GLASS/ EPOXY E-GLASS	STEEL S97	ALUMINIUM ALLOY L65	TITANIUM DTD 5173
SPECIFIC GRAVITY	2.0	1.6	1.5	1.45	1.9	7.8	2.8	4.5
TENSILE* STRENGTH	1.49	0.93	1.62	1.38	1.31	0.99	0.46	0.93
TENSILE* MODULUS	224	213	148	58	41	207	72	110
SPECIFIC* TENSILE STRENGTH	0.73	0.58	1.01	0.95	0.69	0.13	0.17	0.21
SPECIFIC* TENSILE MODULUS	110	133	92	40	22	27	26	24

73

4. CHARACTERISATION OF COMPOSITES

The mechanical properties of isotropic materials can be fully characterized by two elastic constants and a knowledge of tensile, compressive and shear strengths. With composites the situation is rather different, firstly because of their anisotropy and, secondly, because they generally are used in the form of laminated structures. Macro-mechanical analyses can be used to derive the properties of laminated structures from those of the unidirectional ply (Lecture 7), so it is only necessary to characterize the unidirectional material. The elastic constants required for such characerisation can be found from Hooke's Law which relates the stresses and strains in a material. For an anisotropic material in a general three-dimensional state of stress (Fig. 3(a)), Hooke's Law can be written in matrix notation, in terms of the compliance matrix, S_{ij}, as follows:

$$\begin{bmatrix} \varepsilon_1 \\ \varepsilon_2 \\ \varepsilon_3 \\ \gamma_{23} \\ \gamma_{31} \\ \gamma_{12} \end{bmatrix} = \begin{bmatrix} S_{11} & S_{12} & S_{13} & S_{14} & S_{15} & S_{16} \\ S_{21} & S_{22} & S_{23} & S_{24} & S_{25} & S_{26} \\ S_{31} & S_{32} & S_{33} & S_{34} & S_{35} & S_{36} \\ S_{41} & S_{42} & S_{43} & S_{44} & S_{45} & S_{46} \\ S_{51} & S_{52} & S_{53} & S_{54} & S_{55} & S_{56} \\ S_{61} & S_{62} & S_{63} & S_{64} & S_{65} & S_{66} \end{bmatrix} \begin{bmatrix} \sigma_1 \\ \sigma_2 \\ \sigma_3 \\ \tau_{23} \\ \tau_{31} \\ \tau_{12} \end{bmatrix} \quad ; \, S_{ij} = S_{ji}$$

Here there is a full coupling between the direct and shear strains (ε and γ) and the direct and shear stresses (σ and τ).

Because of material symmetries, in the case of a unidirectional composite, with the stress/strain co-ordinate axes referred to the principal material directions, the shear strains, γ, are independent of the direct stresses, σ, and the direct strains, ε, are independent of the shear stresses, τ, so that

$$\begin{bmatrix} \varepsilon_1 \\ \varepsilon_2 \\ \varepsilon_3 \\ \gamma_{23} \\ \gamma_{31} \\ \gamma_{12} \end{bmatrix} = \begin{bmatrix} S_{11} & S_{12} & S_{13} & 0 & 0 & 0 \\ S_{21} & S_{22} & S_{23} & 0 & 0 & 0 \\ S_{31} & S_{32} & S_{33} & 0 & 0 & 0 \\ 0 & 0 & 0 & S_{44} & 0 & 0 \\ 0 & 0 & 0 & 0 & S_{55} & 0 \\ 0 & 0 & 0 & 0 & 0 & S_{66} \end{bmatrix} \begin{bmatrix} \sigma_1 \\ \sigma_2 \\ \sigma_3 \\ \tau_{23} \\ \tau_{31} \\ \tau_{12} \end{bmatrix}$$

Any material having this type of stress-strain law is said to be "orthotropic."

A state of two-dimensional plane stress is usually assumed for individual layers within a laminate (Fig. 3(b)). Taking the plane of the laminate as the "1,2" plane, and setting $\sigma_3 = \tau_{23} = \tau_{31} = 0$, the last equations reduce to

$$\begin{bmatrix} \varepsilon_1 \\ \varepsilon_2 \\ \gamma_{12} \end{bmatrix} = \begin{bmatrix} S_{11} & S_{12} & 0 \\ S_{21} & S_{22} & 0 \\ 0 & 0 & S_{66} \end{bmatrix} \begin{bmatrix} \sigma_1 \\ \sigma_2 \\ \tau_{12} \end{bmatrix}$$

(Note that τ_{31} and τ_{23} may well be present as interlaminar shear stresses, but within the ply itself, they are negligible).

The components of the compliance matrix can be expressed in terms of the more familiar engineering elastic constants, Young's modulus E, Poisson's ratio ν and shear modulus G, as follows:

$$S_{11} = 1/E_1$$

$$S_{22} = 1/E_2$$

$$S_{12} = -\nu_{21}/E_2 = S_{21} = -\nu_{12}/E_1 \quad ,$$

$$S_{66} = 1/G_{12}.$$

There are thus five elastic constants required to characterize the material, four of which are independent since $S_{12} = S_{21}$. The shear modulus, G_{12} is also independent of the other elastic constants.

5. THE MECHANICAL TESTING OF COMPOSITES

5.1 Standard Testing Procedures

Fortunately, it is relatively straight-forward to adopt many of the mechanical testing methods developed for isotropic materials, to determine the mechanical properties of unidirectional composites in the principal material directions. Tensile moduli and strengths are usually determined using 0° and 90° parallel-sided specimens with bonded end-tabs in standard test machines (Fig. 4). Bonded strain gauges allow the determination of ν_{12} and ν_{21} at the same time. References (3) and (4) give details of standard testing procedures.

Compressive properties, particularly strength, are more difficult to determine because of brooming and buckling effects. Large, accurately-bonded, end-restraints, short gauge lengths, and possibly side-restraints must be used on test specimens.

Shear properties can be obtained (by the indirect use of laminate theory) using balanced ±45° tensile specimens (see ref. (5)), or by the torsion of a solid cylindrical rod with the fibres parallel to the longitudinal axis. This latter method can also be used to measure interlaminar shear response, at least to the limit of linearity.

The helically-wound tubular specimen certainly represents the most unified characterisation procedure (Fig. 5). All of the elastic constants and strengths can be determined (see refs. (6) and (7)) by applying axial load with one end free to rotate, torsional load with one end unconstrained in axial movement, and internal pressure. The only objection to using tubular or solid rod specimens is that their microstructures may not be representative of typical laminated panels. Off-axis properties can also be determined with tubular specimens.

5.2   Quality Control Tests

The most popular quality control tests are the flexural·and inter-laminar shear tests. They require only basic testing fixtures and use very simple specimen configurations with no end grips. Flexural tests can be done in three or four point bending and, for pure 0° or 90° specimens, can give valid estimates of strength and modulus.

The short-beam interlaminar shear test uses a three roller jig and a specimen with a small span-to-depth ratio. Although it is convenient and useful for revealing defects such as interlaminar porosity and resin-rich layers, it can not be used as a reliable measure of interlaminar shear strength because of the adverse effects of stress concentrations around the rollers. Testing procedures are detailed in ref. (8).

5.3   Difficulties in Testing Composites

Although straight-forward testing methods can be used for uni-directional composites when stress is applied in the principal material directions, difficulties arise with off-axis* testing and with multi-directional laminates. The major difficulty with off-axis testing is producing a uniform state of stress. Conventional gripping induces severe perturbations (bending and shear) into the stress field, an effect known as shear coupling (Fig. 6(a)). Severe errors would occur in calculated material properties using such a configuration, and for this reason "fixed-grip" testing is suitable only for 0°, 90° or balanced 0°/90° laminates**. The "floating-grip" (Fig. 6(b)) does produce a uniform stress field, but measurements are obviously difficult and results must be carefully interpreted (see refs. (10) and (11)). Similar coupling effects occur with unbalanced laminates (Fig. 7) and with off-angle tubular and cylindrical specimens if appropriate end constraints are not employed.

---

* An off-axis tension specimen is one in which the fibre direction does not coincide with the tension direction.

** A balanced laminate is one in which the mid-plane is a plane of mirror symmetry; often the term "symmetric laminate" is used in place of balanced laminate.

Another problem, especially with bend tests, is the stress concentrations induced at loading points. This, together with the tendency for non-linear behaviour, has restricted the use of such tests to quality control situations, although carefully interpreted results for 0°/90° laminates have given adequate results (see ref. (9)).

Finally, it should be noted that while it is easily realized that the sense in which direct stresses are applied (that is, either tensile or compressive) has a marked effect on material response, it is not as obvious that shear properties are affected in the same way. Consider, for example, the unidirectional 45° material under the two states of pure shear shown in Fig. 8. Clearly, the stress states felt by the fibres and matrix are quite different in the two cases, and different failure modes will result.

6. HYBRID COMPOSITES

A major advantage of laminated structures is the ability to incorporate materials in various combinations, allowing the utilization of desirable properties of one material to overcome the deficiencies in another. A classical example of hybridisation is the aramid-graphite hybrid, in which graphite provides the compression strength which aramids lack, while cost reduction is afforded by the aramids. The effect of hybridisation on the mechanical properties is shown in Fig. 9(a). Aramids are frequently used in hybrid structures where their high strain-to-failure capability provides improved impact resistance (Fig. 9(b)).

REFERENCES

1. Howard, H.B., Merit Indices for Structural Materials, AGARD Report No. 105, 1957.

2. Langley, M., Carbon Fibres in Engineering, McGraw-Hill, London, 1973.

3. Anon., Standard Test Method for Tensile Properties of Fiber-Resin Composites, ASTM D 3039-76, 1976.

4. Anon., Standard Test Method for Compressive Properties of Unidirectional or Crossply Fiber-Resin Composites, ASTM D 3410-75, 1975.

5. Anon., Standard Recommended Practice for Inplane Shear Stress-Shear Strain Response of Unidirectional Reinforced Plastics, ANSI/ASTM D 3518-76, 1976.

6. Pagano, N.J., Halpin, J.C. and Whitney, J.M., Tension Buckling of Anisotropic Cylinders, J. Comp. Mat., vol. 2, p. 154, 1968.

7. Whitney, J.M., Pagano, N.J. and Pipes, R.B., Design and Fabrication of Tubular Specimens for Composite Characterisation, ASTM STP 497, 1972.

8. Sturgeon, J.B., Specimens and Test Methods for Carbon Fibre Reinforced Plastics, Royal Aircraft Establishment, Technical Report 71026, February 1971.

9. Pagano, N.J., Analysis of the Flexure Test of Bidirectional Composites, J. Comp. Mat., vol. 1, p. 336, 1967.

10. Pagano, N.J. and Halpin, J.C., Influence of End Constraint in the Testing of Anisotropic Bodies, J. Comp. Mat., vol. 2., p. 18, 1968.

11. Wu, E.M. and Thomas, R.L., Off-Axis Test of a Composite, J. Comp. Mat., vol. 1, p. 336, 1967.

12. Ashton, J.E., Halpin, J.C. and Petit, P.H., Primer on Composite Materials: Analysis, Technomic, Stamford, Conn., 1969.

13. Tsai, S.W. and Hahn, T.H., Introduction to Composite Materials, Technomic, Westport, Conn., 1980.

Tape

"Broad Goods"

Glass carrier
scrim cloth

Matrix

Individual
fibre
e.g. boron

Removable
release backing

Yarn or tow
of fibres
eg. glass, graphite,
aramid

Removable
release backing
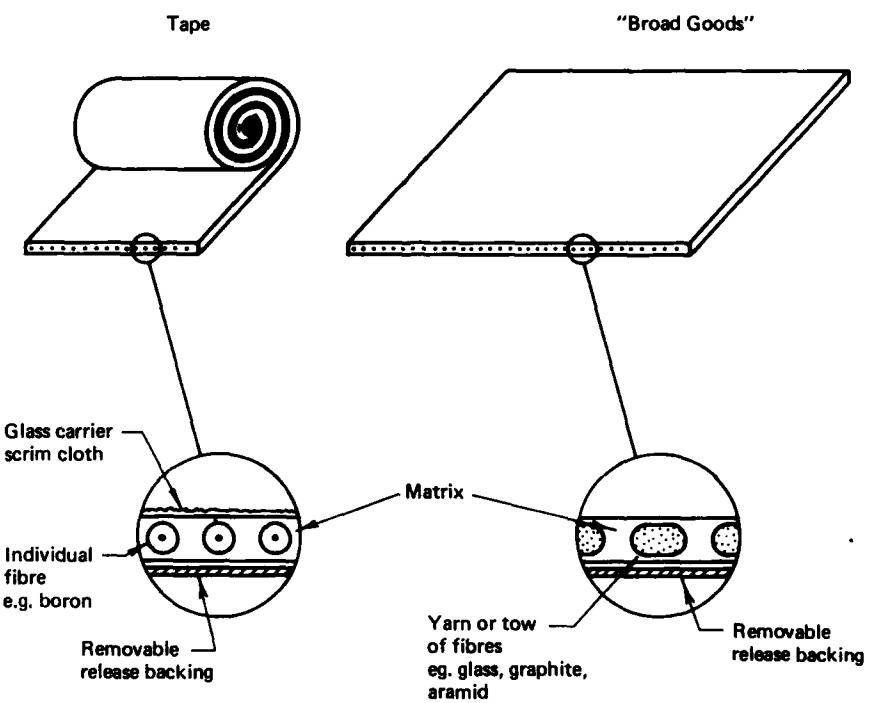
FIG. 1 — AVAILABLE FORMS OF COMPOSITE MATERIALS

79
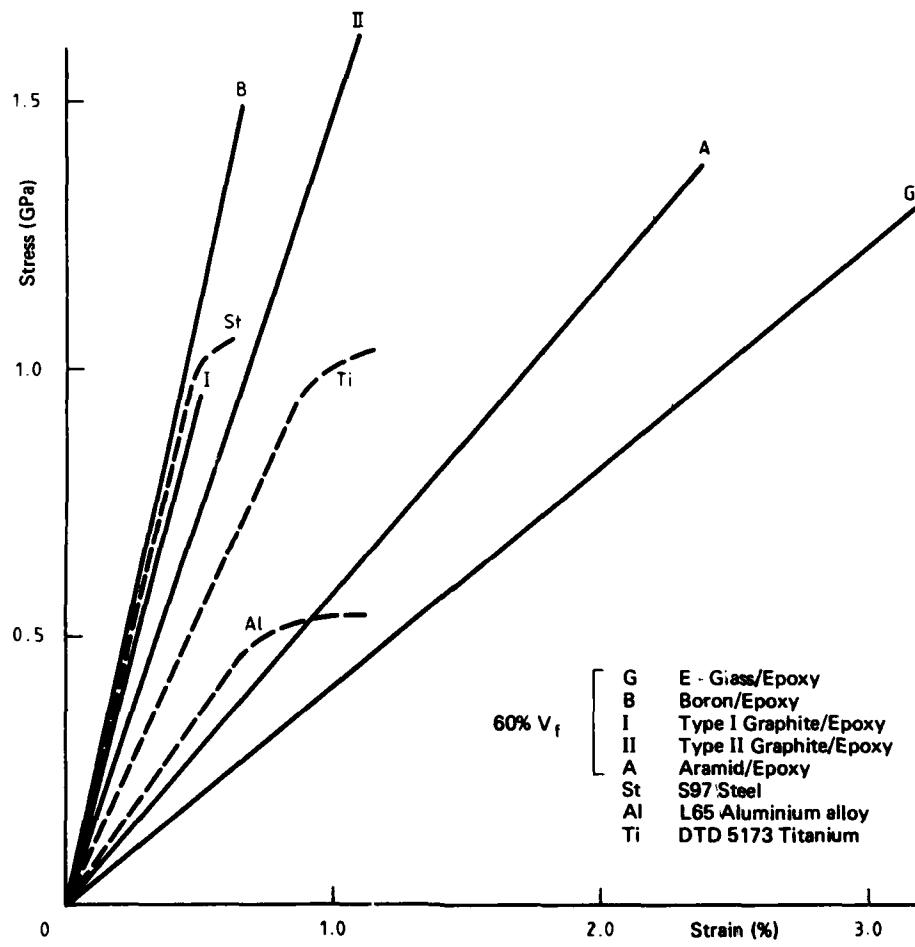
FIG 2 – COMPARISON OF TENSILE PROPERTIES OF COMPOSITES AND METALLIC
AIRCRAFT MATERIALS.

80

$\tau_{13} = \tau_{31}$
$\tau_{23} = \tau_{32}$
$\tau_{12} = \tau_{21}$

(a)

$\tau_{12} = \tau_{21}$

(b)
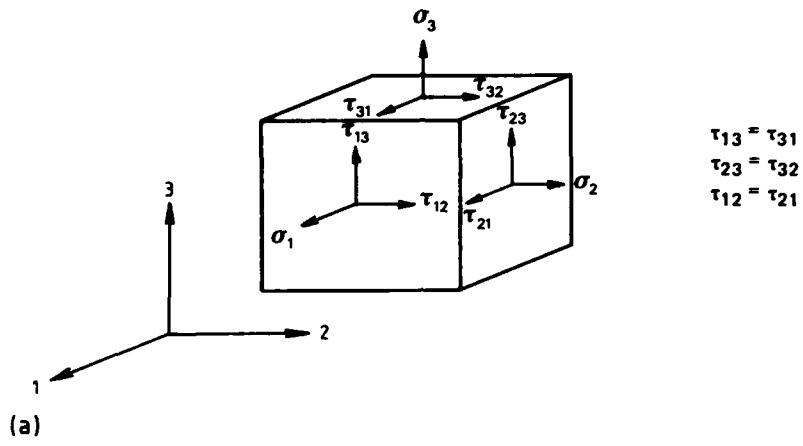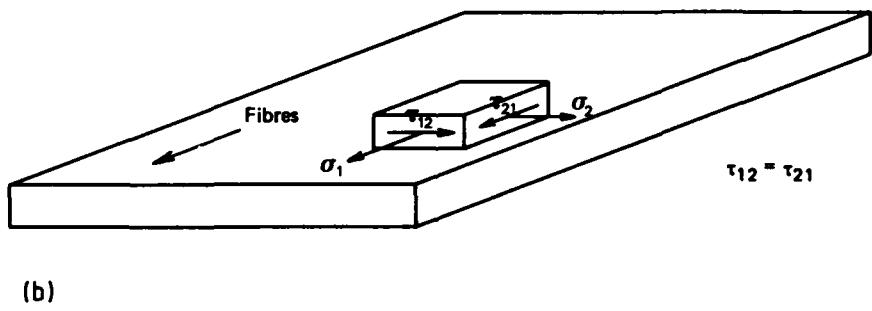
FIG 3 — (a) GENERAL THREE-DIMENSIONAL STRESS STATE
(b) TWO DIMENSIONAL PLANE STRESS STATE IN SINGLE PLY

81
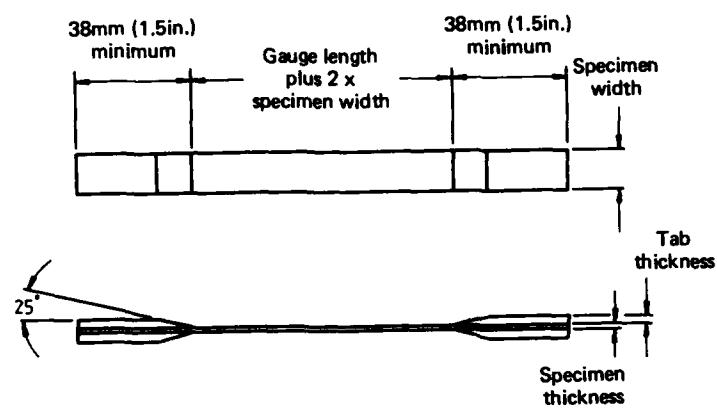
FIG 4 — TYPICAL TENSILE TEST SPECIMEN
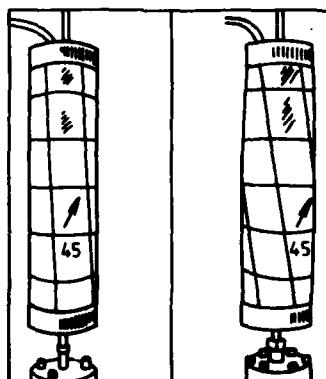
(a)   (b)

FIG 5 — HELICALLY — WOUND TUBULAR SPECIMEN
    (a) TENSION
    (b) INTERNAL PRESSURE
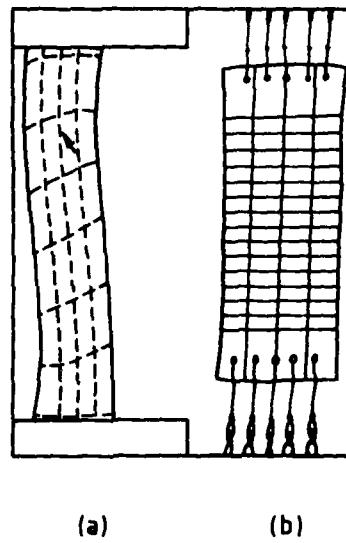
FIG 6 — EFFECTS OF END CONSTRAINTS ON OFF-ANGLE TENSILE RESPONSE
(a) SHEAR COUPLING EFFECTS
(b) UNCOUPLED WITH "FLOATING GRIP"
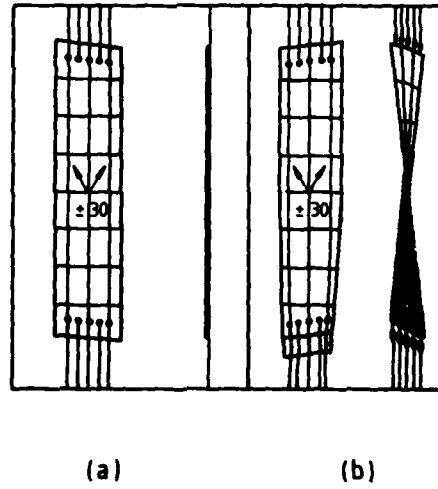
FIG 7 — UNSYMMETRICAL LAMINATE WITH "FLOATING GRIP"
(a) ZERO LOAD
(b) TENSILE LOAD

83
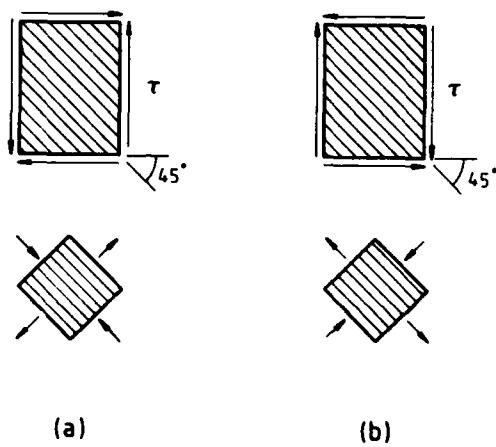
FIG 8 — THE EFFECT OF SENSE OF APPLIED SHEAR IN OFF-ANGLE TESTING

84

(a)

Strength (GPa)

(b)

Strength (GPa)

Energy (GNm)

Aramid to graphite ratio
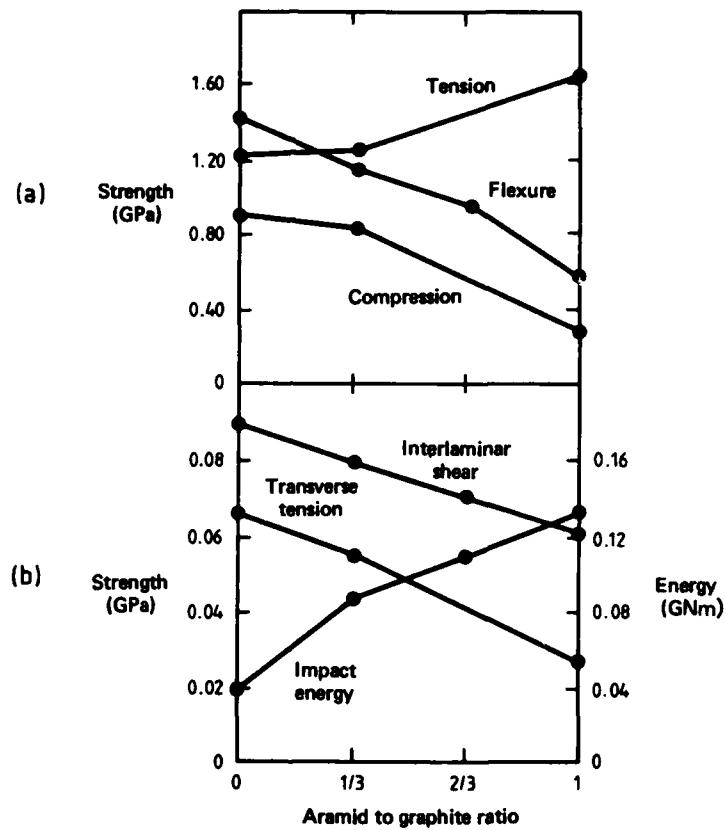
FIG 9 — VARIATION OF LAMINATE MECHANICAL PROPERTIES WITH DEGREE OF HYBRIDISATION FOR ARAMID–GRAPHITE FIBRE UNIDIRECTIONAL COMPOSITES

Lecture 6

COMPONENT FORM AND MANUFACTURE

A.A. BAKER

1. INTRODUCTION

Fibre reinforcement is essentially a one dimensional strengthening process. Since most components are stressed in more than one direction a major function of the forming procedure is to orient the fibres, in the matrix, in the appropriate directions and proportions to obtain the desired mechanical properties. The forming process must also produce the shape of the component and develop the required properties of the matrix. In an ideal fibrous structure the fibres may be aligned with the trajectories of principal stress and be concentrated in direct proportion to the local magnitude of the stress. This ideal is approached only by natural materials such as wood and bone.

The various manufacturing procedures for fibres reinforced plastics may be classified according to the form of the reinforcement; Fig. 1 shows this classification and compares the resulting structures with other more common, fibrous structures, both natural and artificial. At least in principle, all of the procedures based on continuous fibres (and some of the procedures based on discontinuous fibres) allow close tailoring of mechanical properties. These procedures, particularly those based on laminating, are used for manufacturing aircraft components from glass/epoxy, graphite/epoxy, aramid/epoxy and boron/epoxy, and will be the main subject of this paper. Typical generic aircraft components are listed in Table 1 with reference to the forming procedure employed.

TABLE 1: Typical Aircraft Fibre Composite Forms

Laminates	
Type of Structure	Application
sheets	wing skins
sandwich panels	control surfaces
shells	fuselage sections
beams	spars
complex forms	aerofoils
Filament Wound Forms	
closed shells	pressure vessels
open shells	radomes
tubes	drive shafts
secondary formed	helicopter blades
tubes	

86

In general, laminated and filament wound structures are relatively weak in the thickness direction and are thus limited to applications involving two dimensional loading such as those shown in Table 1.

Considerable efficiency is obtained by employing the reinforced material in the most highly stressed regions, for instance in the upper and lower surfaces of components subjected to bending. This is often achieved during component manufacture by using sandwich construction with the composite forming the outer skins which are adhesively bonded to a honeycomb or plastic foam core. It is interesting to note that some natural fibrous materials, such as bone may also employ this construction.

This paper initially outlines general laminating procedures and then describes their application to advanced fibre composites. The paper then goes on to describe the process of filament winding and the related process of braiding. Finally the process of pultrusion is outlined. Joining, a very important aspect of manufacture, is left for treatment in Lecture 8.

2. AN OUTLINE OF GENERAL LAMINATING PROCEDURES

2.1 General

Most reinforced plastic components based on continuous fibres are manufactured by some form of laminating procedure (1) in which sheets of fibres, either woven cloth or warp sheet (unidirectional fibres), are combined with resin and pressed against the surface of a mould. Heat, if required, is then applied to effect a cure. The various laminating procedures adopted, indicated in Fig. 2 will be outlined here. The techniques described here are also applicable to laminates based on random mat materials and mixtures of random mat and cloth, for instance as employed in the hull of a boat. Resin matrices may be polyester or epoxy.

2.2 Liquid Impregnation

In this procedure layers of fibres are placed in a mould cavity which is subsequently evacuated; resin is then forced into the cavity by atmospheric pressure. Problems are caused by the tendency of the resin to foam under vacuum and also by the tendency of the resin to follow the path of least resistance through the fibre network. Considerable improvement in the process is obtained if the resin is applied under positive pressure, usually after the mould has been evacuated. Although this procedure is only occasionally used for advanced fibre composites, it is capable of producing high volume fraction laminates with very good fibre distribution and low void content. It is best if the fibres are pre-coated with a small amount of resin since this aids in maintaining alignment during impregnation.

2.3 Open Die Moulding

Open die moulding involves the use of only one mould surface, over which the layers of fibre are placed - or "laid-up." If dry cloth is used, resin may be applied by brushing or by spraying. Alternatively, cloth

87

or warp sheet pre-impregnated with resin (pre-preg) may be employed. Pre-preg is used for most advanced applications; usually the resin is B staged (partially cured or advanced) to provide desirable tack and flow characteristics.

Various methods are employed to apply pressure to consolidate the lay-up; some of these are indicated in Fig. 2. In contact moulding, generally employed only for fairly low stress applications for glass/polyester composites, pressure is developed by hand rolling over a sheet of plastic film placed over the surface of the lay-up.

The bag procedure involve the use of a flexible plastic membrane which is formed over the surface of the lay-up to form a vacuum-tight bag. In vacuum bagging, the bag is simply evacuated and atmospheric pressure used to consolidate the lay-up against the surface of the mould. Alternatively, gas pressure may be used to apply the consolidation pressure in an autoclave. In this case the bag is evacuated initially to remove air and volatile materials. Vacuum bagging is a very cheap and versatile procedure; however, it can only provide limited consolidation pressure and may produce voided laminates due to the enlargement of bubbles trapped in the resin in regions of low pressure. Autoclave procedures, described in detail later, are used for most high quality laminates employed in the aircraft industry.

Pressure may be applied to the surface of an open mould by means of a flexible plunger. In this procedure, a solid rubber plunger is mounted in a press and used to force the lay-up against the wall of a female mould.

Temperature, if required to effect cure of the resin, is applied to the open mould in various ways, including external methods such as hot air blowers and ovens, or internally by electric elements or steam pipes buried in the mould. Temperatures up to 180°C may be required for high quality epoxy resin systems. Moulds are usually steel or aluminium alloys, particularly wi. internal heating is used. In order to reduce costs, plastic, wood or glass/epoxy open moulds may be used, at least for short or pre-production runs; however, these tend to distort and are difficult to seal under vacuum conditions.

2.4 Matched Die Moulding

Matched die moulding involves the use of matching tool steel male and female dies which close to form a cavity of the shape of the component. These are internally heated, if required, by electric elements or steam pipes. The fibres layers are placed over the lower mould section and the two halves of the mould are brought together in a press. The thickness of the part is usually controlled by lands which are built into the mould. The advantages of matched die moulding are: (i) a very high dimensional control is possible, (ii) a good surface finish is produced on both surfaces, and (iii) production rates can be high. However, the cost of the matching dies (with hardened faces) is very high; also the size of available hydraulic presses, used to apply the closing pressure, limits the size of parts that can be produced.

88

Wet laminating procedures may be used, in which case dry fibre is laid in the mould and the resin added subsequently. If random fibre mat is used, quite complex shapes can be produced; these are often preformed by spraying fibres onto a male mandrel prior to placing in the mould. Advanced fibre composite matched die components are almost always based on pre-preg starting materials.

2.5 Wrapping

Wrapping is an alternative procedure to filament winding for producing tubular components. Prepreg sheet, either warp sheet or cloth, is wrapped onto a removeable metal mandrel and cured under pressure. Special machines are available to perform the wrapping operations. Pressure during elevated temperature cure may be applied by shrink film (applied by a tape winding machine), by vacuum bag, or by autoclave procedures. Alternatively, a silicon rubber bladder may initially be placed over the mandrel prior to wrapping, and then this may be pressurised against an outer mould surface when the laminate has been wrapped in place. Internal pressurisation allows much smaller fibre movement during consolidation of the wrap.

2.6 Continuous Laminating

In this procedure continuous flat shaped or corrugated sheet is continuously fabricated. Sheets of cloth or mat, taken from a large roll, are passed through a resin bath and then brought together between plastic sheets by squeeze rollers which consolidate the layers and form the required section.

3. LAMINATING PROCEDURES FOR ADVANCED FIBRE COMPOSITES

3.1 General

Advanced fibre composite aircraft components are most usually made by a laminating procedure in which plies of pre-preg warp sheet or cloth are laid-up, with the fibres at various prescribed angles, and consolidated against a mould surface under temperature and pressure. Reference (2) gives a good general description of the topics covered here.

The most common ply configuration employed consists of plies of 0°, ±45° and 90°, where the angles are taken with respect to the principal load axis e.g. the spanwise direction in the case of a wing. Considered simply, the 0° fibres provide for the direct loads in the principal direction, the ±45° plies the torsional loads about this axis, and the 90° plies for the transverse loads. The proportion of plies used in each direction depends on the particular application. Thus the skins for a sandwich panel used as a torsion box may consist largely of 0° and ±45° plies with a small number of 90° plies, whereas the skins for a sandwich panel used for a floor beam may have equal proportions of 0° and 90° plies. To avoid distortion, the plies are usually orientated symmetrically about the mid plane of the laminate with equal numbers of +45° and -45° plies.

The laminating procedure is a very versatile method of manufacture; for example, it allows (i) very wide variations in skin thickness, (ii) inclusion of local reinforcements, such as extra ±45° material around fastener hole regions, (iii) inclusion of metallic inserts for joining, (iv) cocuring of stiffners, and (v) formation of honeycomb core regions.

The laminate need not be made up of only one type of ply material. Hybrid constructions involving two or more materials may be employed to improve certain properties or simply to reduce cost. Thus a graphite/epoxy-aramid/epoxy hybrid may be used because it has a higher toughness than graphite/epoxy alone and a higher compression strength than aramid/epoxy alone.

Fabrication of advanced fibre composites, particularly those employed for flight critical components, calls for a very high degree of process control, very much higher than that normally associated with similar procedures for glass/polyester composites. Close control must be exercised over factors such as fibre content, orientation and distribution, resin matrix integrity (freedom from voids, delaminations, cracks), resin properties (including degree of cure), and dimensional tolerances, including distortion.

In order to obtain the required level of control, pre-preg warp sheet or cloth materials are used, employing open die or closed die procedures. Open die laminating, using autoclave procedures, is extensively employed, particularly for large components such as wing and tail skins, doors, fuselage sections and spars. Matched die moulding is only used for long runs of small components, or in fairly large complex components where very high dimensional accuracy is essential e.g. for fan or helicopter rotor blades. Thermal expansion of a rubber insert, or pressure expansion of a rubber bladder, may be used to produce internal pressurisation of shell components, in combination with autoclave or matched die procedures.

3.2 Pre-Preg Materials

Pre-preg materials are based on warp sheet or on woven cloth. Graphite and aramid warp sheet materials usually consist of axially aligned fibres held in position on release film by the tack of the impregnating resin. Boron fibres, however, because of their large diameter (125 μm compared with 8 μm for graphite) and high modulus, are held in place on a light woven glass cloth backing, which is incorporated into the laminate. Warp sheet and cloth pre-preg materials are made by a specialist company to mould to a particular thickness when correctly processed; in the case of most graphite fibre warp sheet this is about 0.13 mm. Then the fibre volume fraction is about 55% to 60%.

A wide variety of graphite and aramid woven fibre materials are available (boron is too stiff to weave into a cloth) having different weaves and tow sizes. Additionally, hybrid woven cloths are available in which two different fibres such as graphite and glass are combined in various arrangements. A typical example is a cloth having a graphite fibre warp and a glass fibre weft. Since cloth is relatively easy to handle dry, pre-preging may be carried out by the component fabricator.

The resin content in pre-preg is usually up to 15% by weight more than required in the laminate, to allow for flow during component manufacture. Until fairly recently, it was considered that resin flow is required to sweep out voids or bubbles. It is now considered by some manufacturers that, with good process control, excess resin is not required - particularly for woven cloth where voids are not as serious since they do not lie in interlaminar regions. Thus, the trend now is to use a zero-bleed pre-preg.

Pre-preg and cloth are available as tape about 75 mm wide or as sheet 1.2 m wide, contained between layers of release paper on rolls. Pre-preg materials are usually stored at a temperature of about -20°C, in which case their usable life is about twelve to eighteen months.

3.3 Ply Cutting and Lay-Up Procedures

Plies are cut from the pre-preg material to the required size and, with the required fibre orientation, are then laid-up onto the surface of the die or moulding tool prior to consolidation under temperature and pressure. The cutting and lay-up operations are performed in a clean room, free of dust which is held at constant temperature and (low) humidity. Various procedures are employed to cut the plies from wide sheet (obtained directly or formed from tape), including Gerber knife, laser or waterjet. These procedures, adapted from modern cloth cutting procedures in the textile industry, are generally numerically controlled. Each cut ply is held on a mylar template which has index holes to allow correct positioning on corresponding pegs on the mould and an identification number which allows correct sequencing of the ply in the thickness of the laminate. The ply is transferred to the laminate stack with a roller when the mylar is positioned on the tool, ply face downwards.

Plies are formed from tape by a tape laying procedure which may be hand controlled or may be partially or fully automatic. Tape is rolled onto the mylar template side by side to produce a sheet which must be free of gaps and excessive overlaps. The automatic procedures often rely on an opaque marking tape attached to the mylar which activates a cutter through a light-sensitive switch. A numerically controlled cutter (e.g. laser) is used to trim the cut edge to the correct contour. Alternatively, tape laying may be used to form the complete lay-up directly onto the mould surface, without the need for separate operations. This procedure requires very uniform high quality tape and very reliable machine operation to ensure that defective material, gaps, or overlaps are not incorporated into the lay-up.

Finally, for thick lay ups, e.g. exceeding about 16 plies, intermediate vacuum bagging operations may be employed to reduce bulk (debulk) so as to minimise movement during subsequent moulding. Vacuum bagging may also be used to preform laminates into deep contours.

3.4 Autoclave Procedures

An autoclave, Fig. 3, is essentially a large pressure vessel (pressurised with air, nitrogen, or carbon dioxide), which is internally heated, and in which the lay-up is consolidated against an open die or mould. Typical

temperatures are 150°C and pressures 1 MPa. A vacuum bag is formed over the lay-up and mould surface, primarily to allow pressure to force the lay-up against the mould surface. Prior to application of gas pressure (from the time of lay-up) the bag is held under vacuum to keep the lay-up in position and to remove air and volatiles. When an intermediate temperature is reached, the vacuum is vented to atmosphere and the temperature and pressure raised to effect cure. During the processing it is most important to insure that the resin is not allowed to gel under vacuum or a voided laminate will result due to the abnormal size of gas bubbles under reduced pressure. Any flaws in the vacuum bag system which may have occurred in the autoclave are detected by loss of the pressurising gas through the vacuum line.

The vacuum bag may be a thin impermeable plastic material, such as nylon, which is disposable, or a preformed silicone rubber, which is reusable. Butyl rubber paste is used to seal the disposable bag, whereas various types of moulded-in ring seals are employed for the reusable bags. Several layers of material are employed over the lay-up inside the vacuum bag (Fig. 4) including a bleeder layer (glass or jute cloth) to distribute vacuum and absorb excess resin, and separator films, (PTFE coated glass cloth, nylon cloth, or plastic film such as nylon or PTFE), porous on top of the lay-up and non-porous underneath, to allow separation of the laminate from the tool surface. The part is generally surrounded by a compressible (cork-neoprene) edge dam which serves to prevent

(a) sideways movement of the part,

(b) overthinning of the edges, and

(c) excess loss of resin from the edges.

Thermocouples are sealed in position in various regions of the lay-up to determine temperature distribution and control heating rate.

Autoclave tools must be vacuum-tight, free from distortions under temperature and pressure and have a low thermal mass to allow fairly rapid heating and cooling. The usual construction is a sheet steel fabrication; however, electroformed nickel is excellent for producing inexpensive, but durable, complex moulds. Moulds based on graphite/epoxy fibre honeycomb construction are also used. These have the advantage of thermal expansion compatibility with the graphite/epoxy laminates; they also resist distortion under pressure and, as a result of their low thermal mass, allow rapid heating and cooling.

Heat may be applied to the autoclave by using fans to circulate the pressurisation gas over electrically or steam heated elements. Alternative-ly, the moulds may be internally heated from built-in electrical resistance elements. This latter method usually produces the best temperature distribu-tion through the part.

92
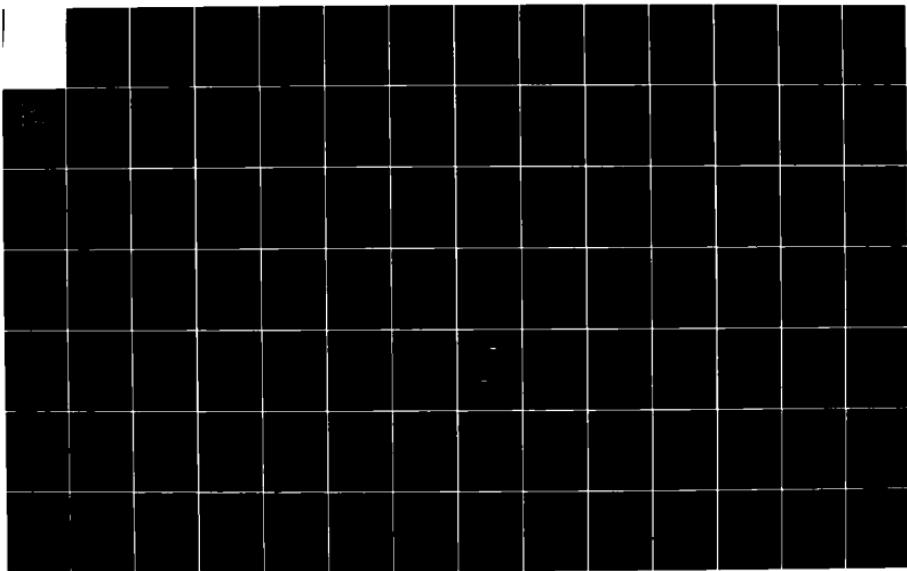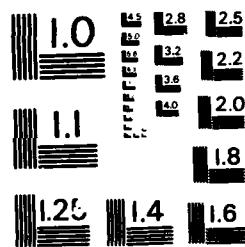
MICROCOPY RESOLUTION TEST CHART

NATIONAL BUREAU OF STANDARDS—1963—A

3.5 Autoclave Manufacture of Some Typical Components

Manufacture of a honeycomb core component is illustrated in Fig. 5. In this case the inner and outer skins are shown to be cocured to the honeycomb; however, in applications where optimum properties are required in the outer skin, the skin would be precured.

Manufacture of sine-wave spars is a fairly complex operation, involving a combination of matched die and autoclave moulding; Fig. 6 shows the major steps. The overall procedure involves (i) lay-up onto a flat tool, (ii) form to shape in a roller jig, (iii) place in matched die tool, (iv) fold out cap plies, (v) place graphite/epoxy preforms into groove, (vi) place on cap plies, (vii) place pressure plate over cap plies, (viii) place vacuum bag assembly over mould, (ix) cure in autoclave.

Quite complex integral structures can be manufactured by autoclave procedures. For example Rockwell International (3) have carried out fabrication studies involving the manufacture of tip-to-tip wing sections, containing the lower skin and integral sine wave spars. The procedure involved (i) preconsolidate and partially cure the spar (Fig. 7 left), (ii) preconsolidate and partially cure the lower skin, (iii) assemble the lower skin and spar (the spars are held in permanent location by barbed metal tacks), and finally (iv) cocure the spars and skins (Fig. 7 right). This procedure involves use of silicone rubber bagging and low bleed (or pre-bled) pre-preg material.

3.6 Matched Die Moulding, Cure Requirements

During matched die moulding it is particularly important that pressure is applied at the correct gellation stage of the resin. The usual procedure is to apply a holding pressure for a dwell period at temperature (typically 150°C) until the onset of gellation and then increase pressure to close the dies. If pressure is applied too early an excessive amount of the, still highly fluid, resin is expelled from the laminate which then cures under low pressure once the dies contact on the lands. The result is a voided laminate with a very poor surface finish. If, however, the pressure is applied after gellation, it is not possible to close the dies and resin flow cannot occur to sweep out voids; an oversize, resin rich, voided laminate results.

3.7 Expansion Moulding Procedures

Thermal Expansion Rubber Techniques

Thermal expansion rubber moulding utilises the high coefficient of expansion of silicone rubber (approximately 10^{-4} °C^{-1}) and its thermal stability. This procedure can be employed to produce complex structures such as integrally moulded skin boxes and complex forms such as sine wave spars. Generally, elastomeric blocks are wrapped with the composite pre-preg or the blocks are placed in position inside a formed lay-up. The assembly is then

placed in a matched die, or an autoclave, which reacts out the expansion forces, allowing accurate formation of the outside face of the component. Often the elastomeric blocks are hollow to avoid development of excessive pressure during moulding.

Zero bleed pre-preg is usually used, since it is difficult to allow for resin bleed in this type of moulding. Vacuum bag debulking is employed to minimise the internal movement required during final moulding.

Bladder Expansion Techniques

This procedure is similar to expansion rubber moulding except that gas pressure is used to expand a rubber bladder wrapped with the pre-preg against the cavity walls of a matched die. Alternatively, the bladder may be placed over a metal mandrel which contains holes to allow access of the pressurisation gas. This procedure is more controllable but less versatile than expansion rubber moulding. Bladder materials are usually cloth reinforced silicone rubber or teflon.

Expansion moulding procedures are often used for the manufacture of complex components involving internal cavities and may be employed with either matched dies or in an autoclave. This procedure is also employed with filament winding, as described in Section 4.4.

3.8 Cure Monitoring

In order to ensure reproducible production of high quality laminates (particularly in matched die moulding) a knowledge is required of the gellation time of the resin. Presently this information is usually obtained by simple laboratory measurements which must be repeated as a given batch of material ages - this problem is avoided by the use of fresh material. Various cure monitoring procedures have been developed to obtain information on the gellation point during the moulding process (4). These procedures are based on measurements of either (i) resin viscosity, (ii) dielectric properties, or (iii) ion conductivity.

Measurement of resin viscosity is the most direct method but it is rather difficult to arrange, particularly with low bleed resin systems, and is difficult to automate. Ion conductivity is based on the mobility of charged ions in the resin system; the mobility and therefore (AC) conductivity of the resin falls as the resin cures.

The dielectric procedure is presently the most highly developed procedure. In this technique two insulated metal electrodes are placed on either side of the laminate. The electrodes are connected to a dielectrometry instrument which measures dielectric properties, particularly the loss tangent. The dielectric properties of the resin are a function of the ability of the dipoles in the resin system to rotate in phase with the electric field provided by the instrument. As the resin begins to gel, the dipole movement becomes more difficult. The change in loss-tangent is detected by the instrument and the indication is used as a signal to apply full pressure to the mould.

94

Eventually presses and autoclaves could be controlled automatically by this procedure however, it does not appear to be widely employed at present.

3.9 Quality Control

(a) Pre-Preg

Pre-preg materials are usually supplied by a specialist company to close specification. However, the aircraft manufacturer generally performs extensive tests (5) to establish that the following items conform to specification: (i) fibre properties, (ii) fibre or resin content, (iii) resin/hardener formulation, (iv) residual volatile material, (v) moisture content, (vi) flow properties, (vii) degree of advancement (age) of the resin system.

Tests on the stage of advancement of the resin would be repeated through the refrigerated storage (-20°C) period to ensure that the pre-preg is used before the resin overages.

(b) Processing

During manufacture of the component the temperature in various regions of the laminate is recorded and plotted, together with details of the pressure cycle including leak rate of the pressurisation gas through the vacuum bag, which is a measure of the integrity of the bagging system and, therefore, the pressurisation cycle.

Test coupons (and possibly even structural details) are laid-up and processed with each major component for evaluation usually of interlaminar shear strength and flexural strength.

(c) Final Laminate

Some of the types of manufacturing faults which can occur in the laminate component are listed in Table 2. Superficial faults, dimension errors and distortion are readily found by inspection. Extensive NDI measurements are performed to inspect for internal flaws. The main techniques employed are C-scan ultrasonics in a water bath, or employing a water jet, to detect voids and delaminations, and radiography to detect foreign objects such as release film) and to examine the condition of honeycomb core regions. Test coupons are mechanically tested to determine interlaminar shear and flexural strength, and structural details representing highly critical regions may be tested under representative loading and environmental conditions.

95

TABLE 2: Manufacturing Faults in Fibre Composite Laminates

Plain Laminates
Voids Delaminations Disbonds - e.g. from metallic inserts Foreign body inclusion - e.g. release film Resin starved areas Resin rich areas Incomplete resin cure Incorrect fibre orientation (including wavy fibres) Incorrect ply sequence Fibre gaps Wrinkled layers Poor surface condition - e.g. poor release from mould Tolerance errors.
Sandwich Panels (In addition to above)
Poor core splice Disbonds from skins Crushed core Core gaps.

4.   FILAMENT WINDING

    4.1   General

        Filament winding (6), (7) is the second major process for producing
high performance fibre composite structures. It is mainly employed to produce
pressure vessels and other shell-like structures. The process involves winding
continuous fibres, combined with resin, over a rotating mandrel, which is
subsequently removed. In some winding modes the resulting structure can be
similar to a laminate; however, in other winding modes a degree of weaving
between the fibres occurs.

        The major advantage of filament winding is that fibres can be layed
under controlled tension precisely onto a curved mandrel surface. Thus, hollow
vessels are readily produced. Since, with some winding patterns, the fibres
can be made to follow a geodesic path (shortest distance between two points on
a curved surface) it is possible to arrange for very efficient utilisation of
the fibres. This is particularly useful in a pressure vessel where, ideally,
all the fibres can be uniformly loaded in tension.

The filament winding procedure is much less versatile than the general laminating procedures described earlier, particularly for complex forms with varying thickness and fibre orientation. However, variants of the procedure have been developed which allow formation of a variety of shapes which are not simple solids of revolution, such as helicopter blades, and could ultimately extend the capability of the procedure to the production of wing torque boxes and fuselage sections.

4.2 Winding Patterns

The basic winding patterns employed are illustrated in Fig. 8. The longitudinal, or polar, winding pattern is obtained by winding over the poles of the mandrel. This method is particularly suited to winding enclosed vessels; however, to obtain the required hoop strength in a pressure vessel, the polar wind must be over-wound with a number of hoop layers, in the same ratio as the biaxial stress ratio. The helical winding pattern is formed by a winding machine with a lathe type of action (Fig. 9) using a controlled out-of-phase movement between the mandrel and the winding head to obtain the correct fibre distribution. Helical winding may be used alone, in which case the optimum winding angle for a pressure vessel is 54.75°, or with hoop windings. The helical winding pattern produces cross-overs which is a disadvantage because the local bending at these points increases fibre stresses; however, the interlocking may improve inter-laminar strength. Helical winding produces an ideal fibre geometry particularly over end closures since the fibres are wound on geodesic paths; however, over all, comparison of the advantages and disadvantages of the winding patterns is rather complex.

Design of filament wound structures is often based on netting analysis which assumes that the fibres provide all the longitudinal stiffness and the matrix provides all the transverse and shear stiffness. However, a more realistic procedure is to use laminate theory which does account for matrix contributions.

4.3 Manufacturing Procedures

The winding machine (Fig. 9) consists of a mandrel and head to feed the reinforcement. Ancillary to this, are devices to control tension in the filaments, which consist of multi-fibre tows often taken from several spools.

In the wet winding procedure, dry fibres are passed through a heated resin bath. Rollers, are used to remove excess resin, force the resin into the fibre strands, and form a flat tape. In order to improve handlability and prevent damage the fibres are usually coated with a light size. Alternatively, a pre-preg may be used, in which case the mandrel must be heated to obtain tack and resin flow. Use of pre-preg allows high winding angles because of the high tack that can be developed, and avoids resin handling problems.

Mandrels may be steel or aluminium if withdrawal is possible. Where simple withdrawal is not possible various types of removable mandrels are employed, including low melting point metal and soluble plastic. Inflatable and collapsible mandrels are also used.

Filament wound vessels can leak under high pressures through voids and cracking in the resin matrix. This problem is generally overcome through the use of metal or rubber liners which are placed over the mandrel prior to winding.

Metallic end closures are usually required in pressure vessels. These are placed on the mandrel and incorporated into the structure during winding.

Glass, aramid and graphite fibres can all be successfully filament wound. However, graphite fibres can cause severe handling difficulties because of their tendency to break up during passage to the mandrel. This problem results from their high stiffness and high coefficient of friction. Frictional problems can be greatly reduced by the use of a light resin coating or size on the fibres.

4.4 Secondary Moulding

Filament winding can also be used to produce components which are not solids of revolution. Components for helicopters and remotely piloted vehicles have been made by this process, which initially involves winding onto an inflatable plastic or rubber mandrel. After winding, the mandrel (covered by the still wet winding) is deflated and placed in a matched die mould; the mandrel is then reinflated to pressurise the composite and effect a cure. Even structures with a honeycomb core can be made by this procedure, in this case employing two stages of winding.

4.5 Manufacture of Helicopter Blades

Filament winding procedures, combined with secondary moulding, are now generally employed to produce the spars for helicopter blades. The winding and moulding procedures involved in a particular case (8), shown schematically in Fig. 10, involve (a) polar winding the 0° fibre spar caps, including wrap around roots, (b) helical winding ±45° inner and outer torque tubes for the spar, and (c) polar winding the trailing edge. The inner torque tube is wound over a rubber bag supported by a metal mandrel. After winding, the metal part is removed so that the torque tube wrap can be pressurised and cured in a matched die mould along with the spar caps. This assembly is then covered with helical windings and remoulded to form the complete spar assembly. The formation of the rest of the blade, including the after-body aerofoil (±45° fibres on a honeycomb core), is indicated in Figure 10.

4.6 Braiding

Braiding is a form of filament-winding in which a number of filament spools, mounted on a ring, produce a woven layer on a central mandrel as it moves through the ring. Although the mechanical properties of braided composites are comparable only with woven cloth, the process offers a number of advantages: (i) non-circular shapes (such as box sections) and complex shapes (such as forks and bends in pipes), including section changes, can be braided, (ii) deposition of the composite is rapid, (iii) continuous forms can be produced as in pultrusion, but with angular, as well as

longitudinal reinforcement and (iv) the braided material can be remoulded.
Glass, aramid and graphite fibres can be braided; however graphite fibres,
even when sized are difficult to handle without excessive fibre damage.

5. PULTRUSION

Continuous uniform sections such as rods, tubes, and beams (I
sections etc.) can be made by pultrusion (2). In this process, schematical-
ly illustrated in Fig. 11, continuous fibres from individual spools are
pulled through a resin bath, combined, and then pulled through a forming die.
The die, usually chromium plated steel, forms the section shape and squeezes
out excess resin; in some cases the die is heated and may then partially
or finally cure the composite. Usually, however, an oven (or, alternatively,
a microwave unit) is used to effect final cure.

Structures with very high fibre volume fractions (approximately 70%)
can be produced, giving excellent unidirectional strength and stiffness.
However, as may be expected, transverse strength is low. This limitation can
be reduced by incorporating glass cloth or mat into the structure.

One of the major problems with pultrusion is that surface damage
occurs due to frictional forces in the die - particularly if the dies are
not provided with a sufficiently gradual section decrease. Friction causes
pieces of semi-cured resin to shear off and attach to the die surface
(where they can cure) and then score the surface of the material following.
This problem can be reduced by periodically stopping the run and allowing the
separate resin particles to attach themselves to the material in the die.
When the run is continued the die is swept clean.

Glass, aramid and graphite fibres can be successfully pultruded.
A resin size is generally used on graphite fibres to avoid handling damage.
Pultruded glass fibre reinforced polyester sections are readily available
off the shelf.

Both polyester and epoxy resins may be used. Sometimes a small
amount of an internal release agent such as an alcohol phosphate is added to
the resin to reduce friction drag during pultruding. However, this addition
can adversely affect the properties of the composite.

6. MACHINING

Graphite/epoxy materials pose no major machining problems.
However aramid/epoxy does cause difficulties due to its inherent toughness,
and specially designed tools are required. Boron/epoxy is very difficult
indeed to machine as a result of the extreme hardness of the boron fibres,
which is close to diamond. Conventional machining operations require diamond
impregnated tools, or alternatively, ultrasonic procedures with diamond
paste.

Machining and drilling of graphite/epoxy (2) can be satisfactorily
performed with tungsten carbide tipped tools. The main difficulty with
drilling is that the composite can be delaminated fairly readily if it is

not firmly supported during drilling (e.g. by sandwiching it between scrap material), and if the rate of drill feed is too high. A particular problem is the tendency for local tearing during drill breakthrough. This difficulty can be greatly reduced by bonding a layer of film adhesive to the exit face of the laminate.

Milling can be performed with conventional tungsten carbide end mills. Damage to the laminate is avoided if the mill passes are made in the fibre direction, since this minimises fibre tear-out. Surface grinding can best be performed with silicon carbide wheels. Cutting and slitting are best performed with diamond impregnated tools.

The advanced procedures employing lasers, or those employing ultrasonic techniques, are effective with all of the advanced composites.

REFERENCES

1. Sonneborn, R.H., Dietz, A.G. and Heysen, A.S., Fibreglass Reinforced Plastics, Reinhold, New York, 1954.

2. Langley, M. (ed.), Carbon Fibres in Engineering, McGraw-Hill, London, 1973, (Chapter 3 by M. Molyneux).

3. Lackman, C.M., O'Brien, W.L. and Loyd, M.S., Advanced Composites Integral Structures Meet the Challenge of Future Aircraft Systems, pp. 125-144 of "Fibrous Composites in Structural Design", ed. by Lenoe, E.M., Oplinger, D.W. and Burke, J.J., Plenum Press, New York, 1980.

4. Instrumental Cure Monitoring - State of Art, Group of Four Papers, Chaired by May, C.A., 22nd National SAMPE Symposium, vol. 22, pp. 618-662, 1977.

5. Carpenter, J.F. and Bartels, T.T., Characterisation and Control of Composite Pre-pregs and Adhesives, SAMPE Quarterly, vol. 7, pp. 1-7, 1976.

6. Rosato, D.V. and Grove, C.S., Filament Winding, Interscience New York, 1964.

7. Ainsworth, L., The State of Filament Winding, Composites, vol. 2, p. 14, 1971.

8. Covington, C.E. and Baumgardner, P.S., Design and Production of Fibreglass Helicopter Rotor Blades, pp. 497-515 of "Fibrous Composites in Structural Design", ed. by Lenoe, E.M., Oplinger, D.W. and Burke, J.J., Plenum Press, New York, 1980.
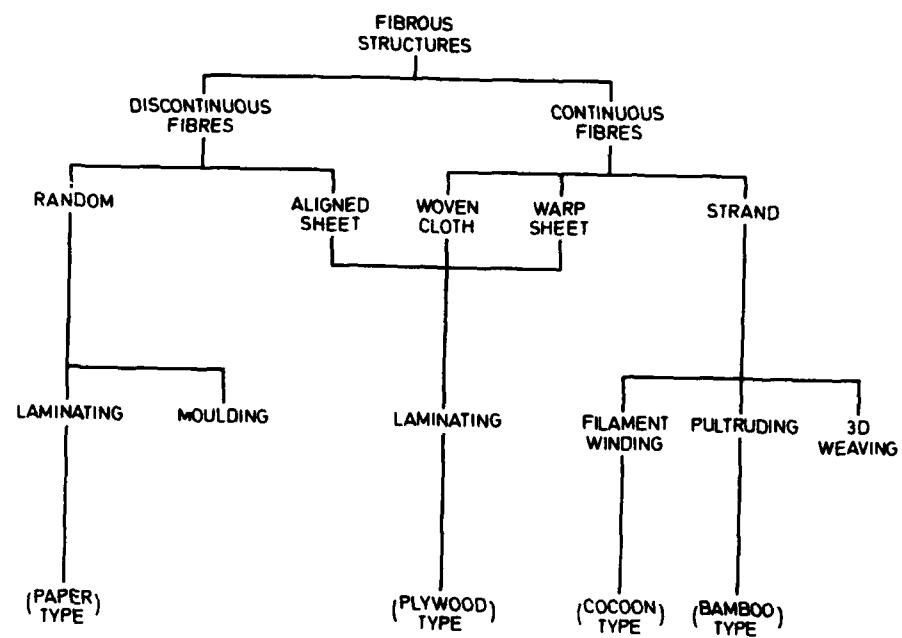
FIG 1   CLASSIFICATION OF MANUFACTURING PROCEDURES
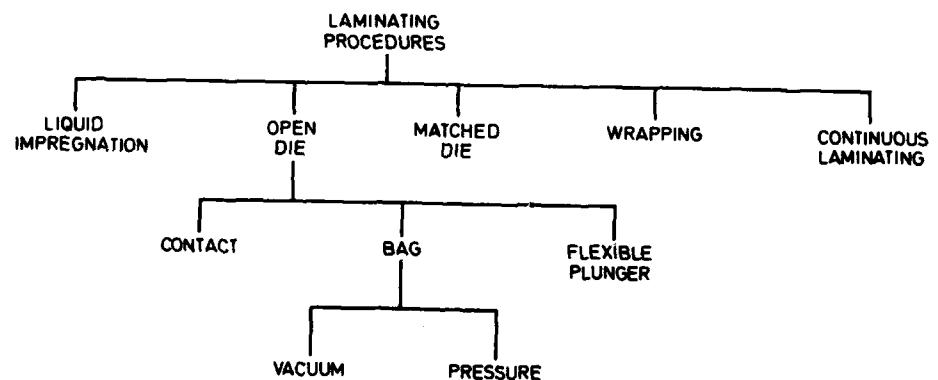
FIG 2   CLASSIFICATION OF LAMINATING PROCEDURES

102

Pressure inlet   Autoclave wall

Lay-up   Bag   Mould base plate

← Vacuum
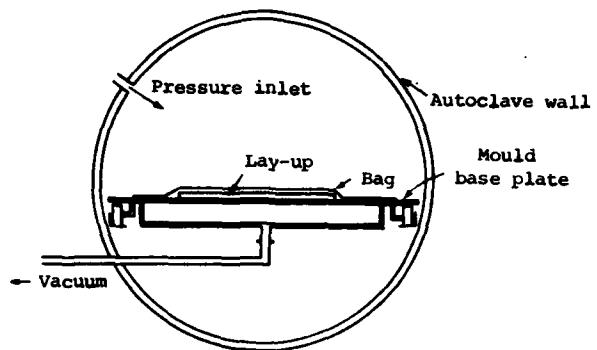
FIG. 3   SCHEMATIC LAYOUT OF AN AUTOCLAVE
Taken from Ref.2

Non-porous release film   Vacuum bag   Pressure plate

Bleeder cloth   Porous release film   Sealant

Mould plate

Edge dam   Lay-up

Vacuum line
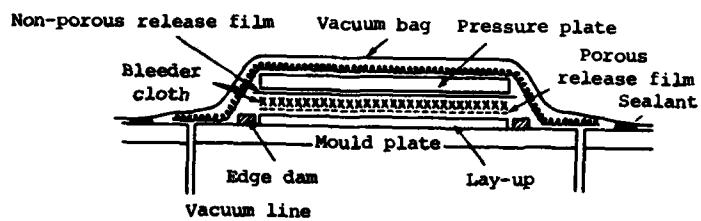
FIG. 4   TYPICAL BAG ASSEMBLY FOR FLAT PANEL MOULDING.
ON OTHER SHAPES PRESSURE PLATES ARE NOT NORMALLY
EMPLOYED. Taken from Ref.2

103

Layup outer
face sheet

TOOL

Position
premachined
honeycomb

Add
Adhesive

TOOL

Layup inner
face sheet

TOOL

Add vacuum
bag

TOOL

Autoclave

Finished part
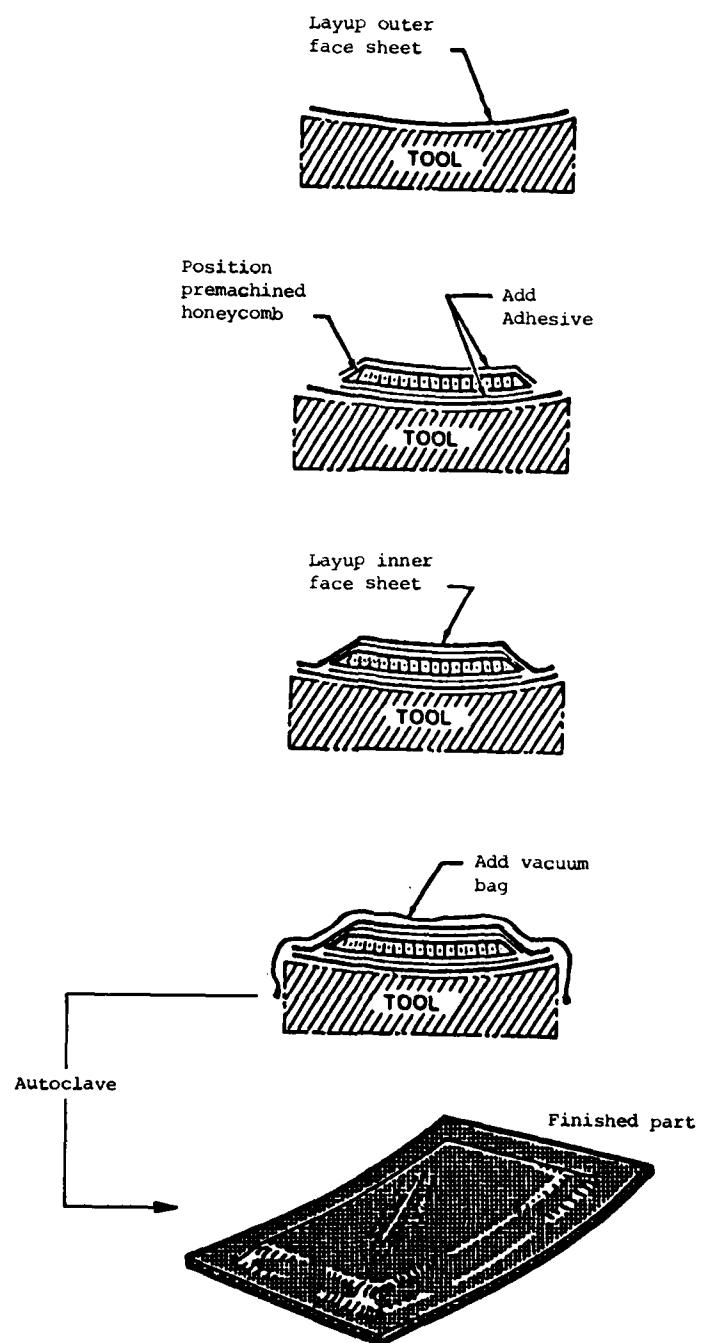
FIG. 5 SCHEMATIC ILLUSTRATION OF THE STEPS IN MANUFACTURE OF A
HONEYCOMB PANEL BY COCURING

104
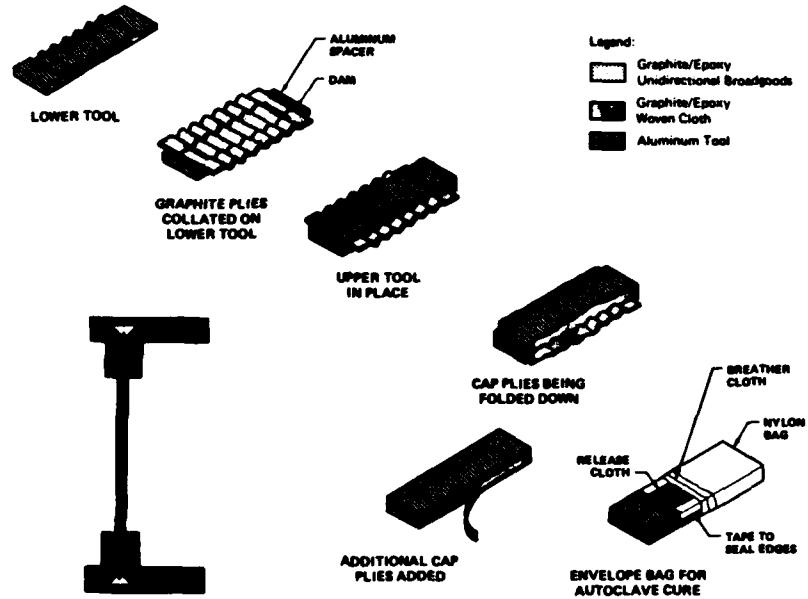
FIG. 6   SCHEMATIC ILLUSTRATION OF STEPS IN MANUFACTURING THE SINE-
WAVE SPAR.
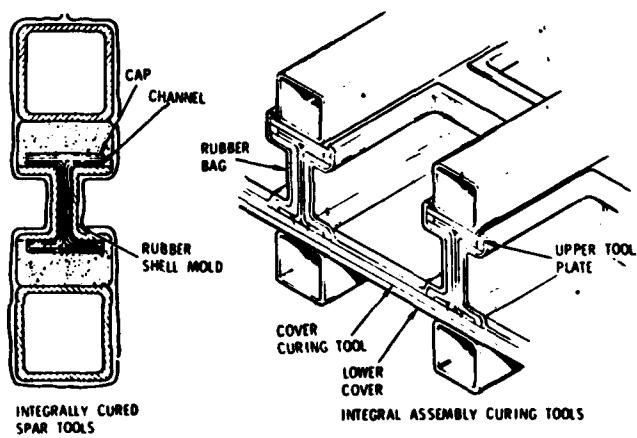
FIG. 7   SCHEMATIC ILLUSTRATION OF PROCEDURE FOR MANUFACTURE OF AN
INTEGRAL WING SKIN/SPAR STRUCTURE. Taken from Ref.3
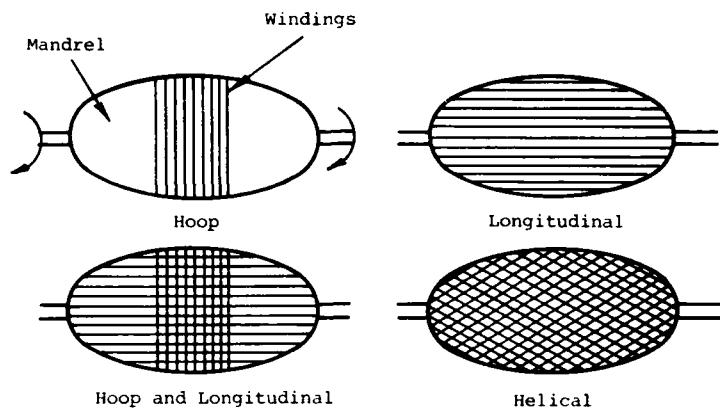
FIG. 8   FILAMENT WINDING PATTERNS
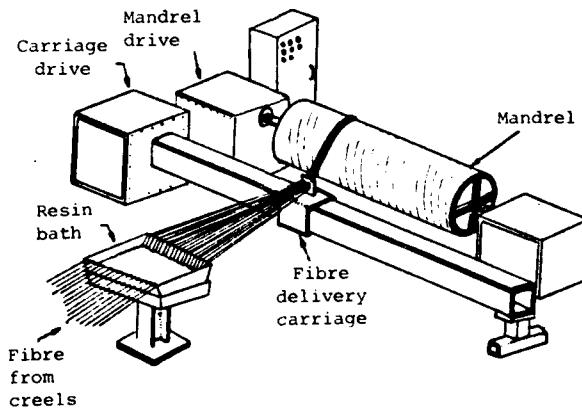
FIG. 9   SCHEMATIC ILLUSTRATION OF A FILAMENT WINDING MACHINE

106

ELECTRO HYDRAULIC
FORM TIP SHOE

TRIM TO LENGTH AND INSTALL
TIP SHOE - BALANCE.
PAINT AND FINAL BALANCE

LAYUP UPPER SKIN, POSITION
SPAR, TRAILING EDGE, LOWER
SKIN AND CORE AND CURE
BLADE BODY

HOT "M INBOARD AND
OUTBO.. ABRASION STRIPS

CURE SPAR ASSY

FILAMENT WIND
OUTER TORQUE
TUBE OVER
INNER SPAR

M/C UPPER SURFACE
AFTER BODY CORE

TRIM
TRAILING EDGE

CO-CURE LOWER SKIN
AND AFTER BODY CORE

CURE
TRAILING EDGE

FILAMENT WIND
INNER TORQUE TUBE

CURE INNER
SPAR

POLAR WIND
UPPER AND LOWER SPAR
CAPS

POLAR WIND
TRAILING EDGE

Manufacturing procedure

FIG. 10   HELICOPTER BLADE
Taken from ref. 8.

107

Storage
containers

Resin
tank

Control
console

Hydraulic
power unit

Pullers

Heated
die

GRP
section

Cut-off
saw
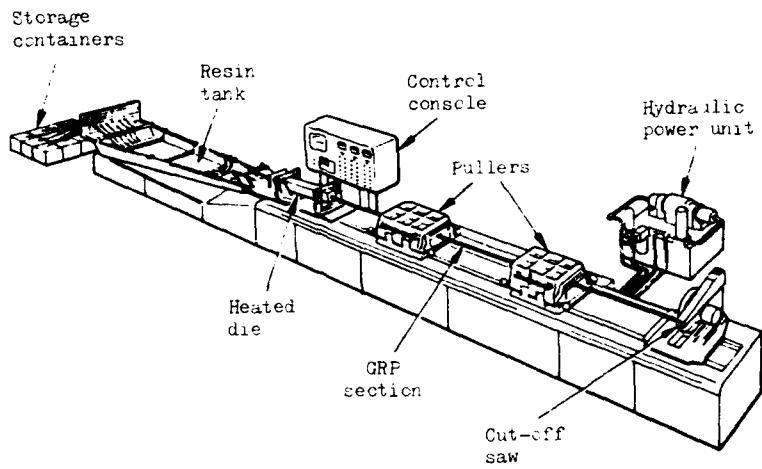
FIG. 11   SCHEMATIC ILLUSTRATION OF A TYPICAL PULTRUSION MACHINE

Lecture 7

STRUCTURAL MECHANICS OF FIBRE COMPOSITES

B.C. HOSKIN and B.I. GREEN

1.   INTRODUCTION

In this lecture the basic theory that is needed for the determination of the stresses, strains and deformations in fibre composite structures is outlined. Attention is concentrated on structures made in the form of laminates because that is the way composite materials are generally utilised.

From the structural mechanics viewpoint, the novel features of composites, compared with conventional structural materials such as metals, are their marked anisotropy and, when used as laminates, their macroscopically heterogeneous nature. However, it should be remarked that there is one classical structural material, namely wood, which is also both anisotropic and, when used in the form of ply-wood, macroscopically heterogeneous. In fact, much of the theory that is needed in the analysis of composite structures is simply an extension of the theory already used for wooden structures.

There is a close analogy between the steps in developing laminate theory and the steps in fabricating a laminate. The building block, both for theory and fabrication,is the "single ply" (also referred to as the "basic ply" or "monoply" or "monolayer" or "lamina"). This is a thin layer of the material (a typical thickness being around 0.125 mm for graphite/epoxy) in which all the fibres are aligned parallel to one another*. The starting point for the theory is the stress-strain law for the single ply referred to its axes of material symmetry. In constructing a laminate each ply is laid up so that its fibres make some prescribed angle with a reference axis fixed in the laminate. All later calculations are made using axes fixed in the laminate - the "structural axes" - so that it is necessary to transform the stress-strain law to these axes. Finally, the individual plies are bonded into a structural entity and so it is necessary to combine the stress-strain laws for the individual plies into a single stress-strain law for the laminate. Since the designer can select his own lay-up pattern, and since the laminate stress-strain law will depend on that pattern, it follows that the designer can "design the material" (as well as the structure).

For more detailed discussions of the topics covered below, see, for example, refs. (1) to (7), and for background material on the theory of anisotropic elasticity see, for example, refs. (8) to (10).

---

* There is some interest in making composite aircraft structures from graphite/ epoxy woven cloth, rather than from unidirectional plies although, generally speaking, more efficient structures can be obtained using the latter form of material. If cloth be used, then some of the statements made here would need to be modified since, of course, cloth has fibres running in two perpendicular directions. However, the theoretical formulae developed below can be readily adapted to apply to a laminate made from cloth; the main difference is in the values of the material constants used in the formulae.

2. STRESS-STRAIN LAW FOR SINGLE PLY IN MATERIAL AXES: UNIDIRECTIONAL LAMINATES

Consider a rectangular element of a single ply with the sides of the element parallel and perpendicular to the fibre direction (Fig. 1). Clearly the direction of the fibres defines a preferred direction in the material so it is natural to introduce a Cartesian set of "material axes" 0-1,2,3 with the 1-axis in the fibre direction, the 2-axis perpendicular to the fibres and in the ply plane, and the 3-axis perpendicular to the plane of the ply. Here interest is in the behaviour of the ply when subjected to stresses acting in its plane i.e., under plane stress conditions; these stresses (also referred to the material axes) will be denoted by σ_1, σ_2 and τ_{12} and the associated strains by ε_1, ε_2 and γ_{12}. (Note that, in composite mechanics, it is standard practice to work with "engineering", rather than "tensor", shear strains). Although a single ply is highly anisotropic, it is intuitively evident that the co-ordinate planes 012, 023, 031 are planes of material symmetry, there being a mirror image symmetry about these planes. Such a material, having three mutually orthogonal planes of symmetry is known as "orthotropic". As is shown, for example, by Tsai (11), the stress-strain law for an orthotropic material under plane stress conditions, referred to the material axes necessarily has the following form:

$$
\begin{bmatrix} \varepsilon_1 \\ \varepsilon_2 \\ \gamma_{12} \end{bmatrix}
=
\begin{bmatrix} 1/E_1 & -\nu_{21}/E_2 & 0 \\ -\nu_{12}/E_1 & 1/E_2 & 0 \\ 0 & 0 & 1/G_{12} \end{bmatrix}
\begin{bmatrix} \sigma_1 \\ \sigma_2 \\ \tau_{12} \end{bmatrix}
\tag{2.1}
$$

Here E_1, E_2 are Young's moduli in the 1 and 2 directions respectively,

ν_{12} is Poisson's ratio governing the contraction in the 2-direction for a tension in the 1-direction,

ν_{21} is Poisson's ratio governing the contraction in the 1-direction for a tension in the 2-direction,

G_{12} is the (in-plane) shear modulus.

There are five material constants in eqn. (2.1) but only four of these are independent because of the following symmetry relation:

$$
\nu_{12}/E_1 = \nu_{21}/E_2
\tag{2.2}
$$

For composites of the type being considered here it should always be borne in mind that E_1 is much larger than either E_2 or G_{12}, because the former is a "fibre-dominated" property whilst the latter are "matrix-dominated" properties.

The above has all related to a single ply, but since the ply thickness does not enter into things, it also applies to a "unidirectional laminate" which is simply a laminate in which the fibre direction is the same in all plies. In fact, most of the material constants for a single ply are obtained from specimen tests on unidirectional laminates, a single ply being itself too thin to test conveniently.

For much of the later analysis it is more convenient to deal with the inverse form of eqn. (2.1), namely,

$$
\begin{bmatrix} \sigma_1 \\ \sigma_2 \\ \tau_{12} \end{bmatrix} = \begin{bmatrix} Q_{11}(0) & Q_{12}(0) & 0 \\ Q_{12}(0) & Q_{22}(0) & 0 \\ 0 & 0 & Q_{66}(0) \end{bmatrix} \begin{bmatrix} \epsilon_1 \\ \epsilon_2 \\ \gamma_{12} \end{bmatrix} \tag{2.3}
$$

where the $Q_{ij}(0)$, which are commonly termed the reduced stiffness coefficients, are given by

$$
Q_{11}(0) = E_1/(1-\nu_{12}\nu_{21}) \qquad Q_{22}(0) = E_2/(1-\nu_{12}\nu_{21}) \tag{2.4}
$$

$$
Q_{12}(0) = \nu_{21} E_1/(1-\nu_{12}\nu_{21}) \qquad Q_{66}(0) = G_{12}
$$

It is conventional in composite mechanics to use the above subscript notation for the Qs, the point of which only becomes evident when three dimensional anisotropic problems are encountered.

3. STRESS-STRAIN LAW FOR SINGLE PLY IN STRUCTURAL AXES; OFF-AXIS LAMINATES

As already remarked, when a ply is incorporated in a laminate, its fibres will make some prescribed angle θ with a reference axis fixed in the laminate. Let this be the x-axis and note that the angle θ is measured from the x-axis to the 1-axis and is positive in the counter-clockwise direction; the y-axis is perpendicular to the x-axis and in the plane of the ply. (See Fig. 2). All subsequent calculations are made using the xy, or "structural", axes so that it is necessary to transform the stress-strain law from the material axes to the structural axes. If the stresses in the structural axes are denoted by σ_x, σ_y and τ_{xy}, then these are related to the stresses referred to the material axes by the usual transformation equations:

$$
\begin{bmatrix} \sigma_x \\ \sigma_y \\ \tau_{xy} \end{bmatrix} = \begin{bmatrix} c^2 & s^2 & -2cs \\ s^2 & c^2 & 2cs \\ cs & -cs & c^2-s^2 \end{bmatrix} \begin{bmatrix} \sigma_1 \\ \sigma_2 \\ \tau_{12} \end{bmatrix} \tag{3.1}
$$

where c denotes cos θ and s denotes sin θ. Also, the strains in the material axes are related to those in the structural axes, namely, ε_x, ε_y and γ_{xy}, by what is essentially the inverse transformation:

$$\begin{bmatrix} \varepsilon_1 \\ \varepsilon_2 \\ \gamma_{12} \end{bmatrix} = \begin{bmatrix} c^2 & s^2 & cs \\ s^2 & c^2 & -cs \\ -2cs & 2cs & c^2-s^2 \end{bmatrix} \begin{bmatrix} \varepsilon_x \\ \varepsilon_y \\ \gamma_{xy} \end{bmatrix} \tag{3.2}$$

Now, in eqns. (3.1), substitute for σ_1, σ_2 and τ_{12} their values as given by eqns. (2.3); then, in the resultant equations, substitute for ε_1, ε_2 and γ_{12} their values as given by eqns. (3.2). After some routine manipulations it is found that the stress-strain law in the structural axes has the form:

$$\begin{bmatrix} \sigma_x \\ \sigma_y \\ \tau_{xy} \end{bmatrix} = \begin{bmatrix} Q_{11}(\theta) & Q_{12}(\theta) & Q_{16}(\theta) \\ Q_{12}(\theta) & Q_{22}(\theta) & Q_{26}(\theta) \\ Q_{16}(\theta) & Q_{26}(\theta) & Q_{66}(\theta) \end{bmatrix} \begin{bmatrix} \varepsilon_x \\ \varepsilon_y \\ \gamma_{xy} \end{bmatrix} \tag{3.3}$$

where the $Q_{ij}(\theta)$ are related to the $Q_{ij}(0)$ by the following equations:

$$\begin{bmatrix} Q_{11}(\theta) \\ Q_{12}(\theta) \\ Q_{22}(\theta) \\ Q_{16}(\theta) \\ Q_{26}(\theta) \\ Q_{66}(\theta) \end{bmatrix} = \begin{bmatrix} c^4 & 2c^2s^2 & s^4 & 4c^2s^2 \\ c^2s^2 & c^4+s^4 & c^2s^2 & -4c^2s^2 \\ s^4 & 2c^2s^2 & c^4 & 4c^2s^2 \\ c^3s & -cs(c^2-s^2) & -cs^3 & -2cs(c^2-s^2) \\ cs^3 & cs(c^2-s^2) & -c^3s & 2cs(c^2-s^2) \\ c^2s^2 & -2c^2s^2 & c^2s^2 & (c^2-s^2)^2 \end{bmatrix} \begin{bmatrix} Q_{11}(0) \\ Q_{12}(0) \\ Q_{22}(0) \\ Q_{66}(0) \end{bmatrix} \tag{3.4}$$

Observe that, in eqns. (3.3), the direct stresses depend on the shear strains (as well as the direct strains) and the shear stress depends on the direct strains (as well as the shear strain). This complication arises because, for non-zero θ, the structural axes are not axes of material symmetry and, with respect to these axes, the material is not orthotropic; it is evident that the absence of orthotropy leads to the presence of the Q_{16} and Q_{26} terms in eqns (3.3). Also, for future reference, note that the expressions for $Q_{11}(\theta)$, $Q_{12}(\theta)$, $Q_{22}(\theta)$ and $Q_{66}(\theta)$ contain only even powers of sin θ and so these quantities are unchanged when θ is replaced by $-\theta$. On the other hand, the expressions for $Q_{16}(\theta)$ and $Q_{26}(\theta)$ contain odd powers of sin θ and so they change sign when θ is replaced by $-\theta$.

112

Analogously to the previous section, the above discussion has been related to a single ply, but it is equally valid for a laminate in which the fibre direction is the same in all plies; a unidirectional laminate in which the fibre direction makes a non-zero angle with the x structural axis is known as an "off-axis" laminate and is sometimes used for test purposes. Formulae for the elastic moduli of an off-axis laminate can be obtained by a procedure analogous to that used in deriving eqns. (3.3). Using eqns. (2.1), with the inverse forms of eqns. (3.2) and (3.1), leads to the inverse form of eqns. (3.3) i.e., with the strains expressed in terms of the stresses; from this result the moduli can be written down. Details can be found in most of the standard texts e.g. p. 54 of ref. (1). Only the result for the Young's modulus in the x-direction, E_x, will be cited here:

$$1/E_x = (1/E_1)c^4 + (1/G_{12} - 2\nu_{12}/E_1)c^2 s^2 + (1/E_2)s^4 \qquad (3.5)$$

The variation of E_x with θ for the case of a graphite/epoxy off-axis laminate is shown in Fig. 3. The material constants of the single ply were taken to be

$E_1 = 137.8$ GPa $\qquad E_2 = 11.71$ GPa $\qquad G_{12} = 5.51$ GPa

$\nu_{12} = 0.25$ $\qquad \nu_{21} = 0.0213$

It can be seen that the modulus initially decreases quite rapidly as the off-axis angle increases from 0°; this indicates the importance of the precise alignment of fibres in a laminate.

4. PLANE STRESS PROBLEMS FOR SYMMETRIC LAMINATES

4.1 General

One of the commonest structural forms for composites is a laminated sheet loaded in its own plane i.e., under plane stress conditions. In order that out of plane bending will not occur such a laminate is always made with a lay-up that is symmetric about the mid-thickness plane. Just to illustrate the type of symmetry meant, consider an 8-ply laminate comprising 4 plies which are to be oriented at 0° to the reference (x) axis, 2 plies at +45°, and 2 plies at -45°. An example of a symmetric laminate would be one with the following ply sequence.

0°/0°/+45°/-45°/-45°/+45°/0°/0°;

on the other hand an example of an unsymmetric arrangement of the same plies would be

0°/0°/0°/0°/+45°/-45°/+45°/-45°.

These two cases are shown in Fig. 4 where z denotes the coordinate in the thickness direction.

4.2 Laminate Stiffness Matrix

Consider now a laminate comprising n plies, and denote the angle between the fibre direction in the kth ply and the x structural axis by θ_k (with the same convention as described in Section 3 above); subject only to the symmetry requirement, the ply orientation is arbitrary. It is assumed that, when the plies are moulded into the laminate, a rigid bond (of infinitesimal thickness) is formed between adjacent plies; as a consequence of this assumption, it follows that under plane stress conditions the strains are the same at all points on a line through the thickness (i.e., that they are independent of z). Denoting these strains by ϵ_x, ϵ_y and γ_{xy} it then follows from eqns. (3.3) that the stresses in the kth ply will be given by

$$\sigma_x(k) = Q_{11}(\theta_k) \, \epsilon_x + Q_{12}(\theta_k) \, \epsilon_y + Q_{16}(\theta_k) \, \gamma_{xy}$$
$$\sigma_y(k) = Q_{12}(\theta_k) \, \epsilon_x + Q_{22}(\theta_k) \, \epsilon_y + Q_{26}(\theta_k) \, \gamma_{xy} \qquad (4.1)$$
$$\tau_{xy}(k) = Q_{16}(\theta_k) \, \epsilon_x + Q_{26}(\theta_k) \, \epsilon_y + Q_{66}(\theta_k) \, \gamma_{xy}$$

If the laminate thickness is denoted by h, and assuming all plies are of the same thickness (which is the usual situation), then the thickness of an individual ply is simply h/n. Now consider an element of the laminate with sides of unit length parallel to the x and y axes. The forces on this element will be denoted by N_x, N_y and N_{xy} (Fig. 5); the Ns are generally termed "stress resultants" and have the dimension "force/length". Elementary equilibrium considerations give

$$N_x = (h/n) \sum_{k=1}^{n} \sigma_x(k), \quad N_y = (h/n) \sum_{k=1}^{n} \sigma_y(k), \quad N_{xy} = (h/n) \sum_{k=1}^{n} \tau_{xy}(k)$$

$$(4.2)$$

Substituting from eqns. (4.1) into eqns. (4.2), and remembering that the strains are the same in all plies, the following result is readily obtained:

$$N_x = A_{11} \, \epsilon_x + A_{12} \, \epsilon_y + A_{16} \, \gamma_{xy}$$
$$N_y = A_{12} \, \epsilon_x + A_{22} \, \epsilon_y + A_{26} \, \gamma_{xy} \qquad (4.3)$$
$$N_{xy} = A_{16} \, \epsilon_x + A_{26} \, \epsilon_y + A_{66} \, \gamma_{xy}$$

where

$$A_{ij} = (h/n) \sum_{k=1}^{n} Q_{ij}(\theta_k) \qquad (4.4)$$

114

The quantities A_{ij} are the terms of the laminate "in-plane stiffness matrix"; given the single ply moduli and the laminate lay-up details they can be calculated routinely by using eqns. (2.4), (3.4) and (4.4). The eqns. (4.3) are generally taken as the starting point for any laminate structural analysis.

4.3   Laminate Stress-Strain Law

As was just implied, it seems to be the current fashion in laminate mechanics to work in terms of the stress-resultants, rather than the stresses; however, for some purposes the latter are more convenient. From the stress-resultants, the average stresses (averaged through the thickness of the laminate) are easily obtained; writing these stresses simply as σ_x, σ_y and τ_{xy}, then

$$\sigma_x = N_x/h \qquad \sigma_y = N_y/h \qquad \tau_{xy} = N_{xy}/h \qquad (4.5)$$

Hence, in terms of these average stresses, the stress-strain law for the laminate becomes

$$\sigma_x = A^*_{11} \varepsilon_x + A^*_{12} \varepsilon_y + A^*_{16} \gamma_{xy}$$

$$\sigma_y = A^*_{12} \varepsilon_x + A^*_{22} \varepsilon_y + A^*_{26} \gamma_{xy} \qquad (4.6)$$

$$\tau_{xy} = A^*_{16} \varepsilon_x + A^*_{26} \varepsilon_y + A^*_{66} \gamma_{xy}$$

where

$$A^*_{ij} = A_{ij}/h = (\sum_{k=1}^{n} Q_{ij}(\theta_k))/n \qquad (4.7)$$

In some cases eqns. (4.6) are more convenient than are eqns. (4.3).

4.4   Orthotropic Laminates

An orthotropic laminate, having the structural axes as the axes of orthotropy, is one for which $A_{16} = A_{26} = 0$; clearly this implies that

$$\sum_{k=1}^{n} Q_{16}(\theta_k) = 0; \qquad \sum_{k=1}^{n} Q_{26}(\theta_k) = 0 \qquad (4.8)$$

Thus, the stress-strain law for an orthotropic laminate reduces to

$$\sigma_x = A^*_{11} \varepsilon_x + A^*_{12} \varepsilon_y$$

$$\sigma_y = A^*_{12} \varepsilon_x + A^*_{22} \varepsilon_y \qquad (4.9)$$

$$\tau_{xy} = A^*_{66} \gamma_{xy}$$

The coupling between the direct stresses and the shear strains, and between the shear stresses and the direct strains, which is present for a general laminate disappears for an orthotropic laminate. Most laminates that are currently used in practice are orthotropic.

It can be readily seen that the following laminates will be orthotropic:

(i) Those consisting only of plies for which $\theta = 0°$ or $90°$; here it follows from eqns. (3.4) that in either case $Q_{16}(\theta) = Q_{26}(\theta) = 0$.

(ii) Those constructed such that for each ply oriented at an angle θ, there is another ply oriented at an angle $-\theta$; since, as already remarked in Section 3,

$$Q_{16}(-\theta) = -Q_{16}(\theta); \quad Q_{26}(-\theta) = -Q_{26}(\theta)$$

there is then a cancellation of all paired terms in the summation (4.8).

(iii) Those consisting only of $0°$, $90°$, and matched pairs of $+$ and $-\theta$, plies are also, of course, orthotropic.

An example of an orthotropic laminate would be one with the following ply pattern:

$$0°/+30°/-30°/-30°/+30°/0°$$

On the other hand the following laminate (whilst still symmetric) would not be orthotropic:

$$0°/+30°/90°/90°/+30°/0°.$$

4.5 Moduli of Orthotropic Laminates

Expressions for the moduli of orthotropic laminates can easily be obtained by solving eqns. (4.9) for simple loadings. For example, on setting $\sigma_y = \tau_{xy} = 0$, Young's modulus in the x-direction, E_x, and Poisson's ratio, ν_{xy}, governing the contraction in the y direction for a stress in the x-direction are then given by

$$E_x = \sigma_x/\varepsilon_x, \quad \nu_{xy} = -\varepsilon_y/\varepsilon_x.$$

Proceeding in this way it is found that

$$E_x = A_{11}^* - A_{12}^{*2}/A_{22}^*, \quad E_y = A_{22}^* - A_{12}^{*2}/A_{11}^*$$

$$\nu_{xy} = A_{12}^*/A_{22}^*, \quad \nu_{yx} = A_{12}^*/A_{11}^* \tag{4.10}$$

$$G_{xy} = A_{66}^*$$

(It is possible to derive analogous, but more complicated, formulae for the moduli of non-orthotropic laminates by solving eqns. (4.6) for simple loadings; see ref. (12).)

As illustrative examples of the above theory consider a family of 24-ply laminates, symmetrical and orthotropic, and all made of the same material but with varying numbers of 0° and ±45° plies. (For the present purposes the precise ordering of the plies is immaterial as long as the symmetry requirement is maintained; however, to ensure orthotropy, there must be the same number of +45° as -45° plies). The single ply modulus data (representative of a graphite/epoxy) are as follows:

$$E_1 = 137.8 \text{ GPa} \qquad E_2 = 11.71 \text{ GPa} \qquad G_{12} = 5.51 \text{ GPa}$$

$$\nu_{12} = 0.25 \qquad \nu_{21} = 0.0213$$

The lay-ups considered are shown in Table 1. Just to recapitulate, the steps in the calculation are as follows:

(i) Calculate the $Q_{ij}(0)$ from eqns. (2.4).

(ii) For each of the ply orientations involved - here $\theta = 0°$, +45°, and -45° - calculate the $Q_{ij}(\theta)$ from eqns. (3.4). (Of course, here the $Q_{ij}(0)$ have already been obtained in (i)).

(iii) Calculate the A_{ij}^* from eqn. (4.7); in the present case eqn. (4.7) becomes

$$A_{ij}^* = [n_1 \, Q_{ij}(0) + n_2 \, Q_{ij}(+45) + n_3 \, Q_{ij}(-45)]/24$$

where n_1 is the number of 0° plies,

n_2 "   "   "   " +45° " ,

n_3 "   "   "   " -45° " .

(iv) Calculate the moduli from eqns. (4.10).

The results of the calculations are shown in Table 1.

TABLE 1: Moduli for Family of 24-ply 0°/±45° Laminates

Lay-Up			E_x	E_y	G_{xy}	ν_{xy}	ν_{yx}
No. 0° plies	No. +45° plies	No. -45° plies	GPa	GPa	GPa		
24	0	0	137.8	11.7	5.51	0.250	0.021
16	4	4	99.6	21.1	15.7	0.579	0.123
12	6	6	79.7	24.5	20.8	0.648	0.199
8	8	8	59.7	26.5	25.9	0.694	0.308
0	12	12	19.3	19.3	36.1	0.753	0.753

The above results have been presented primarily to exemplify the preceding theory; however they also demonstrate some features which are important in design. The stiffness of a composite is overwhelmingly resident in the extensional stiffness of its fibres; hence, at least for simple loadings, if maximum stiffness is required, a laminate is constructed so that fibres are aligned in the principal stress directions. Thus, for a member under uniaxial tension, a laminate comprising basically all 0° plies would be chosen i.e., with all fibres aligned parallel to the tension direction. As can be seen from Table 1, E_x decreases as the number of 0° plies decreases. On the other hand, consider a rectangular panel under shear, the sides of the panel being parallel to the structural axes (Fig. 6). The principal stresses here are an equal tension and compression, oriented at +45° and -45° to the x-axis. Thus, maximum shear stiffness can be expected to be obtained using a laminate comprising equal numbers of +45° and -45° plies; this is reflected in the high shear modulus, G_{xy}, for the all ±45° laminate of Table 1. (For comparison recall that the shear modulus of a typical aluminium alloy is of the order of 27 GPa.)

Before passing on it should also be observed that, whilst for an isotropic material, Poisson's ratio cannot exceed 0.5, this is not the case for an anisotropic material.

4.6 Quasi-Isotropic Laminates

It is possible to construct laminates which are isotropic as regards their in-plane elastic properties i.e., which have the same Young's modulus, E, and same Poisson's ratio, ν, in all in-plane directions and for which the shear modulus is given by $G = E/2(1+\nu)$. One way of achieving this is to adopt a lay-up which has an equal number of plies oriented parallel to the sides of an equilateral triangle. For example, a quasi-isotropic 24-ply laminate could be made with 8 plies oriented at each of 0°, +60° and -60°. Using the same materials data (and theory), as was used in deriving Table 1, it will be found that such a laminate has the following moduli:

E = 54.3 GPa, G = 20.8 GPa, ν = 0.305.

Another way of achieving a quasi-isotropic laminate is to use equal number of plies oriented at 0°, +45°, -45° and 90° i.e., an alternative lay-up which would also give a quasi-isotropic 24-ply laminate (with, incidentally, the same values for the elastic constants as were just cited) could be made with 6 plies at each of 0°, +45°, -45° and 90°.

The term "quasi-isotropic" is used because, of course, such laminates have different properties in the out-of-plane direction. However, it is not usual practice to work with quasi-isotropic laminates; efficient design with composites generally requires that advantage be taken of their inherent anisotropy.

4.7   Stress Analysis of Orthotropic Laminates

The determination of the stresses, strains and deformations experienced by symmetric laminates under plane stress loadings is carried out by procedures that are analogous to those used for isotropic materials. The laminate is treated as a homogeneous membrane having stiffness properties determined as described above. It should be noted, though, that whilst the strains and deformations so determined are the actual strains and deformations (within the limit of the assumptions), the stresses are only the average values over the laminate thickness.

If an analytical procedure is used, then generally a stress function, F, is introduced this being related to the (average) stresses by

$$\sigma_x = \frac{\partial^2 F}{\partial y^2}, \quad \sigma_y = \frac{\partial^2 F}{\partial x^2}, \quad \tau_{xy} = \frac{-\partial^2 F}{\partial x \partial y} \tag{4.11}$$

It can be shown that F satisfies the following partial differential equation:

$$(1/E_y) \frac{\partial^4 F}{\partial x^4} + \{ 1/G_{xy} - 2\nu_{xy}/E_x \} \frac{\partial^4 F}{\partial x^2 \partial y^2} + (1/E_x) \frac{\partial^4 F}{\partial y^4} = 0 \tag{4.12}$$

Solutions of eqn. (4.12) for several problems of interest can be found in ref. (10).

These days most structural analyses are performed using finite element methods, and many general purpose finite element programs contain orthotropic membrane elements in their library. Once the laminate moduli or stiffness coefficients (depending on whether the program is in terms of stresses or stress resultants) are determined as above, these are used as input data for calculating the element stiffness matrix; the rest of the analysis proceeds as in the isotropic case.

As has already been emphasized, the stresses which are obtained from the above procedures are only the average stresses; however, to determine the actual stresses in the individual plies it is only necessary to substitute the calculated values of the strains in eqns. (4.1). An elementary example may clarify this. Consider a rectangular strip under uniaxial tension (Fig. 7) made of that 24 ply laminate considered earlier

119

which had 12 plies at 0° and 12 plies at ±45°; suppose the applied stress is σ_x = 68.9 MPa. The average stress here is uniform in the xy plane and given by

$$\sigma_x = 68.9 \text{ MPa}, \ \sigma_y = \tau_{xy} = 0.$$

Using the values of E_x and ν_{xy} given in Table 1 it follows that the associated strains are

$$\epsilon_x = 0.864 \times 10^{-3}, \ \epsilon_y = -0.560 \times 10^{-3}, \ \gamma_{xy} = 0.$$

The stresses in the individual plies can now be obtained by substituting these values into eqns. (4.1), with the appropriate values of the $Q_{ij}(\theta)$. The results of doing this are shown in Table 2 below.

TABLE 2: Stresses in Individual Plies of 24-Ply Laminate (12 at 0°, 12 at ±45°)

θ	$\sigma_x(\theta)$ MPa	$\sigma_y(\theta)$ MPa	$\tau_{xy}(\theta)$ MPa
0°	118.1	-4.0	0
+45°	19.7	4.0	9.7
-45°	19.7	4.0	-9.7

Thus, the actual stress distribution is very different to the average one. In particular note that transverse direct stresses and shear stresses are developed, even though no such stresses are applied; naturally these stresses are self-equilibrating over the thickness. It follows that there is some "boundary layer" around the edges of the strip where there is a rapid transition from the actual stress boundary values (namely, zero on the longitudinal edges) to the above calculated values. This boundary layer would be expected to extend in from the edges a distance of the order of the laminate thickness (from St. Venant's principle). In the boundary layer, the simple laminate theory presented above is not applicable and a three-dimensional analysis is required; see p. 191 of ref. (5). The matter is of more than academic interest since faults, such as delaminations, are prone to originate at the free edges of laminates because of the above effect.

Finally, when discussing allowable design values for composite structures, it is usual to cite values of strain, rather than stress; clearly strain is the more meaningful quantity for a laminate.

4.8 Stress Concentration around Holes in Orthotropic Laminates

Several analytical solutions for the stresses around holes in (symmetric) orthotropic laminates are cited in ref. (7); details of the derivations of these are given by Lekhnitskii (10). It turns out that the value of the stress concentration factor (SCF) depends markedly on the relative values of the various moduli. This can be illustrated by considering the case of a circular hole in an infinite sheet under a uniaxial tension in the x direction (Fig. 8); here the stress concentration factor at point A in Fig. 8 ($\alpha = 90°$) is given by the following formula:

$$SCF = 1 + [2\{ (E_x/E_y)^{\frac{1}{2}} - \nu_{xy}\} + E_x/G_{xy}]^{\frac{1}{2}} \qquad (4.13)$$

The stress concentration factors for the laminates of Table 1 have been calculated from this formula and the results are shown in Table 3.

TABLE 3: SCF at Circular Hole in Tension
Panel (Laminate Data from Table 1)

Lay-Up		SCF
No. 0° plies	No. ±45° plies	Pt. A
24	0	6.6
16	8	4.1
12	12	3.5
8	16	3.0
0	24	2.0

For comparison, the SCF for an isotropic material is 3. As can be seen, when there is a high degree of anisotropy (e.g. an all 0° laminate), SCFs well in excess of that can be obtained. It should also be pointed out that, as the laminate pattern changes, not only does the value of the SCF change, but the point where the SCF attains its maximum value can also change. Whereas for the first four laminates of Table 3, the maximum SCF does occur at point A, for the remaining laminate the maximum occurs at point B ($\alpha = 55°$) in Fig. 8 and has the value 2.97.

4.9 Laminate Codes

Although the precise ordering of the plies of a laminate has not been of concern in the considerations of this Section, generally there will be other factors which will determine such an ordering. In any case, when a laminate is being called up for manufacture, the associated engineering drawing should

121

list the orientation of each ply. When referring to laminates in a text some
sort of abbreviated notation is necessary to specify the pattern. It is
easiest to describe the code normally used by some examples.

Example 1: Consider an 8-ply laminate with the following (symmetric) lay-
up

$$0°/0°/+45°/-45°/-45°/+45°/0°/0°$$

This is written in code form as

$$[0_2/\pm45]_s$$

Note that

(i)   only half the plies in a symmetric laminate are listed,
the symmetry being implied by the s outside the brackets,

(ii) the degree signs are omitted from the angles,

(iii) in a + and - combination the upper sign is read first.

Example 2: Consider a 50-ply laminate which contains repetitions of the ply
sequence

$$0°/0°/+45°/-45°/90°,$$

the order in the sequence being reversed at the mid-plane to preserve the
symmetry. This would be written in code form as

$$[(0_2/\pm45/90)_5]_s$$

Sometimes, in general discussions a laminate is described by the
percentages of its plies at various angles. Thus, the laminate of example 1
would be described as having "50% 0s, 50% ±45s". Similarly, the laminate
of example 2 would be described as having "40% 0s, 40% ±45s, 20% 90s".

5.   GENERAL LAMINATES SUBJECTED TO PLANE STRESS AND BENDING LOADS

5.1   General

Here the previous restriction to laminates which are symmetric
about the mid-thickness plane will be dropped. It now becomes necessary to
consider the plane stress and bending problems in conjunction, as in-plane
loads can induce bending deformations and vice-versa. Only the outline of the
theory will be given below; for further details, including numerical examples,
see refs. (1) to (5), and (12).

122

5.2 Theory

In distinction to the situation for symmetric laminates, the position of each ply in the laminate now is of importance. Thus, consider an n-ply laminate and denote by z the co-ordinate in the thickness direction, measured from the mid-thickness plane; the kth ply lies between z_k and z_{k+1} (Fig. 9). As before, the total thickness of the laminate will be denoted by h.

It is assumed that when a laminate is subjected to in-plane and/or bending loads, the strain at any point can be written in the form

$$\epsilon_x = \epsilon_x^* + K_x z$$
$$\epsilon_y = \epsilon_y^* + K_y z \qquad\qquad (5.1)$$
$$\gamma_{xy} = \gamma_{xy}^* + K_{xy} z$$

Here the starred quantities are the mid-plane strains and the Ks are the mid-plane curvatures (as in the bending of isotropic plates); both these sets of quantities are independent of z. Substituting from eqns. (5.1) into eqns. (3.3), it follows that the stresses in the kth ply will now be given by

$$\sigma_x(k) = Q_{11}(\theta_k)(\epsilon_x^* + zK_x) + Q_{12}(\theta_k)(\epsilon_y^* + zK_y) + Q_{16}(\theta_k)(\gamma_{xy}^* + zK_{xy})$$

$$\sigma_y(k) = Q_{12}(\theta_k)(\epsilon_x^* + zK_x) + Q_{22}(\theta_k)(\epsilon_y^* + zK_y) + Q_{26}(\theta_k)(\gamma_{xy}^* + zK_{xy}) \qquad (5.2)$$

$$\tau_{xy}(k) = Q_{16}(\theta_k)(\epsilon_x^* + zK_x) + Q_{26}(\theta_k)(\epsilon_y^* + zK_y) + Q_{66}(\theta_k)(\gamma_{xy}^* + zK_{xy}).$$

Now introduce the stress resultants (in the form of forces per unit length and moments per unit length) defined by

$$N_x = \int \sigma_x \, dz, \quad N_y = \int \sigma_y \, dz, \quad N_{xy} = \int \tau_{xy} \, dz$$

$$M_x = \int \sigma_x z \, dz, \quad M_y = \int \sigma_y z \, dz, \quad M_{xy} = \int \tau_{xy} z \, dz \qquad (5.3)$$

where all the integrals are over the thickness of the laminate (i.e., from z = -h/2 to z = h/2); see Fig. 10. Since each of the integrals in eqns. (5.3) can be written in forms such as

$$N_x = \sum_{k=1}^{n} \int_{z_k}^{z_{k+1}} \sigma_x(k) \, dz, \qquad M_x = \sum_{k=1}^{n} \int_{z_k}^{z_{k+1}} \sigma_x(k) \, z \, dz \qquad (5.4)$$

123

it follows that substituting from eqns. (5.2) into eqns. (5.3), and performing some elementary integrations, leads to the result

$$
\begin{bmatrix}
A_{11} & A_{12} & A_{16} & B_{11} & B_{12} & B_{16} \\
A_{12} & A_{22} & A_{26} & B_{12} & B_{22} & B_{26} \\
A_{16} & A_{26} & A_{66} & B_{16} & B_{26} & B_{66} \\
B_{11} & B_{12} & B_{16} & D_{11} & D_{12} & D_{16} \\
B_{12} & B_{22} & B_{26} & D_{12} & D_{22} & D_{26} \\
B_{16} & B_{26} & B_{66} & D_{16} & D_{26} & D_{66}
\end{bmatrix}
\begin{bmatrix}
\epsilon^{*}_{x} \\
\epsilon^{*}_{y} \\
\gamma^{*}_{xy} \\
K_{x} \\
K_{y} \\
K_{xy}
\end{bmatrix}
=
\begin{bmatrix}
N_{x} \\
N_{y} \\
N_{xy} \\
M_{x} \\
M_{y} \\
M_{xy}
\end{bmatrix}
\tag{5.5}
$$

The elements in the above combined "extensional-bending stiffness matrix" are given by

$$
A_{ij} = \sum_{k=1}^{n} Q_{ij}(\theta_k) \, (z_{k+1} - z_k) \tag{5.6}
$$

$$
B_{ij} = \sum_{k=1}^{n} Q_{ij}(\theta_k) \, (z_{k+1}^{2} - z_{k}^{2})/2 \tag{5.7}
$$

$$
D_{ij} = \sum_{k=1}^{n} Q_{ij}(\theta_k) \, (z_{k+1}^{3} - z_{k}^{3})/3 \tag{5.8}
$$

(The above definition for A_{ij} is, of course, equivalent to that of eqn. (4.4).)

Equations (5.5) can be used to develop a theory for the stress analysis of general laminates but this is quite formidable mathematically; it involves the solution of two simultaneous fourth order partial differential equations (see p. 3-43 of ref. (7)).

5.3 Uncoupling of Stiffness Matrix

It can be seen from eqns. (5.5) that the plane stress and bending problems are coupled unless all the B_{ij} are zero. It follows from eqn. (5.7) that the B_{ij} are indeed zero for a symmetric lay-up. (For a symmetric pair of plies, if that ply below the mid-plane has co-ordinates $z_k = -a$, $z_{k+1} = -b$, then its mate above the mid-plane will have $z_k = b$, $z_{k+1} = a$; since each ply has the same Q_{ij} there is a cancellation in the summation (5.7).)

It is possible to achieve an approximate uncoupling of eqns. (5.5) for a multi-ply unsymmetric laminate by making it in the form of a large number of repetitions of a given ply grouping. It can be seen intuitively that such a laminate will be symmetric in "the group of plies" if not in the individual plies; as long as the number of plies in the group is small compared with the total number of plies in the laminate the B_{ij} will turn out to be small quantities. For example, a 48-ply laminate containing 24 groups of ±45° plies laid up in the sequence +/-/+/-/ etc (without there being symmetry about the mid-plane) would be expected to behave much as a symmetrical laminate of the same plies.

6. BENDING OF SYMMETRIC LAMINATES

The moment-curvature relation governing the bending of symmetric laminates out of their plane, as extracted from eqns. (5.5), is

$$\begin{bmatrix} D_{11} & D_{12} & D_{16} \\ D_{12} & D_{22} & D_{26} \\ D_{16} & D_{26} & D_{66} \end{bmatrix} \begin{bmatrix} K_x \\ K_y \\ K_{xy} \end{bmatrix} = \begin{bmatrix} M_x \\ M_y \\ M_{xy} \end{bmatrix} \tag{6.1}$$

Analogously to the definition of orthotropy in plane stress, a laminate is said to be orthotropic in bending if $D_{16} = D_{26} = 0$. However, it is important to note that a laminate which is orthotropic in plane stress is not necessarily orthotropic in bending. For example, consider the 4-ply laminate $[\pm 45]_s$. Here the co-ordinates for the +45° plies may be written as (-h/2,-h/4) and (h/4, h/2) whilst those of the -45° plies are (-h/4, 0) and (0, h/4); h, of course, is the laminate thickness. It is easy to establish that whilst A_{16} and A_{26} are zero, D_{16} and D_{26} are not. On the other hand, a laminate which contains only 0° and 90° plies will be orthotropic in both plane stress and bending. (It is also worth noting that for multi-ply laminates made of "groups of plies", as described in Section 5.3, if the group is orthotropic in plane stress then the laminate will at least be approximately orthotropic in both plane stress and bending.)

For an orthotropic plate in bending, the deflection, w, satisfies the following equation:

$$D_{11} \frac{\partial^4 w}{\partial x^4} + 2(D_{12}+2D_{66}) \frac{\partial^4 w}{\partial x^2 \partial y^2} + D_{22} \frac{\partial^4 w}{\partial y^4} = q \tag{6.2}$$

where q is the applied pressure. Solutions of this equation can be found in refs. (1) and (13) and, in both these references, the related problem of the buckling of laminated plates is also discussed.

7. FAILURE CRITERIA FOR LAMINATES

7.1 General

The problem considered here is broadly that of predicting the ultimate strength of a laminate under plane stress conditions, given relevant strength data for a single ply. This is quite a complex subject on which research is still actively proceeding and only the briefest of outlines can be given; however, detailed reviews can be found in refs. (14) and (15). (At this stage, it is usual to rely largely on test data for laminate strength values).

Using the theory of Section 4 the stresses in the individual plies of a laminate can be determined. Further using the inverse transformation to eqn. (3.1), the stresses at any point in a ply can be referred to the material axes. Hence, the problem can be reduced to establishing a criterion for the ultimate strength of a single ply with the stresses referred to the material axes. As before, these stresses will be denoted by σ_1, σ_2 and τ_{12}.

The available data (established mainly from unidirectional laminate tests) will usually be as follows:

F_{1T}, F_{1C} — ultimate strength in tension and compression, respectively, in fibre direction,

F_{2T}, F_{2C} — ultimate strength in tension and compression, respectively, in transverse direction,

F_{12} — ultimate shear strength.

7.2   Maximum Stress Criterion

The simplest criterion is to assume that failure only occurs whenever any of the following conditions is violated:

$$-F_{1C} \leqslant \sigma_1 \leqslant F_{1T}$$
$$-F_{2C} \leqslant \sigma_2 \leqslant F_{2T} \tag{7.1}$$
$$-F_{12} \leqslant \tau_{12} \leqslant F_{12}$$

Since this criterion does not allow for any interaction between the stress components it is, in general, non-conservative.

7.3   Maximum Strain Criterion

It is possible to establish by test ultimate strains for a single ply (rather than ultimate stresses) and then set up a strain criterion quite analogous to (7.1). However, this also is in general non-conservative.

7.4   Tsai-Hill/Hoffman Criterion

The criterion that is probably most commonly used is one developed by Tsai from a formula proposed by Hill in a different connection (namely, the yielding of an anisotropic metal). In its original form, the Tsai-Hill criterion did not allow explicitly for differences between the tensile and compressive ultimate strengths; Hoffman extended the criterion to cover that situation (which is the usual one). According to the Tsai-Hill/Hoffman criterion, failure occurs if the following inequality is violated:

$$\sigma_1^{~2}/(F_{1T}F_{1C}) - \sigma_1\sigma_2/(F_{1T}F_{1C}) + \sigma_2^{~2}/(F_{2T}F_{2C})$$
$$+(1/F_{1T}-1/F_{1C})\ \sigma_1 + (1/F_{2T}-1/F_{2C})\ \sigma_2 + \tau_{12}^2/F_{12}^2 \leqslant 1 \tag{7.2}$$

126

This criterion does allow for stress interaction effects, as can be seen from Fig. 11 where the criteria (7.1) and (7.2) are compared for the following simplified case:

$$F_{1T} = F_{1C} = 1400 \text{ MPa}$$

$$F_{2T} = F_{2C} = 140 \text{ MPa}$$

$$\tau_{12} = 0$$

There are some theoretical objections to the criterion (7.2) on the grounds of a lack of "tensor invariance"; see refs. (2) and (15). A more refined criterion, often known as the Tsai-Wu criterion, which does not suffer that objection has been developed (15) but it contains another material constant which is difficult to determine accurately.

REFERENCES

1. Jones, R.M., Mechanics of Composite Materials, McGraw-Hill Kogakusha Ltd., Tokyo, 1975.

2. Tsai, S.W. and Hahn, H.T., Introduction to Composite Materials, Technomic Publishing Co., Westport, 1980.

3. Calcote, L.R., The Analysis of Laminated Composite Structures, Van Nostrand Reinhold, New York, 1969.

4. Ashton, J.E., Halpin, J.C. and Petit, P.H., Primer on Composite Materials: Analysis, Technomic Publishing Co., Stamford, 1969.

5. Agarwal, B.D. and Broutman, L.J., Analysis and Performance of Fiber Composites, Wiley, New York, 1980.

6. Broutman, L.J. and Krock, R.H., (eds.), Composite Materials, vols. 7 and 8 (Structural Design and Analysis Parts I and II edited by C.C. Chamis), Academic Press, New York, 1975.

7. Anon, Plastics for Aerospace Vehicles, Part 1, Reinforced Plastics, MIL-HDBK-17A US Department of Defense, Washington, 1971.

8. Hearmon, R.F.S., An Introduction to Applied Anisotropic Elasticity, Oxford, 1961.

9. Lekhnitskii, S.G., Theory of Elasticity of an Anisotropic Elastic Body, Holden-Day, San Francisco, 1963.

10. Lekhnitskii, S.G., Anisotropic Plates, Gordon and Breach, New York, 1968.

11. Tsai, S.W., Mechanics of Composite Materials Parts I and II, AFML-TR-66-149, 1966.

12. Hoskin, B.C. and Green, B.I., Stress Distributions in Fibre Reinforced Plastic Laminates under Simple Loadings, ARL Note SM 396, 1973.

13. Vinson, J.R. and Chou, T-W, Composite Materials and Their Use in Structures, Applied Science Publishers, London, 1975.

14. Vicaris, A.A. and Toland, R.H., Failure Criteria and Failure Analysis of Composite Structural Components, pp. 51-97 of Composite Materials, vol. 7; see ref. (6) above.

15. Wu, E.M., Phenomenological Anisotropic Failure Criterion, pp. 353-431 of Composite Materials, vol. 2, see ref. (6) above.
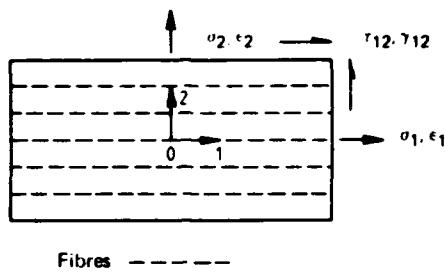
FIG. 1   MATERIAL AXES FOR SINGLE PLY
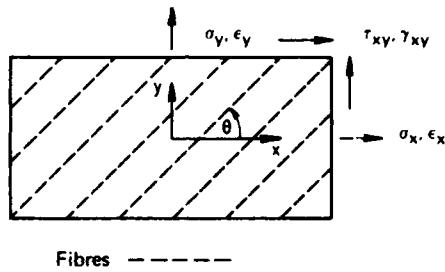
FIG. 2   STRUCTURAL AXES FOR SINGLE PLY

Off-axis angle (degrees)
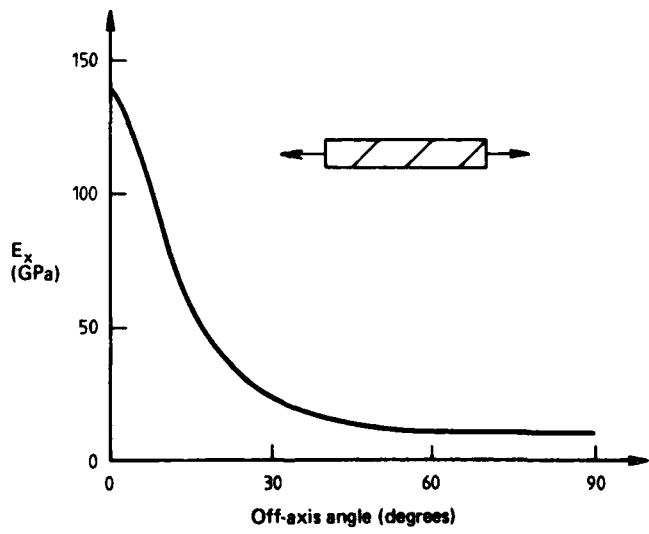
FIG. 3   EXTENSIONAL MODULUS OF OFF-AXIS LAMINATE

0	-45
0	+45
+45	-45
-45	+45
-45	0
+45	0
0	0
0	0

(a) Symmetric   (b) Non-symmetric
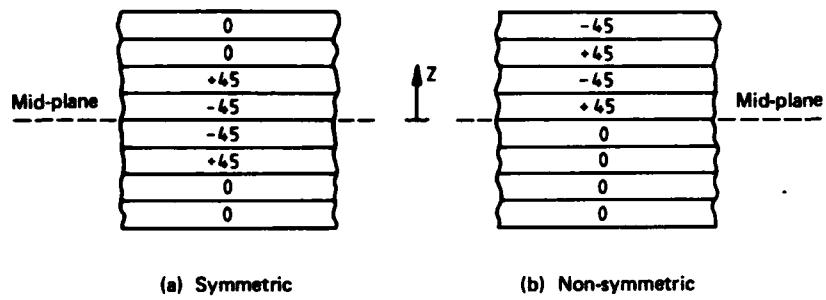
FIG. 4 EXAMPLES OF SYMMETRIC AND NON-SYMMETRIC 8-PLY LAMINATES

FIG. 5 STRESS RESULTANTS
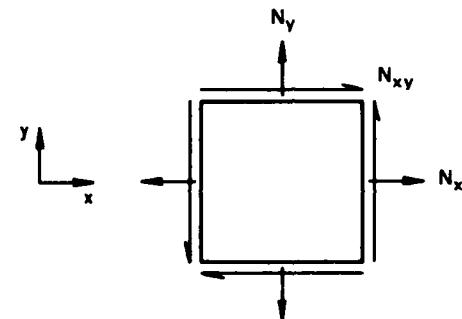
(a) Shear panel   (b) Principal stresses   (c) Fibre directions
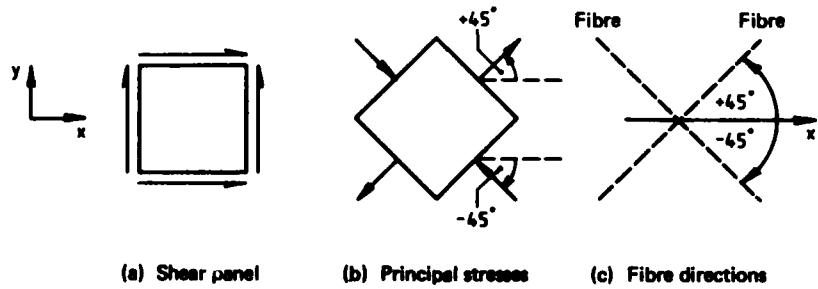
FIG. 6 FIBRE ORIENTATIONS FOR SHEAR PANEL

130
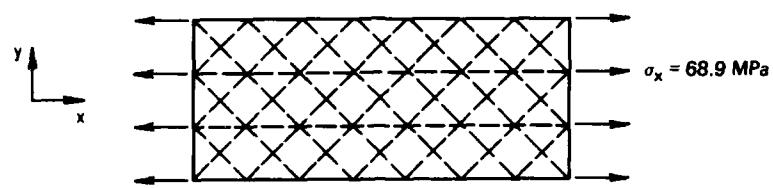
FIG. 7   0°/±45° LAMINATE UNDER UNIAXIAL TENSION
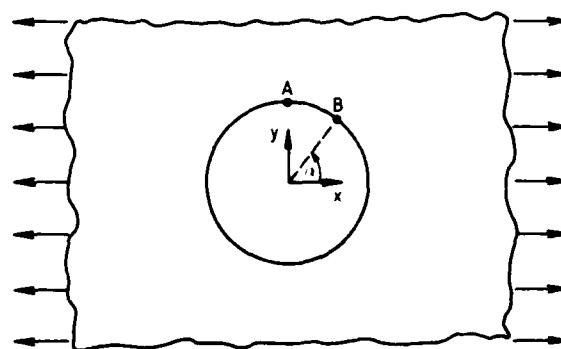
FIG. 8   CIRCULAR HOLE IN INFINITE TENSION PANEL
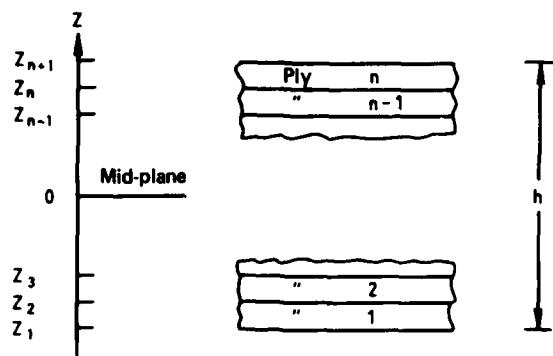
FIG. 9 PLY CO-ORDINATES IN THICKNESS DIRECTION
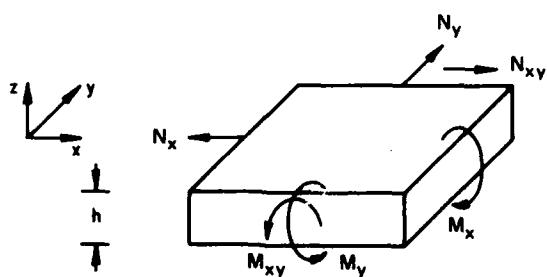
FIG. 10 STRESS AND MOMENT RESULTANTS FOR LAMINATE
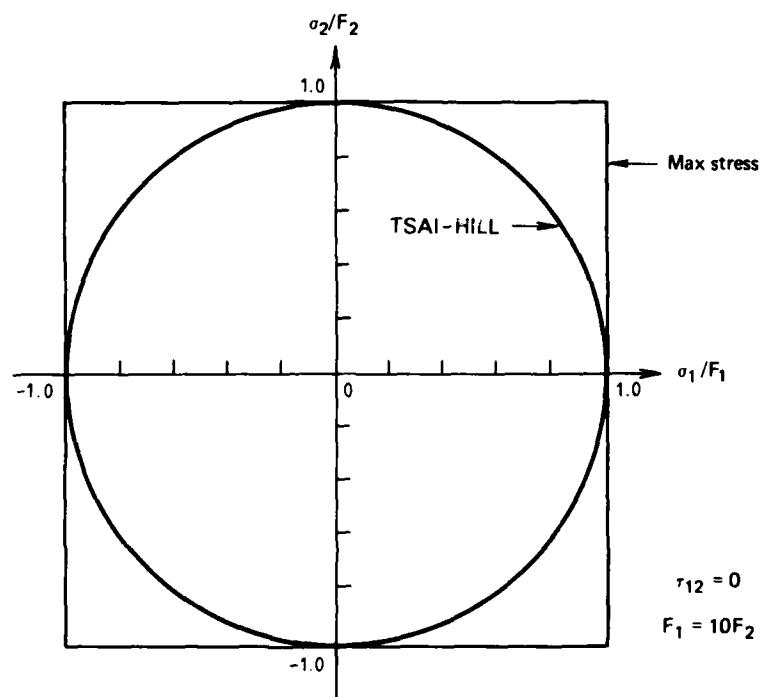
FIG. 11   COMPARISON OF MAXIMUM STRESS AND TSAI-HILL FAILURE CRITERIA
FOR SINGLE PLY

Lecture 8

JOINING ADVANCED FIBRE COMPOSITES

A.A. BAKER

1. INTRODUCTION

Most structures consist of an assembly of a number of individual elements connected to form a load transmission path. These connections or joints are potentially the weakest points in the structure and may determine its viability. For example, in aircraft structures, where minimisation of weight is important, many of the allowable loads are determined by the strength of the joints. This lecture deals with joining of advanced fibre composites, particularly graphite/epoxy, for aircraft applications where the joints are not subjected to significant bending moments.

In general, it is desirable to minimise the number of joints in a structure to minimise both its weight and cost. Fibre composites have an important advantage over metals in this respect, since large one piece components are readily produced. Nevertheless, joints will be required to transmit loads in and out of the composite structure. Usually joints employing metallic members, either aluminium or titanium alloys, are used for this purpose. Metallic members are particularly employed where significant concentrated loads occur or where significant through-the-thickness stresses arise.

The types of composite-to-metal joints can be classified into:

(i) Adhesively bonded,

(ii) Mechanical (a) fastened (bolted, riveted, etc.)

(b) wedge loaded.

(iii) Combinations of (i) and (ii).

In the first type, loads are carried by the surface of the joint elements in shear, through a layer of adhesive or resin. In the second type, the loads are carried by the joint elements in compression on the contacting faces.

A variety of aspects must be considered when comparing the two major procedures, bolting and adhesive bonding, for joining advanced fibre composites to metals. Some of the salient points of comparison are listed in Table 1, which shows that adhesive bonding, where appropriate, produces the most structurally efficient and aerodynamically smooth joint. In general, however, bonding is limited to joining material of equivalent thickness and strength to about 4 mm of a high strength aluminium alloy, unless joints of complex configuration are employed.

134

TABLE 1: Comparison of Bonded and Bolted Composite-
to-Metal Joints for Aircraft Applications

Bonded Joints	
Advantages	Disadvantages
. No stress concentration in adherends. . Stiff connection. . Excellent fatigue properties. . No fretting problems. . Sealed against corrosion. . Smooth surface contour.	. Limits to thickness that can be jointed with simple joint configuration. . Inspection difficult. . Prone to environmental degradation. . Requires high level of pro- cess control. . Sensitive to peel and through- thickness stresses. . Residual stress problems when joining dissimilar materials. . Cannot be disassembled.
Bolted Joints	
Advantages	Disadvantages
. Positive connection. . No thickness limitations. . Simple process. . Simple inspection procedure. . Simple joint configuration. . Not environmentally sensitive. . Provides through-thickness reinforcement - not sensitive to peel stress. . No residual stress problems. . Can be disassembled.	. Considerable stress concen- tration. . Relatively compliant connection. . Relatively poor fatigue properties. . Hole formation may cause damage to composite. . Prone to fretting. . Prone to corrosion.

2.   ADHESIVE BONDING

2.1   General Design Considerations

In adhesive bonding, the aim is to transfer load smoothly from one
adherend to the other, minimising peak shear stresses and peel stresses in
the adhesive layer. Fig. 1 illustrates the elemental joint configurations
appropriate for joining advanced fibre composites to metals. To minimise
manufacturing costs, the simplest joint configuration is chosen which will

135

develop the required strength. For thin section joints, the choice is usually
the lap joint or the double-lap joint, both of which require minimal machining
and only simple manufacturing procedures.

Four main modes of failure of a joint must be considered for design
purposes; these are: (a) shear of the adhesive system, (b) peel of the
adhesive system, (c) peel of the composite, and (d) tension or compression
failure of the adherends. Most joint design procedures aim for tension or
compression failure of the adherends as the lowest static failure loads since
this ensures a joint efficiency of at least 100%, and ensures that the bonded
region does not become the weak link. This approach also usually ensures
that the adhesive is not the weak link under cyclic loading.

The design parameters usually include the following: (i) stiffness
and strength of the adherends, (ii) strength, stiffness and strain to failure
of the adhesive under shear loading - allowing for temperature and degradation
due to representative service environment, (iii) mismatch in stiffness
between the adherends, (iv) mismatch in thermal expansion coefficient between
the adherends, and (v) the direction of the stresses.

Most of the factors influencing the behaviour of structural
adhesive joints are reviewed in ref. (1). The stress-strain behaviour of the
adhesive is a most important materials property affecting joint strength.
This information may be obtained *from tensile tests* on thick adherend lap joint
specimens or from napkin ring tests (end bonded metal cylinders, tested in
torsion). Fig. 2a shows curves for a typical structural film adhesive
obtained from the thick adherend lap test and illustrates the degree of plasti-
city exhibited by these materials; these results were obtained after moisture
conditioning the adhesive to representative environmental conditions.
Similar tests may be performed to determine effects of cyclic or prolonged
static loading. Durability of the joint in service is most reliably assessed
by subjecting structural detail specimens to realistic loading and environmental
conditions. Simple coupon tests are best employed to aid initial design and,
even with sophisticated analytical procedures, should not be relied on to
predict allowable failure loads in composite-to-metal joints.

The most comprehensive design studies on adhesive joints, particu-
larly for advanced fibre composite-to-metal joints have been performed by
Hart-Smith; see refs. (2) and (3). These analytical studies are based on
previous classical work (e.g. by Volkersen, and by Reissner and Goland) but
extended to take account of yielding in the adhesive*, as shown in Fig. 2a,
using the idealised curves shown in Fig. 2b. Based on these studies, Fig. 3
illustrates schematically the strength limitations of various joint designs as

----
* The main weakness in this theory is that it does *not account for* visco-
  elastic effects in the adhesive which have an important bearing on situations
  involving sustained loading.

a function of adherend stiffness. This indicates that single-lap joints (if unsupported) are limited to very thin adherends and that double-lap joints can be greatly increased in thickness capability by tapering the ends of the outer adherends to avoid peel failures. However, for very thick adherends, scarf or stepped-lap joint configurations must be employed.

In the following sections, some of the factors influencing the double overlap joint are first considered in some detail - since this is the simplest effective joint which illustrates most of the important features of composite-to-metal joints. This is followed by a brief description of the other types of bonded joints.

2.2   The Double-Lap Joint

The model used in ref. (2) to estimate the shear stress distribution and load capacity of a double-lap joint is shown in Fig. 4; idealised stress-strain behaviour of the adhesive is assumed (Fig. 2b). The following discussion initially considers the joint overlap length, then briefly considers each of the following parameters in terms of their effect on load capacity of the joint: adhesive plasticity, joint stiffness, adherend stiffness imbalance, adherend thermal expansion mismatch.

Overlap Length:

The idealised shear stress distribution in a well designed joint is illustrated schematically in Fig. 5. This shows a fully developed elastic trough of length $6/\lambda$ (where λ is the exponent of the elastic shear stress distribution as defined on Fig. 5), and two zones at the ends of the joint in which the adhesive is stressed to its yield stress τ_p. The load carrying capacity of the joint (P) is obtained from the area under the shear stress curve. The maximum load (per unit width) that can be carried by the adhesive elastically is τ_p/λ; the rest of the load can be carried by the adhesive plastically, provided that the plastic strain in shear does not exceed γ_p. The maximum joint strength occurs when the plastic zone and the elastic zone are fully developed; increases in overlap length above this do not increase its load carrying capacity.

Whilst in most cases the applied load could be carried with a shorter overlap length, there are several reasons why a length greater than the maximum length indicated in Fig. 5 should be employed. A fully developed elastic zone serves (i) to stabilize the joint against creep in the adhesive by maintaining very low shear stresses in the central region (which is particularly important under hot/wet conditions where the adhesive is relatively weak); (ii) to provide allowance for manufacturing defects, such as voids and debonds; and (iii) to allow for service deterioration such as fatigue damage, debonding and general environmental degradation. In effect, a suitably long overlap length serves to make the joint damage tolerant.

For a balanced joint ($t_i = 2t_o$, Fig. 5) the required minimum overlap length for loading up to the ultimate strength (σ_{ult}) of the adherends - to obtain 100% joint efficiency - is given by

$$\ell_{min} = \frac{t \, \sigma_{ult}}{\tau_p} + \frac{4}{\lambda} \qquad\qquad (2.1)$$

where t is the adherend thickness. The adhesive properties for the hot/wet condition should be assumed for this calculation; an allowance of 25% is usually made for uncertainties.

Effect of Adhesive Plasticity on Strength:

The maximum load carrying capacity P per unit width of a joint in shear, in which the adherends have equal stiffness and expansion coefficient, is given by, using the notation of Fig. 4,

$$P = \sqrt{4 \, \eta \, \tau_p (\tfrac{1}{2} \, \gamma_e + \gamma_p) 4 \, E_o \, t_o} \qquad\qquad (2.2)$$

The quantity $\tau_p(\tfrac{1}{2} \, \gamma_e + \gamma_p)$, Fig. 2b, is the area under the stress-strain curve and is the work to failure per unit volume of the adhesive. The load carrying capacity increases as the square root of this term which is dominated by $\tau_p \, \gamma_p$ for a ductile adhesive; typically γ_p/γ_e is 20 to 50 for an epoxy-nylon adhesive at ambient temperature. Further, since the quantity $\tau_p(\tfrac{1}{2} \, \gamma_e + \gamma_p)$ does not vary much with temperature (see Fig. 2a) joint strength does not vary much with temperature.

Effect of Joint Stiffness on Maximum Strength:

Equation 2.2 shows that, for a stiffness balanced joint, P is proportional to $\sqrt{(E_o \, t_o)}$. Thus, the load carrying capacity of the joint increases as a function of the square root of adherend stiffness. Since, however, the adherend stiffness increases proportionaly to $E_o \, t_o$ and the adherend strength increases proportionaly to t_o, the load bearing capabilities of the adherends increase more rapidly than joint strength. In practice. assuming adherends with the strength and stiffness of aluminium alloy 2024 T3 (and ignoring peel effects, discussed later) the cross-over point occurs at a thickness of about 6 mm where the load capacity of the joint is about 2.5 MN/m (15000 lb/inch) and the strength of the adherends is about 2.9 MN/m.

Effect of Adhesive Thickness:

Equation 2.2 shows that the maximum load carrying capacity, P, increases in proportion to $\eta^{\frac{1}{2}}$, where η is the thickness of the adhesive layer. For most practical joints the adhesive layer thickness is held between 0.13 mm and 0.26 mm. Thicker layers tend to have a high void content, so are not a practical means of increasing strength. However, excessively thin layers reduce joint strength and must be avoided during manufacture; the presence of carrier fibres in structural film adhesives is highly beneficial in preventing excessive adhesive extrusion and, therefore, the formation of thin layers, during joint manufacture.

Effect of Stiffness Imbalance of Adherends:

Fig. 6 shows schematically the situation which arises when the outer members of a double lap joint are stiffer than the inner member. The highest stress occurs at the end of the joint from where the more compliant member projects irrespective of the direction of loading. This results in a reduction of the strength of the joint. Let S be the ratio of stiffness of the inner to the two outer adherends; then S = 1 is a balanced joint. Then, the strength reduction for S > 1 is approximately $\sqrt{(1 + 1/S)/2}$, and for S < 1 the reduction factor is $\sqrt{S(1 + S)/2}$.

Influence of Thermal Expansion Mismatch:

This is an inherent problem with composite-to-metal joints since for aluminium alloys $\alpha = 23 \times 10^{-6}\ °C^{-1}$ and for graphite/epoxy, typically, $\alpha = 0.5 \times 10^{-6}\ °C^{-1}$. For a stiffness-balanced joint the reduction in load capacity of the joint is approximately $2E_o t_o \Delta\alpha\Delta T$. However the critical end of the joint depends on the direction of loading as illustrated schematically in Fig. 7.

Effect of Combined Thermal Expansion Mismatch and Stiffness Imbalance:

In this situation the equations for maximum joint strength are either

$$P = (\alpha_o - \alpha_i)\Delta T E_i t_i + \sqrt{\{2\eta T_p(\tfrac{1}{2}\gamma_e + \gamma_p)2E_i t_i[1 + (E_i t_i/E_o t_o)]\}} \qquad (2.3)$$

or

$$P = (\alpha_i - \alpha_o)\Delta T 2E_o t_o + \sqrt{\{2\eta T_p(\tfrac{1}{2}\gamma_e + \gamma_p)4E_o t_o[1 + (2E_o t_o/E_i t_i)]\}} \qquad (2.4)$$

For this general case, the critical end of the joint cannot be obtained by inspection, the strength being given by the lesser of the two equations.

Peel Stress Limitation on Strength and Methods of Alleviation:

The mathematical model developed in reference (2) to estimate peel stress is shown in Fig. 8. The main simplifying assumption made to the analysis is that the shear stress (τ) at the ends of the adherends is constant. This is appropriate to a situation in which the adhesive has yielded. Peel stresses under tension loading arise at the outer edges of the outer adherends, from the tendency of the outer adherends to bend away from the inner adherend under the moment produced by the shear stresses. The bending is reacted out by the development of a peeling stress (σ_c) in the adhesive layer and adherends which is approximately given by:

$$\sigma_c = \tau \left(\frac{3E_c' t_o}{E_o \eta}\right)^{\tfrac{1}{4}} \qquad (2.5)$$

where E_c' is the <u>effective</u> transverse stiffness of the adhesive <u>system</u>. Thus, for a given adhesive system, σ_c is increased with increasing thickness of the outer adherend and is reduced with increasing stiffness of the outer adherend and increasing thickness of the adhesive layer. Use of a composite in place of a metal for the outer adherend reduces E_c' and, thus, peel stress. Peel stresses can be alleviated by control of these parameters and by geometrical means such as scarfing, to locally reduce t_0 as illustrated in Fig. 9. The influence of scarfing in reducing strength cut-off due to peel is shown schematically in Fig. 3.

The peel problem is particularly serious with fibre composites since they generally have low transverse strength, even compared with the adhesive, particularly if this is the ductile peel resistant type.

2.3 Brief Discussion on the Design of Other Bonded Joints

Single-Lap Joints:

The behaviour of single-lap joints is dominated by peeling effects which arise from bending moments produced by the eccentricity in the load path. Thus, these joints should generally not be employed for fibre composite adherends since these usually have poor transverse strength.

These problems do not arise, however, in a single-lap joint which is supported against bending, e.g. by a substructure to which the joint may be attached or fastened. In this case the double-lap joint analysis is applicable, considering the single-lap joint as a symmetrical half of the double-lap joint.

Scarf Joints:

The shear stress in the adhesive layer is reasonably uniform in a scarf joint, provided the adherends have equal stiffness and thermal expansion coefficients, and the scarf is taken to a sharp edge. Peel stresses and transverse stresses (σ_T) are also very low at low scarf angles θ.

Simple theory gives

$$\tau = \frac{P \sin 2\theta}{2t}$$

$$(2.6)$$

$$\sigma_T = \frac{P \sin^2 \theta}{t}$$

For small scarf angles the conditions for failure in the adherends is given by

$$\theta < \tau_p/\sigma_{ult} \quad \text{radians} \qquad (2.7)$$

However, if the adherends are dissimilar, as in a composite-to-metal joint, the shear stress in the adhesive is not uniform and design becomes more complex. Where joints have adherends with different stiffness the highest stress occurs at the end from which the more compliant adherend extends. For either elastic or plastic analysis, the ratio of the average shear stress to the peak shear stress asymptotes to the adherend stiffness ratio. Problems with stiffness imbalance and thermal expansion mismatch are greatly reduced by employing a multiple scarf configuration. As shown schematically in Fig. 3, scarf joints are capable of joining adherends of any thickness.

Stepped-Lap Joints

Stepped-lap joints can be analysed as a succession of double-laps. (The scarf joint can be considered as a stepped-lap joint having an infinite number of steps). In common with the double-lap joint, the stepped-lap joint has a non-uniform shear stress distribution with high stresses at the ends of each step. However, with suitable design the stepped-lap joint is capable of joining adherends of considerable thickness. In order to increase the load carrying capacity of a stepped-lap joint it is not usually sufficient just to increase the length of the steps, since the load carrying capacity of each step does not increase indefinitely, as discussed earlier for double-lap joints; instead it is necessary to increase the number of steps. Indeed, to avoid overloading some of the end steps of the inner adherend, it may be necessary to reduce their length. The results of an elastic analysis of a stepped-lap joint (such as is used for the wing-to-fuselage joint on the F-18) is illustrated in Fig. 10. Peel stresses are not usually a problem because of the low thickness at the ends of the outer adherend.

Bonded and Bolted Joints

In general an adhesive joint is much stiffer than a bolted (or riveted) joint. Thus, it is not possible to design a bonded and bolted joint where load is effectively shared between the bonded and fastened regions. Fasteners may be used effectively, however, in thick section joints (where failure would normally occur preferentially in the adhesive) to contain local adhesive failure where design stresses are exceeded for any reason (e.g. due to overload or local bond flaws). For this purpose the fasteners should be situated away from high stress regions in the adherends - the centre of the elastic trough in a lap joint is an ideal region. An alternative view, leading to similar conclusions for placement of the fasteners, is that use of adhesive bonding alleviates load in the fastened region, reducing the danger of fatigue failure from the fastener holes.

Rivets are sometimes employed at the ends of a lap joint to reduce peeling stresses. Although mechanically this approach may be effective, particularly for single-lap joints, it is a dangerous procedure in practice since the presence of fastener holes allows entry of moisture and other fluids into the critical high shear stress region and can result in environmentally induced bond failure. It is much safer to use the other procedures for reducing peel stresses, referred to earlier.

2.4   Materials Aspects

Optimum Ply Configuration:

Generally for a bonded joint, the ply content (e.g. proportion of 0°, ±45°, and 90° plies) will be determined by factors other than joint design. However, the strength of the bonded joint (all other aspects taken as constant) depends on the orientation of the fibres at the joint interface. The shear strength of the interface is maximum when the outerlayer of fibres are oriented in the same direction as the applied load and is minimum when the fibres are oriented perpendicular to the applied load. Thus, for a given ply content, the ply configuration should provide 0° fibres on the outer surface for lap joints and on the steps of a stepped lap joint. No particular ply configuration is necessarily optimum for a scarf joint.

Adhesives:

Structural film adhesives are usually employed for forming bonded joints between advanced fibre composite and metal adherends. These adhesives consist of a pre-catalysed modified epoxy such as an epoxy-nitrile, or, for higher temperature applications, an epoxy phenolic, supported by a glass or polymer fibre, usually polyester or nylon, in mat or woven form. Cure temperatures vary from about 110°C for epoxy-nitrile to 180°C for epoxy phenolic. The epoxy-nitrile adhesives are formulated to provide high peel resistance. This results from a dispersion of chemically bonded nitrile rubber particles in the matrix, which consists of a dilute solid solution of the rubber in epoxy resin. These ductile adhesives suffer a makred loss in shear strength and stiffness above about 60°C. The epoxy-phenolic types of adhesive are suitable for use at temperatures up to about 120°C but are brittle and therefore have relatively poor peel resistance at lower temperatures.

The carrier fibres in structural adhesive films serve several purposes, including (i) providing mechanical strength to the uncured resin for handling purposes, (ii) controlling flow and thus inhibiting overthinning of resin during joint formation, (iii) improving peel strength, and (iv) insulating the adherends in the event of complete resin squeeze out; this is important where graphite/epoxy is joined to aluminium alloys, since electrical contact can result in severe galvanic corrosion of the aluminium. However, the carrier fibres can encourage wicking of moisture into the adhesive layer and result in degradation of the metal/adhesive bond. Woven fibres produce more of a problem than mat in this respect since they provide a continuous diffusion path.

Surface Treatment:

The most critical step in joint formation is the production of the correct type of surface for bonding. To ensure good bond strength and durability, metals such as aluminium and titanium alloys are generally degreased, etched, and anodised, to form a stable oxide film. Prior to bonding, the surfaces are coated with a thin layer of a corrosion inhibiting primer - a low solubility chromate in an epoxy resin.

142

Fortunately, in the case of a cured epoxy matrix composite, production of a roughened resin surface, clean from surface contaminants (particularly release films) is all that is usually required. This can be achieved by degreasing and abraiding the area with abrasive paper, or by blasting with a grit such as aluminium oxide to remove the contaminated surface and increase surface energy. Alternatively, during manufacture, a layer of woven nylon cloth is incorporated into the surface of the composite. Prior to bonding, the nylon ply is peeled from the composite exposing a clean surface ready for bonding. The nature of the resulting surface can be controlled to some extent by the weave of the nylon peel ply. However, the resulting surface is usually very rough and tends to entrap air bubbles. There is also a serious danger that small amounts of the peel ply may be left on the surface. It is generally considered that abrasion produces a more reliable surface for bonding.

The requirement for producing a clean surface in the composite (with all the inherent dangers) can be avoided by co-curing the composite with the adhesive. This involves consolidation of composite at the same time as the adhesive is cured, and effectively removes one adhesive/adherend interface.

2.5   Joint Manufacture

Pre-cured Composite:

After surface treatment of composite and metal surfaces, film adhesive is placed between the faying surfaces, and then the parts are supported on a special tool. Thermocouples are placed in position to monitor temperature and temperature distribution, and heat and pressure applied either in a heated press, for relatively small simple components, or in an autoclave for large or complex components. When autoclave curing is used, a vacuum bag is formed over the tool surface to hold the parts in place prior to the cure and to remove air and volatiles. The vacuum is released before gelation of the adhesive and application of full pressure.

Co-Curing

The first half of a composite component is laid up with pre-preg onto a tool, with the configuration required to form the end shape, e.g. steps for a stepped-lap joint. In order to minimise movement during joint formation, the composite lay-up, if consisting of many plies, say 20 or so, is usually debulked at several stages by vacuum bagging operations. The contoured metal part – after appropriate surface treatment and coating with adhesive is placed in position. Finally, the second half of the composite component is formed from pre-preg laid-up over the metal and the composite inner layer. A further vacuum bag is then placed over the part and the assembly cured under normal autoclave conditions.

For this procedure to be successful, the adhesive and resin must be chemically compatible and must cure under a similar temperature, pressure, and time, sequence.

143

2.6 Quality Control

Surface Treatment:

No simple direct methods are available for assessing the quality of surfaces after surface treatment. Thus, close analytical control is maintained over all chemical processes, and control specimens are periodically surface treated, bonded, and tested. In addition, test coupons are usually manufactured along with bonded components (often cut from the component panel) and evaluated using durability and other tests.

Recently the Fokker Aircraft Company produced an instrument which is claimed to measure the quality of surface-treated metallic components by measuring surface free energy. Polarised light tests can be used in some cases to establish the formation of satisfactory oxide films during anodizing of metal surfaces. Other surface examination techniques, such as ellipsometry, can be used to detect contamination and the quality of the anodised film. However, as yet, this has not been used in practical applications.

Bonding Procedure:

The main process quality control here is to measure and record the temperature distribution and the temperature, pressure cycle. The quality of the final component is assessed from the tests on coupons and other specimens manufactured along with the component.

Final Component:

In general, NDI procedures such as ultrasonic (C-scan) and radiography are usually employed. These can detect most significant defects, such as foreign bodies (e.g. separator film), disbonds, delaminations (in co-cured joints), and voids.

3. MECHANICAL JOINTS

3.1 General

This section deals primarily with composite-to-metal joints employing mechanical fasteners, particularly bolts. However, it is worth briefly mentioning an important class of joints which are formed by a wedging action. Joints of this type are employed for various centrifugally loaded applications such as compressor fan blades, as illustrated in Fig. 11, where the outward forces develop the flatwise wedging forces. The major advantage of this type of joint is that holes piercing the composite structure (with the associated stress concentrations) are not required. Wedges may be formed by a bonded - on doubler or, more usually (Fig. 11) by insertion of extra material, such as extra graphite/epoxy layers or glass/epoxy layers. Stress concentrations at the grip exit region are minimised by using the softer glass/epoxy material.

A type of joint, intermediate between the wedge and the conventional bolted joint, is the wrap around joint. This involves the use of tows of fibres wrapped around a loading pin. This configuration has the advantage that

the fibres are continuous and thus stress concentrations are relatively small. Bearing is by flatwise compression on the composite and, in this respect, is similar to that encountered in the wedge joint. Joints of this type are employed for helicopter blades, where the fibres forming the cap of the spar form the wrap around root.

3.2 General Design Considerations - Fastened Joints

Many of the joint configurations used for bonding, Fig. 1, can also be employed for mechanical fastening, since the problems of smoothly trans-ferring load from one adherend to another are quite similar. The main differences are that, in mechanically fastened joints, most of the shear is transmitted through discrete high modulus regions (the individual fasteners), and the shear loads in the fasteners are reacted out by compression (bearing) on the faces of holes passing through the joint members. Some of the shear load is also transmitted by friction through the faces of the members. However, although this is beneficial in improving load transfer in the joint and in reducing bearing loads, friction transfer can not usually be maintained at a high level during prolonged service, due to loss of clamping pressure as a result of vibration and wear. Further, complications may also arise due to fastener bending which may occur from loss of clamping pressure and hole elongation during service. This is particularly a problem with those composites which are relatively soft, and can result in fatigue failure of the fastener. As in metallic joints, three main modes of failure of the joint members must be considered for design purposes (Fig. 12). These are (a) net section tension or compression, (b) shear, and (c) bearing; however, in practice mixed modes of failure often occur. The allowable stresses in each of these modes is a function of (i) the geometry of the joint (including the hole size, plate width and the distance of the hole from the edge of the plate; see Fig. 13), (ii) the clamping area and pressure - allowing for any counter-sink, (iii) the fibre orientation ply sequence, (iv) the moisture content and exposure temperature, and (v) the nature of the stressing (e.g. tension or compression, sustained or cyclic, and any out of plane loads causing bending).

Although practical joints are complex, most can be modelled as simple single or double-lap joints, with single or multiple rows of fasteners. The following discussion on design for graphite/epoxy-to-metal joints considers mainly a double-lap joint (thus avoiding complications caused by bending) with initially a single bolt fastener as shown in Fig. 13. The ply configuration is taken as the 0°/±45° type (with a relatively small amount of 90° plies) commonly employed in aircraft applications. In this section the various failure modes under externally applied loads will be considered; effects of thermal expansion mismatch between the composite and metallic component, whilst, possibly, a significant factor on loading of the joint, have not apparently been considered in the literature and are not covered here.

3.3 Design Criteria For Failure Under Static Loads

Tensile Failure:

Estimation of the static tensile strength of a metallic joint is usually based on net section area. Stress concentration effects are ignored

since it is assumed that they are relieved by local yielding (a dangerous assumption under fatigue loading). Thus one can write:

$$\sigma_{Tu} = P/(w-d)t \qquad (3.1)$$

where σ_{Tu} is the allowable static strength in tension (e.g. the A or B allowable strength for aircraft design) and P the allowable load on the joint.

This situation cannot be assumed for the composite, since generally yielding is not possible (although actually there is some evidence that limited hole softening occurs due to a yielding effect associated with the high interlaminar shear at the edges of the hole). Thus, the simplest relationship that can be assumed is:

$$\sigma_{Tu} = K_T \; P/(w-d)t \qquad (3.2)$$

The problem is to determine the stress concentration factor, K_T, for a loaded hole in a composite plate of given constitution and configuration.

It is instructive, initially, to consider the K_T for an unloaded hole since this case has been solved analytically. The analysis in ref. (4) shows that, for an infinite plate, the effective K_T at the edge of the hole at 90° to the applied load is

$$K_T = 1 + \sqrt{[2\{\sqrt{(E_x/E_y)} - \nu_{xy}\} + E_x/G_{xy}]} \qquad (3.3)$$

where E_x and E_y are the moduli in the direction of the load and normal to the direction of the load, respectively, G_{xy} is the in-plane shear modulus, and ν_{xy} the major Poisson's ratio.

From this equation it can be shown that, typically, K_T varies from 7.5, for a 100% 0° laminate to about 1.8 for a 100% ±45° laminate, and approaches the isotropic value of 3 at about 80% ±45°. The ±45° plies serve to reduce K_T by carrying load around the hole. It is of interest to note that K_T falls below the isotropic value at 100% ±45° plies. To take advantage of the low K_T and high fracture toughness of this construction, British Aerospace, in their experimental Graphite/Epoxy Jaguar Wing used ±45° skins to take the torsional loads, with the 0° plies, required to take the bending loads, separated out into discrete booms.

Since the tensile strength of the laminate falls with increasing ±45° content, it can be shown (5) that the optimum configuration for the holed laminate is given by the maximum value of σ_{Tu}/K ; this occurs at about 50% ±45°.

These considerations, based on the stress concentration factor at 90° to the hole are highly simplified because, in general, the peak stress occurs at some other angle; e.g., for a ±45° laminate the peak occurs at 45° to the loading direction where K_T is about 2. Secondly, the stresses in the individual plies differ according to their orientation, so each ply should be examined separately. Thirdly, biaxial stresses should be considered to

obtain the true failure criterion for each layer. Finally, as mentioned earlier, high interlaminar shear stresses at the edges of the hole (dependent on ply constitution and lay-up sequence) result in a local softening, possibly due to local delaminations, reducing the K_T value.

Various procedures have been developed to obtain K_T values for loaded holes, including finite element procedures, semi-empirical procedures based on experimentation, and analytical procedures. In general, these are rather complex, especially for the purpose of the present discussion. It was shown, however, from experimental studies (5), that equation (3.3) gives a reasonable estimate of the effective K_T for a loaded hole, at least for one representative situation. Although, because of the many differences with the theoretical solution for an unloaded hole, agreement must be considered somewhat fortuitous, the value of K_T so obtained is probably of the correct order at least for present discussion.

Compression Failure:

It will be shown later that fatigue must be considered for the design of joints subjected to compression loading, unlike tension loading where static strength is the design criterion. Although, for an unfilled hole, similar stress concentration factors to those discussed above must be considered for compression, the presence of a fastener stabilises the surrounding material against compression failure.

The mode of failure under compression loading is dominated by the shear properties of the matrix, because the effective shear modulus of the matrix is a major factor determining the stability of the fibres against buckling. The effective shear modulus of the matrix decreases with increasing temperature (up to the maximum service temperature of about 120°C), and also with increasing absorbed moisture; moisture dissolved in the resin matrix (up to a maximum of about 1.5% of the laminate weight) acts as a plasticizer. The compression strength for the hot/wet condition can be as low as 50% of the room temperature/dry condition, and may be even lower, relatively, when the composite contains stress concentrators, such as holes.

Shear Failure:

Estimation of shear or tear-out failure load for a metallic joint is usually based on the following equation:

$$\tau_u = P/2et \tag{3.4}$$

where τ_u is the allowable shear stress and the rest of the notation is as indicated in Fig. 13. There is experimental evidence (5) that this simple relationship also holds for graphite/epoxy laminates containing a significant fraction of ±45° plies, which implies that there is no stress concentration for this type of loading.

147

In contrast, significant stress concentrations appear to arise for an all 0° laminate (not a practical configuration for a bolted joint). With an all 0° laminate splitting is the preferred mode of failure and fairly elaborate precautions are required to inhibit this mode, to allow measurement of the shear strength. When this is done, it is found that the value obtained for τ_u falls well below the apparent in-plane shear strength and the inter-laminar shear strength. Splitting is suppressed for laminates containing plies at significant angles to the 0° direction (e.g. ±45°) since these provide transverse strengthening. Experiments (5) show that an optimum value of strength occurs for the 0°, ±45° family of laminates, again at a combination of 50% 0° plies and 50% ±45° plies.

Bearing Failure:

Bearing loads for a metallic joint are usually estimated from the simple relationship

$$\sigma_{Bu} = P/dt \tag{3.5}$$

where σ_{Bu} is the allowable bearing load, and the other notation is as indicated in Fig. 13. Failure in bearing in a metallic joint occurs by compression yielding of the material at the compression end of the hole. In general, the bearing load is the highest load that can be carried by the joint if e and w are large enough to avoid tension or shear out failures. In a composite, bearing failures occur by local buckling and kinking of the fibres, and subsequent crushing of the matrix. However, according to reference (5), equation (3.5) is applicable.

As a result of this failure mode, σ_{Bu} is quite strongly dependent on the lateral constraint (clamping pressure) provided by the fastener. Experimental studies (5) have shown that an improvement in bearing load of from 60% to 170% can be obtained over pin loading, with a fastener clamping pressure of about 22 MN/m²; above this pressure no further improvement is obtained. Since clamping pressure plays an important role in the bearing strength of composites it will be important (particularly if design is based on constrained bearing) to ensure that this pressure is maintained during the service life.

Bearing stresses initially increase with increasing proportions of 0° plies since these are most efficient in carrying bearing loads. However, with laminates having above about 60% 0° plies, failure occurs by splitting, since the 0° plies have a low transverse strength. The optimum once again appears to occur at about 50% 0° and 50% ±45°. It is found that the bearing strength is further improved, the more homogeneous the ply sequence (dispersion of 0° and ±45° plies). Theoretically, it is well known that interply shear stresses are reduced as the laminate becomes more homogeneous.

The bearing strength may also be expected to be dependent on the moisture content of the resin matrix and the exposure temperature. Whilst, in general, bearing strength probably does decrease with matrix moisture content and test temperature, these adverse effects are considerably reduced if a high

148

level of local lateral constraint is present. Further, some hole softening
in practice leads to better contact of the fastener with the hole, and so
reduces high local loads. Thus, in general, environmental effects do not
appear to affect bearing strength significantly.

3.4 Influence of Fatigue Loading

Open Holes:

In order to discuss the effect of fatigue loading on a graphite/
epoxy laminate with an open hole it is necessary to consider the mechanism
of failure in a little detail; reference (6) includes several papers of
relevance here. Under tension or compression dominated fatigue loading, the
sequence of failure begins in regions of high stress concentration, with
matrix cracking and local debonding of fibres from the matrix. The localised
damage accumulates until it results in more extensive intralaminar cracking.
This reduces the in-plane stress concentration, but increases interlaminar
shear stresses, eventually producing delaminations. The rate of degradation,
and its extent, depend on the interply shear stresses, which are strongly
dependent on ply configuration. More homogeneous configurations generally
produce lower interply stresses.

At this stage, tension and compression behaviour differs greatly.
The effect of the degradation process under fatigue is to reduce the tensile
stress concentration and therefore, at least in the early stages, the
residual strength may show a significant increase. In any event, within the
allowable static tensile strength range the effect of fatigue on residual
strength is usually not detrimental, unless delamination damage is very severe.
Thus, for design purposes, it is necessary only to consider static strength
for laminates subjected to tensile loading.

Under compression loading, although the compression stress
concentrations around the hole are similarly reduced, the loss in section stiff-
ness due to delamination can lead to compression or buckling failure of the
remaining sound material (7). Thus, residual compression strength falls as
a function of fatigue loading; consequently fatigue must be considered in the
design of laminates subjected to compression loading. The extent in the
design of laminates subjected to compression loading. The extent to which
large scale delaminations can grow under fatigue loading and the critical   as
of delaminations for failure under limit loads are subjects of current
research.

The compression strength of the composite is, as mentioned previously,
dominated by the mechanical properties of the matrix. As a consequence, fatigue
properties under compression dominated loading are sensitive to the moisture
content of the matrix and the test temperature.

Filled Holes/Compression Loading:

The above considerations may also be relevant to laminates with a
filled (or loaded hole), even if the fastener is initially a close fit in the
hole. This is because partial bearing failure may occur under fatigue loading
allowing fastener movement and thus spoiling the close fit. In practice, hole

enlargement and loss in residual strength during fatigue loading do not appear to be problems (residual strength may even increase), if load reversal does not occur e.g. for R = -∞ (zero-compression). However, loss of residual strength is marked at R = -1 (tension-compression). The major problem at R = -1 is that of fastener failure, due to fastener bending consequent on hole enlargement. Thus the actual situation under fatigue loading is quite complex. A possible sequence under R = -1 is (i) loss of clamping pressure under fatigue loading, (ii) partial bearing failure and hole enlargement resulting from loss of clamping pressure, (iii) fastener failure, and (iv) final failure due to overloading of adjacent fasteners and holes.

To allow for the presence of delaminations, which may arise due to fatigue damage around stress concentrations or from low energy impact damage, the design allowable for compression dominated cyclic loading is usually given as an allowable strain in the material away from the region of the stress concentrator. The advantage of this approach is generally that no further specification of laminate stiffness is required. Most aircraft manufacturers take the allowable value to be between - 3000 microstrain and -4000 microstrain.

3.5   Multi-Row Bolted Joints

In most practical applications loads are carried by several bolts; an extreme example is a spanwise, skin to spar joint in an aircraft wing. Since, in this case, each bolt reacts out only part of the load the question of interaction between the loads introduced through the bolts, and the running loads, must be addressed.

The simplest approach (8) is to assume a linear relationship of the form:

$$\sigma_{Tmax} = \sigma_T \, K_T + \sigma_B \, K_B \leqslant \sigma_{Tu} \quad \text{(allowable stress)}$$

where σ_B is the bolt bearing stress at the hole under consideration and σ_T is the net section tensile stress caused by the remainder of the load (not reacted by the bolt). The constant K_T accounts for the effective tensile stress concentration resulting from the running load and K_B that resulting from the bearing load. This relationship was validated experimentally (9) and it was found that K_T had values from 1 to 2 and K_B had values from 0.25 to 1 depending on laminate configuration and geometry.

The picture under compression is somewhat different if the hole is filled with a close fitting bolt, since in this case the running compression loads can be reacted out over the region of the hole by bearing on the fastener. In this case the running compression stress (σ_c) and the compression bearing stress (σ_B) are additive with respect to bearing stress;

$$\sigma_{Bu} \leqslant \sigma_B + \sigma_c$$

is the failure criterion.

3.6　Materials and Processing Considerations

Hole Strengthening Procedures:

Several procedures may be employed to improve the strength of the composite under loaded hole conditions. Most of these procedures are based on the incorporation of extra layers into the laminate in the holed region. However, although the composites lend themselves well to modifications of this nature, manufacturing costs are usually greatly increased. Consequently, use is generally confined to critical applications such as highly loaded lugs.

The stress concentration at the edges of a loaded hole in graphite/ epoxy can be reduced significantly either by local reinforcement with a stiffer fibre, such as boron, or by local softening by using local reinforcement with a low modulus fibre, such as glass or aramid; these procedures are also employed to improve damage tolerance of the composites. An effective alterna- tive means of softening the holed area is by incorporation of extra ±45° graphite/epoxy plies, and an alternative means of reinforcement is by incorporation of layers of titanium alloy sheet. The last two methods are also very effective in improving the bearing and shear strength, both by providing additional reinforcement (the titanium alloy is particularly effective in improving bearing strength) and by increasing area.

A simpler and less costly approach is to reinforce the hole with an externally bonded doubler, either made of composite (glass, aramid or graphite) or titanium alloy. The doubler must be appropriately scarfed to minimise shear and peel stresses in the adhesive. In an experimental study in which the weight and thickness of some of these concepts were compared for a given load carrying capacity, it was found that use of extra ±45° graphite/epoxy plies was the lightest solution and use of titanium alloy interleaves the thinnest. However, the use of titanium created considerable manufacturing difficulty because of the bonding pre-treatment required, and the subsequent difficulty in forming holes (tendency to delamination of the material around the hole).

Hole Formation Practice:

Hole drilling in graphite/epoxy, using tungsten carbide tipped drills, causes no particular problem provided simple precautions are taken to avoid delamination. In particular, care must be taken to support the laminate during drilling by sandwiching it either between scrap material or in a drilling guide jig. Delamination on the exit side of the drill can also be prevented by coating the composite on this side with a layer of film adhesive (British Aerospace practice). It is also advantageous to employ a pressure controlled drill and a fairly slow feed rate. Under mass production conditions, some minor delamination damage is inevitable. Provided delamination is not too extensive, the damage can be repaired by local injection of epoxy resin.

Although very good tolerances can be maintained on holes in graphite/ epoxy, interference fit fastening is generally (although not universally) avoided, since excessive interference can result in delamination damage; significant stressing of the hole may also arise subsequently at elevated temperature resulting from differential expansion of the fastener and

laminate. Generally, clearance holes with a tolerance of 0.05 to 0.1 mm are used in most aircraft applications.

For applications where the fastener heads are required to be flush with the surface of the components, countersink depths are limited to avoid the formation of knife edge bearing surfaces which would be very fragile in these materials.

Fastening Procedures:

The fastener spacing and edge distance employed depend on factors such as the type of fastener used, the load transfer requirements, and the ply configuration. Generally, the minimum edge distance ranges from two to three times the fastener diameter, and the minimum allowable fastener spacing ranges from three to four fastener diameters.

For most applications the recommended clamping pressure, σ_z, is about 20 MPa (5); the required torque, T, may be calculated from $\sigma_z = 1.658/d^3$ where a washer of diameter 2.2d is assumed.

Corrosion Prevention:

Graphite/epoxy materials are electrically conducting and cathodic with respect to most structural metals. Thus, to avoid the danger of galvanic corrosion of the metal side of the joint, special precautions are required. Glass, aramid and boron fibre reinforced plastics are non-conducting and thus pose no corrosion problems.

In general, fasteners made from aluminium alloys or steel are avoided unless they can be insulated from the graphite/epoxy composite. The preferred fastener material, particularly for bolts and lock pins, is titanium alloy, although stainless steel is also considered to be suitable. Where the titanium alloy fastener comes into contact with the aluminium alloy side of the joint, an aluminium pigmented coating may be used for corrosion compatibi- lity. Corrosion resistant steel nuts and washers are used, and these may be cadmium plated where they come into contact with aluminium structure.

In areas where graphite/epoxy and aluminium alloy may come into contact, an insulating layer of glass/epoxy or aramid/epoxy is employed. This is usually co-cured onto the surface of the graphite/epoxy laminate during manufacture. In some cases, the insulating layer may also be employed on the outside of the component to allow use of aluminium fasteners.

Fasteners are usually wet set in a corrosion inhibiting sealant, such as a chromate pigmented polysulphide rubber. However, this precaution is not necessary for titanium, unless required for sealing areas containing fuel.

152

REFERENCES

1. Kinloch, A.J., Developments in Adhesives-2, Applied Science Publishers, London, 1981.

2. Hart-Smith, L.J., Adhesive-Bonded Double-Lap Joints, NASA CR-112235, 1973.

3. Hart-Smith, L.J., Analysis and Design of Advanced Composite Bonded Joints, NASA CR-2218, 1974.

4. Lekhnitski, S.G., Anisotropic Plates, 2nd Edition, Gordon and Breach, 1968, p. 171.

5. Collings, T.A., The Strength of Bolted Joints in Multi-Directional CFRP Laminates, Composites, vol. 8 (1), 1977.

6. Fatigue of Filamentary Composites, ASTM STP 636, 1977.

7. Saff, C.R., Compression Fatigue Life Prediction Methodology for Composite Structures, NADC-78203-60, 1980.

8. Hart-Smith, L.J., Mechanically Fastened Joints For Advanced Composites - Phenomenological Considerations and Simple Analysis, pp. 543-575 of "Fibrous Composites in Structural Design", Edited by Lenoe, E.M. et al., Plenum Press, New York, 1980.

Double lap

Single lap

Single scarf

Double scarf

Stepped lap

Double stepped lap
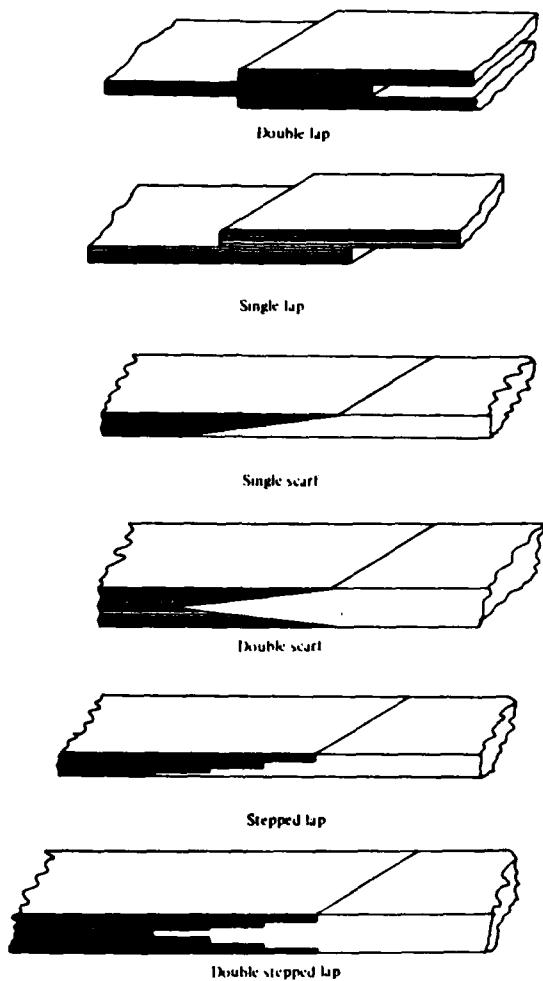
Fig. 1   Schematic illustration of some of the configurations employed for joining composites
to metals by adhesive bonding

154
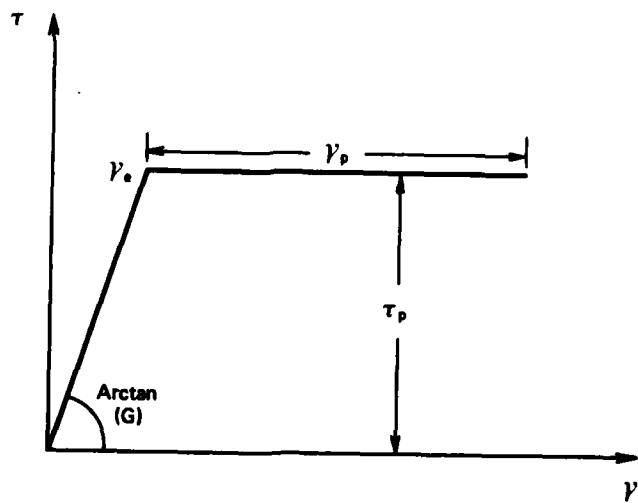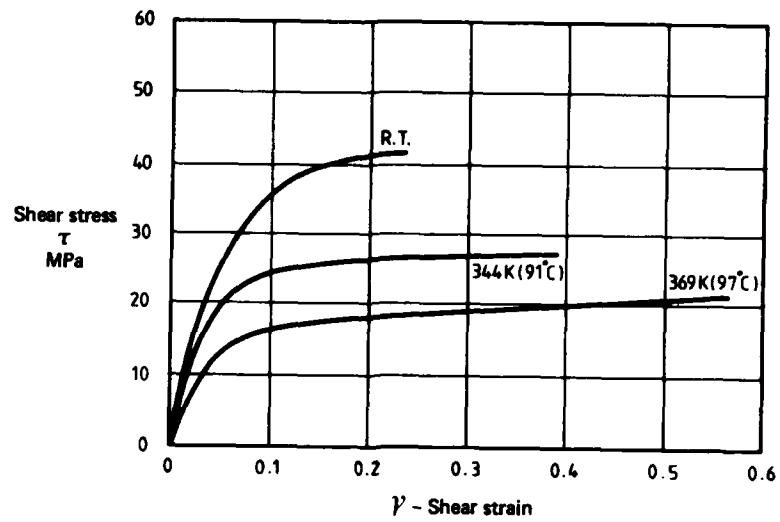
FIG. 2 (a) Plots of shear stress versus shear strain at various temperatures for adhesive FM 300 after exposure to moisture, obtained from thick adherend test
(b) Idealisation of a typical shear stress/shear strain curve for analytical purposes — the aim is to have similar area under the curve τp ($\frac{1}{2}\gamma_e + \gamma_p$) as the real curve

155
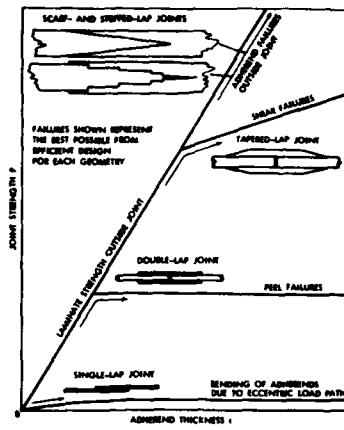
Fig. 3   Schematic illustration of strength limitation of various joint designs as a function of
adherend stiffness; taken from reference (2)
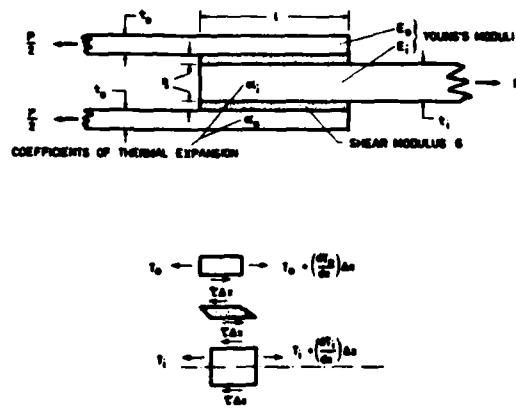
Fig. 4   Schematic of the model employed in (2) to analyse the double lap joint

156

$$\lambda = \frac{G}{\eta} \left(\frac{2}{E_i t_i} + \frac{2}{E_o t_o} \right)$$
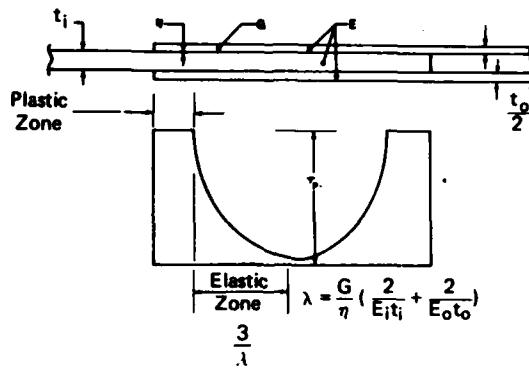
Fig. 5 Schematic illustration of adhesive shear stress distribution in a stiffness balanced joint of optimum length
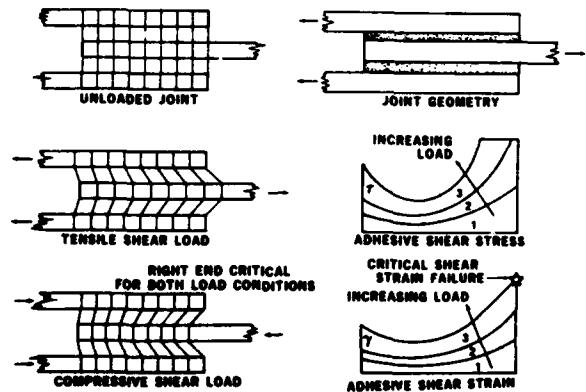
Fig. 6 Schematic illustration of the effect of adherend stiffness imbalance on adhesive shear strength; taken from reference (2)
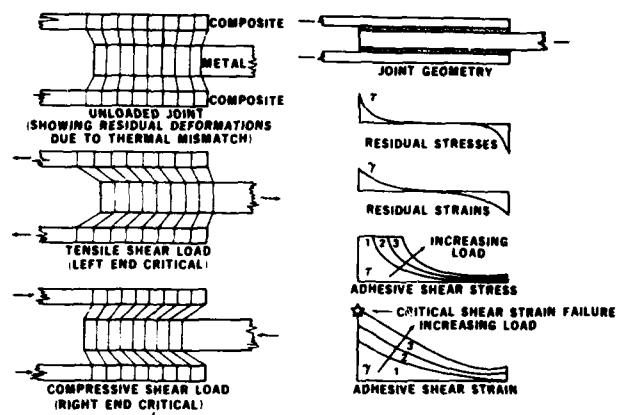
Fig. 7   Schematic illustration of the effect of adherend thermal expansion mismatch on
adhesive shear strength. The lower two diagrams on the right refer to tensile loading;
taken from reference (2)
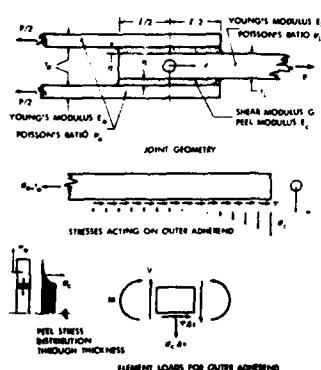
Fig. 8   Model used in ref. (2) to analyse for peel stresses

CHARACTERISTIC FAILURE MODE FOR THICK COMPOSITE ADHERENDS

ALTERNATIVE PEEL STRESS RELIEF TECHNIQUES

BOND PEEL STRESSES

REDUCED BOND PEEL STRESSES

ASSOCIATED SHEAR STRESSES

HIGHER AVERAGE SHEAR STRESS
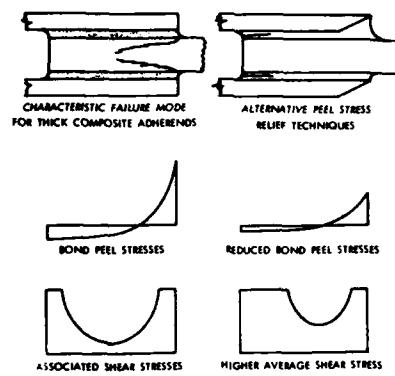
Fig. 9   Schematic illustration of peeling failure mode in a composite inner adherend and
geometrical methods of reducing peel stresses; taken from reference (2)
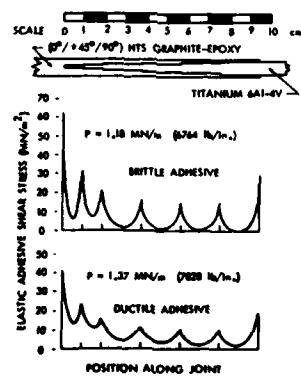
Fig. 10   Illustration of a stepped lap joint employed to join titanium to graphite/epoxy and the
analytical shear stress distribution in the adhesive for two adhesive types; taken from
reference (2)

159
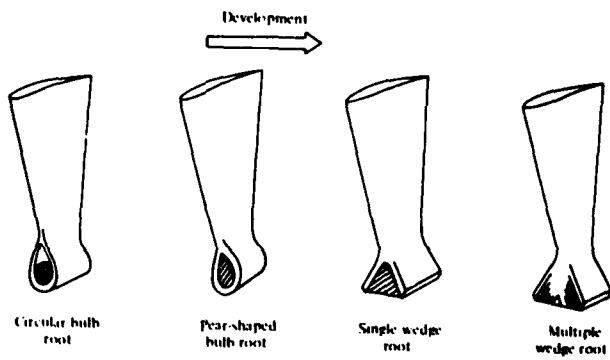
Fig. 11   Development of root configurations, based on a wedging action, for fan blades
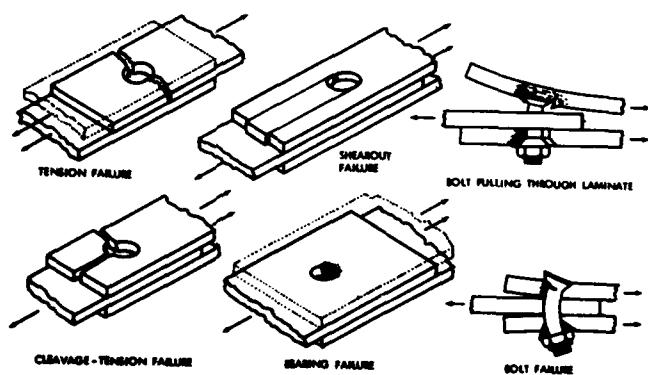
Fig. 12   Modes of failure for bolted joints in advanced fibre composite

160
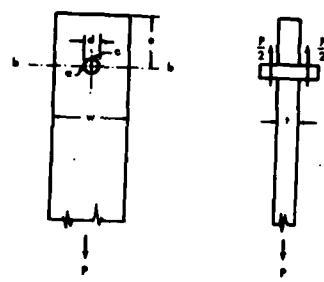
Fig. 13   Geometry of a simple double-lap bolted joint

161

Lecture 9

ENVIRONMENTAL EFFECTS AND DURABILITY

B.C. HOSKIN

1.   INTRODUCTION

In this lecture, key factors which influence the performance of
composite aircraft structures in service will be discussed. These include
environmental effects, especially the effect of moisture absorption from
the atmosphere taken in conjunction with elevated temperatures such as are
encountered by an aircraft structure in high speed flight, and the effect
of cyclic (fatigue) loads.

Bearing in mind that metal aircraft structures have been in
widespread use for almost half a century and that significant uncertainties
still exist there in the general areas of environmental effects and fatigue
performance, it can hardly be considered surprising that significant
uncertainties exist in these same areas for composite aircraft structures,
where there is so much less experience. Another aspect which compounds the
uncertainties for composites is the presence of additional parameters, which
have no analogue for metals, and which can affect performance e.g., the ply
orientations and stacking sequence for a laminate. It is usual practice,
when assessing environmental effects and fatigue performance for design
purposes, to establish a relatively large data base for the particular laminate
patterns it is intended to employ.

For further discussions of environmental effects and fatigue, see,
for example, refs. (1) to (4).

2.   MOISTURE ABSORPTION

The matrix materials, such as epoxy resins, which are commonly used
for present day composites absorb moisture from the atmosphere by what is
essentially a diffusion process. Under ambient temperature conditions, the
rate of diffusion is quite slow, it taking times of the order of weeks (or
even months) for a laminate kept in a humid atmosphere to achieve an equili-
brium moisture distribution. The reverse process, "desorption", also occurs
inasmuch as if a laminate containing moisture is exposed to a dry atmosphere
it will dry out, also by a diffusion process. The amount of moisture in a
laminate is generally expressed in terms of the percentage increase in
laminate weight; for graphite/epoxy laminates exposed for long times in humid
atmospheres weight increases of the order of 1% are encountered.

Since, as will be seen later, the presence of moisture in a laminate
can significantly affect certain of its structural properties, considerable
attention has been devoted to establishing theoretical procedures for
predicting the moisture content. These can be illustrated by reference to the
following example which, although a substantial simplification of the situation
for an aircraft in service where the environmental conditions vary, is
nevertheless representative of the situation encountered in the laboratory in

connection with the moisture conditioning of test specimens. Consider, therefore, an initially dry laminate immersed in a constant humid atmosphere (Fig. 1). It is assumed that moisture only enters the laminate through its flat faces. (When conditioning test specimens, this is often ensured by protecting the side edges of the laminate with some material which is impervious to moisture). If z denotes the co-ordinate in the thickness direction, here measured from one face of the laminate, and t the time, then it has been shown (see, for example, refs. (5), (6), (7) and (8)) that, at least to a good approximation, the ingress of moisture proceeds in accord with Fick's law, namely,

$$\frac{\partial c}{\partial t} = D \frac{\partial^2 c}{\partial z^2}$$
(2.1)

where $c(z,t)$ denotes the moisture concentration in the laminate at depth z at time t,
D denotes the diffusion constant.

As well, there are initial conditions which, for the present case of an initially dry laminate, become simply

$$c(z,o) = 0, \qquad o<z<h$$
(2.2)

where h is the thickness of the laminate. Finally, there are boundary conditions which here are

$$c(o,t) = c(h,t) = c_o$$
(2.3)

where c_o is a constant which can be related to the humidity of the atmosphere in which the laminate is immersed.

Equation (2.1) is a very well known one, and a variety of analytic and numerical solution methods are available (9). For the simple initial and boundary conditions (2.2) and (2.3), the methods of "separation of variables" can be used to obtain the following solution:

$$c(x,t)/c_o = 1 - (4/\pi) \sum_{n=0,1,\ldots} \frac{\sin\{(2n+1)\pi z/h\}}{(2n+1)} \exp\{-D(2n+1)^2 \pi^2 t/h^2\}$$
(2.4)

This last formula gives the concentration of moisture at various depths in a laminate at various times; the general nature of the results is as shown in Fig. 2, where it can be seen that, for sufficiently long times, the moisture concentration approaches a uniform value across the depth of the laminate ("saturation"). The total mass of moisture, m, in a laminate can be obtained by integrating eqn. (2.4) across the depth of the laminate i.e.,

$$m = \int_o^h c(z,t)dz$$
(2.5)

Performing the integration gives

$$m/m_0 = 1 - (8/\pi^2) \sum_{n=0,1,\ldots} \{\exp(-D(2n+1)^2\pi^2t/h^2)\}/(2n+1)^2 \qquad (2.6)$$

where

$$m_0 = c_0 h.$$

For sufficiently small t, it can be shown that eqn. (2.6) is closely approximated by the following simple formula:

$$m/m_0 = (4/h)(Dt/\pi)^{\frac{1}{2}} \qquad (2.7)$$

Thus, in its initial stages, the moisture absorption proceeds at a rate which is proportional to the square root of the time. For this reason, in graphical presentations it is usual to plot the moisture absorption against the square root of the time; when this is done the initial part of the curve is a straight line, and the diffusion constant, D, can be determined experimentally by measurements of the slope of this line.

Two general features of moisture absorption in laminates are:

(i) The higher the ambient temperature, the more rapidly the moisture is absorbed; the diffusion constant is, in fact, quite strongly dependent on the temperature.

(ii) The thicker the laminate, the longer it takes for the saturation condition to be achieved.

These two features are illustrated in Figs. 3 and 4 where the data have been taken from ref. (6).

For a laminate forming part of an aircraft in service it is necessary to replace the simple boundary conditions (2.3) by ones which represent the climatic variations in humidity; it is also necessary to allow for the effects of temperature variations on the diffusion constant. Hinkle (10) has described a program that is underway on moisture absorption in the boron/epoxy skins of the F-15 horizontal tail. There, using the general methodology outlined above, predictions have been made of the moisture absorption over twenty-five years of service life of the F-15. Certain horizontal tails will be periodically removed from service, their moisture content measured, and the measured values compared with the theoretical predictions. Values measured after five years service compared well with the theoretical predictions; at the time of measurement, a typical value of the moisture absorption was 0.6% although higher values (around 0.8%) were predicted at various intermediate times. Another extensive programme on the moisture absorption occurring in service involves graphite/epoxy spoilers on Boeing 737 aircraft operating in various parts of the world (11). A large number of spoilers are again being regularly removed from service and the change in weight of laminate specimens are measured as the specimens are dried out; it appears that weight changes of the order of 0.8% are being measured.

164

One effect of moisture absorption is that stresses can be induced due to swelling (8), especially when there is a moisture gradient across the thickness of a laminate (as in Fig. 2), so that there is unequal swelling of different plies. However, a more important effect of moisture absorption is described in the next section.

3.   EFFECT OF MOISTURE AND TEMPERATURE ON STRUCTURAL PERFORMANCE

It transpires that the main effect of moisture on structural performance comes, not from the moisture alone, but rather when it is taken in combination with elevated temperatures such as occur in high speed flight. Composite components on a supersonic fighter aircraft might be expected to experience temperatures in the approximate range -50°C to 125°C depending on speed and altitude; it is the high end of this range which is seen as being of most importance.

As has already been mentioned in Lecture 4 the effect of absorbed moisture on a resin is to reduce its glass transition temperature. (Broadly, the glass transition temperature of a polymer can be defined as that temperature above which the polymer is soft and below which it is hard). When a fibre/epoxy composite is in a "wet" condition (having a moisture content around 1.2% say), then the glass transition temperature of the epoxy matrix may be reduced by around 40 to 50°C; see ref. (5). Under these circumstances, the maximum temperature seen in service may be approaching the glass transition temperature of the composite matrix. This is where the main potential for reductions in structural performance arises. However, by no means all the structural properties of a composite are reduced significantly from this cause. As would be expected from the above argument, it is only those properties which are strongly dependent on the matrix performance that are affected.

According to Springer (7), the tensile strength and extensional stiffness of fibre dominated laminates (i.e., laminates with a significant proportion of fibres in the principal stress directions) are little affected by temperature over the range -50°C to 125°C regardless of the moisture content, except possibly for a slight decrease in tensile strength when the moisture content exceeds 1% and the temperature exceeds 110°C. (Actually, according to ref. (12), it is the dry, cold (-50°C) condition which is often critical for the tension strength of composite structures). The situation is different for matrix dominated laminates, where substantial reductions in tensile strength and stiffness can occur. (However, such laminates are not generally used for structural applications, although an ever-present problem in composite design is the possibility of hidden load paths i.e., the existence of loads acting in directions which were not anticipated during the design and where, in consequence, no fibres may have been appropriately oriented).

It is the compression properties of composite laminates which are most susceptible to moisture/temperature effects. In a general sense this might be expected because of the nature of fibre composites. Whilst individual fibres can carry tensile loads on their own, it is necessary that they be bonded into a structural entity with some form of support against buckling if they are to carry compression loads; it is the matrix material which provides this bonding and support, and if the general solidity of the matrix is impaired some impairment of a composite's compression properties becomes likely. At

present, relatively little on the compression performance of composites in the "hot, wet" condition has been published in the open literature although, undoubtedly, a large amount of data has been accumulated by aircraft manufacturers in recent years. (For example, in the review by Springer (7) on environmental effects little reference is made to compression performance). A summary of compression strength tests on 48 ply laminates of graphite/epoxy AS/3501-6 with a lay-up comprising 42% 0s, 50% ±45s, 8% 90s is given in ref. (12); there the compressive strength at 120°C with 0.6% moisture absorption appears to be approximately 33% less than the strength in the room temperature dry condition. Broadly similar "representative data" are cited in ref. (13), although there, whilst the laminates, temperature, and reduction in compressive strength are much the same as in ref. (12), a rather larger moisture content (1%) is quoted.

4.   OTHER ENVIRONMENTAL EFFECTS

        The external surfaces of graphite/epoxy aircraft structures are generally painted with a white paint to prevent any long-term degradation due to ultra-violet radiation; the paint also serves to prevent the otherwise high absorption of thermal (e.g. solar) radiation by a "black body". (The paint, however, has no significant effect in reducing moisture absorption although efforts are being made to develop moisture - impervious coatings).

        As regards the susceptibility of graphite/epoxy to attack by fluids such as fuel, hydraulic fluid, and paint strippers, which are commonly encountered in aircraft usage, it appears that only paint strippers have a significantly deleterious effect. (However, it might be noted that some other resin systems, e.g., polysulfones, have shown a susceptibility to attack by hydraulic fluids).

5.   FATIGUE OF COMPOSITES IN NORMAL ENVIRONMENT

    5.1   General

        Turning now to the fatigue of composites, this will be discussed first for a normal environment (i.e., room temperature and moderate humidity). It needs to be said at the outset that the fatigue of composites, and especially advanced composites, is different in many respects from the fatigue of metals. This remark applies not only to the factors which influence fatigue performance (such as type of loading and notch sensitivity) but also to the way in which fatigue damage manifests itself. On this latter point, whilst for a metal fatigue damage eventually appears as a clearly defined crack, in a composite the situation is much more complex. Fatigue damage can take the form of some or all of the following: matrix cracks, fibre/matrix debonds, fibre fractures, and delamination growth (i.e., interply debonds).

        For relatively recent reviews of composite fatigue see, for example, the papers by Hahn (14) and Heath-Smith (15).

    5.2   Tension Dominated Fatigue

        (a)   Plain Laminates

        Here attention is confined to plain laminates (i.e., laminates without stress concentrators) which are subject to tension-tension cycling, so

166

that the fatigue stress ratio, R, (defined as the ratio of the minimum to the maximum cyclic stress) is non-negative. Under these circumstances it has been established that fibre dominated laminates made of advanced composite materials have a much better fatigue performance than structural metals. For example, according to Sturgeon (16), unidirectional graphite/epoxy laminates exhibit almost no sign of a conventional S-N curve. Instead, a wide scatter of lifetimes ranging out to 10^7 cycles is found even when the maximum cyclic stress is around 80% of the ultimate tensile stress (UTS); if the maximum cyclic stress is less than 70% of the UTS then almost no failures are observed in cycling with R = 0 out to 10^7 cycles. This feature is illustrated in Fig. 5 where the data have been taken from ref. (14). Multi-directional laminates do exhibit some sensitivity to fatigue loadings and an S-N curve can be obtained. However, as long as the laminate is fibre dominated, the fatigue performance remains very good. For example, Bevan (17) gives results for $[(\pm45)_2/0_2]_s$ graphite/epoxy laminates which sustained 10^6 cycles with the maximum cyclic stress 80% of the UTS.

The situation is much the same for boron composites (see p. 404 of ref. 14) and, apparently, for aramid composites (4). The good tension fatigue performance of advanced composites is generally attributed to their high Young's modulus; the fatigue performance of the lower modulus glass composites is distinctly poorer (4), although still comparable with that of aluminium alloys.

(b)   Laminates with Stress Concentrators

In structural metals, small holes or other forms of stress concentrators generally have little effect on the static strength, but have a marked effect in reducing fatigue life. The situation for composites seems to be the complete reverse. Because fibre composites are fairly brittle materials, the presence of stress concentrators in them can lead to a significant reduction in their static strength (although the reduction is generally not as severe as would be predicted by the theoretical stress concentration factors discussed in Lecture 7). However, subsequent cycling often leads to no further degradation in strength; indeed, the residual strength after cycling can exceed the original strength (see p. 408 of ref. (14)). This rather paradoxical situation apparently comes about because of the following effect. Although the fatigue cycling can initially cause a limited amount of damage around the stress concentrator, the result of this damage can be to redistribute the stresses (especially in laminates with various ply orientations) so that the effect of the stress concentrator is reduced. Bevan (17), using laminates of the type described earlier, found that the presence of a 2 mm drilled hole in a 25 mm wide specimen could reduce the static strength of the specimen by up to 50%, but that then lives of 10^6 cycles, with the maximum stress in the cycle virtually equal to the (reduced) static strength, could be obtained, and that the residual tensile strength was also very significantly increased. Sturgeon (16) has given generally similar results, except that lesser static strength reductions (around 24%) occurred.

5.3   Compression Dominated Fatigue

For metals, fatigue is governed largely by the tensile stresses; once again the situation seems to be quite the reverse for composites where,

although there is some contradictory evidence, it appears that compressive stresses play the key role. For example, Rosenfeld and Huang (18) carried out tension-compression (R = -1) and zero-compression (R = -∞) fatigue tests on graphite/epoxy laminates (0/±45) with holes and concluded that compressive loads in fatigue produce a significant reduction in fatigue life when compared with results for tension-tension loading; see Fig. 6. They describe the mechanism of failure for compression fatigue as a progressive local fatigue failure of the matrix near a stress riser, thus causing fibre split, progressive delamination, and fibre buckling, which then precipitates laminate failure. Similarly, Ryder and Walker (19) concluded that, for graphite/epoxy, compression markedly reduces fatigue life with a greater reduction corresponding to a larger compression load excursion.

6. FURTHER COMMENTS ON COMPOSITE FATIGUE

6.1 Environmental Effects

Studies of the influence of moisture and temperature on the fatigue performance of composites are still in their relative infancy, and many uncertainties exist. It seems to be implied by data summarised in ref. (12), relating to compression dominated fatigue of graphite/epoxy laminates with moisture levels ranging from 0.6% to 1.5%, that, as long as environmental effects are allowed for in static design a satisfactory fatigue performance can be expected. However, one area where substantial concern has been expressed is the effect of "thermal spikes"; these are relatively large increases in temperature occurring over short time periods (at rates approaching, say, 1°C/sec) corresponding to an aircraft accelerating rapidly to supersonic flight. Especially for "wet" laminates, there is the possibility of damage to the matrix occurring, leading to a degradation in fatigue life and/or residual strength under compression loadings. This type of effect has been observed in a test program on graphite/epoxy structures (20).

6.2 Cumulative Damage

Although its shortcomings are realised, Miner's rule for cumulative damage in metal fatigue generally provides results which are, at least, of the right order of magnitude and have no consistent bias towards either conservatism or non-conservatism (15). There are some very preliminary indications (15), (18) that, for composites, the rule may be markedly non-conservative.

6.3 Statistical Aspects

The indications from specimen tests are that the scatter in the fatigue life of composites is significantly greater than that of metals. (At this stage, of course, there are little statistical data on the fatigue of composite structures but, in reading the following it should be borne in mind that, as a general rule, the scatter in life of built-up structures is usually significantly less than that for simple specimens). The Weibull probability distribution is the one that seems to be most favoured for representing the variation in composite fatigue life (19), (21). According to ref. (19), whereas the number of specimens used for defining the scatter in

composite fatigue life is often taken around 20, the extent of the scatter is such that this cannot be used to justify a survival rate greater than 95%; it is stated that, to justify a survival rate greater than 99%, it is necessary to test at least 100 specimens.

7. FINAL REMARKS

As was stated at the beginning of this lecture, there are currently many uncertainties in all the topics that have been discussed. However, whilst various laboratory programs have identified several areas of potential concern, as far as is known, no major problems have so far arisen due either to environmental effects or fatigue in composite components on aircraft in service. In the case of boron/epoxy, some such components have now been in service for around 10 years; graphite/epoxy components have been in service for a lesser time. Generally, what have been considered to be conservative design procedures have been used for current composite aircraft structures.

REFERENCES

1. Anon., Environmental Effects on Advanced Composite Materials, ASTM STP 602, 1976.

2. Anon., Advanced Composite Materials - Environmental Effects, ASTM STP 658, 1978.

3. Reifsnider, K.L. and Lauraitis, K.N. (eds), Fatigue of Filamentary Composite Materials, ASTM STP 636, 1977.

4. Agarwal, B.D. and Broutman, L.J., Analysis and Performance of Fibre Composites, ch. 7, Wiley, New York, 1980.

5. Browning, C.E., Husman, G.E. and Whitney, J.M., Moisture Effects in Epoxy Matrix Composites, pp. 481-496 of ASTM STP 617, 1977.

6. Shirrell, C.D. and Halpin, J., Moisture Absorption and Desorption in Epoxy Composite Laminates, pp. 514-528 of ASTM STP 617, 1977.

7. Springer, G.S., Environmental Effects on Epoxy Matrix Composites, pp. 291-312 of ASTM 674, 1979.

8. Tsai, S.W. and Hahn, H.T., Introduction to Composite Materials, ch. 8, Technomic Publishing Co., Westport, 1980.

9. Crank, J., The Mathematics of Diffusion, Oxford, 1956.

10. Hinkle, T.V., Effect of Service Environment on F-15 Boron/Epoxy Stabilator, AFFDL-TR-79-3072, 1979.

11. Stoecklin, R.L., Commercial Service Experience of a Graphite-Epoxy Flight Control Component, pp. 289-296 of Ninth National SAMPE Technical Conference, 1977.

12. Weinberger, R.A., Somoroff, A.R. and Riley, B.L., US Navy Certification of Composite Wings for the F-18 and Advanced Harrier Aircraft, pp. 1-12 of AGARD-R-660, 1977.

13. Guyett, P.R. and Cardrick, A.W., The Certification of Composite Airframe Structures, Aeronautical Journal, vol. 84, pp. 188-203, 1980.

14. Hahn, H.T., Fatigue Behaviour and Life Prediction of Composite Laminates, pp. 383-417 of ASTM STP 674, 1979.

15. Heath-Smith, J.R., Fatigue of Structural Elements in Carbon Fibre Composite - Present Indications and Future Research, RAE TR 79085, 1979.

16. Sturgeon, J.B., Fatigue of Multi-Directional Carbon Fibre Reinforced Plastics, Composites, vol. 8, pp. 221-226, 1977.

REFERENCES (CONTD.)

17. Bevan, L.G., Axial and Short Beam Shear Fatigue Properties of CFRP Laminates, Composites, vol. 8, pp. 227-232, 1977.

18. Rosenfeld, M.S. and Huang, S.L., Fatigue Characteristics of Graphite/ Epoxy Laminates under Compression Loading, J. Aircraft, vol. 15, pp. 264-268, 1978.

19. Ryder, J.T. and Walker, E.K., Effect on Fatigue Properties of a Quasi-Isotropic Graphite/Epoxy Composite, pp. 3-26 of ASTM STP 636, 1977.

20. Wolff, R.V. and Wilkins, D.J., Durability Evaluation of Highly Stressed Wing Box Structures, pp. 761-769 of Fibrous Composites in Structural Design (ed. by Lenoe, E.M. et al.), Plenum Press, New York, 1980.

21. Phoenix, S.L., Statistical Aspects of Failure of Fibrous Materials, pp. 455-483 of ASTM STP 674, 1979.
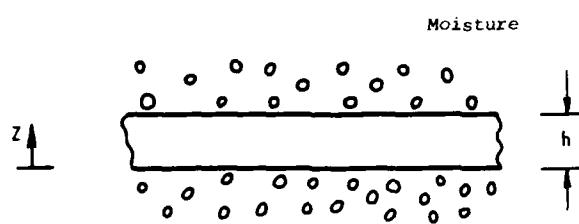
FIG. 1   MOISTURE ABSORPTION BY LAMINATE
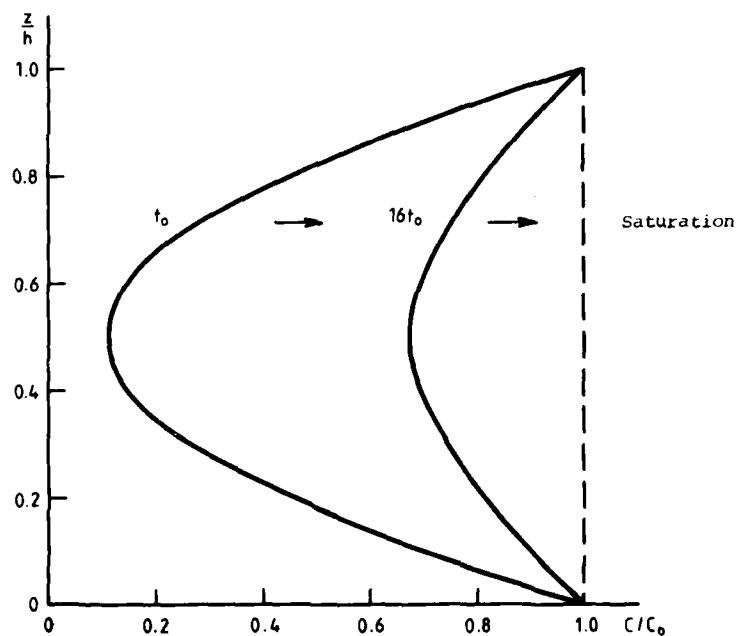
FIG. 2   MOISTURE PROFILES IN LAMINATE AT DIFFERENT TIMES
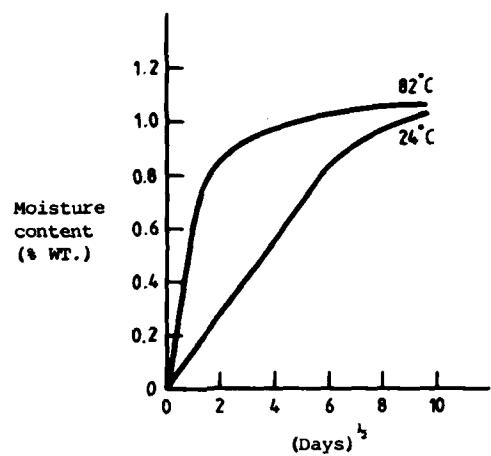
FIG. 3 EFFECT OF TEMPERATURE ON RATE OF MOISTURE ABSORPTION
        (8 PLY Gr/Ep LAMINATE; 75% RH)
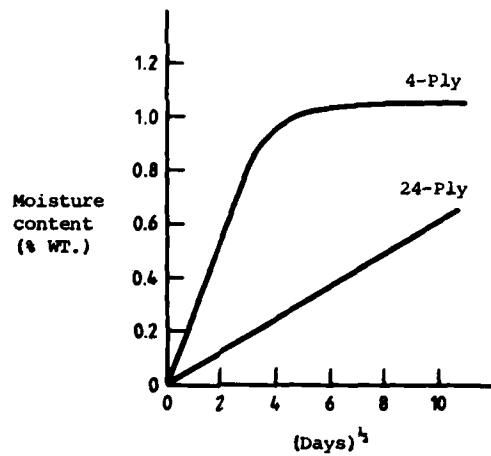
FIG. 4 EFFECT OF LAMINATE THICKNESS ON RATE OF MOISTURE
        ABSORPTION (Gr/Ep LAMINATE; 24°C; 75% RH)

173
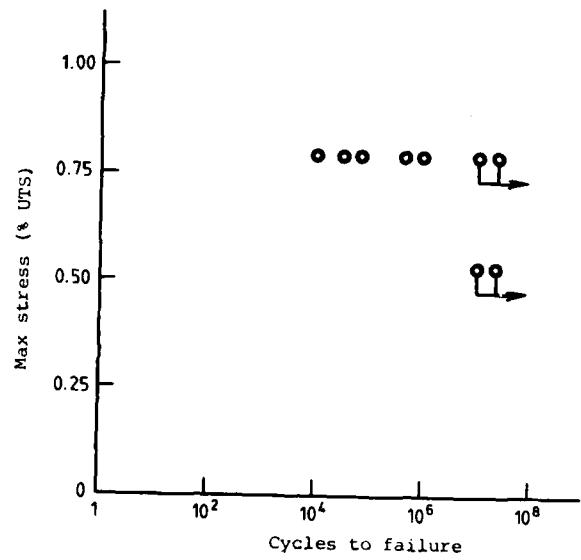
FIG. 5   S-N DATA FOR UNIDIRECTIONAL Gr/Ep LAMINATE
(UTS = 1345 MPa; R = 0)
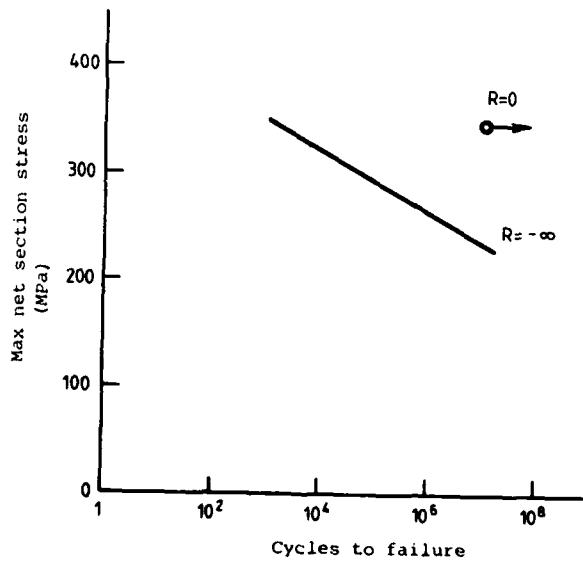
FIG. 6   S-N DATA FOR Gr/Ep (0/±45) LAMINATE UNDER
TENSION (R = 0) AND COMPRESSION (R = -∞)
FATIGUE; REF. 18

174

Lecture 10

DAMAGE TOLERANCE OF FIBRE COMPOSITE LAMINATES

M.J. DAVIS and R. JONES

1.   INTRODUCTION

        The term damage tolerance is used to describe a design philosophy
for military aircraft whereby a component is designed such that structural
integrity is maintained while a defect of a given size is present in the
structure. Modern military aircraft made of metallic materials are designed
on this basis, using fracture mechanics to predict the size of a tolerable
flaw under the applied loads.

        With high performance composites, the field of damage tolerant
design is complex, due to the inhomogeneous nature of the material and the
failure modes, which differ significantly from those in metals. Composites
exhibit near-linear stress-strain characteristics up to failure, while most
metals display some ductile deformation. Thus, composites are less tolerant
of overload. In fatigue, composites again differ from metals in that metals
are sensitive to tension dominated fatigue loading, whereas composites
generally exhibit good resistance to tension fatigue. Composites are, however,
susceptible to local delaminations which may grow under compression fatigue.

        A further complication arises in the manufacturing of composites.
Because of the multi-phase nature of the material and the processes used in
manufacturing, a substantially higher number of defects may exist in a
composite component than would occur in a metallic component. Such defects
also need consideration in the damage tolerance assessment of a component.

2.   NATURE OF DEFECTS

    2.1   Manufacturing Defects

        Defects in composites due to manufacture are usually of two forms:
those produced during the preparation and production of the composite, and
those produced during machining, processing and assembly of the final component.
Typical production defects are shown in Table 2 of Lecture 6. Assembly
defects usually arise as a result of damage to the final product by such
occurrences as scratches, gouges, impact debonding, fibre breakage, incorrect
drilling of holes, over-tightened fasteners, and so on. In any assessment
of the need to repair or reject components, the location and size of the defect,
the type of defect, the load spectrum anticipated for the component, and the
criticality of the component need to be considered.

    2.2   Impact Damage

        The type of damage resulting from impact on composites depends on
the energy level involved in the impact (see Fig. 1). High energy impact,

175

such as ballistic damage, results in through penetration with perhaps some minor local delaminations. Lower energy level impact, which does not produce penetration, may result in some local damage on the impact zone, together with delaminations within the structure, and fibre fracture on the back face. Internal delaminations with little, if any, visible surface damage may result from low energy impact.

Studies (1) on the high energy ballistic damage problem have shown that, for perpendicular impact on boron/epoxy panels, the damage zone size on the entry face is independent of laminate thickness, while the exit face damage zone has been shown to increase linearly with panel thickness. Other work (2) has shown that panel thickness has little effect on residual strength. Also, specimens subjected to tension-tension fatigue after ballistic damage showed little variation in static strength. It was also shown that projectile velocity had no significant effect on residual strength. It was concluded that, while boron/epoxy composites exhibited a substantially larger decrease in static strength when compared to metals, the lower density of boron/epoxy provided a weight saving for structures of comparable damage tolerance.

Low energy impact damage is a major problem in practical fibre-composite structural applications. High and medium levels of impact energy cause surface damage which is relatively easily detected, and therefore repairs may be undertaken. Low energy impact can produce damage which is difficult to observe visually (commonly termed 'barely visible impact damage', BVID). This type of damage is of concern because it may occur at quite low energy levels, and is only detectable using NDI techniques.

The effect of BVID on static and fatigue strengths of graphite/epoxy panels has been studied (3). It was shown that impact degradation is of more concern in compression loading than tension loading. Specimens tested after impact at a standard energy level were compared with specimens with holes. In tension, the standard energy level impact was equivalent to a 3 mm diameter hole. However, for a similar specimen tested in compression it was equivalent to a 25 mm diameter hole. Under reversed cycle fatigue (R = -1.0), the fatigue performance obtained was lower than for specimens with holes.

Studies have been made (4) of energy levels at which incipient damage to graphite/epoxy composites occur. Monolithic specimens of various thicknesses, and other specimens with honeycomb cores, were subjected to impact under drop weight conditions. Two indenters were used: a blunt spherical indenter, and a sharp orthogonal indenter to simulate impact from the corner of a tool box. The specimens were instrumented such that the energy-time history was recorded, giving an accurate measure of the energy required to produce the onset of damage. From the results of these tests, Fig. 2, it can be seen that damage to composites occurs at quite low energy levels, and depends on the thickness of the laminates. As may be expected, a sharp indenter produces damage at a lower energy level than a blunt indenter. (It is important to realise that incipient damage may not necessarily imply damage for which repair is required; this will depend on structural and operational considerations for the component). Honeycomb panels were shown to be more susceptible to impact damage than monolithic panels of the same thickness. From this and other work (5), it may be concluded that graphite/epoxy laminates experience damage at quite low energy levels. It was shown that the energy level required to produce damage in graphite/epoxy sandwich panels was half the energy level for damage in similar panels made from S-glass.

To assess the significance of BVID on graphite/epoxy composites
in service, low energy impacts by typical maintenance equipment may be con-
sidered. Graphical representations of energy levels for a typical tool box,
spanner (wrench), and screw-driver are shown in Fig. 3, plotted against
height of drop. The energy levels for incipient damage for various graphite/
epoxy composite laminates are also shown (dotted lines). From these curves,
it is apparent that accidental tool drops which would hardly cause concern on
metal structures may produce damage in graphite/epoxy structures. For
example, a 16-ply monolithic graphite/epoxy laminate experiences damage from
a sharp screw driver dropped 2 metres, a sharp edged spanner dropped 1 metre,
and a tool box corner dropped 50 mm. Obviously, upper surfaces of an
aircraft are more likely to receive impact from tool drops than lower surfaces.
Since most upper surfaces of an aircraft operate in a compression dominated
load regime, and since it has already been shown that impact damage is more
significant in composite compression members, consideration is required of
maintenance procedures and equipment to provide care and protection of
composite surfaces during maintenance.

2.3 Holes and Slots

Because of the anisotropic nature of composite materials, stress
concentrations due to the presence of holes and slots may be substantially
higher in composites than for an equivalent metallic structure (see Lecture
7). Also, fibre composites generally exhibit near-linear elastic behaviour
to failure. Therefore, the combination of high stress concentrations and the
absence of ductile yielding means that composites are relatively intolerant
of overloads. The results of experimental evaluations of the effects of holes
on fatigue life are discussed in the next section (2.4), and the procedure
for the design of composites with holes is given in Section 3.

2.4 Fatigue

In general, tension fatigue in composites is not a problem, with
fatigue strengths not greatly below static strength. In compression, larger
diameter fibres such as boron produce substantially better fatigue strengths
than smaller diameter fibres.

The problem of fatigue of composites with holes has been considered
in (3) in which experiments were undertaken, involving fatigue regimes of
R = -1.0 (tension-compression), R = 0.05 (tension-tension) and R = 10.0
(compression-compression), on graphite/epoxy composites with holes.

Under tension-tension fatigue, specimens achieved 10^6 cycles at
maximum loads of up to 90% of ultimate strength, indicating that tension
fatigue of composites with holes is not a major concern. For tests involving
compression fatigue, failure lives followed the classical fatigue curves
produced by metals. Thus, these materials with holes are susceptible to
damage under compression fatigue. Further, similar results were obtained for
reversed cycle fatigue, despite the fact that the stress excursion for this
loading is twice the excursion experienced in compression fatigue. Thus it
was concluded that the compressive stress component of a fatigue spectrum is
the dominating parameter in determining the fatigue life of composites with
holes.

177

A further point of interest is the effect of fatigue on the static strength of a composite with holes (see Fig. 4). Here the specimens have been subjected to a substantial proportion of their demonstrated fatigue life (R =-1.0) prior to tensile testing to failure. From these results, Fig. 4, it may be seen that whilst the specimens were near to failure in fatigue, the tensile strength degradation was minimal. The implications of this with regard to the use of proof testing of structures for recertification after fatigue are significant. An interesting and comprehensive review of compressive fatigue life prediction methodology for composite structures is given in ref. (6).

3. DAMAGE TOLERANT DESIGN

3.1   Laminates with Holes

Damage tolerant design for composite materials takes into consideration the types of "defects" which may by design be present in the structure, such as holes and cut-outs, and those defects which may occur inadvertently during manufacture or service, such as delaminations or cracks.

In the case of holes in composite laminates, several different approaches have been successfully developed. These methods are the progressive ply failure approach (e.g. (7), which may use either the Tsai-Hill or the maximum stress failure criterion for individual plies), the average stress failure criterion, and the point stress failure criterion (8). Of these methods, the latter two seem by far the simplest to use and they will now be described.

Consider a hole of radius R in an infinite orthotropic sheet (Fig. 5). If a uniform stress σ is applied parallel to the y axis at infinity, then, as shown in ref. (8), the normal stress σ_y along the x axis in front of the hole can be approximated by

$$\sigma_y(x,o) = \frac{\sigma}{2}\{2+(R/x)^2+3(R/x)^4-(K_T-3)\{5(R/x)^6-7(R/x)^8\}\} \qquad (3.1)$$

where K_T is the orthotropic stress concentration factor, which for an infinite sheet is given by

$$K_T = 1 + [2\{(A_{11} A_{22})^{\frac{1}{2}} - A_{12} + (A_{11} A_{22} - A_{12}^2)/2A_{66}\}/A_{22}]^{\frac{1}{2}}$$

$$= 1 + [2\{(E_x/E_y)^{\frac{1}{2}} - \nu_{xy}\} + E_x/G_{xy}]^{\frac{1}{2}} \qquad (3.2)$$

Here the A_{ij} are the stiffness coefficients for the laminate, where the subscript 1 denotes the direction parallel to the applied stress.

178

The average stress failure criterion (8) then assumes failure to occur when the average value of σ_y over some fixed length, a_o, ahead of the hole first reaches the unnotched tensile strength of the material. That is, when

$$\frac{1}{a_o} \int_R^{R+a_o} \sigma_y(x,o) \ dx = \sigma_o \qquad (3.3)$$

Using this criterion with eq. (3.1), gives the ratio of the notched to unnotched strength as

$$\frac{\sigma_N}{\sigma_o} = 2(1 - \phi)/[2 - \phi^2 - \phi^4 + (K_T - 3)(\phi^6 - \phi^8)] \qquad (3.4)$$

where $\qquad \phi = R/(R + a_o) \qquad (3.5)$

In practice the quantity a_o is determined experimentally from strength reduction data.

The point stress criterion assumes that failure occurs when the stress σ_y at some fixed distance, d_o, ahead of the hole first reaches the unnotched tensile stress.

$$\sigma_y(x,o) \Big|_{x=R+d_o} = \sigma_o \qquad (3.6)$$

It was shown in ref. (8) that the point stress and average stress failure criteria are related, and that

$$a_o = 4d_o \qquad (3.7)$$

The accuracy of these methods, in particular the average stress method, can be seen in Figs. 6 and 7, where a_o was taken as 3.8 mm. The full lines represent predicted strength using the average stress criterion, while the dotted lines are predicted strengths from the point stress method.

With the use of modern structural analyses programs, it is relatively easy to apply these failure criteria to more complex problems. For example, recent tests (9) were carried out on various 16-ply graphite/epoxy laminates (AS/3501-5) with holes. The laminates were:

1. $(0/\pm45_2/0/\pm45)_s$

2. $(0_2/\pm45/0_2/90/0)_s$

3. $(0/\pm45/90)_{2s}$

The results are shown in Table 1, and are compared to predicted values using the average stress method with $a_O = 2.3$ mm.

TABLE 1: Static Strength Predictions; ref. (9)

Hole Size and Placement	Laminate No.	% of unnotched strength	
		Test	Avg. Stress
2-4.8 mm diameter countersunk cf Fig. 8(a)	1	58.9	53.6
"	2	48.1	51.4
"	3	51.8	53.2
2-4.8 mm diameter countersunk cf Fig. 8(b)	3	48.7	45.9
2-6.4 mm diameter countersunk cf Fig. 8(a)	3	53.1	50.3
1-6.4 mm diameter non countersunk	2	54.0	52.6

As can be seen from the examples given, the average stress criterion provides accurate estimates of the strength reduction due to the presence of holes. This method is widely used in the aerospace industry (10), and has been applied to biaxial stress problems (11), to estimation of strength reduction due to battle damage (12), and to problems in which the stress is compressive (13).

3.2   Laminates with Cracks

For the problem of through cracks in a fibre composite panel, see Fig. 9, there have been a variety of approaches which yield accurate results for the reduction in strength due to the presence of a crack. Each is based on fracture mechanics. The most widely used methods are:

(1)   the strain energy density hypothesis (14),

(2)   the compliance approach (15),

(3)   the average and point stress criteria (8).

In the strain energy density hypothesis the strain energy density factor S is defined as:

$$S = r_0 \frac{dW}{dV}$$

(3.8)

where $\frac{dW}{dV}$ is the strain energy density and r_0 is the radius of a core region surrounding the crack tip.. Here,

$$\frac{dW}{dV} = \tfrac{1}{2} \sigma_{ij} \varepsilon_{ij}$$

(3.9)

with the usual tensor summation convention.

The assumptions made in the strain energy density approach are:

(1) Crack growth is directed along a line from the centre of the spherical core (crack tip) to the point on the surf--e $r = r_o$ with the minimum strain energy density factor S_{min}.

(2) Growth along this direction begins when S reaches the maximum critical value S_c which the material will tolerate.

This approach has been useful in the prediction of failure of bonded joints (14) and unidirectional composites (16), as well as for angle ply composites (14). It has also been used for fatigue crack growth pre-dictions (17).

In the compliance method, the strain energy release rate G is calculated from

$$G = \frac{P^2}{2B} \frac{dC}{da} \tag{3.10}$$

where P is the applied load, $C = \delta/P$, a is the crack half-length, B is the thickness, and δ is the deflection measured between the loading points. Failure occurs when G exceeds a critical value G_c, which is a material constant. For metallic structures there is a simple relationship between G and the mode I and mode II stress intensity factors K_I and K_{II}. By con-sidering a composite to be a linear elastic orthotropic material with the crack on one plane of symmetry, G is related to K_I and K_{II} by:

$$G = K_I^2 \{ (a_{11}/a_{22})/2 \}^{\frac{1}{2}} [(a_{22}/a_{11})^{\frac{1}{2}} + (2 a_{12} + a_{66})/2]^{\frac{1}{2}}$$

$$+ K_{II}^2 a_{11} [(a_{22}/a_{11})^{\frac{1}{2}} + (2a_{12} + a_{66})/2a_{11}]^{\frac{1}{2}} (1/2)^{\frac{1}{2}} \tag{3.11}$$

where a_{ij} are the elements of the compliance tensor with the 1 subscript in the direction of the applied load. This procedure has been widely used (18).

For cracks in orthotropic laminates, the stress along the net section beyond the crack tip is given by

$$\sigma_y(x,o) = Y \sigma x/(x^2-a^2)^{\frac{1}{2}} \tag{3.12}$$

where σ is the applied stress, a is the crack half-length and Y is the finite width correction factor. Making use of this, the average stress failure criterion states that failure occurs when

$$\frac{1}{a_o} \int_a^{a+a_o} \sigma_y \, dx = \sigma_o \tag{3.13}$$

which, after using eqn. (3.12), gives

$$Y \, \sigma_N/\sigma_o = \{ (1-\xi)/(1+\xi) \}^{\frac{1}{2}} \tag{3.14}$$

where $\xi = a/(a+a_o)$ $\qquad\qquad\qquad\qquad\qquad\qquad$ (3.15)

and a_o, as previously, is the length of the damage zone in front of the crack. If the point stress criterion is used, this gives

$$\frac{\sigma_N}{\sigma_o} = (1 - \xi_1^2)^{\frac{1}{2}} \tag{3.16}$$

where $\xi_1 = a/(a+d_o)$

As previously discussed, the two criteria are compatible if $d_o = a_o/4$. These criteria are relatively simple and are widely used. Table 2 shows the experimental tensile strengths and the fracture toughness for various laminate constructions as well as the damage zone sizes, d_o. Table 3 shows similar results, but for cracks oriented at an angle to the load direction. From these, and other works (19), (20), it may be seen that the average and point stress methods can accurately predict the reduction in strength due to the presence of cracks. Other interesting works in this field are given in (21), (22).

TABLE 2: Tensile Strength and Fracture Toughness; from Ref. (20)

Laminate construction	Tensile Strength MPa	Fracture Toughness MPa-m$^{\frac{1}{2}}$	d_o (mm)
T300/5208 graphite/epoxy			
$[0/90]_{4s}$	638	13.0	1.01
$[0/\pm45]_{4s}$	542	39.8	1.01
$[0/\pm45/90]_{2s}$	467 - 494	33.2	-
E-glass/epoxy (Scotch ply 1002)			
$[0/90]_{4s}$	424	30.7	1.01
$[0/\pm45/90]_{2s}$	321	24.3	1.01
Boron/epoxy			
$[0_2/\pm45]_{2s}$	697	62.0	1.27
$[0_3/\pm45/90]_{2s}$	691	59.8	1.27
$[0/\pm45]_{2s}$	608	49.9	1.27
$[0/\pm45/90]_{2s}$	421	38.7	1.27
AS/3501 graphite epoxy			
$[0]_{8s}$	1188	90.7	1.93
$[0/90]_{4s}$	500	24.6	0.38
$[0/\pm60]_{4s}$	452	28.0	0.61
$[0/\pm45/90]_{2s}$	480	32.8	0.75
$[0/\pm36/\pm72]_{2s}$	417	36.2	1.2
$[0/\pm30/\pm60/90]_{2s}$	466	27.2	0.45

TABLE 3: Static Tensile Strength Predictions and Test
Results for Slant and Normal Cracks in Gr/Ep AS/3501-5;
ref. (19)

Laminate Construction	Crack Orientation to Load (degrees)	% Unnotched Tensile Strength		d_o mm
		Test	Avg. Stress	
$(0_2/\pm45/0_2/90/0)_s$	45	53.4	50.5	0.575
$(0/\pm45/\pm90)_{2s}$	45	51.4	50.7	0.575
$(0_2/\pm45/0_2/90/0)_s$	90	44.1	44.2	0.575
$(0/\pm45/\pm90)_{2s}$	90	47.2	44.3	0.575

A further extension of the average stress criterion may be considered.
For a notched orthotropic laminate, the fracture toughness K_{1c} is given by

$$K_{1c} = \sigma_N (\pi a)^{\frac{1}{2}} \qquad (3.17)$$

where σ_N is the stress applied to the notched panel at failure, and a is the
crack half-length. This may be expressed in terms of the unnotched strength,
σ_o, by use of eqn. (3.14)

$$K_{1c} = \sigma_o \{ \pi a (1 - \xi)/(1 + \xi) \}^{\frac{1}{2}} \qquad (3.18)$$

It may be shown that as a becomes large, eqn. (3.18) approaches
an asymptote.

$$K_{1c} \rightarrow \sigma_o (\pi a_o/2)^{\frac{1}{2}} \qquad (3.19)$$

As would be expected, K_{1c} is independent of crack length for large
cracks. However, as $a \rightarrow o$, $K_{1c} \rightarrow o$. Since K_{1c} should remain constant and
be independent of crack length, it is necessary to introduce a correction
factor C_o, to provide a modified critical stress intensity K_{1c}' .

$$K_{1c}' = \sigma_N \{ \pi(a + C_o) \}^{\frac{1}{2}} \qquad (3.20)$$

This is analogous to the Irwin type correction factor for plastic
zone effects in ductile materials. Since fibre composites do not yield, C_o
may represent a damage zone ahead of the crack in which matrix cracking and
fibre cracking occur. Use of Eqn. (3.14) again gives,

$$K_{1c}' = \sigma_o \{ \pi(a + C_o) (1 - \xi)/(1 + \xi) \}^{\frac{1}{2}} \qquad (3.21)$$

183

Here, as $a \to o$, $K'_{1c} \to \sigma_o(\pi \ C_o)^{\frac{1}{2}}$. By taking $C_o = a_o/2$, a constant value of K_{1c} is obtained, which is independent of crack length.

$$K'_{1c} = \sigma_o(\pi \ a_o/2)^{\frac{1}{2}} \tag{3.22}$$

3.3   Ballistic Damage

So far, the problems of holes and cracks have been discussed. However, fracture mechanics has also been shown (12), (23), (24), to be applicable to the estimation of the residual strength of ballistically damaged composite panels. The residual strength of damaged tension panels has been derived (12) from the point stress criterion in the form

$$\sigma/\sigma_o = [(W_s - KW_{ke})/W_s]^{\frac{1}{2}} \tag{3.23}$$

where σ is the residual strength of the damaged panel, σ_o is the unnotched strength, K is an experimentally determined constant, W_s is the strain energy derived from the stress strain curve for the unnotched material, and W_{ke} is the kinetic energy per unit thickness imparted to the structure. This model is applicable for the range of impact velocities which do not result in complete penetration. Where through penetration occurs, eqn. (3.4) may be used to estimate the reduction in strength.

The parameter K is dependent on the ratio of panel width to projectile diameter. However, tests (12) have shown that K rapidly asymptotes to a constant value.

3.4   Material Variability

3.4.1   Unnotched condition

For an orthotropic material, the critical stress intensity K'_{1c} is given in Eqn. (3.20) as

$$K'_{1c} = \sigma_N\{\pi \ (a + C_o)\}^{\frac{1}{2}} \tag{3.24}$$

From this it is evident that in the unnotched condition, (a = o), failure is due to an "inherent flaw", of size $C_o = a_o/2$. Therefore the fracture toughness may be affected by factors which influence the inherent flaw size in the unnotched condition. Obviously, one important factor which will influence the inherent flaw size is the quality of the original laminate; a poor quality laminate (with, say a high void content) would exhibit a larger inherent flaw size than a good quality laminate. The reduction in strength due to quality is given by use of Eqn. (3.22)

$$\sigma'_o/\sigma_o = (a_o/a'_o)^{\frac{1}{2}} \tag{3.25}$$

184

where σ_o' is the unnotched strength of the poor quality laminate and a_o' is the characteristic length.

3.4.2 Notched Laminates

The problem of the effect of quality of the laminate in the presence of a large defect, such as a crack, needs consideration from two views: (i) the strength reduction of the poor quality laminate, and (ii) the residual strength reduction due to the defect together with the laminate quality, when compared to the unnotched strength of a good quality laminate. The strength reduction of the poor quality laminate may be determined by evaluating a_o', the characteristic length for the poor quality laminate. This is then substituted in eqn. (3.14).

$$\sigma_N'/\sigma_o' = \{a_o'/(2a + a_o')\}^{\frac{1}{2}} \qquad (3.26)$$

where σ_N' is the notched strength of the poor quality laminate. From this it may be seen that as a_o' increases, (laminate quality decreasing) σ_N'/σ_o' increases; thus the material becomes less sensitive to the presence of the flaw. (Whilst σ_N'/σ_o' increases with a_o', the individual values of σ_N' and σ_o' will decrease).

The comparison of notched strength of the poor quality laminate, when compared to an unnotched good quality laminate is given by

$$\sigma_N'/\sigma_o = \{a_o/(2a + a_o')\}^{\frac{1}{2}} \qquad (3.27)$$

Here, it is apparent that as laminate quality decreases, the notched strength decreases when compared to an unnotched good quality laminate.

3.5 Delaminations

Delaminations in layered composite materials may occur due to a variety of reasons, such as low energy impact or manufacturing defects. The presence of delaminations is of major concern in the vicinity of bonded joints and in compressively loaded components where the delaminations may grow under fatigue loading by out of plane distortion.

An early study into the growth of delaminations (25) arose from the B-1 composite development program. The effects of delamination size, temperature and moisture on AS/3501-5A graphite/epoxy panels was studied. From these tests it is clear that compressive strength degrades with increasing size of delamination and with increasing temperature and moisture content. For example, one laminate, (90/0/±45) with a 12.5 mm delamination in a 38.1 mm wide specimen showed a 20% compressive strength reduction in room environment. A similar specimen tested at 132°C, and 1.3% moisture content, with the same size delamination gave a 50% compressive strength reduction. Recent tests (26) on the fatigue growth of a 50.8 mm diameter delamination (due to impact damage) in a wing box, showed that the effect of impact damage on a full scale structure can be estimated from specimen tests.

To date there have been few analytical studies into delamination growth. A detailed study (27) used the NASTRAN finite element program to determine interlaminar stresses, which were subsequently used to predict accurately delamination growth rates. A similar study (28) into edge delaminations was undertaken, using the strain energy release rate G to predict delamination growth rates. In this work, it appears that the energy release rate remains relatively constant during delamination growth. A detailed three-dimensional analysis (29) of stresses developed during impact has also been undertaken. Sandwich panels with fibre composite faces, and a thick laminate were considered. For the laminate, impact develops large transverse shear stresses in the damage region and it appears that the sub-surface transverse shear stresses are critical. In the case of the sandwich panel the sub-surface 0° plies would be critical.

Finite element analysis has also been used to investigate the static compressive failure of delaminations (30). In this study a detailed three-dimensional finite element analysis of a delaminated graphite/epoxy (viz T300/5208) beam is performed. The orientation of the plies is $(\pm 45/0_2)_{2s}$ and delaminations 12.7 mm, 25.4 mm and 38.1 mm long are considered. The location of the delamination is varied. The maximum strain energy density S at each point along the delamination is computed as is the energy release rate G. The far field failure strain is then estimated on the basis that at failure $G_c = 7.5$ Nm^{-1} and/or $S_c = 9.64$ Nm^{-1}, as given in (31) and (14) respectively. Both failure criteria give a far field failure strain of approximately 4.5×10^{-3} for a delamination 38.1 mm long between the near surface ±45 plies and the 0_2 plies. The failure strain for such a delamination is in good agreement with that given in (26) and again confirms the conclusion given in (26) that estimates of the critical flaw size due to delaminations or impact damage may be obtained from specimen tests. Indeed, as can be seen from Table 4, static failure has been found to occur for a variety of laminates and fibre orientations at approximately 4000 microstrain. Furthermore it has now been clearly shown in (25,30,32) that delamination growth under compressive loading is entirely due to the unsymmetrical nature of the plies above and below the delamination. The compressive forces acting on these plies produce out of plane bending and it is this bending which drives the delamination.

Approximate analytical methods other than the finite element method have also been used (33,34,35). These methods are capable of differentiating between laminates whose stacking sequence is susceptible to delamination growth and those laminate stacking sequences more resistant to delamination.

The cause of the final failure of the bulk material is as yet uncertain although a number of hypotheses have been proposed. It is most probable that failure is due to a combination of out of plane bending due to loss of symmetry and a reduction of the net cross-section.

TABLE 4: Compressive Strength of Various Impact Damaged
Laminates. Specimens listed were impact damaged, then
loaded statically to failure. From ref. (26).

LAYUP	SKIN THICKNESS mm	DELAMINATION AREA mm^2	COMPRESSIVE FAILURE STRAIN μ IN/IN
AS/3501-6 $(\pm45/0_2/\pm45/0_2/\pm45/0/90)_{2S}$	6.91	1290	3780
AS/3501-6 $(+45/90/-45/+22.5/-67.5/-22.5/+67.6/ \pm45/+67.5/+22.5/-67.5/-22.5/\pm67.5/ \pm22.5/0_2/\pm22.5)_S$	6.45	1613	4630
AS/3501-6 $(0/\pm45/0_2/\mp45/0)$ SKIN ON HRP-3/16-5.5 HONEYCOMB CORE	1.07	1161	4270
AS/3501-6 $(\pm45/0*/\pm45/0_2*/90*/0_2*/\pm45*/0_2*/ \pm45*/0*/+45*/0*/\mp45*/0*/-45*/0*/ \pm45*)_S$	12.7	2389	4090
AS/3501-6 $(90*/-45*/\mp67.5/\mp22.5*/0/90*/+22.5*/ 0_2/\pm45*/0*/-22.5*/+45*/+67.5*/+22.5*/ -67.5*/-45*/+22.5_2*/0)_S$	11.1	7097	5460
T300/5208 $(\pm45/0_2/\pm45/0_2/\pm45/0/90)_{2S}$	6.71	1419	4000
T300/5208 $(\pm45/0/90/\mp45/0/90)_{3S}$	6.71	1226	4000

* DOUBLE-PLY MATERIAL, ALL OTHERS SINGLE PLY.

4. DAMAGE TOLERANCE MANAGEMENT

Various papers have shown methods for damage tolerance enhancement
of composite materials. It has been shown (36) that surface treatment of
graphite fibres to enhance bond strength produces a decrease in Izod impact
fracture energy. It is believed that this is due to an alteration in failure
mode which for untreated fibres involves more delaminations, which absorb
more energy. This work also showed that, by use of a plasticiser in the
resin system, a higher strain to failure matrix was produced, which resulted
in an increase in fracture energy.

The effects of laminate stacking sequence on fracture strength have been considered (3), using specimens with the same number of oriented plies, but with differing stacking sequences. The specimens were also slotted. Whilst design procedures would suggest that the laminates would ostensibly have the same unnotched strength, the fracture strengths of the specimens varied by up to 30%. Stronger panels were those with the outer layers at 0° or 90° to the load direction. Specimens with ±45° fibres on the outer faces produced lower fracture strengths. Also, bunching of 0° layers together was shown to produce higher notched strengths, since extensive delamination was possible between the 0° layers, which absorbs more energy.

A major cause of impact related problems in high performance composites is their low strain to failure. Honeycomb face sheets of graphite epoxy have a strain to failure about 1/3 of tha' for S-glass face sheets. Various works have evaluated the concept of hybridisation - mixing the fibre types, thus utilising the advantageous properties of one material to overcome deficiencies of another. Glass fibre face sheets on a graphite core have been compared to an all graphite structure (36). The higher strain to failure of glass fibres led to substantial increases in threshold energies for impact damage, with the energy level required to produce delamination being increased by a factor of 4.

The more recent availability of aramid fibres has added impetus to studies in hybrid composite systems. Aramid fibres (generally known under their trade name "Kevlar") are relatively cheap, and exhibit a high strain to failure, but also have a substantially higher modulus of elasticity than glass fibres. Therefore, they exhibit a high tensile strength without the stiffness penalty of glass fibre composites. Most work using this fibre has concentrated on the aramid/graphite/epoxy hybrid, since the aramid material provides an increase in impact resistance and a reduced material cost, while the graphite fibres provide compressive strength, which the aramid material lacks. Some studies (37) have shown that aramid/graphite hybridisation leads to a doubling of residual strength after impact compared to all-graphite specimens. For unidirectional layups, the same comparison showed an improvement by a factor of 3.

A further concept for improvement of notch sensitivity is that of specific hybridisation. The incorporation of high strain to failure strips in a structure (softening strips) acts to produce a zone where fracture of the structure is arrested by the high displacement capability of the strips. Similarly, the presence of high modulus strips (hardening strips) provides a restraint to opening of a crack, thus assisting arrest of the crack.
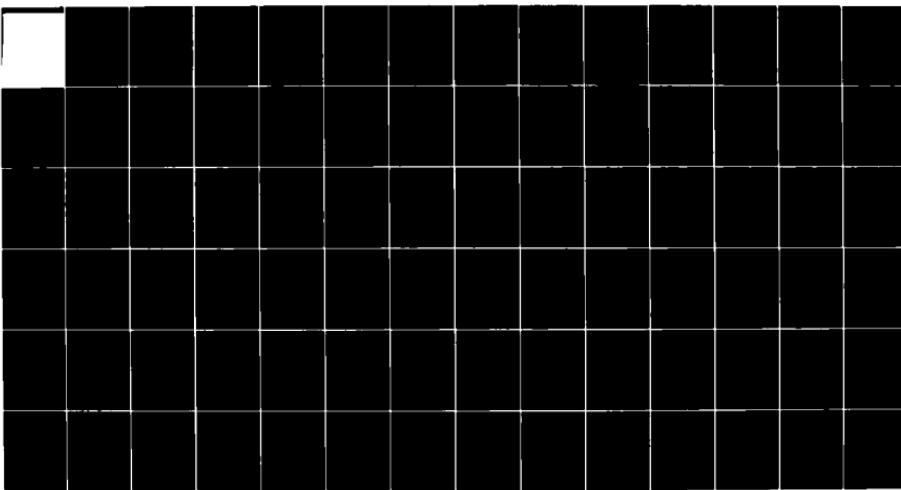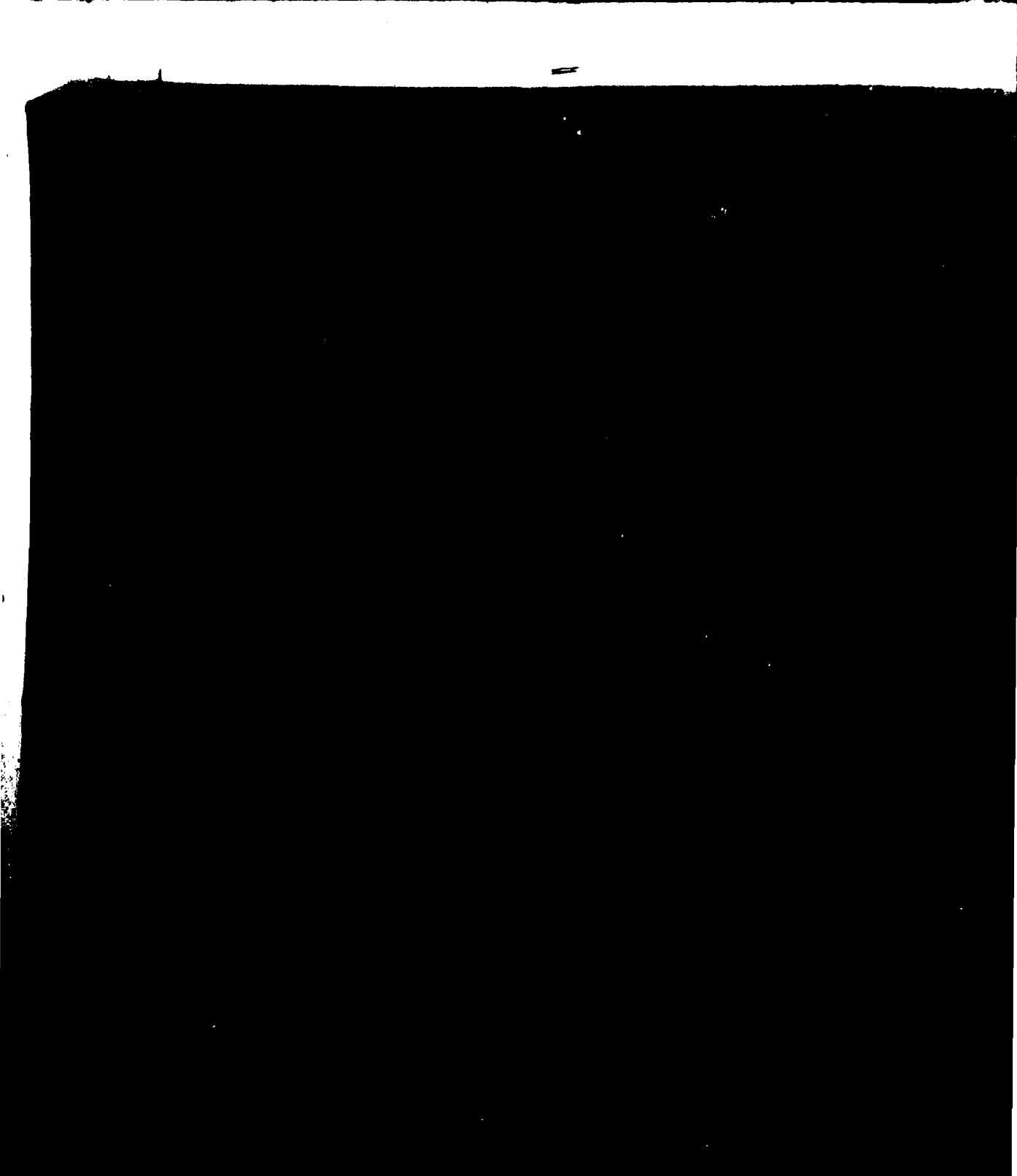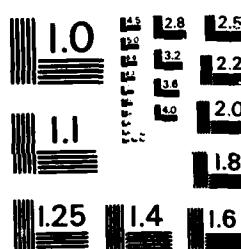
MICROCOPY RESOLUTION TEST CHART
NATIONAL BUREAU OF STANDARDS - 1963 - A

REFERENCES

1. Avery, J.G. and Porter, T.R., Comparison of the Ballistic Response of
   Metals and Composites for Military Aircraft Applications, ASTM STP 568,
   pp. 3-29, 1975.

2. Suarez, J.A., and Whiteside, J.B., Comparison of Residual Strength of
   Composite and Metal Structures After Ballistic Damage, ASTM STP 568,
   pp. 72-91, 1975.

3. Walter, R.W., Johnson, R.W., June, R.R., and McCarthy, J.E., Designing
   for Integrity in Long-Life Composite Aircraft Structures, ASTM STP 636,
   pp. 228-247, 1977.

4. NAEC Report 92-136, Naval Air Engineering Centre.

5. Oplinger, D.W., and Slepetz, J.M., Impact Damage Tolerance of Graphite
   Epoxy Sandwich Panels, ASTM STP 568, pp. 30-48, 1975.

6. Saff, C.R., Compression Fatigue Life Prediction Methodology for Composite
   Structures-Literature Survey, NADC Report No. NADC-78203-60, June 1980.

7. Soni Som, R., Failure Analysis of Composite Laminates with a Fastener
   Hole, AFWAL Report TR-80-4010, 1980.

8. Nuismer, R.J., and Whitney, J.M., Uniaxial Failure of Composite Laminates
   Containing Stress Concentrations, ASTM STP 593, pp. 117-142, 1975.

9. Nuismer, R.J., and Labor, J.D., Applications of the Average Stress
   Failure Criterion: Part 1, Tension, J. Composite Materials, vol. 12,
   p. 238, 1978.

10. Pimm, J.H., Experimental Investigation of Composite Wing Failure, AIAA,
    pp. 320-324, 1978.

11. Daniel, I.M., Behaviour of Graphite Epoxy Plates with Holes Under Biaxial
    Loading, Experimental Mechanics, pp. 1-8, Jan. 1980.

12. Husman, G.E., Whitney, J.M., and Halpin, J.C., Residual Strength Charac-
    terisation of Laminated Composites Subjected to Impact Loading,
    ASTM STP 568, pp. 92-113, 1975.

13. Nuismer, R.J., and Labor, J.D., Application of the Average Stress Failure
    Criterion: Part 2 - Compression, J. Composite Materials, vol. 13, Jan.
    1979.

14. Sih, G.C., Mechanics of Fracture: Linear Response, pp. 155-192 of
    Numerical Methods in Fracture Mechanics, Proceedings of the First
    International Conference, Swansea, (Ed.'s Luxmore, A.R. and Owen, D.R.J.),
    1978.

REFERENCES (CONTD.)

15. Slepetz, J.M., and Carlson, L., Fracture of Composite Compact Tension Specimens, ASTM STP 593, pp. 143-162, 1975.

16. Sih, G.C. and Chen, E.P., Fracture Analysis of Unidirectional Composites, J. Composite Materials, vol. 7, pp. 230-244, 1973.

17. Badaliance, R. and Dill, H.D., Compression Fatigue Life Prediction Methodology for Composite Structures, vol. II, Technical Proposal, McDonnell Aircraft Co., Report No. MDC-A573, February 1979.

18. Barnby, J.T., and Spencer, B., Crack Propagation and Compliance Calibration in Fibre-Reinforced Polymers, J. of Materials Science 11, pp. 78-82, 1976.

19. Morris, D.M. and Hahn, H.T., Mixed Mode Fracture of Graphite/Epoxy Composites: Fracture Strength, J. Composite Materials, vol. 11, p. 124, 1977.

20. Carprino, G., Halpin, J.C. and Nicolais, L., Fracture Mechanics in Composite Materials, Composites, Oct. 1979.

21. Dorey, G., Damage Tolerance in Advanced Composite Materials, RAE Tech. Report TR 77172, Nov. 1977.

22. Kanninen, M.F., Rybicki, E.F., and Brinson, H.F., A Critical Look at Current Applications of Fracture Mechanics to the Failure of Fibre-Reinforced Composites, Composites, pp. 17-22, Jan. 1977.

23. Olster, E.F. and Roy, P.A., Tolerance of Advanced Composites to Ballistic Damage, ASTM STP 546, pp. 583-603, 1974.

24. Dorey, G., Sidey, R. and Hutching, J., Impact Properties of Carbon Fibre/Kevlar Reinforced Plastic Hybrid Composites, RAE Tech. Report 76057, 1976.

25. Konishi, D.Y., and Johnston, W.R., Fatigue Effects on Delaminations and Strength Degradation in Graphite/Epoxy Laminates, ASTM STP 674, p. 597, 1979.

26. Gause, L.W., Rosenfeld, M.S., and Vining, R.E. Jr., Effect of Impact Damage on the XFV-12A Composite Wing Box, 25th National SAMPE Symposium and Exhibition, vol. 25, pp. 679-690, 1980.

27. Ratwani, M.M. and Kan, H.P., Compression Fatigue Analysis of Fibre Composites, NADC Report 78049-60, Sept. 1979.

28. Rybicki, E.F., Schmueser, D.W., and Fox, J., An Energy Release Rate Approach for Stable Crack Growth in Free-Edge Delamination Problem, J. Composite Materials, vol. 11, p. 470, 1977.

REFERENCES (CONTD.)

29. Stanton, E.L. and Crain, L.M., Interlaminar Stress Gradients and Impact
    Damage, pp. 423-440 of Fibrous Composites in Structural Design, (Eds.
    Lenoe, E.M. et al), Plenum Press, New York, 1980.

30. Jones, R. and Callinan, R.J., Analysis of Compression Failures in Fibre
    Composites, Proc. ICCM4, vol, 447-454, Tokyo, October 1982.

31. Ramkumar, R.L., Kulknarni, S.V. and Pipes, R.B., Definition and Model-
    ling of Critical Flaws in Graphite Fiber Reinforced Epoxy Resin Matrix
    Composite Materials, NADC-76228-30.

32. Verette, R.M., and Demuts, E., Effects of Manufacturing and In-service
    Defects on Composite Materials, Proc. Army Symposium on Solid Mechanics,
    1976 - Composite Materials: The Influence of Mechanics of Failure on
    Design. AMMRC-MS-76-2, pp. 123-137, 1976.

33. Rodini, B.T., and Eisenmann, J.R., An Analytical and Experimental
    Investigation of Edge Delamination in Composite Laminates, pp. 441-458
    of Fibrous Composites in Structural Design; see ref. 29.

34. Pagano, N.J., and Pipes, R.B., Some Observations on the Interlaminar
    Strength of Composite Laminates, Int. J. Mech. Sci., vol. 15, p. 679,
    1973.

35. Pipes, R.B., Interlaminar Strength of Laminated Polymeric Matrix
    Composites, AFML-TR-7682, 1976.

36. Bradshaw, J., Dorey, G., Sidey, R., Impact Resistance of Carbon Fibre
    Reinforced Plastics, RAE Technical Report 72240, 1973.

37. Dorey, G., Improved Impact Tolerance in Composite Structures, Ch. 9 of
    a symposium on the Design and Use of KEVLAR(R) in Aircraft, Geneva,
    Oct. 1980.
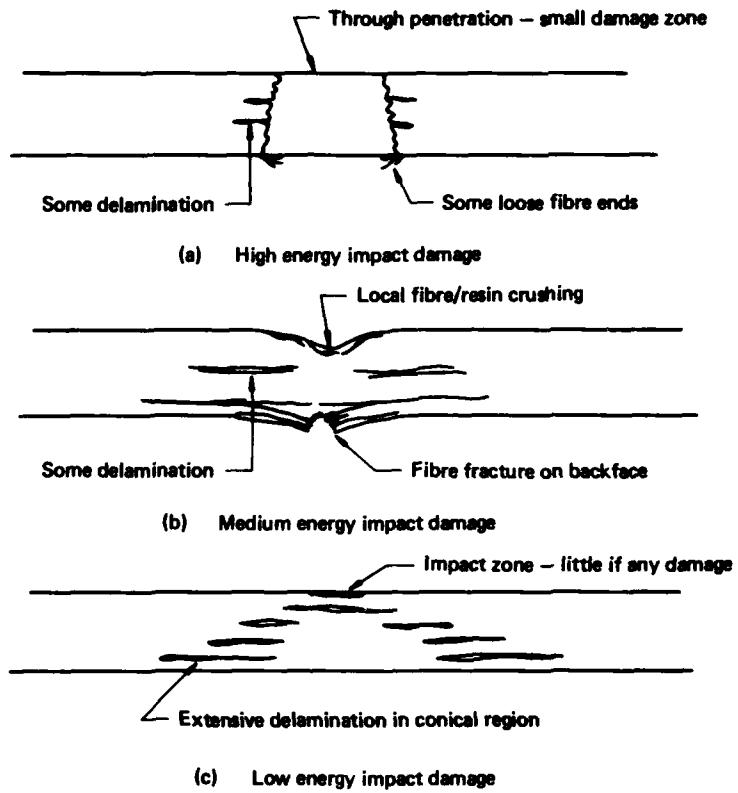
FIG. 1   FAILURE MODES IN LAMINATED COMPOSITES, RESULTING FROM IMPACT
AT VARIOUS ENERGY LEVELS

192
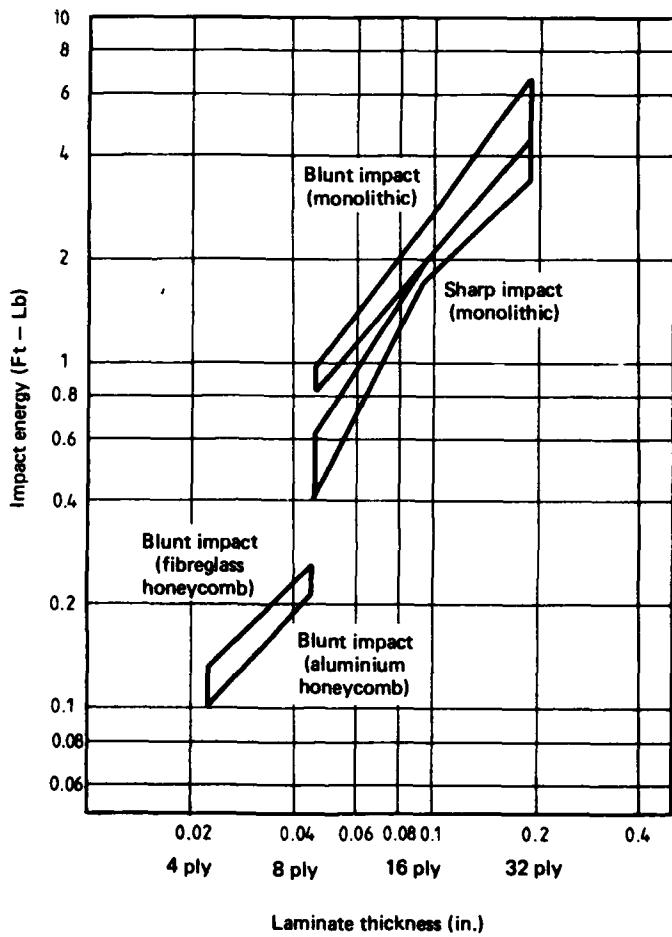
FIG. 2   IMPACT ENERGY FOR INCIPIENT DAMAGE TO GRAPHITE/EPOXY LAMINATES
         FROM [4]

FIG. 2   IMPACT ENERGY FOR INCIPIENT DAMAGE TO GRAPHITE/EPOXY LAMINATES
         FROM [4]

193

Impact
energy
(ft/lb)

C. Toolbox (10 lb)

Blunt
32 – ply monolithic
Sharp

Blunt
16 – ply monolithic
Sharp

Blunt
8 – ply monolithic

Sharp

B. Ratchet wrench (0.532 lb)

8 – ply honeycomb

A. Screwdriver (0.25 lb)

Height tool dropped (in)
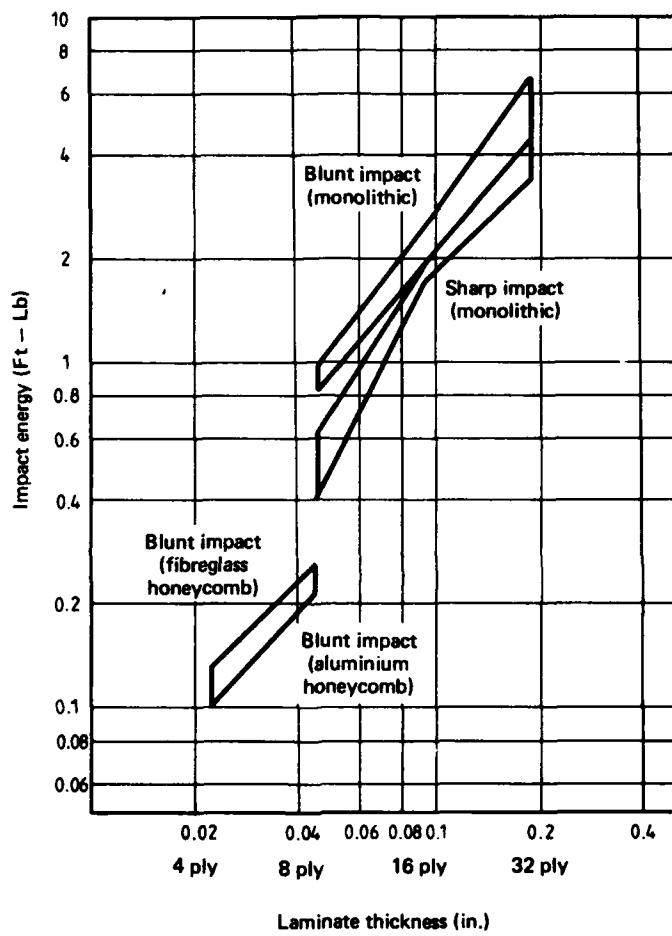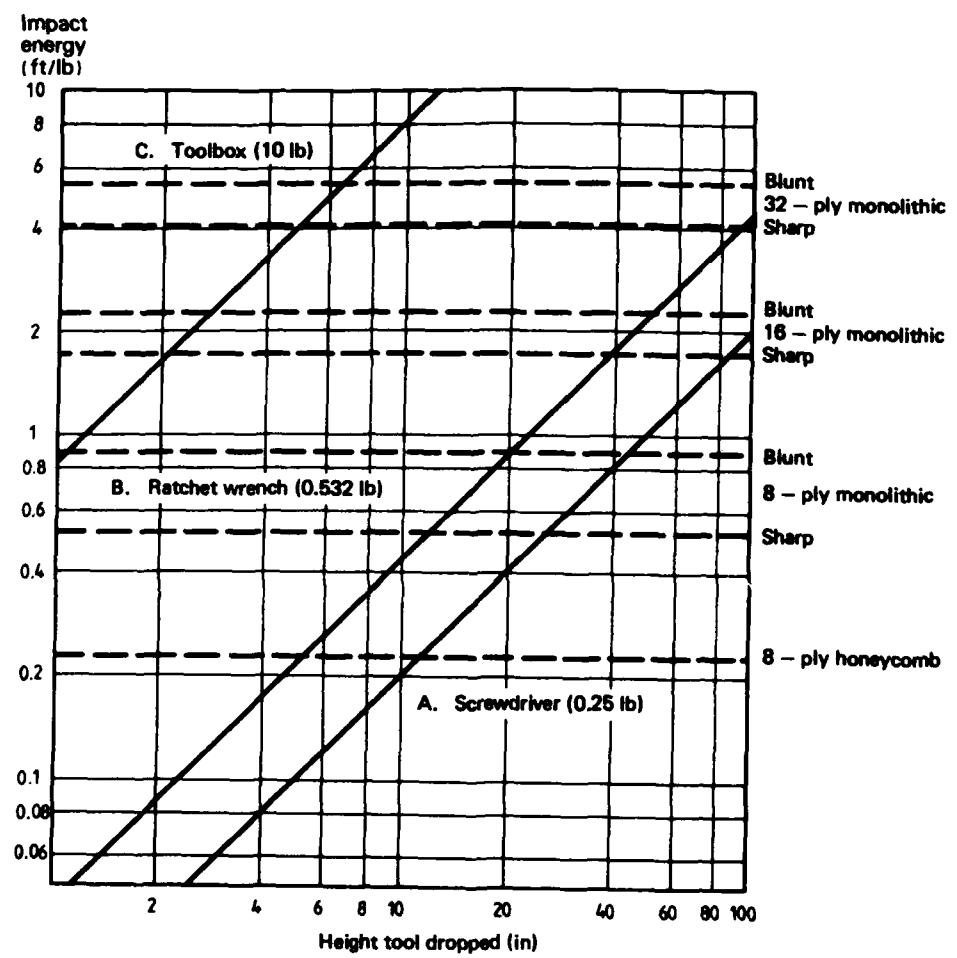
FIG. 3   IMPACT ENERGY, DROPPED TOOLS FROM [4]

194

Material = T300/5209
Laminate = [O / ± 45/90]$_8$

$R = \dfrac{\sigma_{min}}{\sigma_{max}} = \pm 1.0$

□ Residual strength test ~ tension
● Fatigue failure
○ Fatigue cycled and then residual strength tested in tension
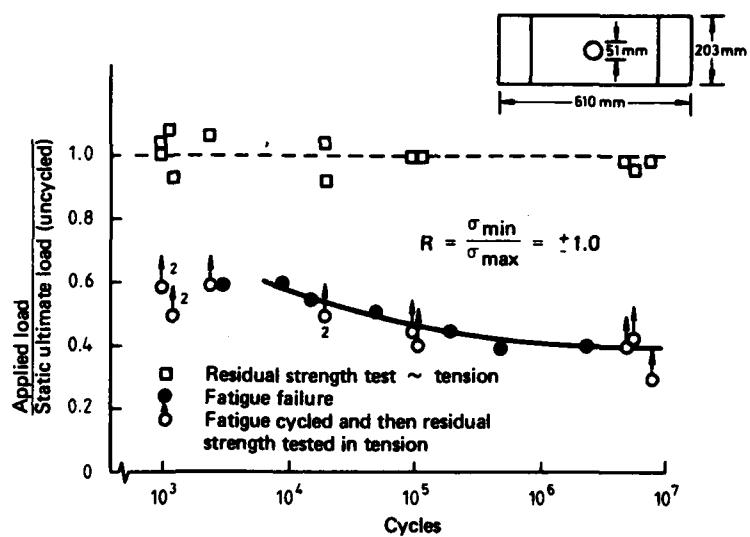
FIG. 4   RESIDUAL STRENGTH OF FATIGUE—CYCLED PANELS FROM [3]

195
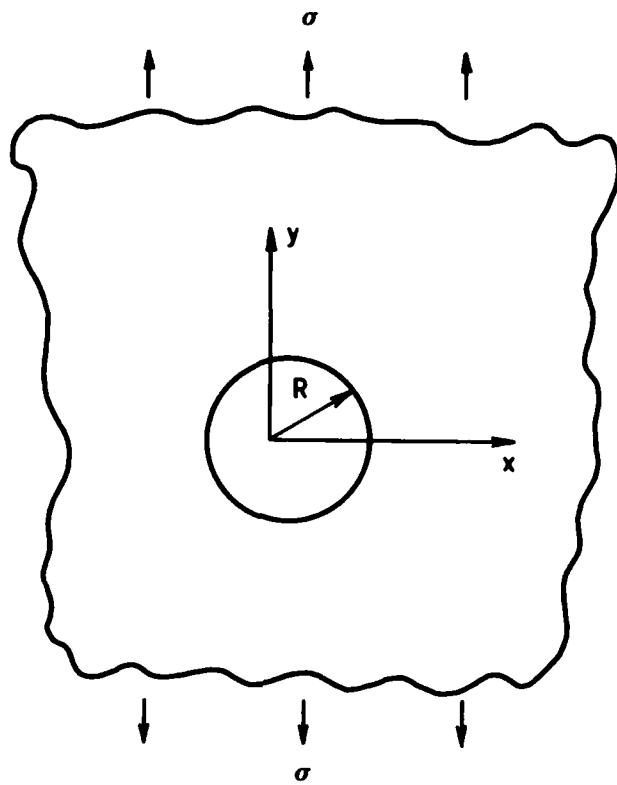
FIG. 5   REFERENCE AXES FOR A HOLE IN ORTHOTROPIC PANEL UNDER
UNIFORM TENSION

196
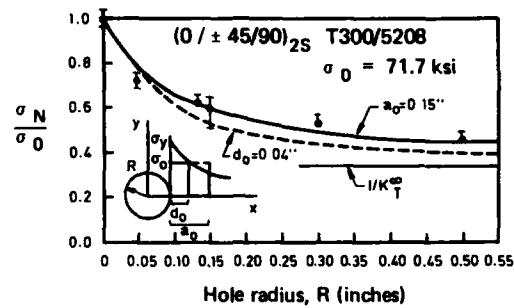
FIG. 6   COMPARISON OF PREDICTED AND EXPERIMENTAL FAILURE STRESSES
FOR CIRCULAR HOLES IN $(0/\pm 45/90)_{2S}$ T300/5208
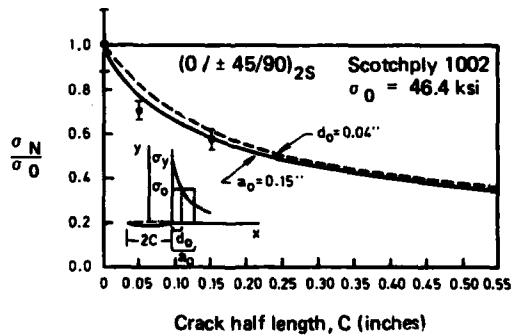
FIG. 7   COMPARISON OF PREDICTED AND EXPERIMENTAL FAILURE STRESSES
FOR CENTRE CRACKS IN $(0/\pm 45/90)_{2S}$ SCOTCHPLY 1002 FROM [12]

209

(b)

(a)
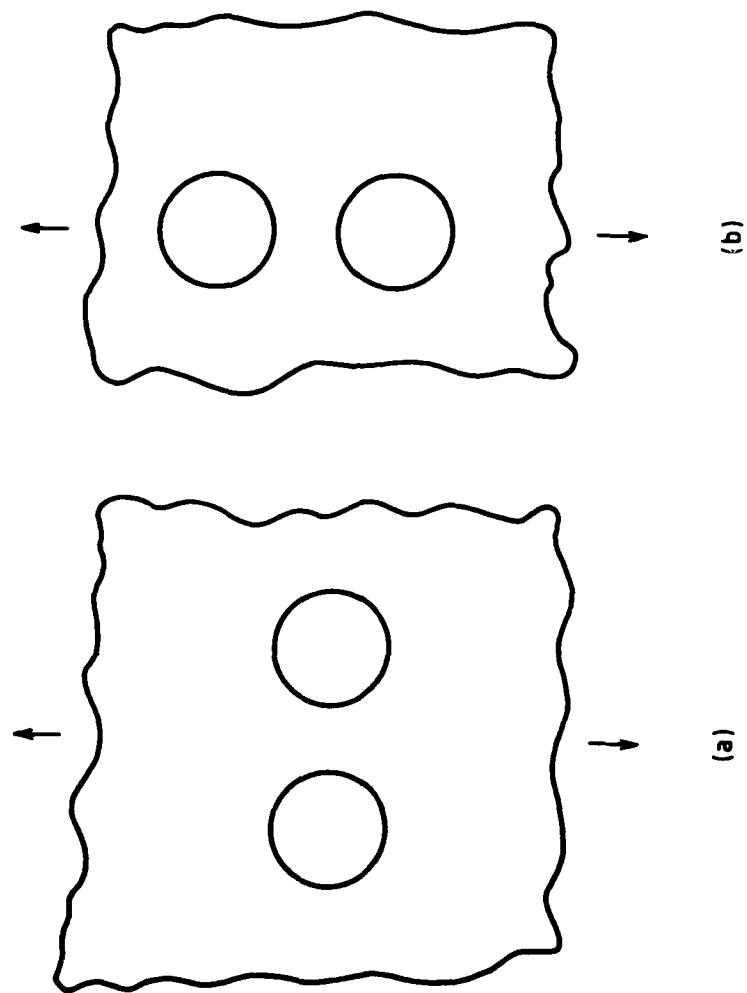
FIG. 8   LOCATION OF HOLES WITH REFERENCE TO APPLIED LOAD

198
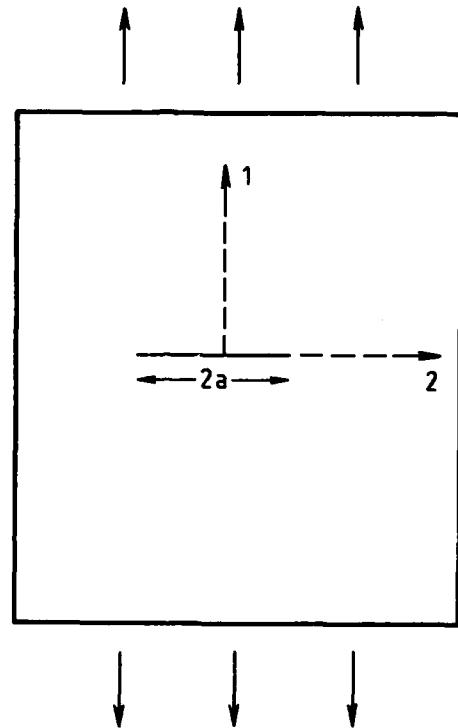
FIG. 9   THROUGH CRACK IN AN ORTHOTROPIC PANEL

Lecture 11

NDI OF FIBRE-REINFORCED COMPOSITE MATERIALS*

I.G. SCOTT and C.M. SCALA

1. **INTRODUCTION**

    Non-destructive inspection (NDI) of F-R (fibre-reinforced) composite
materials can be expected to differ from that of metallic materials because
composites themselves differ markedly from metals and their alloys. F-R
composites are inhomogeneous and markedly anisotropic, they possess a low thermal
conductivity along with a high acoustic attenuation, and they are generally poor
conductors of electricity. High performance structures are conventionally made
from metallic material which is relatively free from unwanted defects;
in-service failures tend to originate from crack initiation at identifiable
defects and occur after crack propagation. Hence NDI procedures can be based
on the detection/location of growing cracks, the importance of which can be
determined using fracture mechanics. No similar predominant failure process has
yet been identified for composite material, no procedure similar to fracture
mechanics has been developed and many of the NDI needs are as yet not clearly
defined.

2. **THE SEARCH FOR DEFECTS**

    For composite materials, much of the NDI is conducted either during,
or immediately after, manufacture of the component and consists of looking for
delaminations, debonds, etc. Subsequently, damage to composites can accrue
from impact, from environmental effects, or from static or cyclic load applica-
tion, all of which have different effects on the defects already present or
may introduce different types of defect altogether.

    A listing of the defects (and related factors) which are likely to
affect the strength of composite material is made in Table 1. A description
of NDI techniques which are applicable to the detection of these defects is
given in Table 2, and principles of operation, capabilities and disadvantages
of each technique are summarised. All the techniques listed in Table 2 will be
discussed further, particularly the most commonly used techniques which are
X-radiography and ultrasonic C-scan. The remainder of those shown are (i) still
undergoing development, or (ii) are not well established either as NDI
techniques or for specific application to composite materials.

---

* This lecture has been prepared by condensing the comprehensive review given
  in (1).

TABLE 1: Factors Affecting Strength of Fibre-Reinforced Composites

Factors related to manufacturing processes
Variation of fibre/matrix ratio; condition of fibre/matrix interface; variation in matrix properties.
Thermal decomposition of matrix; local undercure of matrix.
Lay-up defect - error in ply or fibre orientation, missed plies, gaps between plies or excessive ply overlap.
Dimensional error; inclusion of a foreign object; surface fault/scratch.
Delamination; translaminar cracking.

Factors arising from service use
Degradation of matrix by environment, especially the effect of moisture absorption.
Creep.
Damage zone around stress concentration; impact damage.
Fracture or buckling of fibre; loss of fibre/matrix bond; delamination; matrix crazing; cracks arising from local overload or fatigue processes.

TABLE 2: NDI TECHNIQUES TO DETECT DEFECTS IN COMPOSITE MATERIALS

NAME	OPERATING PRINCIPLES	CAPABILITIES	DISADVANTAGES
X-Radiography	A beam of X-rays is differentially absorbed as it passes through a specimen; rates of absorption are greatest for metals, and vary roughly according to atomic number.	Non-... , but remote capability is depend... on factors such as focussing, sensitivity etc; internal defects can be located and occasionally identified.	Crack detection sensitivity is strongly dependent on crack orientation; contrast between epoxy and carbon rarely permits examination of individual fibres. Distortion which arises at edges of collimated beam of X-rays limits field of view. Discrimination between different types of defect may be difficult.
Ultrasonic C-scan	An ultrasonic pulse, propagating through an object, is scattered or reflected from any interface which separates regions of differing acoustic impedance. The pulse is scattered from a defect or reflected from the front and back surfaces of an object. Amplitude and transit time of reflections yield defect information.	Delaminations in a plane normal to the ultrasonic wave beam can be detected. Cracks can be detected, depending upon their orientation. Large three-dimensional voids are easily detected.	Ultrasound is introduced to specimen via water bath or water jet; water may have a deleterious effect on material particularly if edge delaminations are present. Dependence of sensitivity on orientation may be a problem. Technique is unable to distinguish between delaminations and voids without multiple measurements.
Neutron Radiography	A beam of low energy [or thermal] neutrons is differentially absorbed as it passes through a specimen; rates of absorption are greatest for hydrogen and the organic materials used in composites.	Organic materials are readily examined in close proximity to metals; corrosion products are also emphasised.	Use of nuclear reactor requires specimen to be taken to a reactor site. Hence a portable source is required, together with adequate safety precautions. Californium has been suggested but is expensive and has a short half-life.
Optical Holography	Coherent light from a laser is used to form a hologram of the specimen surface; a speckle pattern can be formed to give surface information or the hologram of a changed surface can be viewed through the hologram of the original surface [live fringes] or two holograms can be compared [frozen fringes].	Surface deformations or surface strains can be determined using a device which is remote from specimen [non-contact]; sensitivities are dependent on mechanical stability of test platform and specimen.	Remains essentially a laboratory technique because of problems with any ambient vibrati·n.
Acoustic Holography	Acoustic holography is analogous to optical holography but in this case the acoustic wave scattered or reflected by an object interferes with an acoustic reference signal. Thus both amplitude and phase information is recorded.	Available as commercial equipment. Detection capabilities are as for C-scan but identification of defects is much better because a three-dimensional picture can be obtained.	Surface defects may cause problems of interpretation.
Thermography	Temperature changes appearing at the specimen surface are measured using sensitive infra-red equipment; temperature changes arise from distortion of an injected heat field by defects or as part of fatigue process or from rubbing of surfaces produced by an applied vibration.	Detects large defects using 'at distance' equipment which frequently can be operated without affecting plant or structure operation.	Thermal techniques are notoriously troubled by changes in ambient conditions; most commonly used equipment is rather expensive. Discrimination between different types of defects is not good even when checked using different thermal techniques.

202

2.1 X-Radiography

X-rays are differentially absorbed in passing through a material according to the atomic number of the elements present. For the organic composite materials, difficulty may be expected in obtaining X-ray images of adequate contrast. Typically, low energy X-rays (a few tens of keV) are used with a beryllium window for composites testing. Currents are held to a few mA and exposures to about one minute. Specimen-to-generator distances vary greatly, usually from 0.3 to 3 metres.

There appear to be contradictory findings about what types of defects can be detected by X-radiography. Harris (2) claims that radiography can be used to identify voids, that fibre/resin debonding or cracks resulting from thermal contraction cannot be distinguished, and that interlaminar cracks cannot be identified. Prakash (3) suggests that thermal cracks are readily detected, as are foreign objects and inclusions, but that interlaminar debonds and fibre debonds are generally hard to detect. Salkind (4) was unable to find void or crack indications in his tests but Nevadunsky et al (5) were able to detect large voids, cracks and porosity in adhesives.

Determination of resin content in a composite should be feasible using X-radiography. However, consideration must be given to the relative absorption coefficients of the particular fibre and matrix in the composite under investigation. Martin (6) determined mass absorption coefficients for a graphite/epoxy composite, both theoretically and experimentally (using attenuation measurements), in an attempt to obtain resin contents. However, neither this method nor an attempt to relate measured film density to resin content worked very well. Forli and Torp (7) studied a glass/epoxy composite in which the absorption coefficient was 20 times higher in the glass than in unpigmented polyester. They were able to determine total glass content from film density measurements, and were also able to observe the reinforcement type and orientation.

Enhancement of some forms of cracks for radiographic testing is possible but the effects on life have yet to be established. Hagemaier and Fassbender (8) tested specimens containing edge delaminations with di-iodobutane (DDB) or s-tetrabromethane (TBE). Radiographs taken an hour later were enhanced, and the chemicals evaporated completely after 2-3 days. However, they noted that DDB was an irritant, while TBE was a severe poison and a potent mutagent which should not be used in the future.

Mention is often made of penetration of suitable materials into voids but the process must surely be very slow unless there is coalescence of microvoids forming a channel to a free surface of the material.

The contrast available from conventional radiographic techniques is usually insufficient to permit resolution of individual fibres. However, Roderick and Whitcomb (9) placed the X-ray source close to a boron/epoxy laminate and a high resolution glass plate, and were able to discern breaks in the tungsten cores (~3 µm diameter) of the boron fibres resulting from

fatigue testing. Crane et al (10) proposed that boron fibres be added to the edge of each composite tape of graphite/epoxy so that fibre alignment could be assessed. Crane (11) also proposed using the fringe patterns, which appear in radiographs due to misaligned fibres, to measure misalignment.

2.2 Ultrasonic C-Scan

The principal established ultrasonic NDI technique for composite materials is the C-scan in which a plane in the object is scanned. An ultrasonic pulse is propagated through the specimen, reflected from a back surface or a defect, and received (usually) by the transmitting sensor. The ultrasonic pulse is scattered or reflected from any defect which differs greatly in acoustic impedance from the surrounding material. The readily available information in the echo signal is the amplitude and the time for the signal to travel from transmitter to receiver. The latter may be measured by means of an electronic gate. The width of the gate may be set to select only a thin plane within the specimen for examination (a similar effect can be obtained by means of focussing transducers) or to average an acoustic parameter through the thickness of the specimen. C-scan testing is usually done in a water tank, although bubbler techniques are available for large structures. A permanent record is available from a Mufax or similar recorder fitted with line-intensification capabilities for amplitude recording. Complications arise when the specimen surfaces are either curved or non-parallel, although Liber et al (12) claim that these are largely overcome by using front-surface triggering of the gate.

Interrogation of a specimen by ultrasonic pulses yields information relating to material acoustic properties and specimen dimensions. Dimensions can be obtained from the signals reflected from the front and back faces of the specimen, and information can also be obtained about non-planar surfaces or the presence of scratches. Similarly, delaminations or cracks normal to the ultrasonic wave beam will be detected. Commonly, frequencies from 1 to 10 MHz are used, for which cracks parallel to the beam or small defects of any nature are unlikely to be seen. Van Dreumel (13) claimed that fibres could be seen and alignment judged, but this probably occurred due to bunching of fibres or to diffraction of waves around bundles of fibres. Small voids cannot be detected unless they appear in large numbers; large voids will be found when their size approaches the wavelength of the probing wave.

Mool and Stephenson (14) made a composite panel comprising eleven layers of boron/epoxy tape sandwiched between aluminium alloy skins. Defects were introduced into the specimen (delaminations, missing plies, extra plies, misaligned filaments, etc.). Commercial through-transmission C-scan equipment was used, which included 5 MHz flat transducers, a long focus 10 MHz transducer, and a short focus 15 MHz transducer. The tests were completely successful, all the artificial defects being positively located, as well as other defects which were confirmed destructively. The higher frequency transducers gave sharper defect definition than the lower frequency transducers but attenuation was very much higher. No indication was given of techniques for identifying an unknown defect.

Liber et al (12) detailed C-scan equipment and test results from cross-ply graphite/epoxy test specimens which underwent cyclic loading. Difficulties associated with detection of standard defects were discussed; initial flaws, designed to simulate in-service flaws, were introduced to the test specimens. A "natural standard for gapless delamination (unbonded but contacting areas of adjacent plies)" was obtained from specimens with drilled holes which were known to contain delaminations extending from the boundary of the hole to the interior of the specimen. For surface defects, it was sometimes observed that, in successive scans, the flaw indication reduced in size; this was traced to water penetration and was largely overcome by sealing edges. Liber et al (12) adopted a realistic approach to flaw type discrimination, stressing the need to interpret ultrasonic indications on the basis of previous experience and knowledge of material.

2.3   Additional NDI Methods

Whitcomb (15) described the fatigue process in composite material as a complicated combination of 'matrix crazing, delamination, fibre failure, fibre/matrix interfacial bond failure, void growth and cracking' and decided that it was 'difficult or impossible to handle using traditional NDE techniques'. Clearly, better (or at least different) techniques are needed, and many alternatives have been proposed as listed in Table 2.

In recent years, neutron radiography has received much attention as a possible new and exciting NDI technique, to complement ultrasonic and X-ray techniques; it is particularly well suited to examining bond lines and to studying composite material in close proximity to metal. Hydrogen, boron and gadolinium exhibit neutron absorption coefficients '2 or 3 orders of magnitude greater than the average value of structural metals' (16). Thus, organic materials such as epoxy adhesives, which contain 8 to 12 percent of hydrogen, exhibit good radiographic contrast; for constant material thickness, variations in film density indicate variations in absorber uniformity caused by voids, inclusions or material inhomogeneities. There may be difficulties in interpretation, e.g. a low absorption inclusion looks like a void, but high absorption inclusions are readily recognised. The neutron radiography technique has been developed using thermal neutrons (i.e. fast neutrons moderated by water or polyethylene) from a nuclear reactor. In-service application awaits the development of a suitable safe, cost-effective, portable neutron source.

Although resin is non-conductive, there is a measurable conductivity associated with bundles of graphite fibres, and eddy current measurements can be used to determine resin content. (For practical applications, present methods for determining resin content are all based on a time-consuming acid-digestion scheme). Eddy current tests were made on a graphite/epoxy combination (8), using test frequencies of 0.5 to 3 MHz and coil diameters of 3 to 1 mm (depending on specimen thickness). Good correlation between resin content and a chosen eddy current parameter (measured on a phase-diagram) was obtained. Owston (17) was confident that eddy currents could be used in various ways (for crack detection, volume fraction and lay-up order measurement)

provided frequencies could be sufficiently increased. Encouraging results were obtained at 25 MHz, and development along these lines will be followed with interest.

Various optical holographic techniques are listed in Table 2. One technique involves measurement of speckle patterns. Speckles appear everywhere in space when a surface is illuminated with laser (coherent) light. The deformation of a structure by mechanical or thermal means modifies the speckle pattern by adding localised regions of high fringe density which are likely to indicate the presence of a flaw. Another technique is the 'live fringe' technique in which a hologram of an unstressed object is recorded and is processed in situ, or very accurately replaced. An interferometric comparison is then made by looking through the hologram at the object, fringes are observed when the latter is slightly strained. The live fringe technique of holographic interferometry produces a measure of changes in surface displacement.

Marchant (18) examined Harrier graphite/epoxy wing tips (approximately 2 m x 1 m x 0.1 m) using live fringes formed from an argon ion lamp. The wing tips were mounted on a heavy steel table which was later isolated from ground-induced vibration. Minor problems were experienced with airborne vibration. Exposure times of about 1s were used and reasonable hologram quality was obtained. Specimens were stressed by heating with a domestic radiator and, although uneven heating occurred, it always seemed possible to make indications of suspect areas reappear with repeated loading. Good agreement with radiographic tests was obtained but doubt was expressed concerning the nature of the defect. It would appear from Marchant's work that, although the technique holds considerable promise, extensive development is still required. Daniel and Liber (19), using a thermally induced frozen fringe technique, show excellent photos of fringe patterns but their discussion is mostly in very general terms. It is not clear to what extent differences between different types of defects can be detected.

Commercial equipment for acoustic holography/imaging frequently includes C-scan as an option. Both amplitude and phase are used to record the hologram. Sheldon (20) used an imaging system in which scan information was stored in a memory. On command, the various configurations could be called up. Using a 5 MHz focussed transducer, 12 mm and 25 mm debonds between graphite/ epoxy skin and honeycomb core were located on the reconstructed C-scan. A focussed image technique used a single focussed transducer imaging on the back side of the test sheet. A crack in a graphite/epoxy wing attachment trunnion was found by imaging and confirmed by C-scan. Damaged specimens were also identified using both techniques. It was generally found that the indicated areas of impact damage were larger than those confirmed visually i.e. damage could well have been more extensive than expected.

For many years thermography has been presented as an NDI technique having great potential - very rapid scanning of large surface areas is possible and equipment can be some distance away from the test surface. Consequently examination can be made with minimal interference to plant operations, and the same equipment can be shifted around to monitor more than one problem area.

That the potential of thermography has not been realised is undoubtedly
because a thermal technique has attendant problems such as the effects of
draughts, variations in surface emissivity, etc., all of which are difficult
to overcome, particularly in the field. Other problem areas are identified
in Table 2.

There are two types of thermal field in materials (21): (i)
stress-generated thermal fields (SGTF) which appear as a consequence of
cyclic loading and wherein maximum temperature rises can be expected where
stresses are highest, e.g. around flaws, and (ii) externally applied thermal
fields (EATF) where normally uniform isotherms are distorted in the presence
of a flaw or a damaged region. Thermography is the science of measuring
temperature change arising from these two thermal fields.

Henneke et al (22) demonstrated the use of SGTF by cylic loading
of a methyl methacrylate specimen containing a central hole; an isotherm
pattern closely related to the calculated stress field was obtained. Further-
more, very good agreement between predicted and measured temperatures was
obtained. Cycling loading tests at frequencies between 15 and 45 Hz were
conducted on boron/epoxy specimens containing a central hole. Early in
testing, heat patterns developed (around the holes) which appeared to be related
to stress fields; subsequent changes in the patterns were attributed to the
development of fatigue damage. Similar successful tests were conducted on
graphite/epoxy laminates containing notches from which matrix cracks propagated.
McLaughlin et al (21) were less successful, probably because their test
frequencies were much lower (0.5 - 5 Hz). Temperature rises were observed for
glass/epoxy specimens containing a part-through hole after only 30 cycles at
1 Hz and at only 10 per cent of the static failure load of the flawed specimen.
No changes were observed for graphite/epoxy material after 1000 cycles at up
to 30 per cent of the static ultimate load. Thus, there appear to be limiting
loading frequencies below which no observable change can be expected.

Thermography is an NDI technique which possesses potential but
much development is needed. Sensitivities commonly quoted are about 0.1 deg
C, temperature ranges are a few deg C and the detectable defect size is a few
mm in diameter. There are many restrictions on the technique and its
application to composite material, but delamination is reasonably easy to
detect. Success-rate seems to vary considerably. Thermography is unlikely to
give any information not found with ultrasonic C-scan, but it is a non-contact
technique which can be used at a distance, and crack growth can be monitored
as it occurs.

3.   ATTEMPTS TO ASSESS STRUCTURAL INTEGRITY

It should be clear that the techniques just described are suitable
for detecting and locating a restricted range of defects in composite material.
Defects differ for different types of composite material but a general
classification based on detectability is not hard to arrange. However, because
of presently incomplete understanding of failure modes, inspections tell very
little about defect severity and even less about the life to failure.

207

Of far greater importance than finding defects is the need to appreciate their importance, i.e. to develop a failure predictor or life indicator. In this section, the measurement techniques described in Table 3 will be discussed with this requirement in mind. Most, it will be seen, go at least part of the way towards this goal.

3.1   Vibration Measurements

The use of a vibration technique to locate defects in structures made from advanced composite materials has been proposed (23). Damage can be detected, located and roughly quantified by measuring changes in natural frequencies of the structure. It is claimed that the severity of the damage can be assessed by additional analysis. This technique is potentially very attractive because properties can be measured at a single point on a structure, and hence access to the whole of a structure is not required. Actual test time can be very small, particularly if the resonant frequencies are excited by an impulse. However, it is necessary to conduct tests on composites in a constant (± 1 deg C) temperature enclosure.

Cawley and Adams (23) readily located damage by saw cuts in a graphite/epoxy plate. One side of a similar plate was damaged by a steel ball; damage was successfully located by vibration techniques and was confirmed by ultrasonic measurements.

Adams and Flitcroft (24) showed that matrix and interface cracking in graphite or glass/fibre reinforced composite material could be detected in the laboratory using a resonant torsion pendulum. The specific damping capacity was measured from the power needed to maintain a constant vibration amplitude at resonance, while the shear modulus was found from the resonant frequency. Crack size was reliably indicated by the amplitude-dependence of these dynamic properties of which damping was the more sensitive measure.

Sims et al (25) were more interested in evaluating specimen life rather than determining the presence of defects. Most of their results were obtained on 0°/90° cross-ply laminate glass/epoxy material. Complex dynamic moduli and damping factors were determined using a simple resonance technique as well as a torsion pendulum technique. For all systems, dynamic moduli decreased while loss factors increased with the introduction of damage. It was concluded that energy dissipated per cycle by the cracks during dynamic testing was proportional to total crack area.

3.2   Measurement of Ultrasonic Attenuation

In any C-scan measurement, the effects of ultrasonic attenuation are evident. However, attenuation is an ultrasonic parameter of value in its own right, measurement of which can be used to assess structural integrity.

TABLE 3 - ATTEMPTS TO ASSESS STRUCTURAL INTEGRITY

NAME	OPERATING PRINCIPLES	CAPABILITIES	REMARKS
Vibration Measurements	A structure or specimen is vibrated through a suitable range of frequencies. Variations in resonant frequencies and amplitudes at or around resonance are measured, from which can be computed the location and severity of damage.	Appears to possess potential for determining damage without regard to nature of damage. It is claimed that the severity of damage can also be measured.	Not fully developed. Access to only one point on a structure is frequently sufficient to permit testing to be conducted.
Ultrasonic Attenuation	An ultrasonic pulse is injected into a specimen. Attenuation is measured by comparing the initial magnitude of the pulse with that after reflection/transmission in a specimen.	Ultimate strength of laboratory specimens has been found to correlate strongly with initial attenuation. Measurements of attenuation caused by the formation of a network of cracks in matrix material have identified structural changes.	Attenuation appears to be frequency dependent but largely independent of life. Access for transducer placement is required (as for other acoustic methods).
Stress Wave Factor	An empirical factor proposed by Vary which purports to measure the efficiency of energy transfer by the tested region of material lying between two transducers. The transmitter injects an ultrasonic pulse into the specimen. The pulse propagates through the specimen, is detected and processed as the number of crossings above a pre-set voltage threshold.	Eventual failure sites in laboratory specimens can be identified.	A highly empirical technique which nonetheless appears to be successful in restricted applications.
Acoustic Emission	Elastic waves resulting from deformation or fracture are detected on the surface of the specimen using a sensitive transducer. Electrical signals from the transducer are conditioned and displayed in various ways.	Differences in time of arrival of signals at an array of transducers permits signal location - there are difficulties with some materials for which acoustic properties vary with direction. Fibre fracture can be distinguished from matrix failure by studying amplitude distributions. Successful safe life predictions have been made in specific cases from proof test measurements.	Retains potential as a failure predictor but has only been successfully used in special cases.

Saluja and Henneke (26) claimed, and were able to justify, that transverse cracks which develop in the weakest plies tend to attain a uniform, equilibrium spacing. These cracks diffract acoustic waves giving rise to a wave attenuation. Attenuation was claimed to give a good indication of damage; it varied with changes in crack-opening for a fixed number of cracks, was sensitive to frequency, and was likely to depend on the number of cracks for a given constant crack-opening. Saluja and Henneke, unlike many other workers, confirmed their findings by destructive examination. Hagemaier and Fassbender (8) found attenuation (which was frequency dependent) correlated well with void content in simple graphite/epoxy laminates. Unfortunately, no correction was made for specimen thickness (number of plies) which turned out to be another variable. Williams and Doll (27) measured attenuation at intervals of 3×10^4 cycles during a compression-compression fatigue test on graphite/epoxy composite material. There appeared to be a correlation between initial attenuation and cycles to fracture, which improved with increasing test frequency.

Attenuation, simply determined, appears to be sensitive to hygrothermal effects for glass/epoxy composites but not for graphite/epoxy composites (28). Accompanying the increased attenuation in the former material is a drastic reduction in flexural strength. However, for both materials (and with the Kevlar material), good correlation between changes in normalised strength and attenuation was found, although no real indication was given for strength reductions greater than 30 per cent. Clearly, confusion could well arise from attenuation results unless it can be shown that degradation from various processes arises from the same physical phenomena, which seems unlikely.

3.3 Stress Wave Factor

The concept of a stress wave factor was developed by Vary and Bowles (29). They studied the inter-relation between various parameters which influence the strength of a unidirectional graphite/polyimide composite. On the basis of their measurements, Vary and Bowles derived the concept of a stress wave factor. This factor was determined by injecting a repetitive ultrasonic pulse into a specimen using a broadband transducer, and detecting the resulting signal some distance away by means of a resonant transducer. The two sensors could obviously be located in various ways. The stress wave factor ϵ was defined by $\epsilon = grn$ where g is the period over which measurement is made, r is the repetition rate of the input pulse, and n is the ring down counts per burst.

Vary and Bowles claimed to be able to predict the relative mechanical strength of a composite material by means of ultrasonic-acoustic measurements made within a relatively 'narrow frequency domain' (0.1 to 2.5 MHz) and without the need for sophisticated equipment. The stress wave factor was shown to correlate strongly with interlaminar shear strength for the particular material. There is no detailed physical basis for any of this work but it is clear that physical properties should be determinable from a study of wave propagation.

Later work by Vary and Lark (30) deals with more specific NDI applications of the stress factor approach. During scanning of tensile specimens of graphite/epoxy composite prior to a test, minimum values of stress factor were observed at a few positions along the specimen. After testing it was confirmed that failure occurred only at the previously indicated positions. It was claimed that stress wave factor 'may be described as a measure of the efficiency of stress wave energy transmission' in a given composite. Hence it was a sensitive indicator of strength variations and could aid in predicting potential failure locations.

3.4   Acoustic Emission

Acoustic emission (AE) is defined by ASTM 610-77 (31) as 'the class of phenomena whereby transient elastic waves are generated by the rapid release of energy from a localised source or sources within a material, or the transient wave(s) so generated'. These waves propagate through a structure and are usually detected by a piezoelectric transducer. The resulting electrical signals can then be processed in various ways to give a wide variety of parameters (32). AE signal analysis has the potential not only to locate sources and thereafter to define defects in a structure, but also to monitor structural integrity during proof-testing and in service. However, the case of a single source in a 'simple' material was only recently addressed by Hsu and Eitzen (33). In practice, the deconvolution of the detected signals into a precise measure of the source function is a complex problem even for relatively uncomplicated metal structures.

There are additional problems which must be solved before AE can be used for routine monitoring of the structural integrity of composite materials; some of these problems have been detailed in the reviews by Williams and Lee (34) and Duke and Henneke (35).

There are numerous specific mechanisms which produce AE in composite materials (36) e.g. fibre fracture, matrix cracking, delamination etc., many of which have already been mentioned. Wave propagation characteristics are complex and are dependent on composite type and design. Signal modification occurs during wave propagation due to geometric spreading of the wave, the effects of structural boundaries, frequency-dependence of attenuation, and the anisotropic nature of composite material. The effects of all these phenomena must be considered during signal analysis. Finally, we need to know the relationship between the AE parameter and the structural integrity of the component.

Several authors have reported success in the use of amplitude distributions to distinguish AE sources and hence identify failure modes (37,38).

In selected special situations, AE has been used successfully for monitoring structural integrity but it is far from viable as a universal method. In an early application, Wadin (39) described how AE counts, measured during a proof test, were used to predict impending failure of the fibre-glass

211

boom of an aerial lift device. His flaw predictions were confirmed destructive-
ly. Fowler (40) and Fowler and Gray (41) developed acceptance-rejection
criteria for fibre-glass tanks, pressure vessels and piping, based on labora-
tory and fatigue tests. They introduced the Felicity ratio, defined as the
load at onset of AE divided by the maximum load previously attained. Their
criteria are based on a combination of total counts, signal amplitude, AE
activity during a load hold and the Felicity ratio.

Hamstad (36) and Wadin (42) discussed the presence or absence of
the Kaiser effect (defined as the lack of detectable AE until previously reached
stress levels are exceeded) in composite materials in terms of the viscoelastic
matrix. Deformation at any stress level is significantly time-dependent,
resulting in time-dependent AE. Thus the absence of a Kaiser effect allows the
determination of a Felicity ratio (as observed by Fowler). This ratio, in
conjunction with observed AE, can be used to assess structural integrity.
Bailey et al (43) used a similar approach to assess impact damage.

In addition to the above, many papers deal primarily with 'data-
gathering'. Future research will need to concentrate on developing a suitable
universal model to describe composite material behaviour, before the potential
of AE as an indicator of structural integrity can be fully realised.

4.   CONCLUSIONS

Detection of manufacturing or in-service defects can be accomplished
using NDI, but the significance of defects remains a major problem. So little
progress has been made in solving this problem that one must perforce look to
other solutions which may enable the prediction of a failure or the identifica-
tion of a failure precursor. Four contrasting techniques have been proposed
for the assessment of structural integrity:-

(i)   Vibration measurements, from which damage (of any
       nature) can be located and a measure of damage
       severity can be obtained.

(ii)   Ultrasonic attenuation, in which changes can be
       related to damage rather than individual defects.
       From measurements of initial attenuation, failure loads
       or cycles to failure could be predicted.

(iii) Stress wave factor, which is a measure of energy trans-
       mission and is essentially a bulk ultrasonic parameter,
       enabling potential failure sites to be predicted.

(iv)   Acoustic emission, which is presently only confirmed
       as a failure predictor derived on the basis of a series
       of tests at various loads (and in some cases loading a
       component to failure).

None of these candidate techniques is entirely satisfactory. Attenuation and stress wave factor techniques appear to have little scope for future development. Both vibration and acoustic emission techniques appear to possess the potential for predicting failure, although considerable research and development is required. However, until this research is undertaken, it will still be necessary to have recourse to the traditional C-scan and X-radiographic techniques.

REFERENCES

1. Scott, I.G., and Scala, C.M., A Review of Non-destructive Testing of Composite Materials, NDT International, vol. 15, pp. 75-86, 1982.

2. Harris, B., Accumulation of Damage and Non-destructive Testing of Composite Materials and Structures. Annales de Chimie-Science de Materiaux, vol. 5, pp. 327-39, 1980.

3. Prakash, R., Non-destructive Testing of Composites, Composites, vol. 11, pp. 217-224, 1980.

4. Salkind, M.J., Early Detection of Fatigue Damage in Composite Materials, J. Aircraft, vol. 13, pp. 764-9, 1976.

5. Nevadunsky, J.J., Lucas, J.J., and Salkind, M.J., Early Fatigue Damage Detection in Composite Materials, J. Composite Matls., vol. 9, pp. 394-408, 1975.

6. Martin, B.G., Analysis of Radiographic Techniques for Measuring Resin Content in Graphite Fiber Reinforced Epoxy Resin Composites, Matls. Eval., vol. 35, pp. 65-8, Sept. 1977.

7. Forli, D., and Torp, S., NDT of Glass Fiber Reinforced Plastics (GRP), Eighth World Conference on NDT, Paper 4B2, Cannes, 1976.

8. Hagemaier, D.J., and Fassbender, R.H., Non-destructive Testing of Advanced Composites, Matls. Eval., vol. 37, pp. 43-9, June 1979.

9. Roderick, G.L., and Whitcomb, J.D., X-ray Method Shows Fibers Fail During Fatigue of Boron-Epoxy Laminates, J. Composite Matls., vol. 9, pp. 391-3, 1975.

10. Crane, R.L., Chang, F.F., and Allinikov, S., Use of Radiographically Opaque Fibers to Aid the Inspection of Composites, Matls. Eval., vol. 36, pp. 69-71, Sept. 1978.

11. Crane, R.L., Measurement of Composite Ply Orientation Using a Radiographic Fringe Technique, Matls. Eval., vol. 34, pp. 79-80, April 1976.

12. Liber, T., Daniel, I.M., and Schraum, S.W., Ultrasonic Techniques for Inspecting Flat and Cylindrical Composite Cylinders, ASTM STP 696, pp. 5-25, 1979.

13. Van Dreumel, W.H.M., Ultrasonic Scanning for Quality Control of Advanced Fibre Composites, NDT International, vol. 11, pp. 233-5, 1978.

14. Mool, D., and Stephenson, R., Ultrasonic Inspection of a Boron/Epoxy – Aluminium Composite Panel, Matls. Eval., vol. 29, pp. 159-64, 1971.

15. Whitcomb, J.D., Thermographic Measurement of Fatigue Damage, ASTM STP 674, pp. 502-16, 1979.

16. Dance, W.E., and Middlebrook, J.B., Neutron Radiographic Non-destructive Inspection in Bonded Composite Structures, ASTM STP 696, pp. 57-71, 1979.

17. Owston, C.N., Eddy Current Methods for the Examination of Carbon Fibre Reinforced Epoxy Resins, Matls. Evaln., vol. 34, pp. 237-44, 250, 1976.

18. Marchant, M., Holographic Interferometry of CFRP Wing Tips, RAE-TR-78105, August 1978.

19. Daniel, I.M., and Liber, T., Non-destructive Evaluation Techniques for Composite Materials, pp. 226-44, Proc. 12th Symp. on NDE, San Antonio, April 1979.

20. Sheldon, W.H., Comparative Evaluation of Potential NDE Techniques for Inspection of Advanced Composite Structures, Matls. Eval., vol. 36, pp. 41-6, February 1978.

21. McLaughlin, P.V., McAssey, E.V., and Deitrich, R.C., Non-destructive Examination of Fibre Composite Structures by Thermal Field Techniques, NDT International, vol. 13, pp. 56-62, 1980.

22. Henneke, E.G., Reifsnider, K.L., and Stinchcomb, W.W., Thermography - An NDI Method for Damage Detection, J. of Metals, vol. 31, pp. 11-15, September 1979.

23. Cawley, P., and Adams, R.D., Vibration Technique for Non-destructive Testing of Fibre Composite Structures, J. Composite Matls., vol. 13, pp. 161-75, 1979.

24. Adams, R.D., and Flitcroft, J.E., Assessment of Matrix and Interface Damage in High Performance Fibre Reinforced Composites, Eighth World Conference on NDT, Paper 4B3, 1976.

25. Sims, G.D., Dean, G.D., Read, B.E., and Western, B.C., Assessment of Damage in GRP Laminates by Stress Wave Emission and Dynamic Mechanical Measurements, J. Matls. Sci., vol. 12, pp. 2329-42, 1977.

26. Saluja, H.S., and Henneke, E.G., Ultrasonic Attenuation Measurement of Fatigue Damage in Graphite-Epoxy Composite Laminates, pp. 260-8, Proc. 12th Symp. on NDE, San Antonio, April 1979.

27. Williams, J.H., and Doll, B., Ultrasonic Attenuation as an Indicator of Fatigue Life of Graphite/Epoxy Fiber Composite, NASA CR 3179, 1979.

28. Bar-Cohen, Y., Meron, M., and Ishai, O., Non-destructive Evaluation of Hygrothermal Effects on Fiber-Reinforced Plastic Laminates, J. Tstg. Eval., vol. 7, pp. 291-6, 1979.

29. Vary, A., and Bowles, K.J., Ultrasonic Evaluation of the Strength of Uni-directional Graphite-Polyimide Composites, NASA TM X-73646, 1979.

30. Vary, A., and Lark, R.F., Correlation of Fiber Composite Tensile Strength with the Ultrasonic Stress Wave Factor, J. Testg. Eval., vol. 7, pp. 185-91, 1979.

31. Annual Book of ASTM Standards, Part 11: Metallography: Non-destructive Testing, p. 676, ASTM, 1977.

32. Licht, T., Acoustic Emission, Bruel & Kjaer Techn. Rev. 2, 1979.

33. Hsu, N.N., and Eitzen, D.G., AE Signal Analysis - Laboratory Experiments Examining the Physical Processes of Acoustic Emission, pp. 67-78, Proc. Fifth International Acoustic Emission Symposium, Tokyo, November 1980.

34. Williams, J.H., and Lee, S.S., Acoustic Emission Monitoring of Fiber Composite Materials and Structures, J. Composite Matls., vol. 12, pp. 348-70, 1978.

35. Duke, J.C., and Henneke, E.G., Acoustic Emission Monitoring of Advanced Fiber Reinforced Composite Materials, 147-162, Proc. Fifth International Acoustic Emission Symposium Tokyo, November 1980.

36. Hamstad, M.A., Deformation and Failure Information from Composite Materials via Acoustic Emission, pp. 229-60, Fundamentals of Acoustic Emission (book), Ed. K. Ono UCLA School of Engineering and Applied Science, 1979.

37. Bailey, C.D., Freeman, S.M., and Hamilton, J.M., Acoustic Emission Monitors Damage Progression in Graphite Epoxy Composite Structures, Matls. Eval., vol. 38, pp. 21-27, August 1980.

38. Rotem, A., The Discrimination of Micro-Fracture Mode of Fibrous Composite Material by Acoustic Emission Technique, Fibre Sci. and Technol., vol. 10, pp. 101-21, 1977.

39. Wadin, J.R., Listening to Cherry Picker Booms, Dunegan/Endevco LT2, March 1977.

40. Fowler, T.J., Acoustic Emission of Fiber Reinforced Plastics, ASCE Fall Convention and Exhibit, Preprint 3092, October 1977.

41. Fowler, T.J., and Gray, E., Development of an Acoustic Emission Test for FRP Equipment, ASCE Convention and Exposition, Preprint 3583, April 1979.

42. Wadin, J.R., Listening to Composite Materials, Dunegan/Endevco LT4, August 1978.

43. Bailey, C.D., Hamilton, J.M., and Pless, W.M., Acoustic Emission of Impact-Damaged Graphite-Epoxy Composites, Matls. Eval., vol. 37, pp. 43-48, 54, May 1979.

216

<u>Lecture 12</u>

REPAIR OF GRAPHITE/EPOXY COMPOSITES

A.A. BAKER

1.   INTRODUCTION

        Graphite/Epoxy composites have many advantages for use as
aircraft structural materials, including their high specific strength and
stiffness, resistance to damage by fatigue loading and their immunity to
corrosion. Thus, extensive use of these composites should reduce the high
maintenance costs associated with repair of corrosion damage normally
encountered with conventional aluminium alloys, particularly those exposed
in a marine environment. Similarly, costs associated with repair of damage
due to fatigue should also be substantially reduced, since the composites
do not in general suffer from the cracking encountered with metallic
structures, particularly cracking resulting from fretting around fastener
holes or from corrosion pitting.

        However, maintenance costs associated with repair of service
contact damage is expected to increase, since graphite/epoxy is essentially
an unforgiving brittle material - unable to yield plastically under overload.
Even quite modest impacts (by metallic standards) can lead to internal
damage in the form of delaminations, which may result in a marked strength
reduction particularly under compression loading. The impacted area may not
be apparent from surface examination because of the absence of permanent
deformation.

        Other more severe handling and environmental damage will also
occur; however this is also common to metallic structures, particularly those
of honeycomb construction.

        It is the purpose of this lecture to consider the repair of
graphite/epoxy aircraft components of various configurations. Typical aircraft
component forms are listed in Table 1. Repairs described here vary from
simple injection of resins into small delaminations and disbonds, to a variety
of patching procedures for damage to areas up to 100 mm or so. Emphasis will
be on repairs that can be carried out under field or depot conditions; however,
some of the repairs described will be more appropriate to factory conditions.
Many of the repairs for composite faced sandwich panels are similar to those
described for metallic honeycomb structures in references (1) and (2). The
following section gives a brief discussion of some of the salient factors
concerning damage, inspection and repair criteria. The rest of the lecture is
concerned with repair methodology.

2.   DAMAGE ASSESSMENT

    2.1   <u>Types of Defects</u>

        Defects may be present initially in the structure due to faulty
manufacture, or they may be introduced during service due to damage resulting
from mechanical contact or environmental effects. Tables 2a, b, c respectively,

list manufacturing faults, mechanical contact damage, and service environment damage, and provide some details on the source of each type of damage. Although it is not the intention here to concentrate on repair of manufacturing damage some mention of this will be made for completeness.

TABLE 1: Typical Graphite/Epoxy Aircraft Structure; Ply Configuration Generally of the ±45°/0°/90° Variety.

(Note that ply thickness is usually about 0.13 mm)

Structure	Typical number of plies	Applications
Honeycomb Panels graphite/epoxy skins; aluminium, fibre glass or nomex core.	2 to 16	Control surfaces, fairings, access doors, flooring.
Sandwich Panels graphite/epoxy skins; PVC foam core,	2 to 6	As above.
Stiffened Panels graphite/epoxy skins with integral graphite/epoxy stiffeners.	16 to 20	Fuselage shells. Tail skins, wing panels.
Monolithic Panels graphite/epoxy skins bolted to aluminium alloy or titanium substructure.	25 to 100	Main torque box, wing and tail.
Monolithic Panels graphite/epoxy skins bolted to graphite/epoxy substructure.	12 to 100	Main torque box.
Channels, Beams graphite/epoxy	16 to 30	Spars (including sine wave spars), ribs.

TABLE 2a: Typical Manufacturing Defects

Defect	Typical Causes
Voids.	. Poor process control.
Delaminations.	. Inclusion of release film.
	. Poor process control.
	. Faulty hole formation procedures.
Disbonds (in bonded joints).	. Poor fit of parts.
	. Inclusion of release film.
	. Poor process control.
Surface damage.	. Poor release procedure.
	. Bad handling.
Misdrilled holes.	. Faulty jigging.

TABLE 2b: Typical Service Mechanical Damage

Defect	Typical Causes
Cuts, scratches.	. Mishandling.
Abrasion.	. Rain/grit erosion.
Delaminations.	. Impact damage.
Disbonds.	. Impact damage.
	. Overload.
Hole elongation.	. Overload/bearing failure.
Dents (with delaminations and crushed core).	. Impact damage.
	. Walk in no-step regions.
	. Runway stones.
Edge damage.	. Mishandling of doors and removable parts.
Penetration.	. Battle damage.
	. Severe mishandling - e.g. fork lift.

219

TABLE 2c: Typical Environmental Damage

Defect	Typical Causes
Surface oxidation.	. Lightning strike. . Overheat. . Battle damage (e.g. laser).
Delamination.	. Freeze/thaw stressing (due to moisture expansion). . Thermal spike (causing steam formation).
Disbonds (in honeycomb panels).	. As for delaminations.
Core corrosion.	. Moisture penetration into honeycomb.
Surface swelling.	. Use of undesirable solvents, e.g. paint stripper.

2.2   Inspection Procedures

Field Procedures:

Visual examination can identify many of the severe forms of damage. However, as mentioned previously, external damage associated with internal delaminations may not be visible - other than possibly as a depression of 0.1 mm or so. The simple coin tap test is very good for detecting delaminations and disbonds in some structures such as honeycomb panels, where support conditions of the damaged material favour its use. Good areas produce a ringing sound, whereas, due to increased damping, disbonded or delaminated regions emit a low pitch or "dead" sound. The usefulness of the technique is limited by the thickness and damping characteristics of the skin.

Pulse-echo ultrasonic procedures, where it is feasible to employ them, are very effective in detecting delaminations and seriously voided regions. Templates may be employed to enable systematic coverage of a component; automatic ultrasonic scanning procedures for field inspection are presently under development.

Depot Inspection:

In addition to the above procedures a wide range of more sophis- ticated procedures are available for depot level inspection. The most versatile is the water bath or water coupled C-scan procedure which automatical- ly maps, in the X Y plane (i.e., the laminate plane), pulse echo or pulse

transmission attenuation. This technique can accommodate very large components and is most effective in detecting voids, delaminations and disbonds since these lie in the X Y plane. The other major technique is radiography which is effective in detecting defects in honeycomb parts, such as water entrapment, core corrosion, core splice separation, and defects in plane laminates such as foreign body inclusion and cracking. In some applications an X-ray absorbent fluid (such as diiobutane) may be forced into disbonded regions to enhance the X-ray image.

2.3 Repair Criteria

A rational basis is required for assessment of the seriousness of flaws in composite components. Three basic decisions are possible: (i) the defect is negligible - in which case it may be disregarded, apart, perhaps, for some cosmetic treatment, (ii) the defect is not negligible but the component is repairable, or (iii) the component is not (economically) repairable and must therefore be replaced.

The decision making process must allow for the nature of the stressing and the environment, the cost of repair compared with replacement (including loss of availability of the aircraft), the reliability and efficiency of the repair and the consequence of failure. A method comparable to linear elastic fracture mechanics as employed to assess the seriousness of crack-like flaws in metals, has yet to be fully developed for composites or bonded components. However, in general, crack-like flaws normal to the loading direction do not occur in these materials and the processes of failure are much more diffuse. Delaminations in the case of composites, and disbonds in the case of bonded joints, are the major forms of damage; these can be treated as single or multiple internal cracks, aligned parallel to the surface of the component.

The problem is to assess whether these flaws have reduced the residual strength of the structure below an acceptable level or whether the flaws may grow in service and thus, at some stage, reduce the residual strength below an acceptable level. Under tension loading the flaws are usually not a serious problem (ignoring possible environmental damage - such as freeze/thaw delamination), since load redistribution can occur and growth is fairly slow; in general, the strain energy release rate does not increase with flaw size. Adhesive bonded joints, in particular, when designed with sufficient safety margin and, especially, sufficient overlap length, allow extensive load redistribution and are thus highly tolerant of flaws.

However, if peel stresses can develop, which is particularly the situation in compression loading, the flaws can grow very rapidly and result in catastrophic buckling failure. Analytical methods are currently being developed to enable assessment of safe flaw size in composite laminates subject to compression; this area is discussed in Lecture 10. Presently the rule of thumb is that delaminations below about 20 to 30 mm in diameter will not reduce residual strength, or grow under compression dominated fatigue loading, when subjected to strains of about 4000 microstrain (which is close to

221

the present ultimate allowable strain) and may therefore be left unrepaired.
Larger delaminations, particularly those in critical areas exposed to high
compression strains, should be repaired.

3.   GENERAL REPAIR APPROACHES

   3.1   Requirements of a Repair Procedure

        The ideal requirement of a repair is to restore structural
capability permanently, with a minimum reduction in functional capability and
a minimum increase in weight particularly on control surfaces where balance
is important. However, implementation of the repair should not require
excessive downtime of the aircraft, should not excessively increase the size
of the damaged area, and should not require elaborate procedures or tooling.
Thus, in practice some compromise between ideal and practical procedures is
required.

        Structural restoration (described more fully later) requires
that the stiffness and strength are restored to the design allowable values
in the operating environment. The functional aspects that must be considered
are: (i) installation constraints, (ii) aerodynamic-acceptability, and
(iii) surface protection.

        Installation constraints that must be considered include:
(a) allowance for clearance in mating surfaces, (b) available fastener length,
(c) requirements for sealing grooves etc., and (d) system installation
requirements (for instance, for support brackets and mounting provisions).

        Aerodynamic acceptability refers to patch repairs applied to the
external surface of the aircraft. Where possible, flush repairs should be
employed to obtain the optimum aerodynamic surface. However, if external (scab)
repair patches are employed, some tapering of the patch is required to ensure
minimum disturbance of the air flow. Since a taper rate of about 50 to 1 is
usually used at the outer ends of bonded patches for structural applications,
this requirement is automatically satisfied. In addition to the patch taper,
the fillet of adhesive around the edge of the patch helps to ensure good
airflow.

        Various protection systems are employed on the surface of the
aircraft, and these must be restored after installation of the repair; included
are the following: (a) external environmental protection e.g. epoxy or
polyurethane paints, (b) lightning strike protection e.g. electrical conductor
mesh (which must be spliced into existing network with conductive material),
(c) fuel tank sealant and surface coatings, (d) heat shielding, heat and flame
resistant material, (e) surface insulation, such as glass/epoxy to avoid
galvanic corrosion of aluminium alloys in contact, (f) wear resistant coatings
such as aramid, thermoplastic sheets, rubber, steel or titanium alloy which
are employed at leading edges.

222

3.2   Major Repair Research and Development Programs

A number of programs on the repair of graphite/epoxy composites have been sponsored by DOD in the US, mostly with the aircraft companies. Some of these are listed in Table 3.

TABLE 3:   Major US Repair Programs for Advanced Fibre Composites

Title/Date/Reference	Company/ sponsor	Objectives
Repair Technology For Boron/Epoxy Composites, 1971 (3)	Grumman/ US Air Force	Repair holes up to 75 mm diameter in boron/epoxy laminates (as used in F14) about 3 mm thick using titanium foil/glass/epoxy bonded patches.
Repair Procedures For Advanced Composite Structures, 1976 (4)	General Dynamics/ US Air Force	Repairs to various types of damage in graphite/epoxy laminates, joints and components with a wide range of configurations and thicknesses, using resin injection, and bonded graphite/ epoxy or titanium alloy patches.
Large Area Composite Structure Repair, 1977 (5) (6)	Northrop/ US Air Force	Repairs to holes up to 100 mm diameter in graphite/epoxy laminates, thickness up to 6 mm, using bonded graphite/epoxy patches.
Field Repair of Composite Structural Components, 1980 (7)	McDonnell- Douglas	Repairs to holes up to 100 mm diameter in graphite/epoxy monolithic skins, thicknesses to 13 mm, using bolted titanium alloy patches.

3.3   Repair Procedures

The repair approaches can be broadly divided into non-patch, usually for minor defects, and patch type, usually for more major defects and damage. However, these procedures may be employed in combination for some types of repair. The two approaches are summarised in Tables 4a and b.

TABLE 4a: Non-Patch Repair Procedures for Minor Damage

Repair Procedure	Applicable Defect
Resin injection.	. Connected voids. . Small delaminations. . Small disbonds.
Potting or filling.	. Minor depressions. . Skin damage in honeycomb panels. . Core replacement in honeycomb panels. . Fastener hole elongation.
Heat treatment.	. Remove entrapped moisture in honeycomb panels. . Dry out absorbed moisture.
Surface coating.	. Seal honeycomb panels. . Restore surface protection.

TABLE 4b: Patch Repairs for Major Damage: All are
Capable of Restoring Ultimate Strain Allowables
to the Limits of Laminate Thickness Noted.

Patch Procedure	Application

Bonded External Patch
 	
 . graphite/epoxy,
   i) co-cured, ii) pre-
   cured layers, iii) pre-
   cured.
 . Titanium alloy foil.
	Repairs to skins, particularly on honey-comb panels, up to 16 plies thick. Well suited for field application.

Bonded Flush Patch
 	
 . graphite/epoxy
   (usually co-cured).
 . Titanium alloy foil
   scarfed or stepped.
	Repairs to skins 16 to 100 plies thick, holes up to 100 mm. May be difficult to employ under field conditions.

Bolted External Patch . Titanium alloy (usual). . Aluminium alloy.	Repairs to monolithic skins 50 to 100 plies, holes up to 100 mm. Suited for field applications.

3.3.1 Repairs to Minor Structural Damage

Injection Repairs:

Resin injection repairs are used for minor disbonds and delaminations. The effectiveness of this approach depends on whether the defect arose during manufacture or was due to mechanical damage during service. Manufacturing flaws, due to local lack of bonding pressure or contamination of the bonding surface, have a surface glaze that must be removed to ensure high bond strength. This can not readily be achieved for internal surfaces; thus these repairs are unsatisfactory. In contrast, internal flaws caused by mechanical damage have a surface which can be bonded reasonably effectively, provided contamination has not occurred, for instance, with moisture (which can be removed by drying) or service fluids such as fuel or hydraulic oil.

The injection procedure, illustrated in Fig. 1, involves the formation of several injection and bleeder holes which must penetrate to the depth of the defect; this requires accurate NDI. If the defect is not penetrated the resin cannot enter the void; if the hole is too deep damage will occur to the material below the void and injection may be inefficient. The resin is usually injected after preheating the repair area to about 65°C; prolonged heating may be required to remove moisture. Resin is injected, by means of an airgun, until excess resin flows from adjacent holes. The procedure is repeated until all holes have been treated; then the holes are temporarily sealed with a layer of protective tape. Finally, pressure is applied to the repair area to improve mating of adjacent regions and to improve or maintain contour. The resin is allowed to gel at room temperature, usually followed by a post-cure at about 150°C.

Similar procedures can be applied to disbonded joints, provided no corrosion or contamination is present in the damaged region. However, in general bonded joints have a large strength margin and injection is unlikely to improve strength, since strong bonds would not be obtained. If disbonds extend to the edge of the bonded region, the procedure is effective in sealing the joint against further damage - e.g. due to ingress of moisture and consequent corrosion or freeze/thaw delamination. Since bond strength is not improved, a sealant or soft adhesive may be the best choice for the injection system. If the disbonds do not extend to the edge of the joint and are reasonably small they are best left alone, because a faulty injection repair would simply provide a path for moisture to the sensitive bond interface which would be damaged by formation of the injection holes.

Filler or Potting Type Repairs:

Potting repairs are made by filling the defective region with a filler compound; minor indentations may be filled in this way provided NDI has ensured that no serious internal matrix cracking or delaminations are present. In the case of lightly loaded honeycomb panels, potting repairs may be made to stabilise the skin and seal the damaged region. The repair in this case, as illustrated in Fig. 2, involves removal of the damaged skin and core, then further undercutting the core to ensure mechanical entrapment of

the potting compound. The resin in the potting compound is then cured at about 150°C. An alternative is to plug the cavity with glass cloth/epoxy prepreg; however, this imposes a higher weight penalty.

Damage in attachment holes, such as minor hole elongations or wear damage, may be repaired with machinable potting compound. Mislocated or oversize holes can be rectified by filling the hole with either aluminium rod (adhesively bonded in position) or machinable potting compound, and redrilling.

3.3.2 Patch Repairs

Patch repairs are generally employed for the repair of major damage and essentially involve replacing the lost load path with new material joined to the parent structure. Thus, the repair is best considered as a joint for the purpose of design; Fig. 3 illustrates the various bonded joint configurations which are applicable to patch repairs and the resulting shear stress distribution in the adhesive. This section outlines the various repair options; design considerations are given later.

Bonded External Patch Repairs:

In this approach the damaged region is removed leaving a straight (or sometimes tapered) hole and a patch with tapered (or stepped) ends is bonded over this region to the parent laminate (Fig. 4). This repair configuration is similar to that of a tapered single overlap joint (Fig. 3); the taper is most important to reduce peel and shear stresses which would otherwise cause failure of the patch, except that it is not required for patches of only a few plies thickness. External patches can be employed reasonably successfully (depending on the stressing requirements of the area) to repair honeycomb skins of thickness up to about 16 plies, suffering from damage up to about 100 mm in diameter. This type of repair will be the most widely employed, since external patches are relatively easily applied under field conditions and graphite/epoxy is presently most widely employed as honeycomb panels. Strength recoveries of from 50 to 100% of ultimate allowables of the parent material can be achieved, depending on laminate thickness.

The main problem with external patches is that, as in a single-lap joint, there is an eccentric load path which results in quite severe bending in the patch and peeling stresses in the adhesive and composite. Out of plane bending under compressive axial loads can also significantly reduce buckling stability. However, these effects are greatly reduced if the patched region is supported by a substructure, such as honeycomb core, which can react out the bending.

When repairs are made to a honeycomb panel, the damaged core is also removed and the region filled either with potting compound, or layers of glass cloth/epoxy prepreg or new core bonded with core splice adhesive; use of honeycomb core is essential in control surfaces to minimise weight increase.

226

The patch is usually bonded to repair area with a film adhesive, using a vacuum bag pressurisation procedure (Fig. 5); a heater blanket may be incorporated into the bag assembly to provide the cure temperature.

Several options exist for the patch; it may be made of (i) graphite/epoxy with a similar ply configuration to the parent laminate, (ii) graphite/epoxy with a quasi-isotropic lay-up (to reduce the danger of lay-up and application errors) in which case it would require to be thicker than the parent laminate, or (iii) titanium foil layers (usually about 0.2 mm thick) adhesively bonded together.

The graphite/epoxy patch may be: (a) formed over the parent laminate from pre-preg tape which is cut to shape and then co-cured with the adhesive, or (b) pre-cured in layers and bonded to the parent laminate during the repair with interleaved layers of adhesive, or (c) preformed to shape and then bonded to the parent material in a subsequent operation. This last option produces the best patch properties, but, since the preformed patch is not compliant, serious 'fit-up' problems may arise on curved surfaces.

The titanium patch is produced by interleaving the foil with adhesive; usually a layer of glass cloth is also employed between each layer of titanium foil to reduce the shear modulus of the patch and thus minimise stress concentrations in the adhesive layer. The main advantages of titanium foil patches are: (i) there is no requirement to control orientation during formation of the patch, and (ii) the properties of the patch are not affected by cure conditions and dissolved moisture in the parent laminate. However, since the titanium patch has a higher thermal coefficient of expansion than the parent material, residual stresses are developed in the adhesive leading to reduction in strength of the patch system. A major disadvantage of titanium is that special surface-treatment is required prior to adhesive bonding.

Flush Patch Repairs:

The flush patch repair configuration, Fig. 4, is similar to a single scarf joint (or a very short overlap single step-joint), Fig. 3, and has therefore the benefit of a (nearly) uniform shear stress distribution in the adhesive layer. In addition, due to the lack of eccentricity in the load patch peel stresses are low. Flush repairs are therefore highly efficient, and are particularly suited to external repairs of thick laminates because of (i) the unlimited thickness of material that can be joined, and (ii) the smooth surface contour that can be produced.

However, flush repairs are much more difficult and time consuming to apply than external patch repairs and so will usually only be employed under depot or factory conditions. A further, significant, disadvantage of flush repairs is that they require the removal of a large amount of undamaged material to form the required taper angle - about 18:1. For example, taking a fairly extreme (but not unlikely) case of a single sided flush repair to a 13 mm thick laminate, with a 100 mm hole, the scarfed diameter would be nearly 600 mm. If, however, a double sided flush patch could be employed the tapered zone length would be reduced by about half.

Single sided flush patches can be employed to repair part-through or full penetration damage. A part-through flush patch, schematically shown in application in Fig. 6, may, as an example, be used to repair a delaminated region in a thick laminate when injection repair is not considered adequate; the material above the delamination is first ground away to leave a recess with the appropriate taper.

Flush repairs are usually based on graphite/epoxy patches with a ply configuration similar to the parent laminate; much less frequently, titanium alloy foil is employed. The graphite/epoxy patches are generally co-cured to avoid severe fit-up problems encountered with pre-cured patches. To cure the patch and adhesive, pressure may be applied by a vacuum bag, heater blanket procedure (Fig. 6). Alternatively, in a depot or factory, temperature may be applied in an oven in combination with a vacuum bag pressurisation system, or best of all where possible, temperature and pressure may be applied in an autoclave.

In an extensive repair study described in reference (5), it was found that peel failure of the longest (outer) 0° fibres in a graphite/epoxy patch occurred, resulting in failure of the patch, unless the ends of the ply were serrated. It was also found that it was necessary with a through thickness repair to scarf the parent laminate to the inner ply. Using this approach, it was possible to produce very efficient repairs to 16 ply laminates with holes - even after representative fatigue loading and environmental exposure.

One sided flush repairs may be employed to repair disbonded regions in composite-to-metal scarf and stepped-lap joints. Here it is particularly important to ensure that the metal surface is free from corrosion and correctly surface treated prior to application of the repair.

External Bolted Patch Repairs:

The external bolted patch repair is similar to a bolted single or double-lap joint, depending on the degree of constraint to bending. A disadvantage of a bolted repair is that quite severe stress concentrations are introduced into the structure at the bolt holes. However, this may not be a significant disadvantage in a mechanically fastened structure. A major advantage of bolted repairs is that the bolts provide transverse reinforcement, with clamping pressure, which is effective in preventing the spread of pre-existing delaminations.

In general, bolted patches are employed for thick laminates (8-15 mm) where the shear stress requirement exceeds the capability of adhesives for external patch repairs, and where the complexity and material removal requirements may preclude use of flush repairs. Moisture problems (referred to later) also limit field applications of bonded repairs in thick material. Thus, bolted repairs would be employed for field repairs of critical monolithic components - such as the F-18 and AV8B Harrier. Titanium alloy is best employed for the metal patch, nut plate and fasteners, since (unlike aluminium alloys) it does not suffer galvanic corrosion when in electrical contact with graphite/epoxy, and also has a fairly low expansion coefficient, thus

minimising thermal and residual stresses. In Fig. 7 is shown schematically
the type of patch configuration investigated in reference (7) and proven to
be highly effective; the patch has a chamfered edge to minimise disturbance
of airflow. The nut plate consists of two sections to allow its blind
insertion and attachment. Tests described in reference (7) have shown that
this repair is capable of restoring the strength in 100 ply thick (13 mm)
laminates with 100 mm diameter holes to over 4000 microstrain which is around
the usual ultimate design allowable.

External Bonded Patch Repairs To Internal Structure:

Repairs to substructure (and other complex composite items) may
be accomplished using external patches, together with resin injection to
diminish the effect of delaminations and disbonds. Although in some cases pre-
formed graphite/epoxy patches may be employed, normally the repair would be
effected with pre-preg materials, co-cured in position with adhesive film,
using vacuum bagging procedures, as illustrated in Fig. 8. The heat source may
be radiant heaters as illustrated, or heat blankets encased in the vacuum bag
assembly. Fasteners may also be employed to reduce peel stresses or reinforce
delaminated regions - possibly after resin injection.

4. MATERIALS ASPECTS

4.1 The Problem of Moisture Removal

Graphite/epoxy laminates may absorb up to about 1.5% moisture
during exposure in humid environments. The moisture is actually absorbed by
the epoxy matrix where (by acting as a plasticizer) it reduces some resin
sensitive mechanical properties, such as compressive strength at elevated
temperature. Moisture can also be trapped in voids and delaminations where
it can cause severe damage due to expansion effects in a thermal spike
exposure or in a freeze/thaw cycle, and, in the case of honeycomb panels,
where it can cause corrosion of the aluminium alloy core.

Moisture can also cause serious problems during repair implementa-
tion if it is not removed by an initial heat treatment. During patch
application the moisture may turn to steam which can (i) split the laminate in
voided regions, (ii) form voids in the adhesive, and (iii) form voids in the
matrix of the repair laminate (if it is being co-cured). Damage in the matrix
can be particularly severe if the heat treatment is performed above its
(reduced) glass transition temperature, when the strength of the matrix is
quite low. In all cases the result may be a severe degradation in mechanical
properties. The problem of moisture removal is a much more serious problem in
a thick laminate (50 plies or more), since days of heating may be required to
effect removal. In general, however, it may not be necessary to remove all
moisture, since only the surface moisture causes problems (i) and (ii)
referred to previously. Rapid surface drying may be achieved by using vacuum
assistance.

Thin laminates (16 plies or less) can be dried out fairly rapidly.
However, if the laminate forms the face of a honeycomb panel, excessive
internal steam formation may result in a blown skin. One approach is to accept

the presence of moisture in the laminate and allow for it in terms of reduced design allowables - both for the patch, if co-cured, and for the adhesive [8]. With pre-cured patches, pre-cured plies or titanium foil patches, referred to earlier, the patches do not suffer from moisture problems; however, the problem of adhesive porosity remains the same.

4.2   Mechanical Preparation

If a patch repair is to be applied, the damaged region is first outlined in the form of a geometrical shape that allows accurate preparation and installation of a patch. In, general the shape will be circular and will encompass the area of damage, as determined by NDI and visual inspection, but will include as little as possible of the sound material.

Graphite/epoxy is best cut with tungsten carbide tipped tools; conventional high speed tools can be used but their useful life is unaccepta- bly short.   Most forming operations for repair purposes can be performed with an end mill cutter or router mounted in an air motor on a portable base. A template may be used to control the outline of the shape of the cut and shims to control its depth. Taper cuts may be made, using shims to allow cuts of one ply depth at a time. Alternatively, a sanding drum (alumina or silicon carbide grit) may be used to cut a smooth taper. In this case the tool may be hand guided (controlled by the operator's observation of ply exposure) or preferably, template guided. The taper may extend through the thickness of the laminate, in the repair of penetration damage, or only part way through, in the repair of delamination damage, as shown in Fig. 6.

Fastener hole formation is required for bolted repairs; in this case the metal patch is used as a template to ensure correct hole alignment. Since the graphite/epoxy skin cannot usually be fully supported during this operation, very slow drill feed rates are required to avoid delamination and splintering damage during break through on the blind face.

4.3   Surface Treatment for Bonding

Graphite/Epoxy Patch:

The most effective treatment for preparing pre-formed graphite/ epoxy patches for bonding is grit blasting (usually with aluminium oxide grit) to remove contaminated surface matrix material. Another approach, which sim- plifies field application, relies on the use of a peel ply, during formation of the patch. Peel ply is a layer of woven nylon cloth incorporated into the surface of the composite during manufacture. Prior to bonding the patch the nylon is peeled off exposing a clean surface ready for bonding. However, it is generally agreed that this procedure produces inferior bonds to grit blasting. This is because the grid like nature of the peeled surfaces encourages air entrapment and also because of the danger of small amounts of the ply remaining on the surface.

By far the most effective procedure, to avoid these difficulties and the danger of subsequent contamination is to co-cure the patch and adhesive.

Graphite/Epoxy Parent Laminate:

The only options for surface treatment of the parent laminate are abrasion or grit-blasting.

Titanium Alloy:

Metals generally require a much more elaborate surface treatment than the organic matrix composites. For durable bonds it is usually necessary to form a stable oxide film (of the required morphology) by chemical etching and/or anodising. In addition the surface is usually coated with a corrosion inhibiting primer. This has the extra function of protecting the metal part prior to bonding and is thus important for patches which must be stored for field application. Chemical treatment under field conditions is best avoided where possible. Titanium alloys are usually surface treated with a proprietary etchant (such as Pasa Jell 107) based on a mixture of hydro-fluoric and nitric acids in an aqueous medium, which is formed into a gel for field application.

4.4   Adhesives

Structural film adhesives are employed for applications where a high level of strength recovery is required. They generally consist of a pre-catalysed modified epoxy such as epoxy-nitrile or, for high temperature applications (60°C to 100°C), an epoxy phenolic, supported by a polymer or glass fibre mat or woven cloth. More recently, these materials have also become available in paste form. Provided the curing conditions can be achieved and moisture does not pose serious problems, these adhesives are preferred for repair applications. A serious disadvantage of the precatalysed adhesives, particularly for repair applications, is that the cure reaction will slowly occur - even under refrigeration to -20°C life is only six months or so. Where this storage and replacement situation cannot be tolerated, and lower mechanical properties can be accepted, two part epoxy-paste adhesives are employed since these have no storage problems and are also simpler to process.

Injection adhesives or resins do not have the same requirements for high peel strength as the adhesives used for bonding patches. However, they are required to have low viscosity and to suffer low shrinkage on cure. Generally two part casting or potting epoxies are used.

4.5   Curing Procedures For Field and Depot Repairs

Heat and pressure are required to cure the adhesive and obtain a uniform non-porous adhesive layer. Under field or depot conditions, these cure requirements are most simply satisfied with a vacuum bag arrangement, as illustrated in Figs. 5, 6 and 8. Although simple vacuum bag arrangements are capable of providing pressures only of one atmosphere, this pressure is usually quite adequate if the patch mates well with the parent material; this condition is easily achieved by co-curing the patch and adhesive. However, higher pressures, if required, can be obtained by means of an oversize caul-plate placed over the patch in the bag assembly.

231

Heat may be applied internally (as shown in Fig. 5) by encasing a heater element under the bag – usually electrical resistance wire embedded in silicon rubber. Alternatively, a reusable combined vacuum bag and heater blanket may be employed consisting of silicon rubber with built in heater wires; this type of arrangement, although apparently quite attractive, has not proven to be very reliable. Heat to effect cure may also be applied externally, for instance in an oven (if the component is removable and of a suitable size), or by heat lamps, as shown in Fig. 8. Heat lamps are a very versatile method of applying heat, through nylon or teflon film vacuum bags; however, it may be difficult to obtain an even heat distribution by this procedure and it is quite common to seriously overheat one spot whilst leaving nearby areas under heated.

The simple vacuum bag procedure suffers from some major drawbacks which are all associated with the low pressures which may be created in some regions inside the bag; these include: (i) entrapped air and volatile materials in the resin matrix and adhesive may tend to expand under the reduced pressure leaving large voids in the cured resin, (ii) moisture absorbed in the graphite/epoxy parent laminate may be evolved more easily under reduced pressure and enter the adhesive, producing voids (and possibly interfering with the cure mechanism) and (iii) air may be drawn into the bond region through any porosity in the parent material producing voids in the patch system – the reduced pressure inside a honeycomb panel may cause the panel to collapse. Thus, although the vacuum bag procedure is reported to yield good results, its use has dangers particularly for critical repairs. A safer alternative is to use gas or mechanical pressure. The problem here is to arrange for the resulting loads to be reacted out. If they cannot be reacted out by surrounding structure, vaccum pads or adhesively bonded anchor points may be employed.

5.   DESIGN OF BONDED REPAIRS

5.1   General Considerations

Repair designs are most simply based on the "equivalent joint", Fig. 3, obtained by considering a section taken through the damaged region. A more detailed and realistic analysis would need to consider the influence of the patch on the surrounding structure; however this aspect is beyond the scope of the present discussion.

Generally, the patch is chosen to match the strength and stiffness of the parent material. The strength of the joint (repair) may be designed to exceed by some margin (e.g. 20-50%) the B allowable*residual ultimate strain of the degraded parent material** or, much less stringently, the B allowable ultimate residual strain of the degraded parent material in the presence of strain concentrators such as holes or representative damage. The first approach is most desirable, if feasible, since it ensures that the adhesive bond can not be stressed to failure, even under the most severe aircraft operating conditions and, further, allows a reserve in strength for disbonds and defects. However, for most practical purposes, it should be quite satisfactory to design for the reduced strain levels.

----

*   B basis ultimate strain allowable is the strain to failure which is equal or exceeded by at least 90% of the population, with a confidence of 95%.

**   After absorption of equilibrium moisture content.

232

For example, the B allowable ultimate residual strength for a
$[(\pm45°/0°/90°)_2]_s$ 16 ply (quasi-isotropic) laminate with 1% absorbed moisture
and tested at 120°C, after representative fatigue loading, is about 9000
microstrain in tension and about 7500 microstrain in compression. Based on
a nominal strain concentration factor of 3 for fastener holes the reduced B
allowables would be about 3000 microstrain tension and 2500 microstrain
compression. However, most design is currently based on an allowable of
about 4000 microstrain which is the practically determined B allowable
ultimate strain for laminates with holes or impact damage - particularly under
compression loading conditions.

5.2   External Patches

The external patch repair can be modelled as a half of a double-
lap joint provided sufficient support is provided by the sub-structure to
overcome bending effects. The following analysis is based on that given in
reference (9) and Lecture 8, and requires initially a shear stress-shear
strain curve for the adhesive at representative service conditions as shown
in Fig. 9a for a typical film adhesive. It is assumed that (i) the patch is
tapered at its ends to reduce peel stresses (very important for patches
thicker than about 8 plies or about 1 mm), (ii) the patch has equal stiffness
and thermal expansion coefficient to the parent material, (iii) the hole
being covered by the patch is straight sided - this is a conservative assump-
tion because any tapering improves the load carrying capacity of the joint.
Then the maximum load carrying capacity of the joint, based on an idealisation
of the stress strain behaviour of the adhesive, Fig. 9b, is given by

$$P = 2\{\eta \ \tau_p (\tfrac{1}{2} \ \gamma_e + \gamma_p) Et\}^{\frac{1}{2}}$$

where τ_p is the effective yield stress of the adhesive, γ_e and γ_p are
respectively the elastic strain to yield and the plastic strain to failure,
η the adhesive thickness, t the thickness of the patch (and the parent material)
and E its modulus.

As an example, taking (for hot/wet conditions)

τ_p = 20 MPa

E   = 72 GPa (typical for graphite/epoxy laminates
                employed in aircraft)

t   = 1.5 mm (12 plies)

γ_e = 0.05

γ_p = 0.5

η = 0.125 mm

gives   P   = 0.75 kN/mm.

233

The allowable load (per unit width) in the patch or parent material, P_u, is given by

$$P_u = E\, e_u\, t$$

where e_u is the allowable ultimate failure strain of the composite; taking this as 4000 microstrain gives

$$P_u = 0.43 \text{ kN/mm}$$

Thus, for the chosen ply thickness in this example, the load capacity of the bonded joint appears to be well above the allowable for the parent material. However, a safe margin is not obtained for external patch repairs for laminates above about 16 plies thick.

If it is considered that the strength of the repair is adequate the next step is to determine the overlap length. The total patch length is twice this plus the diameter of the hole. The minimum design overlap length is given by

$$\ell = \frac{2P_u}{\tau_p} + \frac{4}{\lambda}$$

where λ (the elastic strain exponent) is given by

$$\lambda = \left(\frac{2G}{nEt}\right)^{\frac{1}{2}}, \text{ where } G, \text{the adhesive shear modulus, is given}$$

by τ_p/γ_e

which, using previous figures, gives ℓ as about 60 mm, to which should be added a margin of about 10 mm to allow further tolerance to disbonds or other damage to the bonded region. Thus assuming a hole of 50 mm the total patch size would be 190 mm.

5.3   Flush Repairs - Single Scarf Configuration

Simple Analysis:

If the patch matches the parent material in stiffness and expansion coefficient, simple theory gives

$$\tau = \frac{P \sin\theta \cos\theta}{t} = \frac{P \sin 2\theta}{2t}$$

$$\sigma = \frac{P \sin^2\theta}{t}$$

234

where τ and σ are the shear stress and normal stress acting on the adhesive and θ is the scarf angle. At small θ, the normal stress σ is negligible. The required minimum value of scarf angle θ, for an applied load P, can be obtained from the following, taking τ_p as the peak shear stress,

$$P = E\ e_u\ t = 2\ \tau_p\ t/\sin 2\ \theta$$

Thus, for small scarf angles the condition for reaching the allowable strain e_u in the adherends is:

$$\theta < \tau_p/E\ e_u \quad \text{radians}$$

Taking e_u as 4000 microstrain, τ_p as 20 MPa, and E as 72 GPa, gives

$$\theta \leqslant 3°$$

Thus, the minimum length of the scarf taking the laminate thickness as 13 mm is about 250 mm, which, for a hole size of 100 mm, gives a total patch length of 600 mm.

Repairs To Laminates:

The above simple theories are based on the assumption that the shear stress in the adhesive layer is constant. However, if the patch or parent material varies in stiffness with thickness - as does a composite laminate - the shear stress can no longer be taken as constant. In addition, when a composite patch is produced its edges are stepped rather than scarfed; however, since the steps are very short the shear stress in the adhesive may be taken as constant on each step. Thus the repair is essentially a single step-lap joint, Fig. 3, with very short steps.

The distribution of shear stress in the adhesive can be approximately obtained from the following simple analysis, based on a simplification of that given in reference (5), which ignores shear lag effects and yielding in the adhesive.

From load equilibrium on each ply step of length Δx, it follows that

$$\tau = \Delta P/\Delta x$$

If it is assumed that the load increment ΔP on each step is proportional to the relative stiffness of the ply, such that for any layer

$$\frac{\Delta P}{P} \approx \frac{\text{stiffness of ply}}{\text{Total stiffness}}$$

then τ varies through the laminate thickness approximately as does the ply stiffness. Thus, for a $[(0°/\pm45°/90°)_2]_s$ laminate the stiffnesses are in the ratio

$$1\ (0°)\ :\ 0.23\ (\pm45°)\ :\ 0.07\ (90°)$$

This shows (on the basis of the above reasoning) that very high shear stresses occur on the 0° plies. These can lead to shear, or more likely, peel failure, unless they are relieved, for instance by serrating the ends of the plies, as described in reference (5). Serrations reduce the effective stiffness of the end of the ply and thus act in a similar way to tapering in an external patch.

An approximate estimate of the required step length Δx can be made by assuming the adhesive is stressed to its shear yield stress, τ_p, and each of the plies are loaded individually; then

$$\Delta x = \frac{E_p e_u}{\tau_p} \times \text{ply thickness}$$

where E_p is the ply stiffness (typically around 120 GPa for the 0° plies.) Taking e_u as 4000 microstrain, gives a ply length about 3 mm. The length for the ±45° and 90° plies could be shorter but in practice would probably be made the same length. Thus, for a laminate 100 plies (13 mm) thick the scarf length is 300 mm.

6.   CERTIFICATION OF REPAIRS

The question of certification must be addressed when repairs are made to critical structure. When sufficient experience has been gained with the design procedures, certification may satisfactorily be based on a stress analysis of the patched structure, together with data on materials allowables, obtained from tests on environmentally conditioned specimens of the various materials. However, at this stage it is unlikely that all of the important factors have been fully appreciated for instance, to mention a few, the influence of bending, due to load eccentricity, on compression buckling strength and long term effects such as creep and stress relaxation on the adhesive. Consequently, at this stage the design information must be supplemented by mechanical tests on structural details representing the patched region.

A reasonable test procedure would be to expose the specimens to moisture and other relevant environmental agents for a prolonged period (at elevated temperature to aid diffusion) and then (i) test under static loads to ensure structure will withstand ultimate design loads, (ii) test under cyclic loading (mission related) for say three lifetimes (or possibly less allowing for life consumed), and (iii) after cyclic loading, test under static loads to ensure that the ultimate residual strength has not fallen below the allowable level.

REFERENCES

1. Adhesive Bonded Aerospace Structures, AFML-TR-77-206, AFFDL-TR-77-139, 1977.

2. Structural Sandwich Composites, US MIL-HDBK-23A, 1968.

3. Lubin, G., Dastin, S., Mahon, J., and Woodrum, T., Repair Technologies For Boron Epoxy Structures, 27th Annual Technical Conference, 1972, Reinforced Plastics/Composites Institute. The Society of the Plastics Industry.

4. Studer, V.J., and La Salle, R.M., Repair Procedures For Advanced Composite Structures, vols. 1 and 2, AFFDL-TR-76-57, 1976.

5. Myhre, S.H., and Beck, C.E., Repair Concepts For Advanced Composite Structures, J. Aircraft, vol. 16, no. 10, 1979.

6. Myhre, S.H., and Labor, J.D., Repair of Advanced Composite Structures, J. Aircraft, vol. 18, no. 7, 1980.

7. Watson, J.C. et al., Bolted Field Repair of Composite Structures, NADC-77109-30, McDonnell Aircraft Co., 1979.

8. Rosenzweig, E.L., Environmental and Fatigue Evaluation of Field Repair Concepts, Proceedings of International Workshop Defence Applications of Advanced Repair Technology For Metal and Composite Structures, US Naval Research Laboratory, Washington DC, July 1981.

9. Hart-Smith, L.J., Analysis and Design of Advanced Composites Bonded Joints, NASA CR-2218, 1974.

237

Nozzle for injection of repair material

Air gun

Delaminated area

Graphite Epoxy skin

Aluminium honeycomb

Drill holes approximately ¼ inch from edge of delamination

Delamination   Repair material

Section A-A
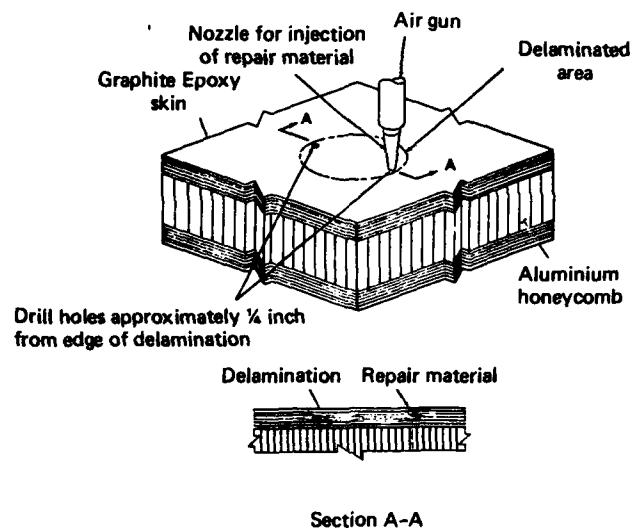
FIG. 1   ILLUSTRATION OF METHOD OF REPAIRING DELAMINATION IN THE COMPOSITE SKIN OF A HONEYCOMB PANEL BY THE RESIN INJECTION PROCEDURE
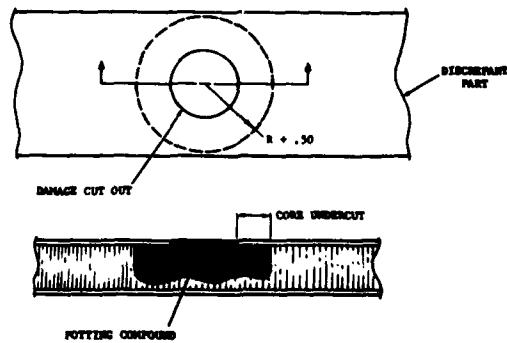
FIG. 2   ILLUSTRATION OF A POTTED REPAIR TO A DAMAGED HONEYCOMB REGION

238
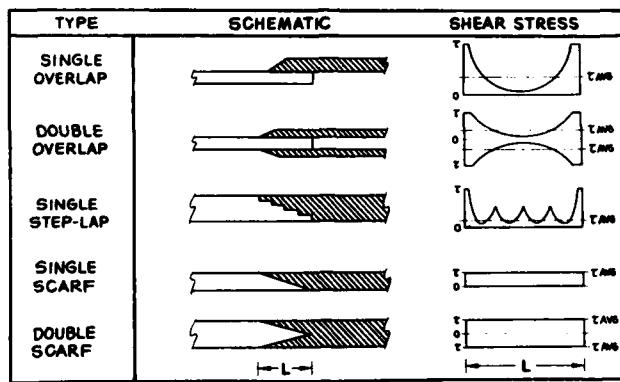
FIG. 3   ILLUSTRATION OF THE MAIN TYPES OF JOINT CONFIGURATES EMPLOYED FOR
BONDED PATCH REPAIRS AND RIGHT THE TYPES OF SHEAR STRESS
DISTRIBUTION

External patch repair
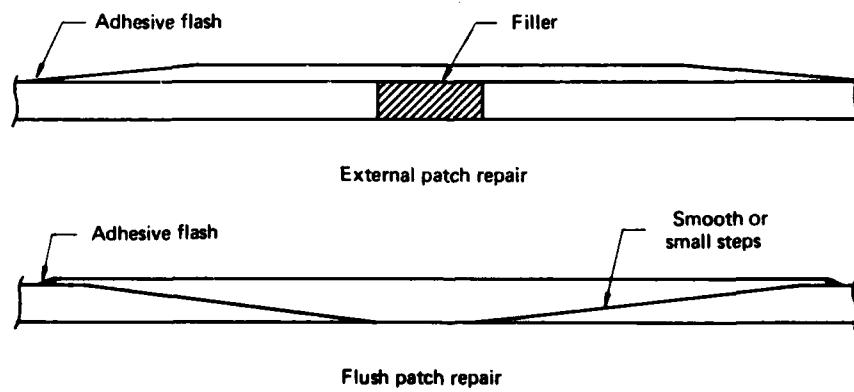
Flush patch repair

FIG. 4   ILLUSTRATION OF THE TWO MAIN TYPES OF PATCH REPAIR
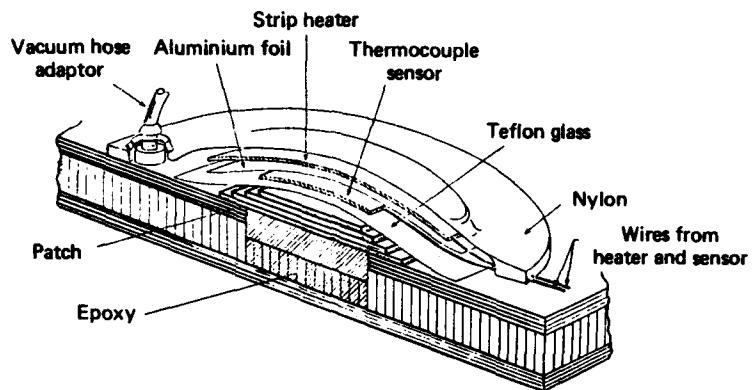
FIG. 5   ILLUSTRATION OF THE VACUUM BAG AND PATCH ARRANGEMENT EMPLOYED
TO BOND AN EXTERNAL REPAIR PATCH
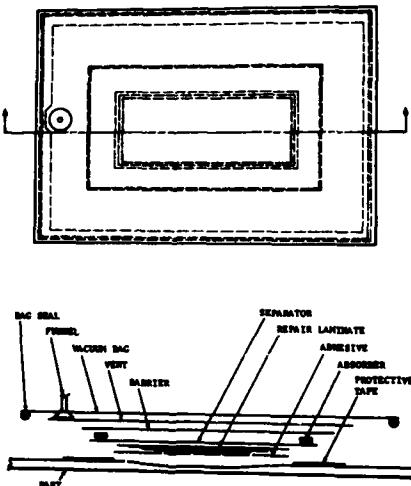
FIG. 6   ILLUSTRATION OF THE VACUUM BAG AND PATCH ARRANGEMENT EMPLOYED
TO BOND A FLUSH REPAIR PATCH

Fasteners
External titanium patch
Damage
Drill holes as indicated (use plate as template)
Monolithic wing skin
Cut away
Internal titanium back up plates
Captive plate nut
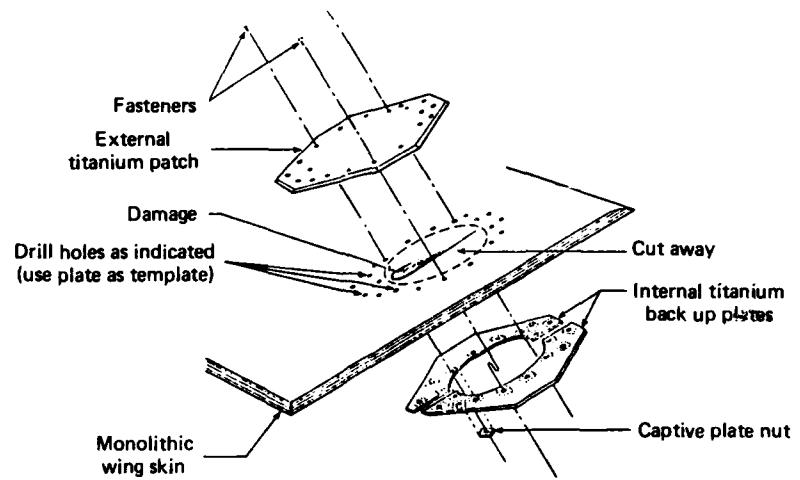
FIG. 7   ILLUSTRATION OF A BOLTED, TITANIUM EXTERNAL PATCH REPAIR FOR THICK MONOLITHIC GRAPHITE/EPOXY LAMINATES SUCH AS EMPLOYED AS AIRCRAFT WINGS

ALUMINUM FOIL TENT
HEAT SOURCE
THERMOCOUPLE
VACUUM HOSE
VACUUM BAG
REPAIR LAMINATE
VENT PLY
BAG SEALANT
OUTER SKIN

VACUUM BAG
VENT PLY
SEPARATOR FILM
VACUUM FUNNEL
REPAIR LAMINATE
BAG SEALANT
SECT A-A
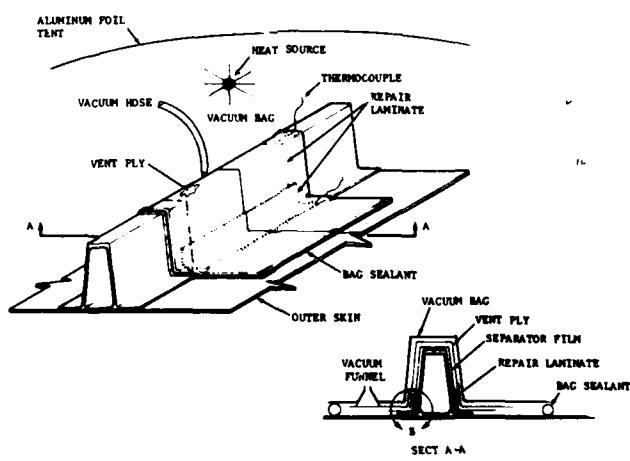
FIG. 8   ILLUSTRATION OF AN EXTERNAL PATCH REPAIR TO INTERNAL AIRCRAFT STRUCTURE, SHOWING USE OF AN EXTERNAL HEAT SOURCE

241
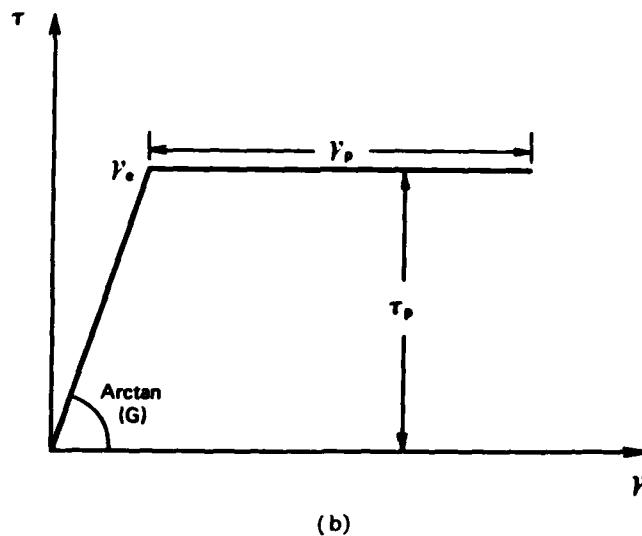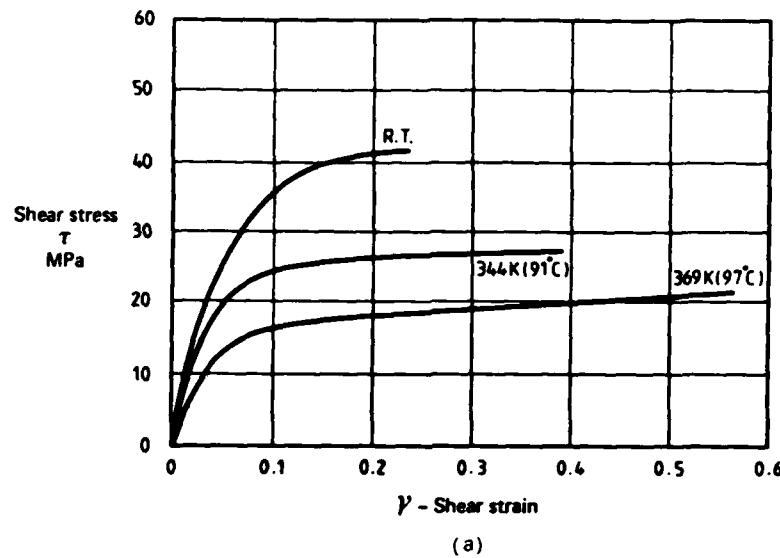
FIG. 9   (a) PLOTS OF SHEAR STRESS VERSUS SHEAR STRAIN AT VARIOUS TEMPER-
ATURES FOR ADHESIVE FM 300 AFTER EXPOSURE TO MOISTURE, OBTAINED
FROM THICK ADHEREND TEST
(b) IDEALISATION OF A TYPICAL SHEAR STRESS/SHEAR STRAIN CURVE FOR
ANALYTICAL PURPOSES — THE AIM IS TO HAVE SIMILAR AREA UNDER THE
CURVE τ_p ($\frac{1}{2}\gamma_e + \gamma_p$) AS THE REAL CURVE

242

Lecture 13

AIRCRAFT APPLICATIONS

B.C. HOSKIN and A.A. BAKER

1.   INTRODUCTION

          As has already been described in the first lecture, composite
materials, especially graphite/epoxy, are being used to a significant extent
in present day aircraft and all the signs are that this use will increase.
Just to recapitulate, major composite applications include:-

          F-14:   boron/epoxy horizontal tail skins,

          F-15:   boron/epoxy horizontal and vertical tail
                   skins,

          F-16:   graphite/epoxy horizontal and vertical
                   tail skins and control surfaces,

        F/A-18:   graphite/epoxy wing skins, horizontal and
                   vertical tail skins, and control surfaces,

          AV-8B: graphite/epoxy wing (skin plus substructure),
                   horizontal tail skin, forward fuselage, and
                   control surfaces,

          B-1:   graphite/epoxy horizontal tail (skin plus
      (prototype) substructure),

      Boeing 757):(graphite/epoxy control surfaces,
      Boeing 767) (graphite-aramid/epoxy fairings, cowlings, etc.,

      Lear Fan 2100: "almost all" graphite/epoxy structure.

In this lecture the nature of some of these applications will be discussed
further and an indication given of what seem to be the general design rules
that are evolving. Also, some matters that need special attention for
composite structure (such as lightning protection and erosion protection)
are touched on. Brief mention is made of composite applications in helicop-
ter construction.

          For further details on particular applications see, for
example, ref. (1) (F-14), ref. (2) (F/A-18 and AV-8B), refs. (3) and (4)
(AV-8B), ref. (5) (various USAF aircraft) and ref. (6) (various demonstrator
items for civil aircraft).

2.   TYPICAL COMPOSITE CONSTRUCTIONS

      2.1   Skin Structure for Wings, Tails and Control Surfaces

          At present the most common application of composites in aircraft
structures is for the skin of wings, tails and control surfaces. Generally

243

such skins are made in the *form* of "monolithic" laminates i.e., without discrete stiffeners, such as stringers, on their inner surfaces. Orthotropic lay-ups are used and these can be readily analysed by the stressing procedures described in an earlier lecture.

Consider first the skin of a main wing box. This is primarily required to carry direct stresses in the spanwise direction due to the wing bending more or less as a cantilever beam and shear stresses due to the wing twisting (Fig. 1); there will also be generally smaller direct stresses in the chordwise direction due to fore-and-aft bending. The simplest design approach is to use a laminate pattern (defined with respect to a reference axis in the spanwise direction) which consists of 0° plies to carry the span-wise direct stresses, ±45° plies to carry the shear stresses, and 90° plies to carry the chordwise direct stresses (Fig. 2). Naturally, the number of plies of each orientation depends on the specific application but, as an example, according to ref. (2) the basic pattern for the F/A-18 wing skin comprises 46% of 0° plies, 50% of ±45° plies, and 4% of 90° plies. The required thickness of skin usually decreases markedly as one proceeds from the wing root to its tip. This is something that can be easily achieved using composites; it is only necessary to cut plies successively shorter prior to lay-up. Thus, a wing skin might be 100 plies thick at its root but less than 20 plies thick at its tip.

The situation is much the same for the skin of a vertical tail (where the spanwise direction is, of course, upwards) and a fixed horizontal tail, and the laminate patterns are *likely* to be broadly similar to that described above for a wing. However, fighter aircraft often have all-moving horizontal tails ("stabilators" or "tailerons") and then, in order to provide adequate torsional strength and stiffness, it may be necessary to have a higher percentage of ±45° plies, even up to 80%, say. Also, the required skin thickness for a horizontal tail will generally be rather less than that for a wing and, at the tip, only a few plies may be required.

For a control surface hinged to a wing, say, (Fig. 3) there is likely to be, relatively speaking, a much larger amount of chordwise bending and, consequently, its skin may be expected to contain a larger proportion of 90° plies.

2.2 Metal Substructures for Components with Composite Skins

Composite skins are widely used with some form of metal sub-structure. This is the case, for example, in the F/A-18 wing and in the F-14, F-15, F-16 and F/A-18 tail units. The substructure usually comprises aluminium alloy members (spars and ribs) but sometimes titanium alloy members are used. The F/A-18 main wing box has five aluminium alloy spars but these have only relatively small flanges so that the composite skin carries most of the bending loads. A generally similar type of construction is used in the F-16 vertical tail. The horizontal tails of fighter aircraft are commonly of small thickness with an interior structure comprising full-depth aluminium honeycomb core. For an all-moving tailplane, a metallic spar/spindle is used and there may be light front and rear spars as well. An example of this type of construction, taken from ref. (5), is shown in Fig. 4.

When metallic spars and ribs are used, the composite skin is generally attached to them by mechanical fasteners. As described in an earlier lecture, when the skin is graphite/epoxy and the substructure an aluminium alloy, either titanium or stainless steel fasteners are employed to prevent galvanic corrosion. (For the same reason, thin sheets of some electrically insulating material such as glass/epoxy are inserted between adjacent areas of the composite and the metal.)

If a wing is built in the form of two half-wings, as is the case with the F/A-18, the wing-to-fuselage attachment needs special considera- tion. Composites are not well suited to carrying high bolt bearing loads and, because of this a titanium fitting, which is bonded to the graphite/epoxy skins, is used at the root of the F/A-18 wing. This has been described in Lecture 8 and it will be recalled that a stepped-lap joint is employed; see also ref. (2). The titanium fitting is then connected to the fuselage by lugs in the usual fashion. Broadly similar bonded joints are used for the root fittings of the F-14, F-15 and F/A-18 horizontal tails.

2.3   All-Composite Wings and Tails

Both the AV-8B wing and the prototype B-1 horizontal tail are virtually all-composite structures; as well as having graphite/epoxy skin, they also have graphite/epoxy sub-structure. For example, the AV-8B wing, which incidentally is made continuous tip-to-tip (rather than in two halves as in the F/A-18), has eight graphite/epoxy spars. Because the main function of the web of a spar is to carry the vertical shear loads, the web comprises mainly ±45° plies, although there may be a small percentage of 90° plies also (Fig. 5). In both the AV-8B and B-1 applications the spar webs are corruga- ted in the spanwise direction to give increased compression strength; the results are the so-called "sine wave" spars.

3.   DESIGN PRINCIPLES FOR COMPOSITE STRUCTURE

Naturally, the design principles for composite aircraft structures are still evolving but the following gives an indication of what seems to be current thinking.

According to ref. (2), the design strains at the ultimate load condition for the graphite/epoxy components of the F/A-18 wing have been restricted to 5000 microstrain in zones of low fastener bearing stresses; in regions of higher bearing stresses the strain is further restricted. (For a 50% 0°, 50% ±45° laminate of graphite/epoxy with a Young's modulus of, say, 80 GPa, 5000 microstrain converts into an ultimate design stress of approx- imately 400 MPa.) Somewhat lower ultimate design strains, namely, between 4000 and 4500 microstrain are recommended in ref. (7). For a reasonably extensive discussion of the design allowables for a typical graphite/epoxy system see, for example, ref. (8).

Dastin and Erbacher (9) have given what they consider to be the general design principles for composite structure; these are reproduced (verbatim) in Tables 1 and 2 below.

245

TABLE 1: General Design Practice (ref. 9)

Serial	Practice	Reason
1	Filamentary controlled laminates - minimum of three layer orientations.	To prevent matrix and stiffness degradation.
2	0/90/±45 laminate with a minimum of one layer in each direction.	0° layers for longitudinal load, 90° layers for transverse load, ±45° layers for shear load.
3	A + 45° and a - 45° ply are in contact with each other.	To minimise interlaminar shear.
4	45° layers are added in pairs (+ and -)	In-plane shear is carried by tension and compression in the 45° layers.
5	When adding plies try to maintain symmetry.	To minimise warping and interlaminar shear.
6	Minimise stress concentrations.	Composites are essentially elastic to failure.
7	±45° plies, at least one pair on extremes of laminate. However, for specific design requirements (applied moments) 0° or 90° plies may be more advantageous in direction of moments.	Increases buckling (strength) for thin laminates; better damage tolerance; more efficient bonded splice.
8	Maintain a homogeneous stacking sequence banding several plies of the same orientation together.	Increased strength.

246

TABLE 2: General Design Practice for Joints (ref. 9)

Serial	Practice	Reason
1	3D edge distance and 6D pitch for bolted joints.	Bearing strength.
2	Design bonded step joints rather than scarf joints.	More consistent results, design flexibility.
3	Bonded joints - no 90° plies in contact with Ti.	Reduction in lap shear strength.
4	Bonded joints - ±45° plies on last step.	To reduce peak loading.
5	When adding plies use a 0.3 in (7.6 mm) overlap in major load direction using a wedge type pattern.	Requires approximately 0.3 in (7.6 mm) to develop strength.

4.   EROSION PROTECTION

The erosion resistance of composite materials, especially the resin matrix component thereof, is poorer than that of metals. Thus, for the leading edges of aerodynamic surfaces it is usual to employ either an all-metal structure or else to bond, over a composite skin, a metallic layer.

5.   LIGHTNING PROTECTION

Early composite aircraft structures used mainly glass or boron fibres. Since both these materials are essentially non-conductors of electricity, structures made of them are very susceptible to damage from lightning strikes; an account of the damage sustained by boron/epoxy structures under 100 kA and 200 kA simulated lightning strikes has been given by Clark (10). The sort of protection schemes used for boron/epoxy components can be exemplified by that adopted for the F-14 horizontal tail (ref. 1). There, 50 mm wide and 0.1 mm thick aluminium foil strips are bonded on to the composite skin at 100 mm centres. Fibreglass strips are located between the foil strips to preserve aerodynamic smoothness.

Carbon is, of course, quite a reasonable electric conductor but, with graphite/epoxy structures, it is still common to incorporate some form of lightning protection; again this may take the form of bonded metallic foil on the external surface of a component.

6. HELICOPTER APPLICATIONS

In the preceding parts of this lecture attention has been limited to applications of composite materials in fixed wing aircraft, but there is just as much interest in their applications to helicopters; see, for example, refs. (11), (12), (13) and (14). Whilst consideration has been given to the use of composites for many parts of a helicopter structure, there has been especial interest in two areas, namely, rotor blades and drive shafts.

All the composite materials that have been discussed in these lectures, whether using glass, graphite, boron or aramid fibres, have been seen as having distinct advantages for rotor blades (although boron is now probably ruled out on a cost basis). Pinckney (12) lists the following such advantages:

(i) Improved aerodynamic efficiency is obtainable with composite blades because they can be readily manufactured in more complex airfoil shapes than are achievable with metal construction; Pinckney cites 20% increases in the lift-to-drag ratio from this cause.

(ii) Although factors outside structural design may impose a minimum weight on a helicopter blade, there are still some circumstances where the weight saving that is generally achievable with composites can be utilised.

(iii) According to Pinckney, the most significant advantage of the use of composites comes from the ability that exists to tailor the dynamic frequencies and structural responses of the blade element to its operating parameters. The blade frequencies can be controlled by selecting appropriate laminate patterns to give requisite bending and torsional stiffness.

Helicopters make an extensive use of connecting drive shafts e.g., the usually long such shaft to the tail rotor. Since lack of stiffness is generally a potential problem with these, only the advanced high modulus composites are usually considered suitable for this application (and not glass). The main function of a drive shaft is to transmit a torque, so, with a reference axis taken parallel to a generator of the shaft the laminate pattern is likely to comprise ±45° plies, with some 0° plies to provide increased bending strength (Fig. 6). (Actually, in the application described in ref. (13) more 0° plies are used than ±45° plies; however, other applications described in ref. (11) seem to use all ±45° plies). According to Salkind (11), a composite drive shaft may be easier to balance dynamically than an equivalent metal one, because of its higher internal damping.

248

REFERENCES

1. Forsch, H., Advanced Composite Material Applications to F-14A Structure, pp. 30-39 of ASTM STP 674, 1979.

2. Weinberger, R.A., Somoroff, A.R., and Riley, B.L., US Navy Certification of Composite Wings for the F-18 and Advanced Harrier Aircraft, pp. 1-12 of AGARD-R-660, 1978.

3. Huttrop, M.L., Composite Wing Substructure Technology on the AV-8B Advanced Aircraft, pp. 25-40 of Fibrous Composites in Structural Design (ed. by Lenoe, E.M. et al), Plenum Press, New York, 1980.

4. Watson, J.C., Preliminary Design Development AV-8B Forward Fuselage Composite Structure, ibid pp. 41-62.

5. Goodman, J.W., Tiffany, C.F., and Muha, T.J., Structural Assurance of Advanced Composite Components for USAF Aircraft, pp. 25-35 of AGARD-R-660, 1978.

6. Vosteen, L.F., Composite Aircraft Structures, pp. 7-24 of Fibrous Composites in Structural Design; see ref. 3 above.

7. Goodman, J.W., Lincoln, J.W., and Petrin, C.L., On Certification of Composite Aircraft Structures for USAF Aircraft, AIAA Aircraft Systems and Technology Conference, Dayton, Paper AIAA-81-1686, August 1981.

8. Ekvall, J.C. and Griffin, C.F., Design Allowables for T300/5208 Graphite/ Epoxy Composite Systems, AIAA 22nd Structures, Structural Dynamics and Materials Conference, Atlanta, Part 1, pp. 416-422, 1981.

9. Dastin, S.J., and Erbacher, H.A., Experiences with Composite Aircraft Structures, SAMPE Engineering Series, vol. 25, pp. 706-715, 1980.

10. Clark, H.T., Lightning Protection for Composites, pp. 324-342 of ASTM STP 546, 1974.

11. Salkind, M.J., VTOL Aircraft, pp. 76-107 of Applications of Composite Materials, ASTM STP 524, 1973.

12. Pinckney, R.L., Helicopter Rotor Blades, ibid. pp. 108-133.

13. Zinberg, H., and Symonds, M.F., The Development of an Advanced Composite Tail Rotor Driveshaft, Preprint 451, 26th Forum of American Helicopter Society, 1970.

14. Various Authors, Special Composite Structures and Materials Issue, Journal of the American Helicopter Society, vol. 26, no. 4, October 1981.

Torque

Verti.
Shear

Spanwise bending moment
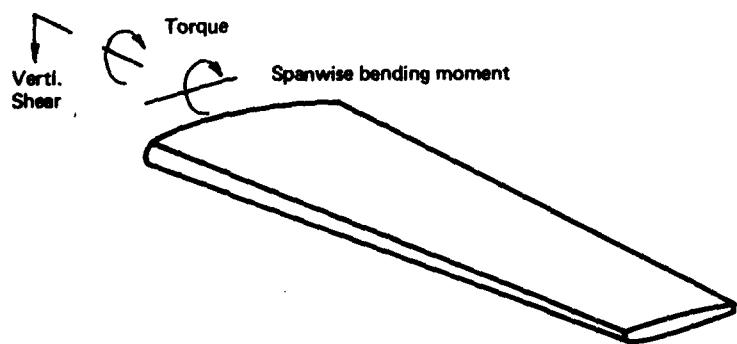
FIG. 1   MAIN REACTION LOADS AT WING SECTION

±45°   90°   0°   Ref. Axis (spanwise)
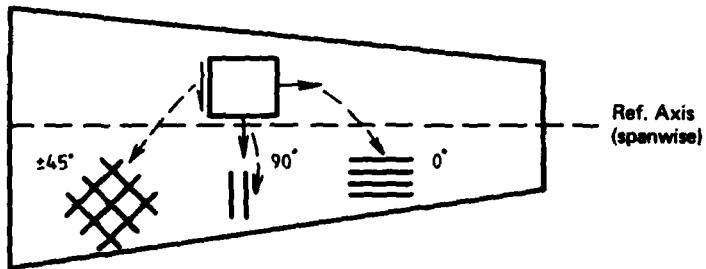
FIG. 2   MAIN PLY ORIENTATIONS FOR WING SKINS

90°   Ref. Axis (spanwise)
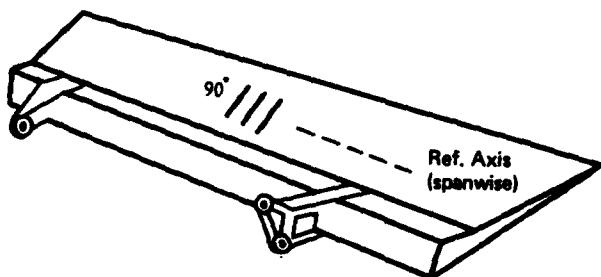
FIG. 3   HINGED CONTROL SURFACE (SPOILER)
(0°, ± 45° PLIES NOT SHOWN)

Graphite/epoxy
cover

Aluminium
honeycomb
core

Titanium
spar/pivot
fitting

Graphite/epoxy
cover
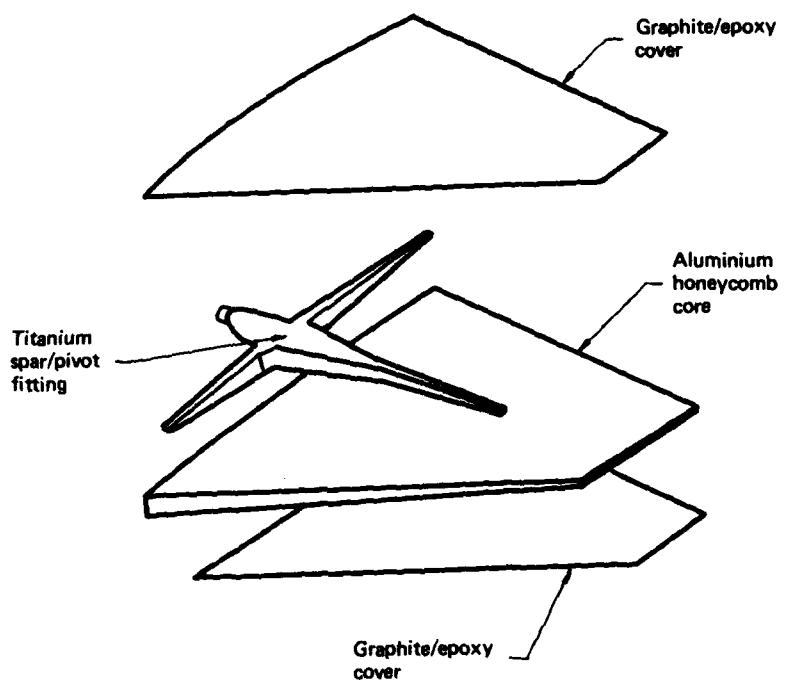
FIG. 4   REPRESENTATIVE COMPOSITE ALL-MOVING HORIZONTAL TAIL PLANE
CONSTRUCTION (FRONT AND REAR SPARS NOT SHOWN)
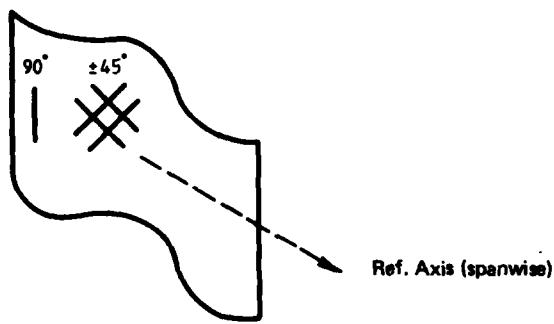
FIG. 5 MAIN PLY ORIENTATIONS FOR WEB OF SINE WAVE SPAR
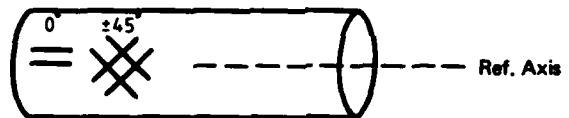
FIG.6 MAIN PLY ORIENTATIONS FOR A DRIVE SHAFT

Lecture 14

AIRWORTHINESS CONSIDERATIONS

B.C. HOSKIN

1.   INTRODUCTION

As has been seen in the preceding lectures, the use of composite
materials raises some problems which are different to those for metal aircraft
structures. These problems, in turn, raise questions about specific
airworthiness requirements for composite aircraft structures. At this stage,
few formal such specific requirements exist. As an example, consider the
matter of the effect of the moisture/temperature environment on structural
performance. Although the US Military Standard on Aircraft Structural
Integrity (1) states that the standard applies "to metallic and non-metallic
structures", and although the US Military Handbook (2) details general design
procedures for composite structures, neither document specifies a procedure
for allowing for environmental effects in the structural integrity program,
including the static and fatigue tests on full-scale articles. In the UK,
according to ref. (3), written in 1980, airworthiness requirements for UK
military aircraft containing composite structure only "exist in draft form".
(Nevertheless, ref. (3) gives quite a detailed account of key aspects of the
airworthiness certification process for composite structures.)

Despite the fact that, to date, composites have been used much
more widely in military, than in civil, aircraft the US civil authority has
produced an Advisory Circular (4) setting forth an acceptable means of com-
pliance with the "certification requirements of composite aircraft structures
involving fibre reinforced materials e.g., graphite, boron and glass
reinforced plastics."

The certification of the several US military aircraft built to
date, which do contain significant amounts of composite structure, seems to
have been achieved basically by following the procedures for metal aircraft, but
with additional requirements, sometimes of an ad hoc nature, agreed between
the certifying authority and the manufacturer for the composite components;
see refs. (5) and (6).

It is not the aim of the present lecture to attempt to define a
path to certification, but rather to give a general description of the type
of approach that is evolving. As will be seen, two main problems are:

(i)   the proper allowance for environmental effects
       (moisture and temperature) in the full scale
       static and fatigue tests, and

(ii)   the implications of the apparent increase in scatter
       in both the static and fatigue strengths of composite,
       as compared with metal, structure.

(With regard to scatter, as experience in the manufacture of composite structures has increased, there are indications that the scatter in static strength can be reduced to levels which are comparable with metals i.e., with a coefficient of variation (defined as standard deviation/mean) of around 5%. On the other hand, it is generally agreed that the scatter in fatigue strength of composites is much higher than that for metals although, even here, it should be borne in mind that most of the composite fatigue data obtained so far has been for simple specimens; it is well known, and is consistent with extreme value statistics, that the fatigue scatter decreases as the size and complexity of the specimens increase.)

Brief mention is also made of some other special problems for composites.

2.   DEMONSTRATION OF STATIC STRENGTH

2.1   General

The design procedure to establish the static strength of a metal aircraft generally involves, firstly, a detailed theoretical structural analysis (now almost always done using a finite element structural "model") and, secondly, a large amount of structural testing on specimens of varying degrees of complexity. These last can be conveniently, if somewhat arbitrarily, categorised as follows (Fig. 1):

(i) Coupon Tests

These are tests on small, plain specimens used to establish basic material properties (e.g. ultimate tensile strength). Enough tests are done on such specimens, so that "allowable values", which take account of statistical effects (i.e., scatter), can be established. Two allowable values are defined for any particular design quantity (e.g., ultimate tensile strength): the A- allowable, which is the value achieved by at least 99% of the population, at the 95% confidence level, and the B-allowable which is the value achieved by at least 90% of the population, at the 95% confidence level. An allowable value, F_a, for a quantity, F, is calculated from test data by a formula of the type

$$F_a = F_m(1 - K \times CV) \tag{2.1}$$

where F_m is the mean test value,

CV is the coefficient of variation of the test values,

K is a statistical parameter, which depends on the relevant probability distribution (generally assumed to be normal), the number of samples, and whether an A or B allowable is required.

For metals, it is usual to work with A-allowables and in ref. (3) tables are given showing the reduction of an A-allowable below a mean value, for various coefficients of variation and sample size.

254

(ii) Structural Detail Tests

Structural details are still small specimens but contain typical, if elementary, structural features. Examples might be tension specimens with open or filled bolt holes, simple lap joint specimens and so on. If wished, it is possible to obtain allowable values for the strength of such details.

(iii) Sub-Component Tests

A sub-component is a full scale representation of a moderate size region of a structure. Examples would be a compression panel forming part of a wing skin, part of a major splice, etc. Generally, these specimens are already too large for it to be practicable to test enough of them to establish useful A-allowable values.

(iv) Component Tests

A component is a full scale representation of a major region of a structure. An example might be a sizeable length of the main wing box or a complete major joint. Here only a very limited number of specimens (say 1 or 2) may be able to be tested.

(v)   Full Scale Article Test

This is the test on a virtually complete aircraft structure. Almost certainly, only one test specimen will be available.

The above discussion has been from the design point of view, but, from the airworthiness point of view it is the full scale article tests which are seen as providing the key verification of static strength. Generally, there are two series of static tests on a full scale article. The first is to establish that, at design limit load (DLL), no unacceptable deformations occur. The second is to establish that, at ultimate load, which by definition is 150% DLL, failure does not occur.

Turning now to composites, as has already been seen, certain of the strength properties there are significantly degraded due to moisture/temperature effects, and, possibly, although to a lesser extent, due to load cycle effects as well. It is clearly necessary that a composite aircraft must have sufficient static strength even when it is in the most environmentally degraded form it will achieve in service. The question is, how is that to be demonstrated? The prospect of enclosing a complete aircraft in a humidity chamber, and spending many months in moisture conditioning the structure, then possibly subjecting the structure to a certain amount of temperature and load cycling, before finally carrying out the static tests, is a daunting one. This is especially so if, because of scatter, it is unclear what inferences can be drawn from the results of a single test anyway.

Before going on, it might be mentioned that the matter of whether a composite structure should be given a certain amount of load cycling before being statically tested is rather contentious; the same argument could certainly be applied to a metal structure, but there it has usually been accepted that the static test can be carried out on a new structure.

255

2.2   Test Programs for Composite Structures

The same broad program as was just outlined for a metal structure is generally followed for a composite structure. Again, a finite element structural model is developed for the theoretical analysis and, again, tests will be carried out on specimens of varying complexity. Points of difference are discussed below.

(i)   Coupon and Structural Detail Tests

Since these two specimen types are of a generally small size there are no major difficulties in conditioning them to whatever is considered an appropriate moisture level (typically of the order of a 1% weight increase). As indicated earlier, the specimens may, or may not be, subjected to some specified amount of spectrum load/temperature cycling (equivalent to 1, or possibly 2, lifetimes) before being statically tested to failure. It is usual to test according to the test matrix of Table 1.

TABLE 1:   Environmental Tests

Moisture	Temperature		
	Cold	RT*	Hot
"Dry"			
"Wet"			

*RT = room temperature

Enough coupon tests are done on the main laminate patterns to establish "allowable" values for each temperature/moisture combination. (Although the situation is by no means clear, there seems to be a trend towards accepting B-allowables for composite design, it being considered that, because of increased scatter, an unacceptably large amount of testing is necessary to establish A-allowables. The airworthiness implications of working with B-allowables, which are distinctly less conservative than A-allowables, are still to be assessed.) Enough structural detail tests are done to establish the worst environmental condition for each type of detail; then, enough tests are done for this worst condition, and also for the RT/dry (base) condition, to establish allowable values for the detail in these two conditions.

As well as establishing design allowables, these tests also provide "knock-down" factors (i.e., reduction factors) for both environmental effects and variability. Comparison of, say, the "RT, dry" value and the "hot/wet" value of an allowable provides an environmental knock-down factor. Similarly, comparison of any mean value with its associated allowable value provides a variability knock-down factor.

As discussed in Lecture 7, because the stresses in a multi-directional laminate can vary markedly from ply to ply, allowable values are likely to be cited in terms of strain, rather than stress.

(ii)   Sub-Component and Component Tests

The sub-components and components selected for test will initially be based on the predictions of the finite element model (as, indeed, will have been the structural details). It will usually still be feasible, although time consuming, to moisture condition sub-components and components prior to test. (Again, they may, or may not be subjected to load/thermal cycles prior to test). They are then statically tested to failure under the most severe environmental condition, and the failure strain measured. These tests establish mean values of ultimate strains in the environmentally degraded condition. It is also important to note the region and nature of the failure and to ensure that there are "structural detail" tests relevant to the region, and that, there, the sam.. failure mode occurred. If this is not the case, then such tests must be done. Then, assuming that the scatter in the sub-component and component tests is the same as that in the detail tests (which is certainly open to criticism, but which is probably conservative), application of the variability knock-down factor to the mean values just determined gives allowable values for the full scale structure in the environmentally degraded condition. In addition, if a component has not been tested with the environment included, then the environmental knock-down factor must also be applied.

(iii) Full Scale Article Test

The full scale article is tested in the "RT, dry" condition. The main difference between this test for a composite and a metal aircraft is that, for a composite, the structure is much more extensively strain gauged. This test then serves, firstly, to validate the finite element model; if the strain gauge results show regions of high strain in areas where no component or sub-components were tested, then it is necessary that such testing be done. Then, concentrating on the ultimate load test, the measured strains at 150% DLL are compared with the knocked-down design allowables as established in (ii). If the measured strain exceeds the allowable value, failure is deemed to have occurred and some redesign is necessary.

Although there are uncertainties at various stages in the above, the general approach seems reasonable. It can be seen that, for composite aircraft, virtually all the development testing (on small and large specimens) becomes an integral part of the airworthiness certification.

2.3   Proof Tests

For some composite components in service, certain airworthiness authorities have required that every production component be given a proof test, generally to a load slightly in excess of design limit load. In such cases, the components are given a thorough NDI both before and after test.

3. DEMONSTRATION OF FATIGUE STRENGTH

The situation with regard to demonstration of a satisfactory
fatigue performance for composite aircraft structure is far from clear. The
full scale fatigue tests that have been carried out on current aircraft con-
taining composites have generally been the same as would have been used for
an all-metal aircraft i.e., a test to N lifetimes (where N may be 2, 4 or
whatever) in a normal environment. (Of course, most such aircraft are
mainly metal anyway). Again the prospect of doing a fatigue test on a full
scale aircraft with the moisture/temperature environment fully represented
is a daunting one. Also, insufficient data are yet available on the fatigue
of large composite structures to give any real basis for selecting a scatter
factor.

The full scale test in a normal environment will certainly
continue to be performed to verify metal structure and it may sometimes serve
to reveal unsuspected problems with the composite structure. However, it
seems that the main verification of the fatigue performance of the composite
structure will be based on sub-component and component testing in an
appropriately humid environment and with the temperature cycling (especially
the thermal spikes) accurately represented. Depending on what is eventually
considered to be an adequate scatter factor for composite structural fatigue,
these tests may or may not be performed in association with the static test
program as previously described.

Because of the apparently large scatter in composite fatigue
life which, if the same sort of fatigue test philosophy as has been used in
the past for metal structures were applied, would seem to necessitate testing
composite structures for excessively long periods (say, the order of 30 or
more lifetimes), serious consideration is being given to adopting a different
test procedure. For example, the composite taileron for Tornado is only
being tested to one lifetime but an "enhanced" (i.e., more severe than
actual) load spectrum is being applied (ref. 7). (This sort of approach has
previously been used for metal rotor blades for helicopters.)

It should not be inferred from the above that the fatigue of
composites is necessarily a cause for major concern; it is more a matter of
there being difficulties in establishing a convenient test demonstration.
A detailed discussion of the fatigue problem from the airworthiness point of
view is given in ref. (3).

4. DAMAGE TOLERANCE

An understanding of the damage tolerance requirements for
composite aircraft structures is still in its early stages. Many uncertain-
ties exist about the nature and extent of the damage which should be
postulated in any damage tolerance requirements. Currently delaminations
seem to be the type of damage in which there is most interest. Also, though
this is very conjectural, there seems to be a line of thought that, in a
large sheet structure, a laminate should be able to tolerate a delamination
having a length dimension of the order of 20 mm without any serious
degradation in its performance occurring over 1 lifetime.

258

5. A PROPOSED SCHEDULE OF ENVIRONMENTAL TESTS FOR COMPOSITE CERTIFICATION

Goodman et al. (8) have proposed an approach to the certification of composite structures, paying particular attention to the inclusion of environmental effects in the structural test program. (The matter of scatter is less thoroughly addressed.) The approach takes cognisance of the temperature seen by a particular component and, also, of its method of construction, namely, whether bolted, bonded, or co-cured. The key features of the approach are summarised in Table 2 below which has been taken verbation from ref. (8).

TABLE 2: Typical Full Scale Structural Tests for 350°F (177°C) Curing Graphite/Epoxy Composite Safety-of-Flight Components (ref. 8)

Service Temperature	Assembly Method	Static Strength	Durability	Damage Tolerance
Less than 180°F (82°C)	Bolted, bonded, or co-cured	Conventional room temperature static test	Conventional room temperature accelerated fatigue test	Room temperature accelerated damage growth tests
180°F (82°C) to 250°F (121°C)	Bolted	Room temperature increased loads		Accelerated worst-case moisture/ temperature environmental damage growth tests
	Bonded or co-cured	Worst case elevated temperature test, pre-conditioned for worst case moisture absorption	Accelerated average moisture/ temperature environmental fatigue test	
More than 250°F (121°C)	Bolted, bonded, or co-cured	By individual agreement with procuring authority		

6. FLAMMABILITY

In ref. (4), requirements with respect to the flammability of composite structures for US civil aircraft are given. Simply, these require that existing levels of safety for metal aircraft should not be decreased by the use of composite structure. For aircraft exterior structure and engine compartment materials that are to be fire-resistant, the following test is considered acceptable for demonstrating compliance. Two sheets specimens, each 24 in. by 24 in., are separately positioned perpendicular to a 2000°F

flame produced by a modified oil burner consuming 2 gallons of kerosene per hour. One of the specimens is of the composite material and has a thickness equal to the thickness of the component being evaluated; the other is of aluminium alloy with the thickness that would be appropriate if the component had indeed been made of aluminium alloy. The burner is positioned so that it takes the flame approximately 5 minutes to penetrate the aluminium specimen. The requirement is then that it should take at least as long for the flame to penetrate the composite specimen.

Although it is not strictly an airworthiness matter, it is convenient to refer here to a problem which, for a short time, caused substantial concern about the large scale use of graphite fibres in aircraft. This was what sometimes was termed "the carbon fibre release problem" which arose in the following conceived situation. When a graphite structure is involved in a conflagration, very fine carbon fibres may be released into the atmosphere. These fibres may permeate electrical equipment in the vicinity of the conflagration and, since carbon is an electrical conductor, short circuits may result. (A scenario, sometimes described in the above connection, was of an aircraft fire in the neighbourhood of an airport with the possible consequent long term disruption of airport communication and navigational equipment.) An intensive study of this problem was undertaken in USA (9) and the conclusion appears to have been that the problem is nowhere near as serious as was conceived.

7.   FORCE MANAGEMENT

The term "force management" refers to the procedures adopted when an aircraft enters service to ensure that it maintains a satisfactory standard of airworthiness during that service. A main activity here has always been the measurement of the loads experienced by an individual aircraft, and then assessing the rate of consumption of its fatigue life. In practice, this has generally involved applying Miner's cumulative damage rule to the actual load spectrum and relating the results to the life established under the (usually different) fatigue test spectrum. There are two complications in this area for composite structures. Firstly, as remarked in Lecture 9, there are some indications that Miner's rule may be quite unsatisfactory for composites; if that proves to be the case then some alternative procedure will have to be developed so that the fatigue performance in service can be related to that demonstrated in the fatigue test. Secondly, because of the effect of moisture absorption on structural performance, it may well be important to monitor the moisture absorption in service "by tail number", along with the loads. As also was indicated in Lecture 9, some monitoring of moisture absorption in service is already being done by measuring the weight increase in "traveller specimens", but a form of continuous monitoring would be much more convenient. Attention is being paid to identifying an appropriate physical property of a composite which can be both readily correlated with moisture absorption and can also be readily measured; for example, in ref. (10), moisture induced resistivity changes in graphite/epoxy were studied.

REFERENCES

1. Anon., Military Standard, Aircraft Structural Integrity Program, Airplane Requirements, MIL-STD-1530A (11), US Department of Defense, 1975.

2. Anon., Plastics for Aerospace Vehicles, Part 1, Reinforced Plastics, MIL-HDBK-17A, US Department of Defense, 1971.

3. Guyett, P.R., and Cardrick, A.W., The Certification of Composite Airframe Structures, The Aeronautical Journal (RAeS), vol. 84, pp. 188-203, 1980.

4. Anon., Composite Aircraft Structure, US Department of Transportation, Federal Aviation Administration, Advisory Circular, AC 20-107, 1978.

5. Weinberger, R.A., Somoroff, A.R., and Riley, B.L., US Navy Certification of Composite Wings for the F-18 and Advanced Harrier Aircraft, pp. 1-12 of Certification Procedures for Composite Structures, AGARD-R-660, 1978.

6. Goodman, J.W., Tiffany, C.F., and Muha, T.J., Structural Assurance of Advanced Composite Components for USAF Aircraft, ibid, pp. 25-35.

7. Rogers, G.W., The Fatigue Certification of the CFC Tornado Taileron, ICAF Conference, Netherlands, 1981.

8. Goodman, J.W., Lincoln, J.W., and Petrin, C.L., On Certification of Composite Structures for USAF Aircraft, Paper AIAA-81-1686, AIAA Conference, Dayton, August 1981.

9. Anon., Assessment of Carbon Fibre Electrical Effects, NASA Conference Publication 2119, 1980.

10. Belani, J.G., and Broutman, L.J., Moisture Induced Resistivity Changes in Graphite Reinforced Plastics, Composites, vol. 9, pp. 273-277, 1978.
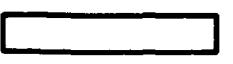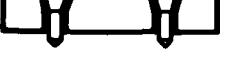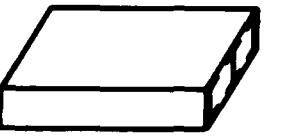
Serial	Type	Example ←— L —→	Typical dimension, L m
1	Coupon		0.1
2	Structural detail		0.2
3	Sub-component		1.0
4	Component		3.0
5	Full scale aircraft		30

FIG. 1   RANGE OF SPECIMENS IN STRUCTURAL TEST PROGRAMME

DISTRIBUTION

AUSTRALIA

Department of Defence Support

Central Office

Secretary

Aeronautical Research Laboratories

Director
Library
Superintendent - Structures
Divisional File - Structures
Superintendent - Materials
Divisional File - Materials
Authors: B.C. Hoskin
          A.A. Baker
          I.G. Scott
          J.G. Williams
          R. Jones
          M.J. Davis
          B.I. Green
          A.W. Rachinger
          C.M. Scala
L.M. Bland
N.E. Ryan
B.J. Wicks
J.H. Auld
J.Y. Mann
J.M. Finney
C.A. Patching
C.K. Rider

Materials Research Laboratories

Director/Library

Defence Research Centre Salisbury

Library

RAN Research Laboratory

Library

Government Aircraft Factories

Library

Department of Defence

Central Office

Chief Defence Scientist)
Deputy Chief Defence Scientist)
Superintendent Science and Technology Programmes) (1 copy)
Controller, Projects and Analytical Studies)
Defence Central Library
Document Exchange Centre, DISB (17 copies)
Joint Intelligence Organisation
Librarian H Block, Victoria Barracks, Melbourne
Director General - Army Development (NSO) (4 copies)

Navy Office

Navy Scientific Adviser
Directorate of Naval Aircraft Engineering
Superintendent Aircraft Maintenance and Repair

Army Office

Army Scientific Adviser
Library, Royal Military College

Air Force Office

Air Force Scientific Adviser
Technical Division Library
Director General Aircraft Engineering
HQ Support Command (SENGSO)
Library, RAAF Academy, Point Cook
Directorate of Quality Assurance (Central Office)

Department of Aviation

Library
Airworthiness Group (200 copies)

Statutory, State Authorities and Industry

CSIRO Central Library, Melbourne
QANTAS (Engineering Library)
TAA (Engineering Library)
Ansett (Engineering Library)
Library, Commonwealth Aircraft Corporation
Library, Hawker de Havilland, Bankstown
Dunlop Aviation, Bayswater

Universities and Colleges

Adelaide	Barr Smith Library
Australian National	Library
Flinders	Library
James Cook	Library
LaTrobe	Library
Melbourne	Engineering Library
Monash	Library
Newcastle	Library
New England	Library
New South Wales	Physical Sciences Library
	Head, Mechanical Engineering Dept.
Queensland	Library
Sydney	Library
	Head, Aeronautical Engineering
Tasmania	Engineering Library
Western Australia	Library
RMIT	Library
	Head, Aero. Eng. Dept.

CANADA

CAARC Co-ordinator Structures
National Aeronautics Establishment, Library
De Havilland Aircraft of Canada, Library
Defence Research Establishment Pacific, Library
McGill University, Library
Toronto University, Institute of Aerophysics, Library

FRANCE

ONERA, Library
Service de Documentation, Technique de l'Aeronautique

GERMANY

Fachinformationszentrum:Energie, Physic,
    Mathematik GMBH

INDIA

CAARC Coordinator Structures
National Aeronautical Laboratory, Library
Hindustan Aeronautics, Bangalore, Library

INTERNATIONAL COMMITTEE ON AERONAUTICAL FATIGUE

Distributed through Dr. G.S. Jost (23 copies)

ISRAEL

      Technion - Israel Institute of Technology, Library

ITALY

      Associazone Italiana di Aeronautica end Astronautica

JAPAN

      National Aerospace Laboratory, Library

NETHERLANDS

      National Aerospace Laboratory (NLR), Library

NEW ZEALAND

      Air Department, RNZAF Aero Documents Section

SWEDEN

      Aeronautical Research Institute
      SAAB Library

UNITED KINGDOM

      CAARC Co-ordinator Structures
      Royal Aircraft Establishment, Farnborough, Library
      Royal Aircraft Establishment, Bedford, Library
      National Engineering Laboratories, Library
      British Library, Science Reference Library
      British Library, Lending Division
      Aircraft Research Association Library
      British Aerospace, Warton, Library
      British Aerospace, Hatfield, Library
      British Aerospace, Kingston, Library
      British Aerospace, Weybridge, Library
      Shorts, Belfast, Library
      Westland, Yeovil, Library
      Cranfield Institute of Technology, Library
      Bristol University, Engineering Library
      Cambridge University, Engineering Library
      Imperial College, Engineering Library

UNITED STATES OF AMERICA

      NASA Scientific and Technical Information Centre
      Air Force Wright Aeronautical Laboratories, Dayton, Library
      Naval Air Development Centre, Warminster, Library
      NASA Langley Research Centre, Hampton, Library
      NASA Lewis Research Centre, Cleveland, Library

Air Force Institute of Technology, Dayton, Library
Bell Helicopter Textron, Fort Worth, Library
Boeing Commercial Airplane Co., Renton, Library
Boeing Vertol Co., Philadelphia, Library
Cessna Aircraft Co., Wichita, Library
General Dynamics, Fort Worth, Library
General Dynamics, San Diego, Library
Grumman Aerospace, Bethpage, Library
Lockheed-California, Burbank, Library
Lockheed-Georgia, Marietta, Library
McDonnell-Douglas, St. Louis, Library
McDonnell-Douglas, Long Beach, Library
Northrop Corporation, Hawthorne, Library
Rockwell International, El Segundo, Library
Sikorsky Aircraft, Stratford, Library
MIT, Cambridge, Library
Polytechnic Institute of Brooklyn, Aero. Labs., Library
Cornell Aeronautical Laboratories, Library

TTCP

Dr. A.R. Somoroff, Naval Air Systems Command, Washington DC, USA
Mr. R. Maxwell, Royal Aircraft Establishment, Farnborough, UK
Dr. K. Street, Defence Research Establishment Pacific, Victoria B.C.
    Canada

Spares (40 copies)

Total (415 copies)

Department of Defence Support
DOCUMENT CONTROL DATA

1. a. AR No	1. b. Establishment No	2. Document Date	3. Task No
AR-002-919	ARL-STRUC-REPORT-394/ ARL-MAT-REPORT-114	October 1982	DST 82/002

4. Title	5. Security a. document	6. No Pages
LECTURES ON COMPOSITE MATERIALS FOR AIRCRAFT STRUCTURES	UNCLASSIFIED b. title c. abstract U U	264 7. No Refs 233

8. Author(s) Edited by B.C. HOSKIN and A.A. BAKER	9. Downgrading Instructions -

10. Corporate Author and Address AERONAUTICAL RESEARCH LABORATORIES P.O. Box 4331, Melbourne, Victoria 3001	11. Authority (as appropriate) a.Sponsor b.Security c.Downgrading d.Approval

12. Secondary Distribution (of this document)

Approved for Public Release.

Overseas enquirers outside stated limitations should be referred through ASDIS, Defence Information Services Branch, Department of Defence, Campbell Park, CANBERRA ACT 2601

13. a. This document may be ANNOUNCED in catalogues and awareness services available to ...

No limitations.

13. b. Citation for other purposes (ie casual announcement) may be (select) unrestricted(XXXXXXXXXX

14. Descriptors		15. COSATI Group
Composite materials.	Surface properties.	1104
Fiber reinforced plastics.	Damage tolerance.	0103
Dissimilar materials bonding.	Nondestructive tests.	
Durability.	Aircraft structures.	
Laminates.	Aircraft repair.	
Adhesive bonding.	Airframes.	

16. Abstract

     This report is an edited version of notes prepared in connection with a series of lectures on Composite Materials for Aircraft Structures that was given at the Aeronautical Research Laboratories during November 1981. The aim of the lectures was to provide a broad introduction to virtually all aspects of the technology of composite materials for aircraft structural applications. Topics covered included: the basic theory of fibre reinforcement; material characteristics of the commonly used fibre, resin, and composite systems; component form and manufacture; structural mechanics of composite laminates; joining composites; environmental effects, durability and damage tolerance; NDI procedures; repair procedures; aircraft applications; airworthiness considerations.

PF 65

This page is to be used to record information which is required by the Establishment for its own use but which will not be added to the DISTIS data base unless specifically requested.

16. Abstract *(Contd)*

17. Imprint
Aeronautical Research Laboratories, Melbourne.

18. Document Series and Number	19. Cost Code	20. Type of Report and Period Covered
STRUCTURES REPORT 394/ MATERIALS REPORT 114	214655 (50%) 364750 (50%)	

21. Computer Programs Used

22. Establishment File Ref(s)

END

DATE
FILMED

11 83

DT